

**EXPERIMENTAL MODELS OF STEM CELL COMMITMENT  
AND HUMAN DISEASE**

**By**

**Lea-Anne Harrison B.Sc. (Hons)**

**Thesis submitted to**

**The University of Leicester**

**For the degree of**

**DOCTOR OF PHILOSOPHY**

**Department of Cancer Studies and Molecular Medicine**

**Division of Cellular Interaction and Cell Signalling**

**The University of Leicester**

**March 2007**

UMI Number: U227443

All rights reserved

INFORMATION TO ALL USERS

The quality of this reproduction is dependent upon the quality of the copy submitted.

In the unlikely event that the author did not send a complete manuscript and there are missing pages, these will be noted. Also, if material had to be removed, a note will indicate the deletion.



UMI U227443

Published by ProQuest LLC 2013. Copyright in the Dissertation held by the Author.  
Microform Edition © ProQuest LLC.

All rights reserved. This work is protected against  
unauthorized copying under Title 17, United States Code.



ProQuest LLC  
789 East Eisenhower Parkway  
P.O. Box 1346  
Ann Arbor, MI 48106-1346

## Abstract

A stem cell is a cell that maintains its own numbers and can self-renew whilst at the same time producing indefinite numbers of differentiated pluripotent progeny. The aim of this thesis was to test the hypothesis that stem cells and their progenitors are important in metaplasia in the gastrointestinal (GI) tract across species. Immunohistochemistry (IHC) was employed to identify and analyse potential stem cell markers in human tissue. Putative stem cell location was mapped using a thymidine analogue to label slow cycling cells in human tissue. Zebrafish were investigated to examine deoxycholic acid (DCA), as a model for bile acid stimulation on stem cell fate, and whole animal histology was evaluated. Finally, the liver fatty acid binding protein (L-FABP) promoter was used to direct placental cadherin (P-cadherin) expression in the GI tract in a transgenic murine model. Transgene expression was confirmed using reverse transcriptase polymerase chain reaction (RT-PCR) and the resulting phenotype was investigated.

IHC analysis showed P-cadherin was expressed in the putative stem cell compartment in human oesophageal and Barrett's mucosa. Iododeoxyuridine (IUdR) labelling identified the stem cell compartment in human tissue. Double labelling, using IUdR with Ki-67 further identified a small stem cell side population in the basal compartments. The zebrafish model showed a mucin cell phenotype in the DCA stimulated animals, which was absent from controls. In the transgenic mouse model, although neoexpression of P-cadherin was demonstrated in the small bowel by RT-PCR, there was no obvious phenotype observed. However, there was an increase in stem cell division in the small bowel.

In conclusion, the data generated in this thesis support the hypothesis that stem cells play a pivotal role in human disease. It would appear that the previously undefined stem cell compartment can now be elucidated and that P-cadherin upregulation is a feature of this location.

## Acknowledgements

First and foremost I would like to thank my supervisors Professor Janusz Jankowski and Dr Jacqui Shaw who have both contributed invaluable to this thesis. I would like to thank you both for your guidance, expertise and constant support and encouragement. I have learnt a great deal as a result of your supervision and I will be forever grateful for all of your thoughts, constructive criticism and direction during my time as a PhD student.

I am indebted to many members of the laboratories at CRUK, London for their practical and intellectual assistance at various stages throughout this project. In particular I would thank, Emma Nye, Gordon Stamp, Robert Goodlad, Stuart McDonald, George Elia, Nikki Mandir, Sean Preston and Richard Poulson.

I would like to thank the members at Daniolabs, Cambridge, who made my stay with you both enjoyable and incredibly productive. In particular I would like to extend a special thank you to Angeleen Fleming and Clare Chappell who contributed greatly to my understanding of the subject that is zebrafish! My thanks must also be given to David Hopwood for his invaluable EM expertise.

I would also like to extend my appreciation to members of the Robert Kilpatrick Clinical Sciences Building workforce. In particular to members of the histopathology department such as Rebecca Harrison, Kevin West, Angus McGregor, and far too many more to mention, who significantly aided this work when it came to pathological examination and diagnosis. There have been too many academic staff, post-docs, Ph.D., M.D., M.Sc. and B.Sc. students to name individually, but I would especially like to acknowledge; Howard Pringle, John Halsall, Linda Potter, Lindsay Primrose, Leanne Hart, Angie Gillies and Karen Kulbicki. You have all contributed to making my time here both enjoyable and interesting and I appreciate all of your technical advice and constructive input to this PhD investigation. Separately I would like to mention Paul Atherfold, Jolanta Obszynska, Karen Page and Toryn Poolman, while all of the above also applies to you, in addition I would like to thank you for your friendship and for making my days at work and in the laboratory as enjoyable as possible.

Also I would like to thank Coconut for being such a great companion and constant source of entertainment. While it could be argued that you don't understand the process of a PhD, you always seemed to know when I needed a break and took me out in the fresh air to clear my thoughts and prepare me for another day.

A special gratitude must be conveyed to my family and friends, for their unwavering support and encouragement. To my Dad, Peta and Ella-Rose, thank you for always having faith in me, especially at times when I wasn't so sure. I would particularly like to mention my Mum, truly the most amazing lady I have ever known. Not only have you taught me so much but you have always had faith in me and supported me every step of the way. Thank you for always being there and knowing exactly the right words, and not only for being the best proof reader I could ask for, but especially for teaching me that taking things one step at a time is the best way to get things done.

Last, but by no means least, I would like to thank my partner Ben who has provided me with encouragement, understanding and companionship during the last three years. I know that you have given up a lot to be there for me, always supporting me in everything that I do. So, while the support you've given me over the years isn't unexpected, I wanted you to know that it is certainly not unappreciated. Thank you for always being there as my sounding board after all those hard days, always being able to see things from a different view point and giving me great advice with a calm head, and of course for your ability to make sure I never had any computer worries and for reminding me every 10 minutes to "back up my work"! Mostly thank you for always keeping me warm and safe, and for being my safe port of call in my turbulent PhD waters. I couldn't have done this without you.

## Contents

<b>Abstract</b> .....	<b>i</b>
<b>Acknowledgements</b> .....	<b>ii</b>
<b>Contents</b> .....	<b>iii</b>
<b>List of Figures</b> .....	<b>x</b>
<b>List of Tables</b> .....	<b>xiii</b>
<b>Abbreviations</b> .....	<b>xv</b>
<b>Units of Measurement Abbreviations</b> .....	<b>xviii</b>
<b>Publications and Presentations Arising from this Work</b> .....	<b>xi</b>
<b>Chapter 1: Introduction</b> .....	<b>1</b>
<b>1.1 Epithelial Development</b> .....	<b>2</b>
<b>1.2 The Gastrointestinal Tract</b> .....	<b>3</b>
<b>1.3 Stem Cells</b> .....	<b>4</b>
1.3.1 <u>Adult Oesophageal Stem Cells</u> .....	6
1.3.2 <u>Stem Cells of the GI Tract</u> .....	8
1.3.2.1 <i>Adult Gastric Stem Cells</i> .....	8
1.3.2.2 <i>Adult Small Intestine Stem Cells</i> .....	8
1.3.2.3 <i>Adult Colonic Stem Cells</i> .....	9
<b>1.4 Molecular regulation of stem cell function in the GI tract</b> .....	<b>9</b>
1.4.1 <u>Cell adhesion molecules</u> .....	10
1.4.1.1 <i>Cadherin's</i> .....	11
1.4.1.2 <i>Integrins</i> .....	11
<b>1.5 Diseases of the oesophagus</b> .....	<b>12</b>
<b>1.6 Metaplasia of the oesophagus</b> .....	<b>13</b>
<b>1.7 Elucidating the putative Barrett's stem cell</b> .....	<b>15</b>
1.7.1 <u>Label Retaining Cells</u> .....	16
1.7.2 <u>Radioactive Markers</u> .....	16
1.7.2.1 <i>Iododeoxyuridine (IUdR)</i> .....	17
<b>1.8 Model Systems</b> .....	<b>18</b>
1.8.1 <u>Ex vivo Models</u> .....	18
1.8.2 <u>Animal Models</u> .....	19
1.8.2.1 <i>Animal Models of BO</i> .....	20
1.8.2.2 <i>The Zebrafish – A Novel Model of BO?</i> .....	26
<b>1.9 Hypothesis and Aims</b> .....	<b>27</b>

<b>Chapter 2: Materials and Methods .....</b>	<b>28</b>
<b>2.1 Materials .....</b>	<b>29</b>
2.1.1 <u>Tissue Samples</u> .....	29
2.1.1.1 <i>Human Tissue</i> .....	29
2.1.1.2 <i>Mouse Tissue</i> .....	29
2.1.1.3 <i>Zebrafish Tissue</i> .....	29
2.1.2 <u>Clinical Trial Protocol</u> .....	30
2.1.3 <u>Cell Lines</u> .....	31
2.1.4 <u>Primary Antibodies</u> .....	32
2.1.5 <u>General Reagents</u> .....	34
2.1.5.1 <i>Cell Culture: Buffers and reagents</i> .....	34
2.1.5.2 <i>IHC: Buffers and reagents</i> .....	34
2.1.5.3 <i>Competent Cell Transformation and Plasmid Preparation</i> .....	36
2.1.5.4 <i>Sequencing</i> .....	36
2.1.5.5 <i>DNA Restriction</i> .....	36
2.1.5.6 <i>DNA Extraction</i> .....	36
2.1.5.7 <i>RNA Extraction</i> .....	37
2.1.5.8 <i>Reverse Transcription</i> .....	37
2.1.5.9 <i>Polymerase Chain Reaction</i> .....	37
2.1.5.10 <i>Agarose Gel Electrophoresis</i> .....	37
2.1.6 <u>PCR Primer sequences</u> .....	38
<b>2.2 Methods .....</b>	<b>40</b>
2.2.1 <u>Tissue Processing</u> .....	40
2.2.1.1 <i>Human Tissue</i> .....	40
2.2.1.2 <i>Clinical Trial Tissue</i> .....	40
2.2.1.3 <i>Mouse Tissue</i> .....	40
2.2.1.4 <i>Zebrafish Tissue</i> .....	42
2.2.2 <u>Cell Culture</u> .....	44
2.2.2.1 <i>Routine Cell Culture</i> .....	44
2.2.2.2 <i>Deoxycholic Acid Zebrafish Stimulation</i> .....	44
2.2.2.3 <i>IUdR Reconstitution</i> .....	45
2.2.2.4 <i>In Vitro Culture of TE-7 and OE-21 cell lines</i> .....	45
2.2.2.5 <i>Preparation of TE-7 and OE-21 cell lines</i> .....	46
2.2.3 <u>Primary Explants</u> .....	46
2.2.3.1 <i>Ex Vivo Culture of Barrett's Mucosal Biopsies</i> .....	46
2.2.3.2 <i>Preparation of Primary Explant Mucosal Biopsies</i> .....	47
2.2.4 <u>Immunostaining of Human Tissue Sections</u> .....	47
2.2.4.1 <i>Dewaxing and Rehydrating</i> .....	47
2.2.4.2 <i>Haematoxylin and Eosin Staining of FFPE Sections</i> .....	47
2.2.4.3 <i>Microwave antigen retrieval</i> .....	47
2.2.4.4 <i>Proteinase K digestion antigen retrieval</i> .....	48

2.2.4.5	<i>Pressure cooking antigen retrieval</i>	48
2.2.4.6	<i>Non-specific antigen and hydrogen peroxidase blocking</i>	48
2.2.4.7	<i>Streptavidin-Biotin-Horseradish Peroxidase Detection (ABC-HRP)</i>	48
2.2.4.8	<i>Streptavidin-Biotin- Alkaline Phosphatase Detection (ABC-AP)</i>	49
2.2.4.9	<i>IHC for Bromodeoxyuridine (BrdU)</i>	49
2.2.4.10	<i>Double Staining</i>	50
2.2.4.11	<i>Dehydrating and Mounting</i>	51
2.2.4.12	<i>Human IHC Tissue Controls</i>	52
2.2.4.13	<i>Evaluation of Immunostained Sections</i>	52
2.2.5	<b><u>Immunostaining of Mouse Tissue Sections</u></b>	53
2.2.5.1	<i>Mouse IHC for P-cadherin, Clone 56</i>	53
2.2.5.2	<i>Mouse IHC for P-cadherin, Clone PCD-1</i>	53
2.2.5.3	<i>IHC for Phospho-Histone (H3)</i>	54
2.2.5.4	<i>Mouse Tissue IHC Controls</i>	55
2.2.6	<b><u>Immunostaining of Zebrafish Tissue Sections</u></b>	55
2.2.7	<b><u>Competent Cell Transformation</u></b>	56
2.2.8	<b><u>Plasmid Preparation</u></b>	56
2.2.8.1	<i>'Mini' Plasmid Preparations</i>	56
2.2.9	<b><u>Sequencing</u></b>	57
2.2.10	<b><u>DNA Restriction</u></b>	58
2.2.11	<b><u>DNA Extraction</u></b>	58
2.2.12	<b><u>RNA Extraction</u></b>	58
2.2.13	<b><u>Reverse Transcription</u></b>	59
2.2.14	<b><u>Polymerase Chain Reaction</u></b>	60
2.2.15	<b><u>Agarose Gel Electrophoresis</u></b>	61
2.2.16	<b><u>Statistical Analysis</u></b>	62

## **Chapter 3: Stem Cell Compartment Identification and Mapping of LRC**

	<b>Location in Human Tissue</b>	<b>63</b>
<b>3.1</b>	<b>Introduction</b>	<b>64</b>
<b>3.2</b>	<b>Aims</b>	<b>66</b>
<b>3.3</b>	<b>Materials and Methods</b>	<b>66</b>
<b>3.4</b>	<b>Results</b>	<b>67</b>
3.4.1	<i><u>Tissue Morphology</u></i>	67
3.4.2	<i><u>IHC on Clinical Cases</u></i>	70
3.4.2.1	<i>Immunoreactivity Controls</i>	70
3.4.2.2	<i>P-cadherin, 610227</i>	71
3.4.2.3	<i>Ki-67, NCL-Ki67</i>	74
3.4.2.4	<i><math>\beta</math>-catenin, 610153</i>	77
3.4.2.5	<i><math>\beta</math>1-integrin, 4B7</i>	80

3.4.2.6	<i>Statistical Analysis for IHC Data</i> .....	83
3.4.3	<b><u>BrdU IHC on Control Cells and Tissues</u></b> .....	86
3.4.3.1	<i>Cytoblock Immunoreactivity Controls</i> .....	86
3.4.3.2	<i>Primary Explant Immunoreactivity Controls</i> .....	89
3.4.4	<b><u>P-cadherin IHC on Cytoblock Control Cells</u></b> .....	91
3.4.4.1	<i>Cytoblock Immunoreactivity Controls</i> .....	91
3.4.4.2	<i>Cytoblock Immunoreactivity Tissues</i> .....	91
3.4.5	<b><u>IHC on Experimental Cells and Tissues</u></b> .....	94
3.4.5.1	<i>Immunoreactivity Controls</i> .....	94
3.4.5.2	<i>Primary Explant P-cadherin Immunoreactivity Tissues</i> .....	94
3.4.5.3	<i>Clinical Trial P-cadherin Immunoreactivity Tissues</i> .....	97
3.4.5.4	<i>Clinical Trial E-cadherin Immunoreactivity Tissues</i> .....	100
3.4.6	<b><u>Method Development for BrdU IHC on Clinical Trial Tissues</u></b> .....	103
3.4.7	<b><u>BrdU IHC on Clinical Trial Tissues</u></b> .....	106
3.4.8	<b><u>High Powered Microscope Analysis on BrdU IHC on Clinical Trial Tissues</u></b> .....	108
3.4.9	<b><u>Labelling Index of IUdR LRC's in Clinical Trial Tissues</u></b> .....	111
3.4.10	<b><u>Double Labelling IHC on Clinical Trial Tissues</u></b> .....	112
3.4.10.1	<i>Experimental Tissue Controls</i> .....	112
3.4.10.2	<i>Clinical Trial Experimental Tissues</i> .....	113
3.4.10.3	<i>Statistical Analysis for Double Labelling IHC</i> .....	120
<b>3.5</b>	<b>Discussion</b> .....	<b>121</b>

**Chapter 4: The Role of Bile Acid Stimulation and Suppression in the Normal *in Vivo* System of the Zebrafish ..... 129**

<b>4.1</b>	<b>Introduction</b> .....	<b>130</b>
<b>4.2</b>	<b>Aims</b> .....	<b>131</b>
<b>4.3</b>	<b>Materials and Methods</b> .....	<b>131</b>
<b>4.4</b>	<b>Results</b> .....	<b>132</b>
4.4.1	<i>Tissue Morphology</i> .....	132
4.4.2	<b><u>Zebrafish IHC</u></b> .....	134
4.4.2.1	<i>Experimental Controls</i> .....	135
4.4.2.2	<i><math>\beta</math>1-integrin, Ab89918</i> .....	135
4.4.2.3	<i><math>\beta</math>-catenin, Ab6302</i> .....	135
4.4.2.4	<i>Pan-cadherin, Ab16505</i> .....	138
4.4.3	<b><u>DCA Zebrafish Stimulation Experiment</u></b> .....	140
4.4.3.1	<i>DCA Zebrafish Stimulation Statistics</i> .....	144
4.4.4	<b><u>EM on DCA Stimulated Zebrafish</u></b> .....	145
<b>4.5</b>	<b>Discussion</b> .....	<b>147</b>

<b>Chapter 5: P-cadherin Transgenic Mouse Model .....</b>	<b>152</b>
<b>5.1 Introduction.....</b>	<b>153</b>
<b>5.2 Aims.....</b>	<b>155</b>
<b>5.3 Materials and Methods.....</b>	<b>155</b>
<b>5.4 Results .....</b>	<b>156</b>
5.4.1 <u>Characterisation of P-cadherin Transgene Plasmid Construct .....</u>	156
5.4.2 <u>Generation of Experimental Animals .....</u>	163
5.4.3 <u>Genotyping of Transgenic Animals.....</u>	167
5.4.4 <u>Mouse IHC .....</u>	170
5.4.4.1 <i>Immunoreactivity Controls.....</i>	170
5.4.4.2 <i>P-cadherin, Clone 56 .....</i>	170
5.4.4.3 <i>P-cadherin, Clone PCD-1 .....</i>	171
5.4.4.4 <i>Phosphohistone H3.....</i>	174
5.4.4.5 <i>Phosphohistone Statistics .....</i>	177
5.4.5 <u>Expression of P-cadherin Transgene mRNA in Transgenic Mouse Tissues .....</u>	179
5.4.6 <u>Protein Analysis .....</u>	182
5.4.7 <u>Assessment of Proliferation and Fission .....</u>	183
<b>5.5 Discussion .....</b>	<b>185</b>
 <b>Chapter 6: Conclusions and Future Perspectives .....</b>	 <b>190</b>
 <b>Chapter 7: References.....</b>	 <b>196</b>
 <b>Appendices:</b>	
<b>Appendix 1: Study Documentation to Accompany the “STEMcell Assessment in Neoplastic Tissues” (SAINT) Clinical Trial .....</b>	<b>211</b>
<b>Appendix 2: IHC Data on All Six Clinical Cases and Each Marker Studied ....</b>	<b>215</b>
<b>Appendix 3: IHC Pan-cadherin Staining in the Transitional Zone Epithelium in the Zebrafish .....</b>	<b>240</b>
<b>Appendix 4: NCBI Blast Data.....</b>	<b>242</b>
<b>Appendix 5: Full Version of Mice Breeding Family Tree.....</b>	<b>246</b>
<b>Appendix 6: Full Genotyping Data for P-cadherin Transgenic Animals .....</b>	<b>249</b>
<b>Appendix 7: Statistical Raw Data and Analyses .....</b>	<b>253</b>
<b>Appendix 8: Publications Arising from this Work.....</b>	<b>267</b>

## List of Figures

<b>Figure 1.1</b>	Differentiation of human tissues.....	<b>2</b>
<b>Figure 1.2</b>	Topographical organisation of squamous oesophageal epithelium.....	<b>4</b>
<b>Figure 1.3</b>	Model of the organisation of proliferating and differentiating cells in the human oesophagus.....	<b>7</b>
<b>Figure 1.4</b>	Architecture and location of proliferating cells in human oesophageal epithelium.....	<b>8</b>
<b>Figure 1.5</b>	Architecture and location of stem cells in the GI tract.....	<b>9</b>
<b>Figure 1.6</b>	The metaplasia-dysplasia-adenocarcinoma sequence for oesophageal epithelial cells in Barrett's oesophagus.....	<b>13</b>
<b>Figure 1.7</b>	Cellular aberrations during carcinogenesis in Barrett's oesophagus.....	<b>15</b>
<b>Figure 1.8</b>	Plasma percentage and half life number for IUdR.....	<b>17</b>
<b>Figure 1.9</b>	Evolutionary time line.....	<b>24</b>
<b>Figure 2.1</b>	Layout of zebrafish sections on slide.....	<b>44</b>
<b>Figure 3.1</b>	H&E staining of a sample of clinical cases.....	<b>68</b>
<b>Figure 3.2</b>	H&E staining of control cells and tissues.....	<b>69</b>
<b>Figure 3.3</b>	H&E staining of clinical trial patient tissues.....	<b>70</b>
<b>Figure 3.4</b>	P-cadherin IHC analysis on experimental tissues.....	<b>72</b>
<b>Figure 3.5</b>	Ki-67 IHC analysis on experimental tissues.....	<b>75</b>
<b>Figure 3.6</b>	$\beta$ -catenin IHC analysis on experimental tissues.....	<b>78</b>
<b>Figure 3.7</b>	$\beta$ 1-integrin IHC analysis on experimental tissues.....	<b>81</b>
<b>Figure 3.8</b>	BrdU IHC analysis on experimental control cells.....	<b>87</b>
<b>Figure 3.9</b>	BrdU IHC analysis on primary explant control tissues.....	<b>90</b>
<b>Figure 3.10</b>	P-cadherin IHC analysis on cytoblock experimental controls and cytoblock control cells.....	<b>92</b>
<b>Figure 3.11</b>	P-cadherin IHC analysis on primary explant tissues.....	<b>95</b>
<b>Figure 3.12</b>	P-cadherin IHC analysis on clinical trial tissues.....	<b>98</b>
<b>Figure 3.13</b>	E-cadherin IHC analysis on clinical trial tissues.....	<b>101</b>
<b>Figure 3.14</b>	BrdU IHC comparison analysis on experimental control tissues using different counterstains.....	<b>104</b>

<b>Figure 3.15</b>	BrdU IHC analysis on clinical trial tissues.....	<b>107</b>
<b>Figure 3.16</b>	High powered BrdU IHC analysis on clinical trial tissues.....	<b>109</b>
<b>Figure 3.17</b>	Double labelling IHC analysis on cytoblock control tissues.....	<b>113</b>
<b>Figure 3.18</b>	Double labelling IHC analysis on clinical trial experimental tissues.....	<b>114</b>
<b>Figure 4.1</b>	Cross section through a one month old zebrafish.....	<b>132</b>
<b>Figure 4.2</b>	Zebrafish (7d.p.f.) gut regions.....	<b>133</b>
<b>Figure 4.3</b>	Cross section at four key sites showing major anatomical features of the zebrafish digestive tract.....	<b>134</b>
<b>Figure 4.4</b>	IHC analysis of antibodies used in zebrafish tissue.....	<b>137</b>
<b>Figure 4.5</b>	Pan-cadherin IHC analysis on zebrafish tissue.....	<b>139</b>
<b>Figure 4.6</b>	H&E analysis of first DCA stimulation experiment.....	<b>143</b>
<b>Figure 4.7</b>	High powered H&E analysis of the first DCA stimulation experiment.....	<b>144</b>
<b>Figure 4.8</b>	High powered H&E analysis of the second DCA stimulation experiment.....	<b>144</b>
<b>Figure 4.9</b>	Zebrafish EM analysis.....	<b>146</b>
<b>Figure 5.1</b>	Colony screen PCR of P-cadherin transformed DH5- $\alpha$ competent cells and mini prep DNA agarose gel.....	<b>157</b>
<b>Figure 5.2</b>	Restriction digest analysis.....	<b>157</b>
<b>Figure 5.3</b>	5' end region of P-cadherin transgene plasmid DNA sequence analysis for the primer into the promoter region.....	<b>159</b>
<b>Figure 5.4</b>	P-cadherin transgene plasmid DNA sequence analysis for the primer into the vector 3' end region.....	<b>160</b>
<b>Figure 5.5</b>	P-cadherin transgene plasmid DNA sequence analysis for the primer into the fatty acid binding promoter region.....	<b>161</b>
<b>Figure 5.6</b>	pBluescriptPCAD plasmid map.....	<b>163</b>
<b>Figure 5.7</b>	Founder line 4044a (line 1) breeding strategy and family tree.....	<b>165</b>
<b>Figure 5.8</b>	Founder line 4045a (line 2) breeding strategy and family tree.....	<b>166</b>
<b>Figure 5.9</b>	Optimisation of the genotyping PCR method prior to batch analysis.....	<b>168</b>
<b>Figure 5.10</b>	Optimised PCR method trial prior to batch analysis.....	<b>168</b>
<b>Figure 5.11</b>	A representative sample of genotyping analysis for 33 experimental animals..	<b>169</b>
<b>Figure 5.12</b>	P-cadherin IHC analysis on mouse experimental control tissues.....	<b>172</b>

<b>Figure 5.13</b>	P-cadherin IHC analysis on mouse experimental control tissues.....	<b>173</b>
<b>Figure 5.14</b>	Phosphohistone H3 IHC analysis on mouse experimental control tissues.....	<b>175</b>
<b>Figure 5.15</b>	Phosphohistone labelling index scores for control wild type, heterozygous and homozygous animals in the areas of SB1, SB2, SB3, LB1 and caecum intestinal mucosa.....	<b>178</b>
<b>Figure 5.16</b>	RT-PCR primer design.....	<b>179</b>
<b>Figure 5.17</b>	Expression of P-cadherin transgene mRNA in RT-PCR for wild type and homozygous animals from line 1, 4044a.....	<b>181</b>
<b>Figure 5.18</b>	RT-PCR transgene P-cadherin expression data for three separate homozygous animals from line 1, 4044a.....	<b>182</b>
<b>Figure 5.19</b>	Cell proliferations and crypt fission in the mid small intestine and colon.....	<b>183</b>

## List of Tables

<b>Table 1.1</b>	Comparative genetics of animal models of Barrett's metaplasia.....	<b>25</b>
<b>Table 2.1</b>	A summary of the human samples used along with primary characterisation details.....	<b>30</b>
<b>Table 2.2</b>	Cell lines used and their tissue of origin.....	<b>32</b>
<b>Table 2.3</b>	Primary antibodies used in this study.....	<b>33</b>
<b>Table 2.4</b>	Mouse genotyping, sequencing and RT-PCR primers.....	<b>39</b>
<b>Table 2.5</b>	Antibody details and conditions for IHC.....	<b>52</b>
<b>Table 2.6</b>	RT reaction mix composition.....	<b>60</b>
<b>Table 2.7</b>	The composition of a PCR reaction.....	<b>61</b>
<b>Table 3.1</b>	Intensity of cytoplasmic P-cadherin staining in human tissues of the MDCS.....	<b>83</b>
<b>Table 3.2</b>	Intensity of membranous P-cadherin staining in human tissues of the MDCS.....	<b>83</b>
<b>Table 3.3</b>	P-cadherin statistical analysis.....	<b>83</b>
<b>Table 3.4</b>	Intensity of nuclear Ki-67 staining in human tissues of the MDCS.....	<b>84</b>
<b>Table 3.5</b>	Ki-67 statistical analysis.....	<b>84</b>
<b>Table 3.6</b>	Intensity of membranous $\beta$ -catenin staining in human tissues of the MDCS.....	<b>84</b>
<b>Table 3.7</b>	Intensity of cytoplasmic $\beta$ 1-integrin staining in human tissues of the MDCS.....	<b>85</b>
<b>Table 3.8</b>	Intensity of membranous $\beta$ 1-integrin staining in human tissues of the MDCS.....	<b>85</b>
<b>Table 3.9</b>	$\beta$ 1-integrin statistical analysis.....	<b>85</b>
<b>Table 3.10</b>	Labelling index of IUdR positive LRCs in the human gastric mucosa, normal squamous, Barrett's and adenocarcinoma tissue.....	<b>111</b>
<b>Table 3.11</b>	Proportion of IUdR positive LRCs in each topographical location of the human gastric mucosa, normal squamous and Barrett's tissue.....	<b>111</b>

<b>Table 3.12</b>	Proportion of IUdR, Ki-67 and negative cells in the human normal oesophageal mucosa.....	<b>120</b>
<b>Table 3.13</b>	Percentage of IUdR, Ki-67 and negative cells in the human normal oesophageal mucosa.....	<b>120</b>
<b>Table 4.1</b>	Zebrafish DCA stimulation experiment, survival rates and health scores.....	<b>140</b>
<b>Table 5.1</b>	Information on transgenic experimental animals used in subsequent experiments.....	<b>167</b>
<b>Table 5.2</b>	Genotyping PCR optimisation conditions.....	<b>167</b>
<b>Table 5.3</b>	Genotyping results for all experimental animals investigated in the batch analysis.....	<b>169</b>
<b>Table 5.4</b>	Phosphohistone statistical analysis.....	<b>178</b>

## Abbreviations

ABC-HRP	Streptavidin biotin complex-horseradish peroxidase
ABC-AP	Streptavidin biotin complex-alkaline phosphatase
AMV	Avian myeloblastosis virus
ANOVA	Analysis of variance
AP	Alkaline phosphatase
APC	Adenomatous polyposis coli
ATCC	American Type of Culture Collection
BM	Barrett's metaplasia
BMDCs	Bone marrow-derived cells
BMP	Bone morphogenetic protein
BO	Barrett's oesophagus
BrdU	Bromodeoxyuridine
BSA	Bovine serum albumin
CAMs	Cell adhesion molecules
cDNA	Complementary DNA
CNS	Central nervous system
DAB	3, 3' - Diaminobenzidine
DCA	Deoxycholic acid
dH <sub>2</sub> O	Distilled water
DMEM	Dulbeccos Modified Eagles Medium
DMSO	Dimethylsulphoxide
DNA	Deoxyribonucleic acid
DNase	Deoxyribonuclease
dNTP	Deoxyneucleotide 5' triphosphate
d.p.f.	Days post fertilisation
ECACC	European Collection of Cell Cultures
E-cadherin	Epithelial cadherin
EM	Electron microscopy
FABP	Fatty acid binding protein
FBS	Foetal bovine serum
FCS	Foetal calf serum
FFPE	Formalin fixed paraffin embedded

GAPDH	Glyseraldehyde-3-phosphate dehydrogenase
GI	Gastrointestinal
GOJ	Gastro-oesophageal junction
GOR	Gastro-oesophageal reflux
GORD	Gastro-oesophageal reflux disease
H&E	Haematoxylin and Eosin
Hes-1	Hairy and Enhancer of Split homologue-1
<i>H. pylori</i>	<i>Helicobacter pylori</i>
HRP	Horseradish peroxidase
IBL	Interpapillary basal layer
ICC	Immunocytochemistry
I-FABP	Intestinal fatty acid binding protein
IgG	Immunoglobulin G
Igs	Immunoglobulins
IgSF	Immunoglobulin superfamily
IHC	Immunohistochemistry
IMS	Industrial methylated spirits
IM	Intestinal metaplasia
IUdR	Iododeoxyuridine
LB1	Large bowel 1
LB medium	Luria-Bertani medium
L-FABP	Liver fatty acid binding protein
LRC	Label retaining cell
LREC	Leicestershire Local Research Ethics Committee
LWT	London wild type
MDCS	Metaplasia-dysplasia-carcinoma sequence
M.O.M	Mouse on mouse
mRNA	Messenger ribonucleic acid
Msi-1	Musashi-1
NBF	Neutral buffered formalin
N-cadherin	Neuronal cadherin
NCBI	National Center for Biotechnology Information
NPA	No primary antibody
OA	Oesophageal adenocarcinoma

---

OD	Optical density
PBL	Papillary basal layer
PBS	Phosphate buffered saline
PBT	Phosphate buffered saline with Tween 20
P-cadherin	Placental cadherin
PCR	Polymerase chain reaction
PCNA	Proliferating cell nuclear antigen
PK	Proteinase K
PNACL	Protein and Nucleic Acid Chemistry Laboratory
PSA	Picryl sulfonic acid
RNA	Ribonucleic acid
RNase	Ribonuclease
rpm	Revolution per minute
RPMI	Roswell Park Memorial Institute media
RT	Reverse transcription
RT-PCR	Reverse transcriptase polymerase chain reaction
SAINT	STEMcell Assessment in Neoplastic Tissues
SB1	Small bowel 1
SB2	Small bowel 2
SB3	Small bowel 3
SCJ	Squamo-columnar junction
SDS	Sodium dodecyl sulphate
St-ABC	Streptavidin binding complex
TA	Transit amplifying
TAE	Tris-acetate EDTA buffer
<i>Taq</i>	<i>Thermophilus aquatcius</i>
TBS	Tris buffered saline
TBS-T	Tris buffered saline with Tween 20
TD	Terminally differentiation
TGF- $\beta$ 1	Transforming growth factor-beta one
TL	Tuebingen Long Fin
UP-water	Ultra-pure water
VAB	Veronal acetate buffer
ZFIN	Zebrafish International Resource Center

## Units of Measurement Abbreviations

bp	Base pair
g	Gram
L	Litre
M	Molar
mg	Milligram
ml	Millilitre
mM	Millimolar
mosmol	Milliosmol
m <sup>2</sup>	Meter squared
nm	Nanometre
pmol	Picomole
U	Units
µg	Microgram
µl	Microlitre
µm	Micrometre
V	Volts
°C	Degrees centigrade
%	Percentage

## **Publications and Presentations Arising from this Work**

### **Published Abstracts**

- Harrison LA, Nye E, Stamp G, Wright NA, Goodlad R, Jankowski JA. Transgenic mouse model for P-cadherin expression. *Gut* 2006; 55 (suppl II) A9-A9, 032.
- Harrison L, Nicholson AM, Harrison R, McDonald S, Wilson G, Atherfold PA, Wright N, Jankowski JA. The saint trial (stem cell analysis and identification by IUDR labelling of neoplastic tissue): Identification of Barrett's stem cells. *Gut* 2007; 56 (suppl II) A10-A11, 031.

### **Award Presentations**

- P-cadherin Transgenic Mouse Model: a potential role in mucosal modelling. LA. Harrison, E. Nye, G. Stamp, N. Mandir, J. Shaw, R. Goodlad, NA. Wright and JA. Jankowski. Selected for oral presentation, PhD Researcher of the Year, CSMM Campbell Prize Day, June 2006.

### **National Presentations**

- Transgenic mouse model for P-cadherin expression. J. Obszynska, L. Harrison, R. Harrison, N. Wright, and J. Jankowski. Poster presentation, BSCB annual conference, September 2003.
- Transgenic mouse model for P-cadherin expression. LA. Harrison, E. Nye, G. Stamp, NA. Wright, R. Goodlad, and JA. Jankowski. Oral presentation, BSG annual conference, March 2006.
- The SAINT trial (stem cell analysis and identification by Iododeoxyuridine (IUdR) labelling of neoplastic tissue); identification of Barrett's stem cells. LA. Harrison, AM. Nicholson, R. Harrison, S. McDonald, G. Wilson, PA. Atherfold, N. Wright, and JA Jankowski. Oral presentation, BSG annual conference, March 2007.

***\*Details of each of the abstracts pertaining to the above work can be found in Appendix 8\****

## **Chapter 1: Introduction**

## 1.1 Epithelial Development

Epithelial development is clearly of major importance to multicellular organisms. During gastrulation the three primary germ layers, the ectoderm, mesoderm and endoderm, are developed (Montero and Heisenberg, 2004). These germ layers become distinguishable during late blastula/early gastrula stages of embryogenesis, and each gives rise to a characteristic set of tissues, including, the epithelia (Figure 1.1) (Evers and Starr, 2006).

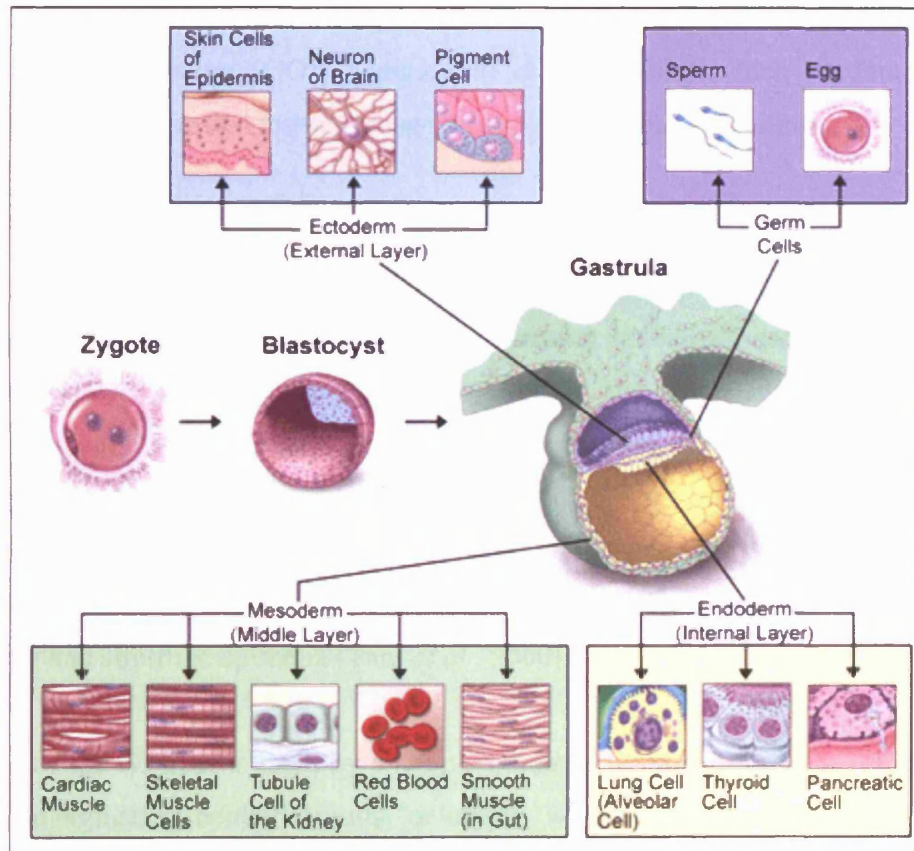


**Figure 1.1 - Differentiation of human tissues.** Fertilisation leads to the formation of a zygote. During the next stage, cleavage, mitotic cell divisions transform the zygote into a tiny ball of cells called a blastula. This early embryonic form undergoes a massive reorganisation called gastrulation forming a gastrula with three germ layers (ectoderm, light blue; mesoderm, light green; and endoderm, light yellow). In all vertebrates, these are the forerunners of all adult tissues and organs [taken from (The National Center for Biotechnology Information, 2006)].

Epithelia are continuous sheets of cells covering the surfaces of the body, and are involved in absorption and secretion. They stand on a basement membrane, which provides a site of attachment for the epithelium, and acts as a selective filtration barrier. Epithelia are avascular and rely on diffusion for exchange of oxygen and metabolites. Specialised cell-cell junctions allow binding and communication between adjacent cells. Cells in epithelia show a polarity along the axis between the external and internal environment, and their apical free surfaces often exhibit modifications (Alberts *et al.*, 2002).

There are two major types of epithelia: covering or lining epithelia and glandular epithelia, however these can be sub-classified depending on their characteristics, such as cell shape, number of layers, or particular specialisations. The shape of the cells, and their organisation are important to the particular function of each type of epithelia (Evers and Starr, 2006).

Within the body there are several “transitional zones”, which act as a boundary between two different epithelial tissues, and these are usually highly variable. Examples of these transitional zones can be found at the anal canal, the uterine cervix, the prostate gland and the gastro-oesophageal junction (GOJ), (Jankowski *et al.*, 2000a) which borders the gastric columnar glandular tissue and the oesophageal simple squamous epithelium.

## **1.2 The Gastrointestinal Tract**

The gastrointestinal (GI) tract has a unique epithelium, showing constant turnover and regeneration, yet it maintains a high degree of structural order with secretory, digestive and absorptive functions (Jankowski and Wright, 1992). The exact turnover time of these epithelial cell lineages is not known, while Jankowski *et al.*, (2000) stated that this occurs every 3-10 days, Brittan and Wright (2002), suggested a time of 2-7 days. While the exact time has not been defined it is known that this takes place under normal homeostasis and increases after damage, which is common with other rapidly renewing tissues such as the bone marrow and stratified epithelia (Tani *et al.*, 2000).

The surface of the GI tract is lined by a simple columnar epithelium that is folded to form a number of invaginating epithelial units, or crypts, which are embedded in the connective tissue. Each crypt contains approximately 250 cells, depending on its species and anatomical location (Booth and Potten, 2000).

The human oesophageal mucosa has distinctly different anatomical features compared to the rest of the GI tract, being organised in a similar fashion to the skin. A deep layer of stratified squamous epithelial cells line the oesophagus and form a protective smooth lining enabling food to pass to the stomach (Jankowski and Wright, 1992). The oesophageal epithelium is composed of three layers; 1) the basal compartment or muscularis mucosa, which is adjacent to the basal laminae and capillaries, is 1-4 cells thick and used for local movement of the mucosa; 2) the parabasal compartment or lamina propria, contains 10-30 cuboidal cells, with varying degrees of differentiation, which are regularly organised and provide vascular support for the epithelium; 3) and finally the superficial compartment or lining epithelium, which is

composed of 20-30 post mitotic end cells that will eventually be shed into the lumen (Jankowski and Dover, 1993).

The sub-mucosa lies underneath these three compartments and is a loose connective tissue layer containing blood vessels, lymphatics, nerves, and mucous secreting glands. Two layers of smooth muscle line the sub-mucosa; the inner layer is circular, and the outer layer is longitudinal. These layers of smooth muscle are used for peristalsis (Mills, 2006). The underlying connective tissue forms papillae that extend into the epithelium at regular intervals (Figure 1.2).

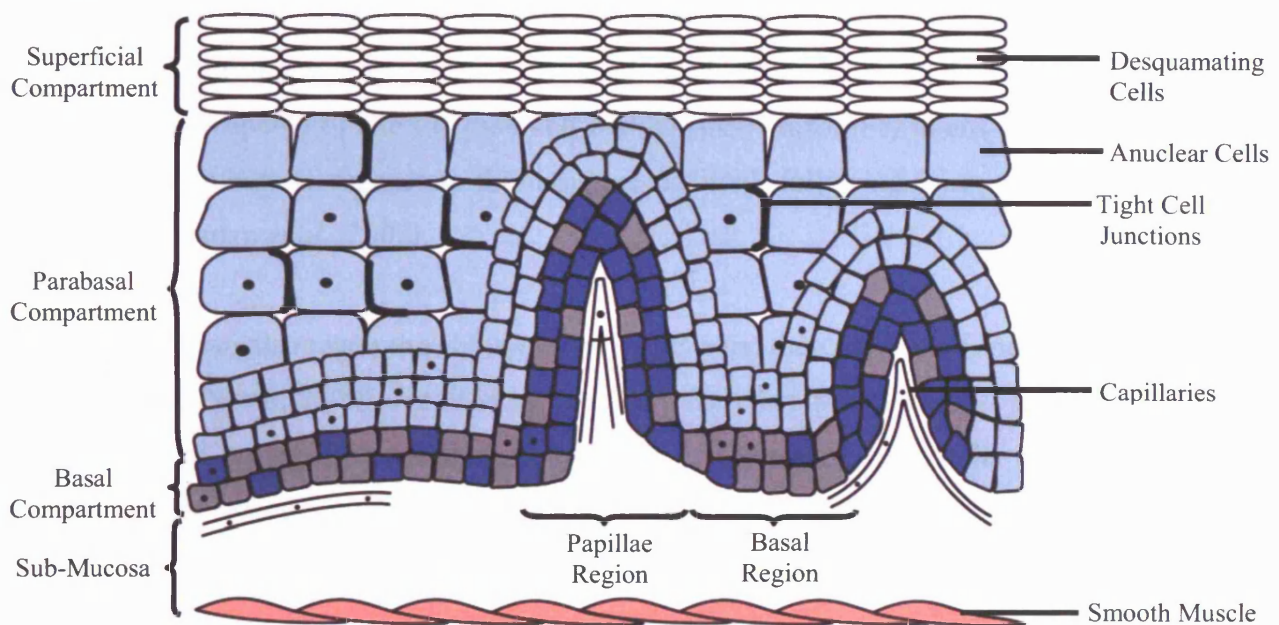


**Figure 1.2 – Topographical organisation of squamous oesophageal epithelium.** Basal, parabasal and superficial compartments are shown, along with the key histological details of this tissue [adapted from Jankowski *et al.*, (1992)].

### 1.3 Stem Cells

The concept of a stem cell came into being over one hundred years ago, as one of the organising principles of developmental biology. The existence of a stem cell, viewed as the ultimate origin of self renewal in self-maintaining tissues was first postulated by Regaud in 1901, based on his studies of spermatogenesis (Regaud, 1901a; Regaud, 1901b).

The definition of a stem cell is a cell that maintains its own numbers and can self-renew (clonogenic) whilst at the same time it can produce indefinite numbers of differentiated pluripotent progeny. In the GI tract these progeny, termed the transit amplifying (TA) or daughter cells are capable of differentiating into all GI epithelial cell lineages in order to regenerate the entire adult cell repertoire within intestinal crypts, gastric glands or the

oesophageal epithelium (Brittan and Wright, 2003). The TA cells undergo a finite number of divisions, but each time they divide they lose some of their capacity for self-renewal (non-clonogenic) (Jankowski *et al.*, 2000a). Stem cells are relatively undifferentiated and in most tissues they do not have the functional specialisations of the progeny that they give rise to (Brittan and Wright, 2003).

Differences occur in the operational definition of stem cells. It is now generally accepted that “stemness” is not a single property, but a number of properties that may manifest under different conditions (Booth and Potten, 2000). Thus, a stem cell must be undifferentiated (relative to the other epithelial cell types, but not necessarily relative to embryonic cells) and capable of proliferation and self-maintenance, producing many differentiated progeny. They must also be capable of altering their self-maintenance probability to ensure the expansion of stem cell numbers to regenerate the tissue, if required, following injury (Booth and Potten, 2000; Marshman *et al.*, 2002).

A stem cell can also retain the ability to switch between these options if and when appropriate (Booth and Potten, 2000). Adult stem cells may therefore possess a vast potential for tissue regeneration, previously only thought possible of embryonic stem cells (Marshman *et al.*, 2002). This regeneration process is regulated throughout life by proliferation of a multipotential stem cell population and terminal differentiation (TD) of stem cell progeny (Watt, 2002).

Stem cell division normally gives rise, through asymmetric cell division, to one daughter stem cell and one daughter cell that undergoes differentiation (Watt and Hogan, 2000). Such ‘invariant asymmetry’ is rare in adult mammalian tissues. In most mammalian tissues, stem cell division has three possible outcomes: the generation of two stem cells, two TA cells or one daughter cell of each type. In the steady state, the balance between stem and TA cell numbers is maintained in the tissue as a whole by multiple feedback loops (‘populational asymmetry’) (Jankowski *et al.*, 2000a; Watt and Hogan, 2000).

Little is known about either the stem cell compartment of the human oesophageal epithelium in health or disease (Jankowski *et al.*, 1993; Parkin, 1998), or the organisation and control of the stem cell hierarchy. However, since the publication of two papers in 1998, describing the *in vitro* growth of human embryonic stem cells derived either from the inner cell mass of the early blastocyst (Thomson *et al.*, 1998) or the primitive gonadal regions of early abortive

foetuses (Shamblott *et al.*, 1998), the field of stem cell research has progressed (Alison *et al.*, 2004).

Epithelial stem cells are important because epithelial cells cover a large proportion of the surface of our bodies and most human tumours derive from epithelial tissue. All functional GI stem cells lie in specific epithelial zones immediately adjacent to the mesenchyme and therefore the topographical position of stem cells seems to be of utmost importance in the maintenance of tissues (Jankowski and Wright, 1992). Epithelial cell-renewal is under the strict control of cell-cell and cell-extracellular matrix interactions between the epithelium and the connective tissue (Ishizuya-Oka, 2005).

The epithelium undergoes constant change with the underlying mesenchyme having spatially distinct compartments dedicated to control of stem cell activity (Sancho *et al.*, 2004). A vital balance between senescence, cell apoptosis, proliferation and/or differentiation of new cells must be maintained in order to regulate homeostasis in the GI tract (Brittan and Wright, 2003). Programmed cell death occurs by either extrusion into the gut lumen or by phagocytosis by neighbouring cells (Que and Gores, 1996).

This homeostatic control has led to the concept of a stem cell 'niche' (Alison *et al.*, 2002) which is thought to play an important role and govern all aspects of stem cell behaviour (Ishizuya-Oka, 2005). Functionally, a 'niche' provides an optimal setting for stem cell survival and function, and is characterised by its persistence upon removal of the stem cells and, conversely, if stem cells are extracted from their niche, they cease to retain their stem cell potential, or 'stemness', and become committed to differentiation (Spradling *et al.*, 2001). This specialised microenvironment is believed to be created and maintained by the mesenchymal cells of the underlying lamina propria (Brittan and Wright, 2003) and disruption within this microenvironment leads to diseases or disorders such as cancer in the human GI tract (Ishizuya-Oka, 2005). Although understanding how this niche affects stem cells is clinically important, its mechanisms still remain mostly unknown at the molecular level, mainly due to difficulties in the identification of the stem cells within the GI tract (Ishizuya-Oka, 2005).

### 1.3.1 Adult Oesophageal Stem Cells

In the squamous oesophagus the epithelium is divided into distinct zones; the basal zone (adjacent to the basal lamina) contains stem cells and their progeny, while the parabasal

(middle) layer contains TA cells and the superficial layer (adjacent to the lumen) contains differentiating or TD cells (Jankowski and Wright, 1992). The basal zone is made up of a layer of cells that adhere to the basement membrane and these are either segmented into a flat interpapillary basal layer (IBL) or a papillary basal layer (PBL) (Seery, 2002) (Figure 1.3). Cellular proliferation is limited to the basal zone, and cells are thought to migrate from this area towards the oesophageal lumen (Jankowski *et al.*, 1993) where cell loss occurs by the shedding of squamous cells at the surface; they eventually lose attachment with underlying cells and desquamate (Logan *et al.*, 1978).

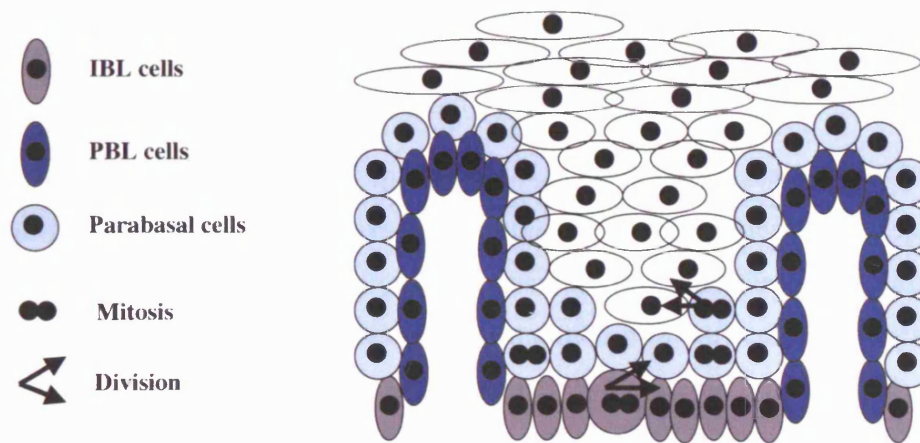


**Figure 1.3 – Model of the organisation of proliferating and differentiating cells in the human oesophagus.** The IBL cells constitute the stem-cell compartment (grey). Transit amplifying cells are proposed to reside in the PBL (dark blue) and parabasal layers (light blue). Suprabasal cells that can no longer divide and are undergoing terminal differentiation are shown in white. Arrows indicate the direction of cell movement [adapted from Seery and Watt (2000)].

Seery and Watt (2000) state that there is also a difference in the symmetry of cell division within these layers and that cells in mitosis appear to be more common in the parabasal layers than the PBL which are in turn more common than those in the IBL (Figure 1.4). In the PBL, cells divide symmetrically yielding two daughter cells which are both in contact with the basement membrane, whereas cell division on the IBL is perpendicular to the basement membrane and is asymmetrical with one daughter cell remaining in the IBL and the other moving into the epibasal layers. Cells in the IBL have similar mitotic properties to those of stem cells within the rest of the GI tract. They have a low proliferative index and when they do divide one remains in the niche to maintain stem cell numbers and the other progresses to achieve a high proliferative index. For this reason IBL cells are thought to be putative stem cells of the oesophagus.

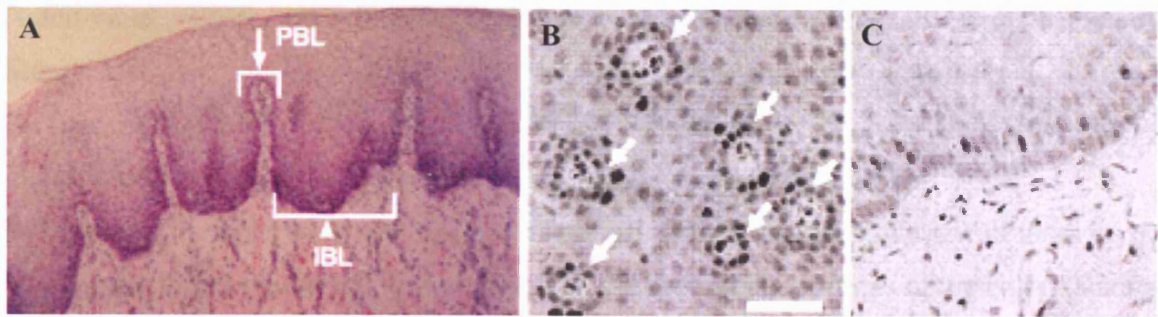


**Figure 1.4 - Architecture and location of proliferating cells in human oesophageal epithelium,** (A) Haematoxylin and eosin staining. Note the tall papillary structures at regular intervals (overlaid by PBL; arrow) separated by relatively flat interpapillary regions (IBL; arrowhead), (B, C) Ki-67 labelling of (B) PBL and (C) IBL. Cross-sections through individual papillae are indicated by arrows in (B). The scale bar represents 180mm in (A) and 70mm in (B, C) [taken from Serry and Watt (2000)].

### 1.3.2 Stem Cells of the GI Tract

While the factors maintaining the GI epithelium in a steady state remain to be elucidated, this epithelium represents a remarkable system for studying the biological features of stem cells and their hierarchies (Karam, 1999). In many areas of the GI tract characterisation of the stem cell location has already been documented and the mouse in particular has become a model system for investigating stem cells of the GI tract.

#### 1.3.2.1 *Adult Gastric Stem Cells*

The gastric glandular epithelium invaginates to form numerous short pits continuous with long tubular glands (Helander, 1981; Karam and Leblond, 1992). The acid-secreting region of the stomach contains at least four epithelial cell lineages: the pit, parietal, zymogenic (also know as the chief) and endocrine cell, and can be divided into isthmus, neck and base regions (Karam, 1999). In the stomach, epithelial cell migration is bidirectional, and cells that are thought to be stem cells are located at the neck/isthmus region of the gastric gland (Jankowski and Wright, 1992; Karam and Leblond, 1993) (Figure 1.5). These produce cells that migrate downwards to the base of the gland, becoming zymogenic cells or parietal cells (Karam, 1999), and upwards differentiating into mucus-secreting pit cells.

#### 1.3.2.2 *Adult Small Intestine Stem Cells*

The small intestinal epithelium invaginates to form small crypts continuous with large evaginating villi. Although the crypts are much smaller than the villi, they are much more numerous (Wright and Alison, 1984). In addition to the proliferative precursor cells, the crypts contain lysozyme and cryptidine-producing Paneth cells at the bottom and the stem cells are located just above these cells (Potten *et al.*, 1997) (Figure 1.5). The absorptive, goblet, enteroendocrine and caveolated cells are all scattered along the crypt-villus unit

(Potten *et al.*, 1997) and while they migrate outwards, the Paneth cells migrate inwards (Karam, 1999).

### 1.3.2.3 Adult Colonic Stem Cells

The epithelial lining of the colon invaginates to form numerous crypts, the size of these crypts and their lining cell types vary in the ascending and descending portions of the colon (Karam, 1999). In the colon the stem cells are located at the crypt base (Chang and Leblond, 1971) at cell position 4-5, (Potten *et al.*, 1997) (Figure 1.5). Cell types in the colon include vacuolated-columnar, goblet, enteroendocrine and caveolated cells which are found throughout the crypt wall (Karam, 1999).

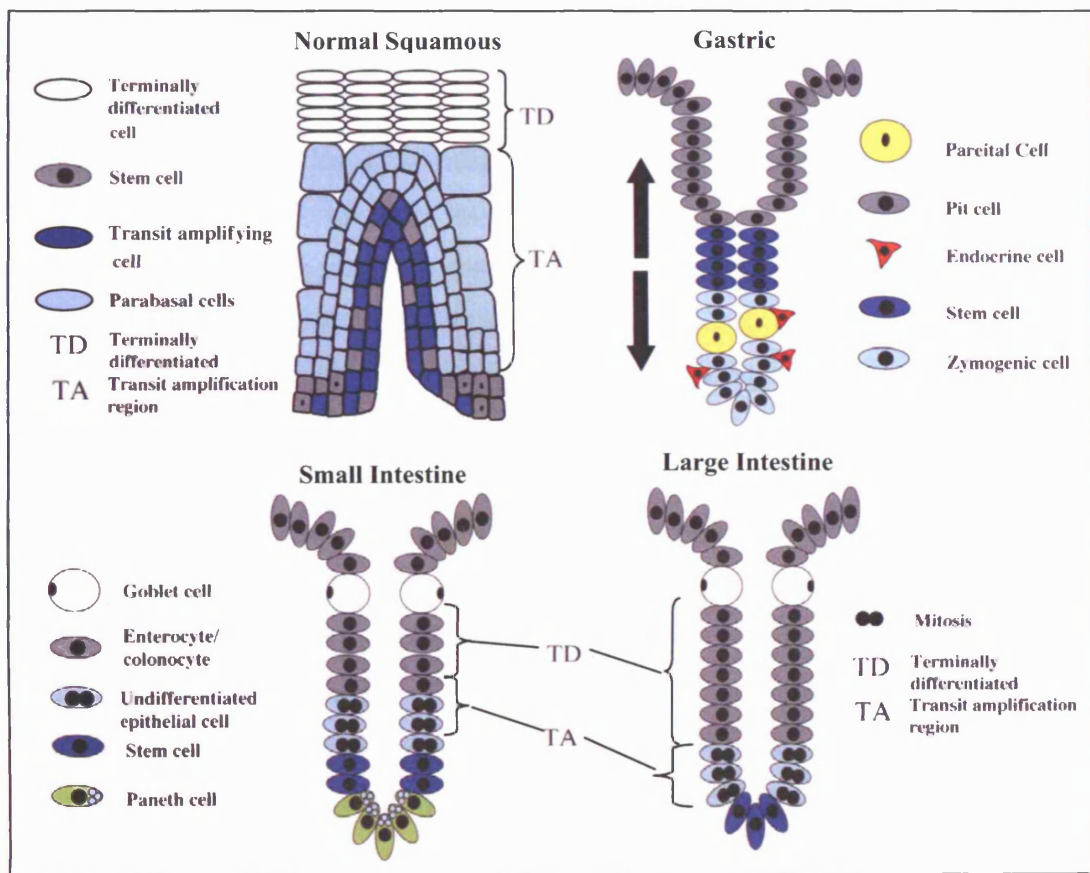


**Figure 1.5 - Architecture and location of stem cells in the GI tract.** Stem cells of the gut are stationary and anchored in specific locations, in the oesophagus they are located at the base, in the stomach they are found within the neck region and in the small intestine and colon they are also located at the crypt base [this figure has been adapted and reproduced with kind permission from Stuart McDonald © (2006) Histopathology Unit, London Research Institute, Cancer Research UK, London].

## 1.4 Molecular regulation of stem cell function in the GI tract

Recent progress in cell and molecular biology is gradually beginning to shed light on some of the key signalling pathways in the cell-renewal of the intestinal epithelium and the molecular control of tissue-specific stem cell behaviour is becoming particularly apparent within the GI

tract (Ishizuya-Oka, 2005). The major players in the homeostatic control of the adult epithelium include the Wnt, transforming growth factor-beta one (TGF- $\beta$ 1), bone morphogenetic protein (BMP), Notch and Par polarity pathways (Sancho *et al.*, 2004), which are also involved in embryonic organogenesis and/or adult carcinogenesis.

At present, only fragmentary information is available on their precise functions in the GI tract. Nevertheless, there is a growing body of evidence that such signalling pathways have conservative functions throughout the intestine of terrestrial vertebrates, suggesting the usefulness of experimental animals to clarify molecular mechanisms regulating epithelial cell-renewal (Ishizuya-Oka, 2005).

#### 1.4.1 Cell adhesion molecules

Cell adhesion molecules (CAMs) are found on the surfaces of all cells, where they bind to extracellular matrix molecules or to receptors on other cells. As well as having a structural role, CAMs function as signaling receptors, transducing signals initiated by cellular interactions, which regulate many diverse processes, including cell division, migration, and differentiation. CAMs are essential for maintaining stable tissue structure, however, cell adhesion must be dynamic to facilitate the mobility and turnover of cells (Thomas and Speight, 2001).

It has been established that the initial step in the metastatic cascade is the detachment of tumour cells from the primary tumour via dysregulation of normal cell-cell and cell-matrix interactions (Nair *et al.*, 2005). CAMs are distinct proteins which mediate these interactions and this process is normally tightly regulated, however in malignant tumors many of these processes are impaired, and it has been shown that many of the characteristics of tumor cells are attributable to the aberrant expression or function of CAMs (Thomas and Speight, 2001).

In recent years, a plethora of information has contributed to the in depth understanding of these molecules. Adhesion between individual cells allows an intact layer to be formed, which is selectively permeable. In addition, the orchestrated regulation of multiple adhesion molecules allows the gradual transition from basal secretory cells to apical absorptive cells in the crypt-villus gradient (Perry *et al.*, 1999).

There are five families of CAMs (cadherins, integrins, CD44, immunoglobulin superfamily (IgSF), and selectins) and alterations in their expression relate both to prognosis and tumour

behaviour in squamous cell carcinoma and adenocarcinoma of the oesophagus (Nair *et al.*, 2005).

#### 1.4.1.1 *Cadherin's*

Cadherins form a highly conserved superfamily of cellular adhesion molecules, which lead to stable cell-cell contacts that maintain tissue integrity (Handschuh *et al.*, 1999). The majority are transmembrane glycoproteins, and are adhesive only in the presence of calcium. They mediate adhesion by a homotypic interaction with cadherins on neighbouring cells (Hermiston *et al.*, 1996). All members of the cadherin superfamily are transmembrane proteins, with few exceptions, and are characterised by a unique domain, called cadherin motif or extracellular domain (Takeichi, 1990). The major classical cadherins are epithelial (E), neural (N) and placental (P) named according to the tissue that they were first located in (Handschuh *et al.*, 1999). Cadherins exhibit tissue specific distributions; E-cadherin is present in most tissues outside the nervous system (Takeichi, 1990), whereas P-cadherin expression is limited to stratified epithelia and placenta (Shimoyama *et al.*, 1989). These cadherins play major roles in vertebrate morphogenesis and are expressed widely throughout development. Antibodies to specific cadherins perturb a variety of developmental processes, and many gene knockouts are lethal at early stages of development (Gallin, 1998). The adhesive function of most cadherins is dependent on catenins,  $\alpha$  and  $\beta$ , that promote a link to the cytoskeleton. Unfortunately, cadherins and catenins seem to play a pivotal role in pathologies such as cancer and skin disease.

#### 1.4.1.2 *Integrins*

One of the best studied classes of CAMs is the integrin superfamily of cell surface receptors. Integrins are heterodimeric cell surface glycoproteins that primarily mediate the attachment of basal keratinocytes to extracellular matrix proteins found in the basement membrane (Li *et al.*, 1998). Integrins not only anchor the epidermis to the underlying basement membrane but are also required for wound repair and contribute to skin inflammation. They regulate the balance between proliferation and differentiation, and perturbed integrin expression contributes to the pathogenesis of benign and neoplastic conditions (Watt, 2002). Integrins can also mediate intercellular adhesion and activate cellular signalling pathways controlling epithelial cell survival, proliferation and differentiation (Juliano and Varner, 1993).

Integrins are one of the most important CAMs expressed by stratified squamous epithelium. Altered expression of these molecules has been found in oral carcinoma, where loss of CAM

expression is often seen in poorly differentiated lesions. However, upregulation of certain integrins, such as  $\alpha\beta6$ , has consistently been found in oral cancer, suggesting that it may play an active role in disease progression (Thomas and Speight, 2001).

### **1.5 Diseases of the oesophagus**

The mechanisms which control the proliferation and differentiation of cells, as well as the failure of these processes, are fundamental to most diseases. This is well illustrated in diseases of the oesophagus, which present an instructive spectrum of pathological changes, including benign inflammation, three types of metaplasia, dysplastic changes and two common types of cancer (adenocarcinoma and squamous cell carcinoma) (Jankowski and Dover, 1993).

There are a number of diseases of the oesophagus and conditions such as adenocarcinoma at the GOJ are becoming increasingly common in Western countries (Cameron *et al.*, 1995; Devesa *et al.*, 1998). Despite the fact that these types of cancers are among the most common fatal tumours in the world, comparatively little is known about the cell biology and organisation of this tissue (Seery, 2002).

One condition that predisposes to the development of oesophageal adenocarcinoma (OA) is Barrett's Oesophagus (BO). Here the normal squamous epithelium of the oesophagus is replaced by atypical columnar epithelium of the stomach. An English surgeon Norman Rupert Barrett (1903-1979), first described the modification of the epithelium of the lower oesophagus, characterised as a transition from Barrett's metaplasia (BM) through a carcinoma sequence (Jankowski *et al.*, 1999). This condition is thought to arise from chronic gastro-oesophageal reflux disease (GORD) and it has been reported that patients with BO have an estimated 30-150 fold higher risk, compared to the general population, of developing oesophageal cancer (Tytgat, 1995).

Most people develop BO in adult life, mainly as a result of GORD, although any insult that causes distal oesophageal irritation, such as chemical injury, also predisposes to metaplasia (Jankowski *et al.*, 2000a). Genetic factors may occasionally play a part in a small proportion of BM because it may have a familial association and occur in twins (Poynton *et al.*, 1996). Oesophageal metaplasia is thought to give rise to most, if not all, oesophageal and GOJ adenocarcinomas with the rate of neoplastic change each year between 0.2 and 2%. The resulting adenocarcinoma has a uniformly poor prognosis. Once diagnosed, patients have a median survival time of less than 1 year and fewer than 10% of patients survive for more than

5 years despite combined chemotherapy and surgery. The ideal requirement is to detect lesions at an early stage because surgical resection has proven survival benefits (Jankowski *et al.*, 2000b).

### 1.6 Metaplasia of the oesophagus

Several decades ago, studies of the age dependence of cancer suggested that carcinogenesis is a multistage process, and that between six and seven successive genetic hits are needed to convert a normal cell into an invasive cancer. Since then specific genetic mutations have been identified, and in 1988 Vogelstein *et al.*, published the famous colorectal adenoma-carcinoma sequence model. More recently there has been an interest in a model for the origin of OA, termed the metaplasia-dysplasia-carcinoma sequence (MDCS). In this model it is proposed that oesophageal cancer begins with metaplasia, which is secondary to GORD. From here a proportion of people will go on to develop dysplasia, and a fraction of these to invasive carcinoma (Figure 1.6) (Scott and Jankowski, 2001). The natural history of the MDCS in the oesophagus is of a similar length to the adenocarcinoma sequence in the colon, with a significant lead time before cellular invasion across the basement membrane. Cancer preventative strategies are targeted at this stage, aiming to halt, retard or preferably reverse the malignant process (Preston *et al.*, 2007).

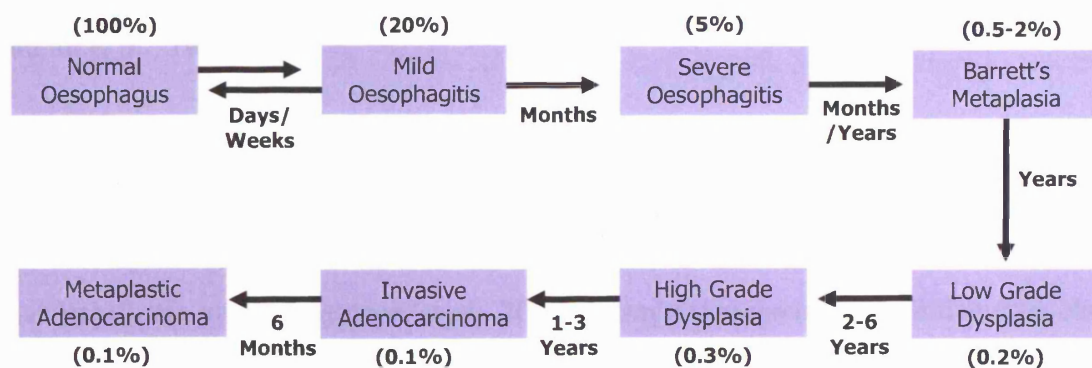


**Figure 1.6** – The metaplasia-dysplasia-adenocarcinoma sequence for oesophageal epithelial cells in Barrett's oesophagus. Prevalence rates in the adult population for each stage and approximate times for progression between stages are shown [adapted from Scott and Jankowski (2001)].

BM consists of a simple columnar epithelium that is folded to form glandular invaginations in the mucosa. As discussed, most proliferative GI cells are transitory and are shed from the epithelial surface into the lumen in a short time frame as they are replaced from below by new cells as a result of stem-cell division. The development of metaplasia and progression to adenocarcinoma occurs over a long period, enabling time for successive genetic events to take place (Jankowski *et al.*, 2000a). There is no direct evidence for the role of stem cells in BM,

however, as they are the only permanent residents of the epithelia, and are induced to undergo altered differentiation as a result of chronic epithelial damage, it is the stem cells of the native oesophagus or adjacent oesophageal glandular tissue which are the most likely candidates for causing metaplasia and subsequent dysplasia (Jankowski *et al.*, 1999).

Having said this, the pathogenesis of BM is still unclear, although three main theories exist. Firstly, the “*de novo* metaplastic theory” that stem cells are directly exposed to acid reflux and metaplasia arises spontaneously. This conjecture has support from studies carried out in mucinosis in the squamous epithelium of the vagina (Jankowski *et al.*, 2000a; Sodhani *et al.*, 1999). Secondly, the “transitional zone metaplasia theory” that claims cells at the GOJ (transitional zone) migrate to the distal oesophagus or gastric cardia in response to noxious luminal agents and colonise the tissue (Fitzgerald, 2005; Jankowski *et al.*, 2000a). To highlight the pluripotency of these transitional zone cells Fass and Sampliner (2000) reported that in response to oesophageal injury these cells can exhibit either a columnar phenotype in the oesophagus or a squamous phenotype when in the gastric cardia. Thirdly, the “duct-cell metaplasia theory” states that stem cells, located in the glandular neck region of oesophageal ducts, may selectively colonise the oesophagus when squamous mucosal damage occurs (Jankowski *et al.*, 2000a; Scott and Jankowski, 2001). The basis for this mechanism of metaplasia is the ulcer-associated cell lineage that occurs adjacent to ulceration in the GI tract (Schmidt *et al.*, 1999).

Overall, approximately 15% of malignancies worldwide (1.2 million/year) can be attributed specifically to chronic infections, and examples include bladder cancer due to schistosomiasis, liver cancer due to Hepatitis B and C infection, and cervical cancer due to human papilloma virus (Houghton *et al.*, 2006). Many other cancers are initiated by chronic inflammation secondary to other aetiologies, such as OA due to gastro-oesophageal reflux (GOR), colon cancer due to inflammatory bowel disease, and lung cancer due to smoking. These examples represent the “tip of the iceberg”, since most cancers do not arise in a normal tissue environment but require some initial degree of tissue alteration. As indicated the link between infection, chronic inflammation, and cancer has long been recognised and could reveal a fourth potential source of malignancy in the form of bone marrow-derived cells (BMDCs). Recent studies have suggested that BMDCs may possess an unexpected degree of plasticity and often home to sites of chronic injury or inflammation (Jiang *et al.*, 2003; Krause *et al.*, 2001).

A prime example of this is seen with *Helicobacter pylori* (*H. pylori*) in gastric cancer where BMDCs have been shown to home to and repopulate the gastric mucosa and contribute over time to metaplasia, dysplasia, and cancer (Balkwill and Mantovani, 2001; Houghton *et al.*, 2004; Wang *et al.*, 1998). In particular, this may occur where tissue injury induces excessive apoptosis that overwhelms or compromises the supply of endogenous tissue stem cells (Anderson *et al.*, 2001). The exact mechanism for this has not been established and there is little information on the long-term consequences of recruiting pluripotent cells to areas of chronic inflammation where signals for cell growth and differentiation may be altered.

These findings suggest a fourth potential source of malignancy for the pathogenesis of BM, whereby that epithelial cancers could originate from a bone marrow derived source, where a stem cell migrates to the area. Although currently there is no clear evidence to support this, if proved it has broad implications for the multistep model of cancer progression. What is known is that invasive OA arises after progression through a sequence of cellular aberrations (Figure 1.7).

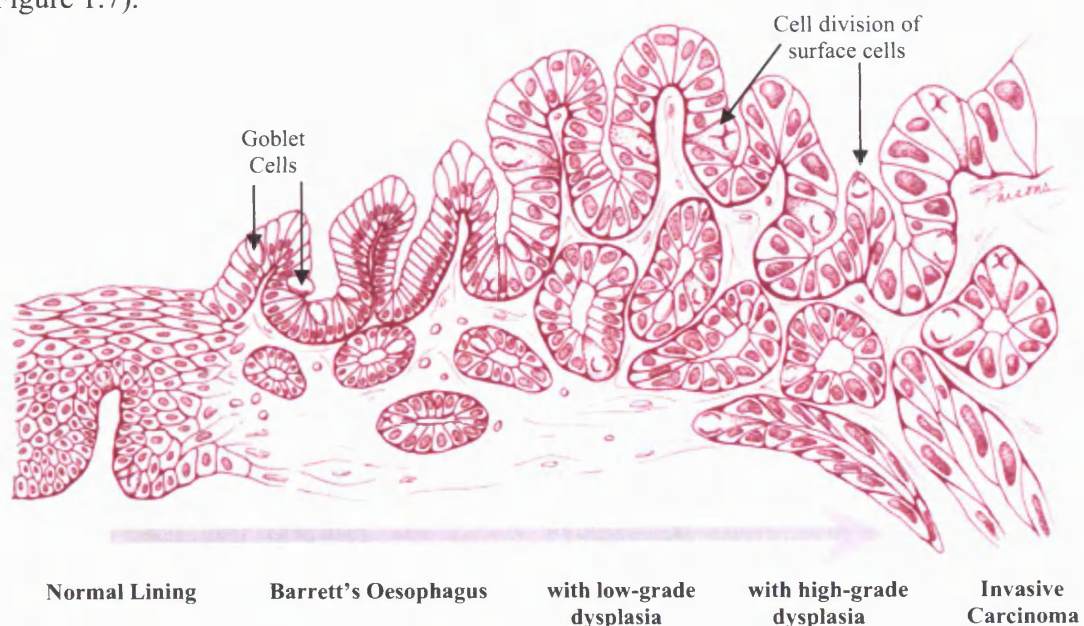


**Figure 1.7 – Cellular aberrations during carcinogenesis in Barrett's oesophagus.** The pathophysiological changes observed from normal oesophageal epithelial cells, through Barrett's oesophagus to invasive carcinoma are often associated with prosurvival signalling pathways and mutations that result directly or indirectly in carcinogenesis-promoting molecular and cellular aberrations [adapted from Buttar and Wang (2004)].

### 1.7 Elucidating the putative Barrett's stem cell

Although our understanding of the biology of BM is increasing, fundamental questions still remain. Firstly, and probably most importantly is which cells in the normally squamous lined oesophagus give rise to the columnar BM tissue? Secondly, where do the stem cells lie in the metaplastic Barrett's mucosa?

### 1.7.1 Label Retaining Cells

It is clear that tumours are heterogeneous and it seems likely that a small percentage of tumour cells cause and propagate cancer. In this context experimental evidence has established that stem cells and cancer are linked because labelled carcinogens are retained most avidly by slow cycling label retaining cells (LRCs) (Jankowski and Wright, 1992).

As mentioned the GI epithelium is in a steady state of regeneration with most cells having a limited lifespan as they are constantly being renewed by cells dividing to form new cells, migrating to where they are needed, differentiating into the cell types required at a given place and then undergoing apoptosis and being lost into the lumen. Stem cells in the gut lining divide to replenish those cells being lost and have a unique biological property of being able to undergo an essentially infinite number of divisions and divide more slowly. This property allows them to replace cells as they mature and die, while maintaining the stem cell population. There remains uncertainty as to how this progression occurs and how the process differs in the normal to cancerous situation. In particular, whether one single basic cell undergoes differentiation into all the multiple cell lineages or whether different groups (clones) of cells progress to be different kinds of cells.

Stem cells have a high capacity for self renewal but in many tissues stem cells divide less frequently than TA cells (Wright, 2000). This slow cycling property would seem prudent as DNA synthesis can be error-prone and so stem cell division is most likely restricted. In 1975, Cairns proposed that when stem cells undergo a series of DNA replications and asymmetric cell divisions then at each division the same DNA template strands would always co-segregate to form the DNA complement of the new stem cell (Cairns, 1975). Therefore, following each cell division, the newly synthesised DNA strand is eliminated in the subsequent division. The 'immortal' DNA strands are passed down through the stem-cell generations, ensuring that newly replicated DNA strands are never retained in the stem-cell compartment for more than one generation (Smalley and Ashworth, 2003). This suggests that selective retention of the template DNA strand during stem cell division, provides a means of protection against DNA replication errors (Brittan and Wright, 2003).

### 1.7.2 Radioactive Markers

Radioactive markers can be used to identify LRCs by utilising two characteristics of stem cells, namely longevity and slow cycling times (Jankowski and Wright, 1992). Two techniques can be used to label slow cycling LRCs; continuous labelling over days or weeks

to target label in the residual stem cells or alternatively labelling for at least six hours and waiting for the faster cycling cells to dilute their label so that only the stem cells subsequently retain their label (Jankowski and Wright, 1992).

#### 1.7.2.1 Iododeoxyuridine (IUdR)

IUdR is an antiviral agent and also used as a radiosensitiser in radiation therapy. IUdR is a halogenated pyrimidine that can be incorporated into DNA in place of thymidine through DNA replication (Yan *et al.*, 2006). When given systematically IUdR is incorporated into the DNA of dividing cells and is rapidly metabolised in both rodents and humans, principally with cleavage of deoxyribose and subsequent dehalogenation by hepatic and extrahepatic metabolism. Studies have indicated that when it is given by bolus infusion its plasma half-life is less than 5 minutes (Kinsella, 1996). Figure 1.8 shows the plasma percentage and half life for IUdR. At 35 minutes post infusion, the percentage of IUdR in the plasma is less than 1% and is therefore unlikely to be labelling cells after this time.

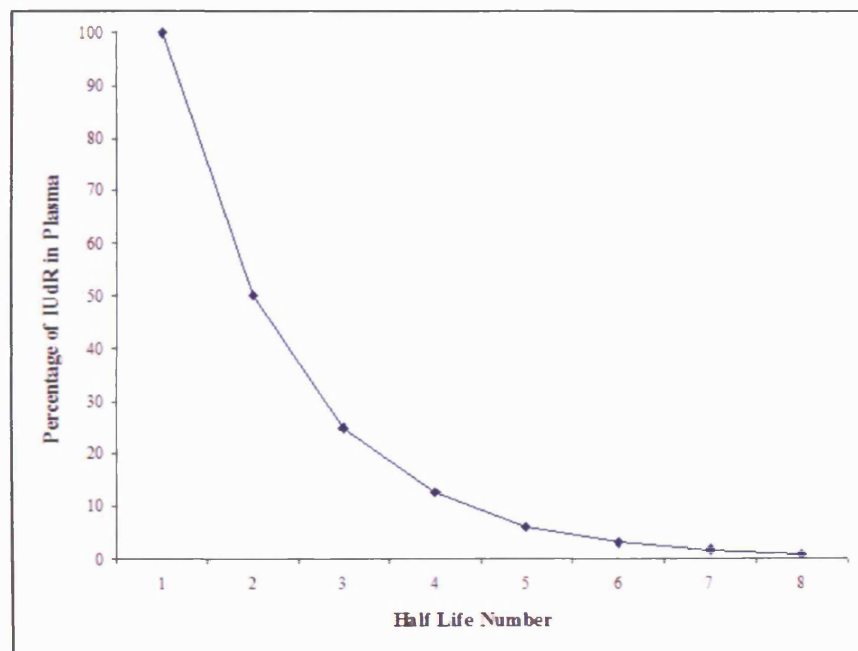


**Figure 1.8: Plasma percentage and half life number for IUdR.** Graph to show the decrease in percentage of IUdR with each half life cycle.

Most cells which incorporate IUdR will be lost into the oesophageal lumen following normal differentiation and regulation. Cells which retain IUdR 14 days post infusion indicate a prolonged lifespan and must be dividing more slowly. These cells are classified as a LRCs and it is our hypothesis is that these cells represent the Barrett's stem cell. LRCs are the only *in vivo* marker of stem cell biology and by identifying the exact site of the stem cells in BM it may be possible to compare gene expression in these cells with the stem cells of normal

squamous oesophageal mucosa. This may then allow for the identification of the cells of origin and aid the understanding of the molecular changes that occur in the initial transition from normal oesophageal mucosa to BM.

The drawback with this method is that not all LRCs are stem cells and may represent slowly cycling proliferative cells and mesenchymal or inflammatory cells. Also not all stem cells will be dividing at the time of the label and so definitive identification of the Barrett's stem cell is not possible. However, using this cell marker at different time points allows the progress of differentiation in normal tissue and tumour tissue to be followed. This has the potential to be an additional marker to predict tumour aggressiveness and patient survival and in this study it will be utilised to label the putative stem cells in the oesophageal compartment and Barrett's mucosa.

## 1.8 Model Systems

### 1.8.1 *Ex vivo* Models

Many transformed oesophageal cell lines have been reported but they are only temporary surrogate models of both native (squamous) and columnar (BM) tissue. These cell lines are far removed from the *in vivo* environment and may contain several mutations, which may detract from their reliability as models. Therefore, the establishment of non-transformed, or primary cell model systems, obtained from endoscopic biopsy samples, would be an invaluable resource. These models are extremely arduous to generate and possibly change phenotype when cultured *ex vivo*. However, recent advances in both the monolayer and tissue explant culture of alimentary mucosa have been reported throughout the alimentary tract and they have been successfully cultured in expanding populations for at least 4 weeks, throughout the GI tract (Jankowski and Wright, 1992).

The study of epidermal mucosa has been advanced greatly by the availability of non-transformed immortal cell lines. In the GI mucosa there are no similar cell lines available for the application of study to GI stem cells and perhaps this area in particular requires further investigation, although there are encouraging reports regarding culture of rat intestinal 'stem cells' *ex vivo* and subsequent generation of intestinal lineages in homografts (Campbell *et al.*, 1993; Evans *et al.*, 1992).

Much of the available information regarding GI stem cells is restricted to either *in vivo* or *ex vivo* animal models, or human *in vitro* models, and therefore the validity of the assumptions

made with regard to human stem cells *in vivo* is as yet unknown. The development of models with greater similarity to the normal human epithelia would greatly increase our knowledge and understanding of stem cell biology and in turn lead to clinical and therapeutic advancement.

### 1.8.2 Animal Models

With the limitations of *in vitro* experiments the use of animal models enables high throughput science excluding the 'noise' of human epidemiological studies and generating results over a relatively short period of time (Preston *et al.*, 2007).

Several animal models have been examined in order to investigate the potential for refluxed material to cause pre-malignant or malignant changes in the oesophagus. Unfortunately, at present, there are no suitable evasive animal models to simulate the conditions of BO, and those which have been reported all require simultaneous major surgical intervention with consequential changes in bacterial flora, physiology as well as tissue viability (Janusz Jankowski, personal communication).

Other carcinomas have established animal models of neoplastic progression, for example there are numerous animal models of colon cancer. However, in contrast to the oesophagus, the pathological and genetic processes underlying the transition from benign to malignant disease in the colon are well established (Fearon and Vogelstein, 1990; Vogelstein *et al.*, 1988). For this reason it has been possible to create animal models of the disease by disrupting critical genes. One example is targeted germline deletion of *Apc* exon 14 which leads to the formation of colonic tumours (Colnot *et al.*, 2004), but the *Min/+* mouse (*Apc<sup>+/+</sup>*) is probably the best known model, despite its tumour bulk arising in the small intestine (Preston *et al.*, 2007).

Various animal models have also been developed to clarify gastric carcinogenesis but it was not until the apparent mechanism of gastric cancer was clarified in recent years and the recognition of the pathogenicity of *H. pylori* that animal models could be developed to confirm the association between *H. pylori* and gastric cancer (Kodama *et al.*, 2005). Persistent *H. pylori* infection has recently been achieved in Japanese monkey and Mongolian gerbil models, with results demonstrating that the sequential histopathological changes in the gastric mucosa closely mimic the gastric mucosal changes caused by *H. pylori* infection in humans (Fujioka *et al.*, 2002; Kodama *et al.*, 2005; Tatematsu *et al.*, 2005).

Accepting the wide discrepancies between species in the development of cancers, particularly with regard to diet and xenobiotic substances, no animal model will ever be able to exactly replicate human disease (Preston *et al.*, 2007). Therefore it is important to ask if a suitable and practical animal model of BO is available and if so, which species would provide such a model?

#### 1.8.2.1 *Animal Models of BO*

Bremner *et al.*, (1970) documented the first animal model of BO in dogs and illustrated the causal role of acid reflux in the generation of an oesophageal columnar epithelium, but failed to demonstrate malignant progression. Others working with canines later established cancer formation took nearly 6 years when either cardiectomy or total gastrectomy was performed (Kawaura *et al.*, 2001).

Porcine models have also been proposed in the study of BO and one such study showed that healthy pigs had GOR levels in the distal oesophagus in amounts that are equivalent to pathological reflux in man. The significance of this level of reflux in the pig is uncertain and is probably physiologically normal for this animal as there was no endoscopic or histological evidence of oesophagitis (Kadiramanathan *et al.*, 1999). These findings may allow the porcine model of GOR to be useful in the study of BO, as surgical disruption is not required to induce reflux.

Chronic oesophagitis due to GOR is rarely reported in the cat (Han *et al.*, 2003) although feline models have also been explored as possible models of human GORD. The effects of myotomy or duration of acid exposure on feline models has been evaluated. Animals which had myotomy performed in the GOJ resulted in lowered oesophageal sphincter pressure and reflux oesophagitis similar to that seen in patients with chronic GORD (Poorkhalkali *et al.*, 2001). A similar outcome was seen with acid perfusion, which induced acute experimental oesophagitis and also decreased lowered oesophageal sphincter pressure (Geisinger *et al.*, 1990; Zhang *et al.*, 2005) although no disease pathology was observed.

Even rabbits have been examined with regard to the lack of appropriate animal models to investigate the mechanisms of mucosal damage and defence in reflux oesophagitis. Lanis *et al.*, (1999) showed that oesophageal mucosal lesions mimicking human reflux oesophagitis could be induced in rabbits with repetitive acid and pepsin exposure.

Rodents models are more practical on many levels, and like colorectal carcinoma, the first rodent models of BO involved the use of chemical carcinogens. Squamous cell carcinoma, adenocarcinoma, and mixed adenosquamous carcinoma are three cancers which have been induced in experimental animals (Su *et al.*, 2004). In the rat intraperitoneal injections of nitrosamines led to the formation of squamous cell carcinomas in 40-65% of the animals studied in a 6-12 week treatment schedule (Bulay and Mirvish, 1979). The addition of surgically induced duodeno-oesophageal reflux to this model increased the frequency and changed the histological type to OA, indicating that duodeno-oesophageal reflux plays a role in the development of OA (Attwood *et al.*, 1992). Others have reproduced OA formation on the background of glandular metaplasia in this way (Pera *et al.*, 1989), but some have only succeeded in squamous differentiation (Seto *et al.*, 1991).

Several surgical models without the addition of exogenous carcinogens have also been studied in the rodent. In these, successful methods of increasing the tumour number include the oxidative stress of intraperitoneal iron (Chen *et al.*, 1999; Goldstein *et al.*, 1998) and a high fat diet (Clark *et al.*, 1994).

In a rat surgical model of gastro-duodeno-oesophago reflux, anastomosing the distal oesophagus to the jejunum, 83% of animals developed cancers, with a predominance of adenocarcinomas occurring at the site of the anastomosis, surrounded by columnar epithelium (Miwa *et al.*, 1996). A similar number of cancers were found in the duodeno-oesophageal reflux, but notably, none were seen in the GOR group. Surgical experiments enabling bile and pancreatic juice to reflux in isolation, concluded that pancreatic juice was the more potent promoter of oesophageal squamous cancers (Yamashita *et al.*, 1998). Pera and colleagues (1993) reproduced this work, but significantly half their tumours were adenocarcinomas.

Oberg *et al.*, also examined the importance of reflux by creating several surgical models including: an oesophagoduodenostomy to induce gastroduodenal reflux; an oesophagoduodenostomy and a total gastrectomy for duodenal reflux; and also a Roux-en-Y reconstruction to exclude all reflux (Oberg *et al.*, 2000). Severe reflux oesophagitis was seen in all reflux-induced groups, without any direct evidence of BM, and although OA did develop, the tumours were sub-mucosal and the greatest number of tumours arose in the absence of any reflux. This indicates that there was no correlation with the human MDCS, and that these surgical models were a poor representation of human disease progression. Buskens *et al.*, (2006) completed a detailed histopathological study of oesophago-

gastrojejunostomised rats, and succeeded in causing long segment BO, suggestive of true metaplastic spread rather than mechanical spread. However, the model again failed to mimic human malignant progression, as the adenocarcinoma appeared to be a mechanical, post surgical phenomenon rather than a product of the MDCS. Other rat models appear to be more representative of the MDCS, with BO seen in Wistar rats 10 weeks after gastrectomy and duodeno-oesophageal reflux inducing surgery, and OA detected 10 weeks after that (Sato *et al.*, 2002). It is likely that strain differences are responsible for some of the discrepancies between results and should be considered when examining these data.

As discussed a variety of models have been proposed for studying GOR but it appears from this review of the literature that currently there is no satisfactory animal model of BO as those proposed and implemented all have certain drawbacks. Most existing models are post operative rodents, which lack the physiological levels of either bile or gastric acid constantly refluxing into the oesophagus, some requiring the addition of exogenous carcinogens, but none reliably mimicking what we currently know of the MDCS. In detailed histopathological studies of the MDCS, most have found similarities in the reflux-induced oesophageal metaplasia, but some of the resulting adenocarcinomas differed significantly between humans and the model systems, usually occurring along side squamous cell tumours or even lacking the appearance of disease pathology. Surgical models, in which the lower oesophageal sphincter is excised or incised, tend to disrupt the oesophageal sphincter anatomy in an unphysiological manner and pharmacological models can only be used in short term experiments.

Having said this, animal models still provide one of the best chances of elucidating the mechanisms involved in the transition from BO to OA, and in this sense other potential animal model systems need to be investigated. When looking for a suitable model perhaps it would be prudent to look for an animal, which closely mimics the human environment. In Figure 1.9 an evolutionary time line can be seen, which details the human relationship to many of the other animal models systems that have been discussed above and utilised in the study of BO. Our closest relation in the animal world is the primate, our primary concestor, one which we diverged from 5 to 7 million years ago, and therefore it would seem logical to assume that these would be the best models to use for study, as they may most accurately reflect the human setting. However, for emotive and practical reasons primates are rarely used as model systems to study BO, and as discussed, it is our tenth concestor, one which we diverged from 75 million years ago, the rodent, which appears to be the most widely utilised

model. There have also been reported cases of utilising our eleventh concestors, which we diverged from 85 million years ago, the dogs, cats and pigs. However, these studies have shown little practical use due to the amount of time needed for follow up, differences in disease progression and the ethical considerations of using such large and ambulant creatures.

Considering all of the above the field is desperate for a suitable and reliable animal model although, as has been seen in other carcinomas such as gastric and colon cancer, the suitable animal model could not be refined until the pathological and genetic processes underlying the transition from benign to malignant disease had been defined.

In this study we propose to use a new animal model system, the zebrafish. While the zebrafish is our 20 concestor, having diverged from humans 440 million years ago, their use may be more practical than it would seem at first glance. In Table 1.1 the comparative genetics are evaluated for the most regularly used BO model systems and we compare them to the proposed model system of the zebrafish. The cornerstone of animal models of BO has been surgically induced reflux in the rat, and while the rodent GI tract may accurately reflect the human GI tract in most other respects, it lacks the upper GOJ and the squamo-columnar junction (SCJ) is present between the forestomach and gastric body. Other animal models more accurately reflect human anatomy where a GOJ marks the differentiation between the squamous and columnar epithelium however these do not induce the same type of cancer as seen in humans, and those that do require the addition of carcinogens or major surgical intervention (Table 1.1).

Animal models, in particular rodents, have no doubt forwarded our scientific understanding of BO and the MDCS and will continue to unravel some of the complex host/environment interactions, but will in all likelihood never be able to provide all the answers. This is because without all the mutations in all the necessary genes the phenotype of the tumour may sometimes be similar to the human, but the underlying process will never be identical and may therefore not accurately reflect the human setting (Preston *et al.*, 2007). With this in mind it should be considered a possibility that novel models of BO have the potential to unravel the mysteries that the rodent model has thus far not been able to achieve. In this study the zebrafish will be examined as a potential successor.

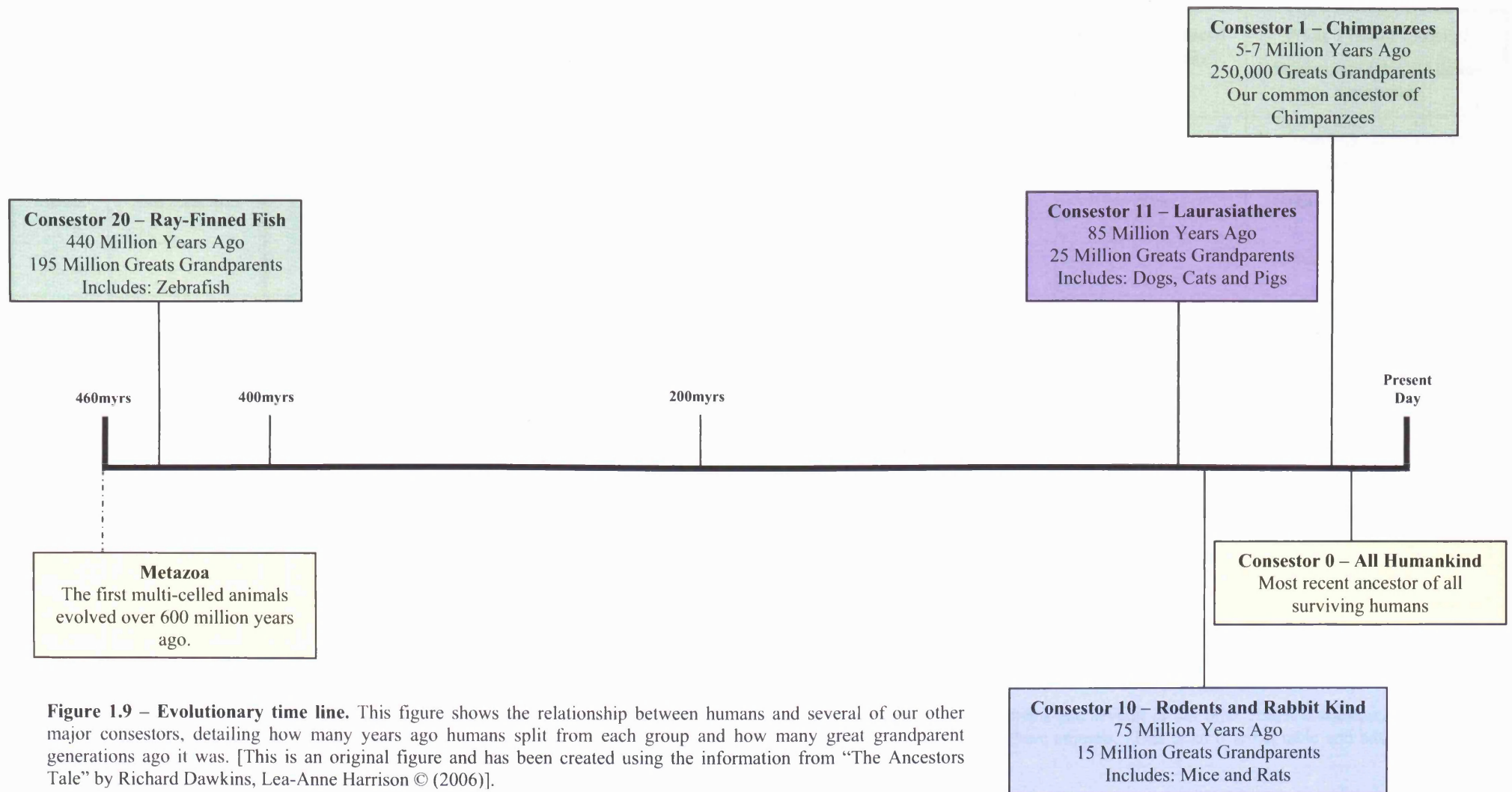


**Figure 1.9 – Evolutionary time line.** This figure shows the relationship between humans and several of our other major constors, detailing how many years ago humans split from each group and how many great grandparent generations ago it was. [This is an original figure and has been created using the information from “The Ancestors Tale” by Richard Dawkins, Lea-Anne Harrison © (2006)].

Common Name	Species	Diploid Chromosome Number	Number of Great Grandparents between Human and Species	Gastro-oesophageal Junction	Histopathology (Where squamous/mucin junction lies)	Cancer is Induced Physiologically?	What Type of Cancer? Squamous/Adeno/Adeno-squamous
Human	<i>Homo sapiens</i>	46	N/A	Yes	Squamous-columnar junction at gastric junction	Yes	Squamous carcinoma and Adenocarcinoma
Mouse	<i>Mus musculus</i>	40	15 million	Yes	Squamous-columnar junction at gastric junction	Yes	Squamous carcinoma with carcinogens Adenocarcinoma with severe reflux injury
Rat	<i>Ratus norvegicus</i>	42	15 million	No	Squamous-columnar junction between forestomach and gastric body	Oesophagus and in stomach under different conditions	Squamous carcinoma with carcinogens. Adenocarcinoma with severe reflux injury (involving duodenal juice)
Dog	<i>Canis familiaris</i>	78	25 million	Yes	Squamous-columnar junction at gastric junction	Has been induced in lower oesophagus	Adenocarcinoma is the only cancer induced (in published literature)
Cat	<i>Felis catus</i>	38	25 million	Yes	Squamous-columnar junction at gastric junction	No	N/A
Pig	<i>Sus scrofa</i>	38	25 million	Yes	Squamous-columnar junction at gastric junction	No	N/A
Zebrafish	<i>Danio rerio</i>	50	195 million	Yes	Squamous-columnar junction at gastric junction	Not known	Not known

**Table 1.1 – Comparative genetics of animal models of Barrett’s metaplasia.** This table shows the relationship between humans and several of our other major conspecifics, detailing the comparative genetic information, along with information regarding the histopathology and the pathogenesis of cancer within these animals. [This is an original table and has been created using the current literature, Lea-Anne Harrison © (2006)].

### 1.8.2.2 *The Zebrafish – A Novel Model of BO?*

Zebrafish (*Danio rerio*), are becoming an increasingly accepted organism for modelling human disease (Rubinstein, 2003). Their major advantage (and one of the reasons developmental biologists first began using zebrafish in the mid 90s) is that they are a vertebrate that closely resemble humans in a number of characteristics. Zebrafish embryos develop most of the major organ systems present in mammals, including the cardiovascular, nervous and digestive systems in less than one week (Rubinstein, 2006). Although at the macroscopic level their tiny size belies their phylogenetic closeness, at the tissue, molecular and genetic level the similarities are striking, with their genome size being similar to humans, and a high degree of homology between protein functional domains (Goldsmith and Solari, 2003).

Zebrafish lie close behind the rodents in terms of similarity making them a useful vertebrate model. Zebrafish are highly prolific, and a single pair of adults will breed weekly, generating 100-200 offspring with each mating. Development is rapid, with the basic body plan having been laid out within 24 hours and the fish being free swimming by 72 hours (Westerfield, 2000). Additional characteristics that makes them advantageous for scientific study is their small size, of between 3.7-4.1mm in length (Angeleen Fleming, personal communication), transparency, and ability to absorb compounds (Rubinstein, 2006). This model therefore offers the throughput of *in vivo* technology but with the relevance of a vertebrate.

Thus, zebrafish are ideally suited for use as an *in vivo* model for elucidating the complex mechanisms of intestinal epithelial development and describe paradigms that may be investigated in mammals; such as the role of caudal genes controlling intestinalisation in development as well as in diseases like BM and OA. Also, a BM zebrafish model would be well suited to high throughput compound screening for development of new drugs (Goldsmith and Solari, 2003).

## **1.9 Hypothesis and Aims**

The aim of this thesis is to test the hypothesis that stem cells and their progenitors express conserved gene families that are important in determining cell fate across species in health and disease. A number of key objectives will be investigated towards realising this aim:

- Firstly, potential molecular markers of the oesophageal stem cell compartment will be examined.
- Secondly, a review of the location of LRCs and their role as putative stem cells of the oesophageal epithelium and Barrett's mucosa will be examined using a human model system.
- Thirdly, environmental factors such as the role of bile acid stimulation in the induction of metaplastic change within the transitional zone epithelium will be studied. This will be looked at using the high throughput zebrafish model system.
- Finally, the role of aberrant P-cadherin expression in the GI tract will be investigated in order to explicate the normal and potential pathological roles of P-cadherin expression. This will be investigated using a P-cadherin knock-in transgenic mouse model.

## **Chapter 2: Materials and Methods**

## 2.1 Materials

All chemical reagents were ‘analar’ grade and purchased from Sigma, unless otherwise stated.

### 2.1.1 Tissue Samples

#### 2.1.1.1 *Human Tissue*

All tissue samples analysed were obtained from patients attending for routine upper GI endoscopy at the Leicester Royal Infirmary, University Hospitals NHS Trust. Patients were recruited with informed consent as part of “The analysis of tissues from oesophageal, gastric and small bowel epithelium” Trial. The study was approved by, the Leicestershire Local Research Ethics Committee (LREC) (Ethics reference number: 8500; LREC reference number: 6885). All diagnoses were confirmed by a consultant GI histopathologist. A summary of the human samples used along with primary characterisation details can be found in Table 2.1. Six cases of oesophageal adenocarcinoma were kindly provided for use in this investigation by Dr. M. Anderson. These were taken from patients with a sex ratio of roughly one third female to two thirds male, with an age range of between 55-75 years.

#### 2.1.1.2 *Mouse Tissue*

All mouse tissue samples analysed were obtained from Cancer Research UK, Clare Hall under the project licence of Dr. R.A. Goodlad (PPL 70/5134, 19b1). All experimental animals were from one of two initial founder lines, either 4044a or 4045a, and test crosses were set up to generate wild type, heterozygous and homozygous experimental animals. The animals were of various ages when culled and both male and female animals were used, however in each experiment animals were matched according to gender, age and weight.

#### 2.1.1.3 *Zebrafish Tissue*

All zebrafish tissue samples analysed were obtained from a collaborative project involving Daniolabs, Cambridge. Fish were reared under standard conditions (Westerfield, 2000), in a pH range of 6.8-7.2, although animals can tolerate a pH range of 5.0-8.0 with no noxious effect due to the fact that zebrafish are tolerant to standard chemical solvents, and readily absorb most chemicals and drugs. Embryos were collected from natural spawnings, staged according to established criteria (Kimmel *et al.*, 1995), and reared in embryo medium. All experimental animals were between 3 to 4 days post fertilisation (d.p.f.), when each experiment began and all animals were either of the Tuebingen Long Fin (TL) or London Wild Type (LWT) strain. All experiments were conducted on animals prior to the age of independent feeding and as such the work was unlicensed.

Case Number	Tissue Set Number	Tissue Type	Gender	Age
1	1	Normal Stomach	Male	65
2		Normal Squamous		
3		Oesophagitis		
4		Barrett's Metaplasia		
5	2	Normal Stomach	Male	51
6		Normal Squamous		
7		Oesophagitis		
8		Barrett's Metaplasia		
9	3	Normal Stomach	Male	47
10		Normal Squamous		
11		Oesophagitis		
12		Barrett's Metaplasia		
13	4	Normal Stomach	Female	75
14		Normal Squamous		
15		Oesophagitis		
16		Barrett's Metaplasia		
17	5	Normal Stomach	Female	59
18		Normal Squamous		
19		Oesophagitis	Male	41
20		Barrett's Metaplasia		
21	6	Normal Stomach	Male	76
22		Normal Squamous		
23		Barrett's Metaplasia	Male	42
24		Oesophagitis		

**Table 2.1 – A summary of the human samples used along with primary characterisation details. Both male and female patients were used with a mean age of 57 years.**

### 2.1.2 Clinical Trial Protocol

To assess the labelling properties of IUdR, fresh tissue samples were obtained by the author from patients with OA as part of the “STEMcell Assessment in Neoplastic Tissues” (SAINT) Clinical Trial. The study was approved by the LREC (Ethics reference number: 09122; LREC reference number: 7213).

Patients who were scheduled to undergo an oesophagectomy for treatment of OA or high grade dysplasia were approached pre-operatively. Informed consent was obtained after detailed information had been given to the patient. Consent was granted from the patients involved in this study in accordance with the ethical policies of the University Hospitals Leicester NHS Trust LREC. Pre-operatively patients attended the hospital as a day case patient to receive an intravenous infusion of IUdR which was performed by the trial research nurse. Prior to the infusion all patients were given a pre-clinical assessment by Professor Janusz Jankowski and vital signs were also recorded. After this time the research nurse then inserted a venflon into a vein on the patients arm and, after the appropriate dispensing check, an intravenous infusion of IUdR at a dose of 200mg per m<sup>2</sup> body surface area (max dose of 400mg) was given over a 30 minute period. IUdR was obtained from the Pharmacie du Chav in Lausanne, Switzerland, and imported to the UK in accordance with the EU Clinical Trials Directive.

During the infusion of IUdR the patient was monitored closely by a trained physician/research nurse. Following the infusion the vital signs were recorded and patients were monitored every 30 minutes for a further 3 hours. An example of this monitoring form can be found in Appendix 1, page 214. All procedures were performed at Leicester Royal Infirmary and after the final assessment patients were allowed to go home. At the time of resection tissue samples were collected and processed as detailed in section 2.2.1.2.

Thus far, 2 patients have been recruited to the trial and these can be identified as ST001 and ST002. Of these, matched pairs of biopsies were obtained from normal squamous oesophagus, gastric mucosa and OA tissue. Further tissue was obtained from BM for one patient only (ST002), which is most likely due to the fact in 30-70% of people with OA cancer the Barrett's area is overgrown by the tumour (Janusz Jankowski, personal communication). Prior to use of the tissue in immunohistochemistry (IHC) experiments, a 6µm section was cut and stained with Haematoxylin and Eosin (H&E) to ensure that the tissue preservation was sufficient to confirm diagnosis. Staining was graded according to location and frequency.

### 2.1.3 Cell Lines

Two GI cell lines were used as positive and negative controls for immunocytochemistry (ICC) (Table 2.2). The culture media for maintaining cell lines was as follows; OE-21 cells were cultured in Roswell Park Memorial Institute (RPMI) 1640 Medium with L-Glutamine

and TE-7 cells were cultured in Dulbecco's Modified Eagles Medium (DMEM) with Glutamax-1, pyridoxine and 4500mg/L glucose. All cells were maintained in their appropriate growth media, in a 5% CO<sub>2</sub> humidified atmosphere at 37°C. Cell lines were originally purchased from either the American Type of Culture Collection (ATCC), or the European Collection of Cell Cultures (ECACC).

Cell Line	Tissue of Origin	Morphology	Supplier
OE-21	A human oesophageal squamous cell carcinoma cell line, also known as JROECL21. It was established in 1993 from a squamous carcinoma of mid oesophagus of a 74 year-old male patient. The tumour was identified as pathological stage II and showed moderate differentiation (Rockett <i>et al.</i> , 1997).	Epithelial	ECACC
TE-7	A human oesophageal adenocarcinoma cell line (Nishihara <i>et al.</i> , 1993).	Epithelial	ATCC

**Table 2.2 - Cell lines used and their tissue of origin.**

#### 2.1.4 Primary Antibodies

The optimised concentrations at which primary antibodies were used for various applications are shown in Table 2.3.

Target Antigen	Manufacturer	Catalogue Number	Clone	Isotype	Positive Control	Negative Control	Experimental Species	Final Concentration/ Dilution Factor
<b>P-cadherin</b>	BD Transduction Laboratories	610227	56	Mouse IgG <sub>1</sub>	Normal Squamous	NPA Isotype Matched	Human/ Mouse	IHC/ICC: 2.5µg/ml IHC: 5µg/ml
<b>E-cadherin</b>	Abcam	Ab1416	HECD-1	Mouse IgG <sub>1</sub>	Normal Breast	NPA Isotype Matched	Human	IHC: 13.3µg/ml
<b>β1-integrin</b>	Cancer Research UK	β1-4B7	4B7R	Mouse IgG <sub>1</sub>	Normal Breast	NPA Isotype Matched	Human	IHC: 1:200
<b>β-catenin</b>	BD Transduction Laboratories	610153	14	Mouse IgG <sub>1</sub>	MCF-7 Cell Line	NPA Isotype Matched	Human	IHC: 0.5µg/ml
<b>Ki-67</b>	Novocastra Laboratories	NCL-Ki67	MM1	Mouse IgG <sub>1</sub>	Tonsil/ BrdU infused MCF-7 cyto block	NPA Isotype Matched	Human	IHC: 0.5µg/ml
<b>PCNA</b>	DakoCytomation	MO879	PC10	Mouse IgG <sub>2a</sub>	BrdU infused MCF-7 cyto block	NPA	Human	IHC: 0.8µg/ml
<b>BrdU</b>	DakoCytomation	MO744	Bu20a	Mouse IgG <sub>1</sub>	BrdU infused MCF-7 cyto block	NPA Isotype Matched	Human	IHC: 6.3/18.8µg/ml ICC: 6.3/18.8µg/ml
<b>β1-integrin</b>	Abcam	Ab8991	2B1	Mouse IgG <sub>1</sub>	N/A	NPA	Zebrafish	IHC: 1.25µg/ml
<b>β-catenin</b>	Abcam	Ab6302	Polyclonal	Rabbit IgG	N/A	NPA	Zebrafish	IHC: 10µg/ml
<b>Pan-cadherin</b>	Abcam	Ab16505	Polyclonal	Rabbit IgG	N/A	NPA	Zebrafish	IHC: 2µg/ml
<b>Zns5</b>	ZIRC, University of Oregon	N/A	2/1F4	Mouse IgG <sub>1</sub>	Zebrafish Brain	NPA	Zebrafish	IHC: 1:100
<b>P-cadherin</b>	Invitrogen	132000Z	PCD-1	Rat IgG <sub>2a</sub>	Mouse Placenta/Oesophagus	N/A	Mouse	IHC: 10µg/ml
<b>Phospho-Histone H3</b>	Upstate	06-570	Polyclonal	Rabbit IgG	Mouse Embryo	NPA	Mouse	IHC: 4µg/ml

**Table 2.3 - Primary antibodies used in this study.** (IHC = Immunohistochemistry; ICC = Immunocytochemistry; IgG = Immunoglobulin G).

### 2.1.5 General Reagents

#### 2.1.5.1 *Cell Culture: Buffers and reagents*

**Deoxycholic acid (DCA):** Sigma, D2510.

**Dimethylsulphoxide (DMSO):** Sigma, D5879.

**DMEM with Glutamax-1, pyridoxine and 4500mg/L glucose:** Invitrogen, Paisley, Renfrewshire (incorporating Gibco BRL).

**Embryo medium:** NaCl (5mM), KCl (0.17mM), CaCl<sub>2</sub> (0.33mM), Mg<sub>2</sub>SO<sub>4</sub> (0.33mM), 10-5% Methylene Blue, pH 7.2.

**Ethanol:** VWR, 20821.321.

**Foetal bovine serum (FBS):** Sigma, F7524. This was heat inactivated at 56°C for 30 minutes and stored at -20°C.

**Foetal calf serum (FCS):** Biowest.

**Insulin:** Invitrogen, Paisley, Renfrewshire (incorporating Gibco BRL).

**Isopentane:** BDH, 294526G.

**Medium 199 with Glutamax-1, Earles salts and NaHCO<sub>3</sub>:** Sigma, M4530.

**OCT Embedding Medium:** Raymond A Lamb, LAMB\OCT.

**Penicillin and streptomycin solution:** Invitrogen, Paisley, Renfrewshire (incorporating Gibco BRL).

**Phosphate buffered saline (PBS):** Invitrogen, Paisley, Renfrewshire (incorporating Gibco BRL).

**RPMI 1640 medium with L-Glutamine:** Cambrex Bio Science.

**Tricaine:** Sigma, A5040. Made up to a 4mg/ml concentration.

**Trypsin:** Invitrogen, Paisley, Renfrewshire (incorporating Gibco BRL).

**95% Oxygen cylinder:** BOC Gases, Guildford, Surrey.

#### 2.1.5.2 *IHC: Buffers and reagents*

**Ammonium Nickel sulphate:** BDH, 10029.

**Blocking solution:** Tris buffered saline (TBS) with 3% bovine serum albumin (BSA) (ICN Biomedicals: 160069) and 0.1% Triton X (Sigma: T8532).

**Citrate buffer:** Citric Acid (10mM sodium citrate, Fisher, C/6200/53), pH to 6.0.

**Dimethylformamide (DMF):** Fisher, D/384/08.

**3, 3'- Diaminobenzidine (DAB):** DAB (500µl, Sigma, D5637), TBS (9.5ml), H<sub>2</sub>O<sub>2</sub> (100µl, 3% (v/v)).

**3, 3'- Diaminobenzidine (DAB) Sigma Fast Tablet Sets:** DAB (0.7mg/ml), Urea hydrogen peroxide (0.2mg/ml), Tris buffer (0.06M) (Sigma, D9292).

**Di-sodium tetraborate (0.1M) pH 8.5:** BDH, 10267.

**Eosin:** Eosin Yellowish (14.4mM, DBH, 341973), Calcium chloride ( $5 \times 10^{-4}$  %), Formaldehyde ( $3.9 \times 10^{-2}$  %).

**Formalin 10%:** Formalin (40% formaldehyde) (100ml), dH<sub>2</sub>O (1L).

**Haematoxylin:** Haematoxylin (0.1% (w/v), BDH, 340 374T), Aluminium potassium sulphate (105.4mM, Fisher, A/2440/53), Citric acid (4.8mM, Fissons, C/6200), Chloral hydrate (302.2mM, Fisher, C/4280/53), Sodium iodate (0.93mM, DBH, 30171).

**Histoclear:** Fisher, H/0468/17.

**Hydrochloric acid:** Fisher, H/1200/PB15.

**Hydrogen peroxide (12%):** Fisher, H/1650/17.

**Industrial Methylated Spirits (IMS):** Genta Medical, I99050.

**Isotype control:** IgG<sub>1</sub> Negative Control (DAKO Cytomation, X0931).

**Mountant:** DPX mountant (VWR, 3 6029 414) and Aquamount (VWR, 362263H) as appropriate.

**Neutral buffered formalin (NBF) 10%:** Formalin (40% formaldehyde) (100ml), Sodium phosphate, monobasic, monohydrate (4g), Sodium phosphate, dibasic, anhydrous (6.5g), dH<sub>2</sub>O (1L).

**Normal serum:** Normal rabbit serum (DAKO Cytomation, X0902) and normal goat serum (DAKO Cytomation, X0907).

**Nova Red Substrate Kit:** Vector Labs, SK-4800.

**Proteinase K (PK):** Roche, 3-115-836.

**Red developer:** Fast-red TR salt hemi (zinc chloride) salt (Sigma: F2768), Naphthol AS-BI phosphate (Sigma: N2250), and Levamisole (Sigma: L9756).

**Secondary antibodies:** Biotinylated rabbit anti-mouse immunoglobulin (DAKO Cytomation, E0413) and goat anti-rabbit immunoglobulin (DAKO Cytomation, E0466).

**Tertiary detection:** Streptavidin binding complex conjugated with horseradish peroxidase (ABC-HRP), (DAKO Cytomation, K0377) and Streptavidin binding complex conjugated with alkaline phosphatase (ABC-AP) (DAKO Cytomation, K0391).

**TBS:** Tris (50mM, Roche, 708 976), Sodium chloride (300mM, Fisher, S/3160/63), pH 7.65.

**Toluidine blue:** 0.1% solution in 0.1% sodium borax.

**Vector M.O.M Basic Kit:** Vector Labs, BMK-2202.

**Veronal acetate buffer (VAB):** Sodium acetate (7.772g), Sodium barbitone (11.772g), NaCl (11.68g), dH<sub>2</sub>O (1800ml) and pH to 9.2 using HCl, then make up to 2L with dH<sub>2</sub>O.

**Xylene:** Fisher, X/0200/17.

### 2.1.5.3 Competent Cell Transformation and Plasmid Preparation

**Luria-Bertani medium (LB):** Bacto tryptone (10g), Bacto yeast extract (5g), NaCl (5g), then make up to 1L with dH<sub>2</sub>O.

**LB Agar:** For each 250ml of LB medium add 3.75g of Agar.

**RapidPURE™ Plasmid Mini Kit:** Q-BIOgene, 2066-400.

**Subcloning efficiency™ DH5α™ competent cells:** Invitrogen, 18265-017.

### 2.1.5.4 Sequencing

**Big Dye:** Version 3.1, PNACL.

**Centri-sep Columns:** Princeton Separations, CS-901.

**QIAquick Purification Kit:** Qiagen, 28104.

### 2.1.5.5 DNA Restriction

**BSA (100x):** Diluted down to a 10x stock.

**EcoRV:** New England Biolabs, R0195S.

**EcoRV Digestion Buffer (NEBuffer 3):** Tris-HCl (50mM), NaCl (100mM), MgCl<sub>2</sub> (10mM), dithiothreitol (1mM), pH 7.9.

**HindIII:** New England Biolabs, R0104S.

**HindIII Digestion Buffer (NEBuffer 2):** Tris-HCl (10mM), NaCl (50mM), MgCl<sub>2</sub> (10mM), dithiothreitol (1mM), pH 7.9.

**SacI:** New England Biolabs, R0156S.

**SacI Digestion Buffer (NEBuffer 1):** Bis Tris Propane-HCl (10mM), MgCl<sub>2</sub> (10mM), dithiothreitol (1mM), pH 7.0.

**SmaI:** New England Biolabs, R0141S.

**SmaI Digestion Buffer (NEBuffer 4):** Potassium acetate (50mM), Tris-acetate (20mM), magnesium acetate (10mM), DTT (1mM), pH 7.9.

### 2.1.5.6 DNA Extraction

**Tail lysis buffer:** (For 100ml) 5ml kcl (1M), 1ml Tris HCL (1M) pH 8.3, 0.25ml MgCl<sub>2</sub> (1M), 10ml 0.1% Gelatin. Add 82.85ml of distilled H<sub>2</sub>O, then autoclave. Leave to cool, add 0.45% (ml) NP40, 0.45% (ml) Tween 20. Add PK before use at a final concentration of 200µg/ml, or a 1/25 dilution.

**Proteinase K (PK):** Roche, 3-115-836.

### 2.1.5.7 RNA Extraction

**Chloroform:** Sigma, C2432.

**Glycogen:** Invitrogen, 10814-010.

**Isopropanol alcohol:** Fisher, P/7500/17.

**Tri Reagent:** Sigma, T9424.

### 2.1.5.8 Reverse Transcription

**Avian Myeloblastosis Virus (AMV) buffer:** Tris-HCl (250mM, pH 8.3), KCl (250mM), MgCl<sub>2</sub> (50mM), Dithiothreitol (50mM), Spermidine (2.5mM).

**AMV reverse transcriptase:** Promega, M5101.

**Deoxyneucleotide 5' triphosphate (dNTP) mix:** Roche, 1 969 064.

**Dynabeads® Oligo (dT)<sub>25</sub>:** Invitrogen, 610-50.

**Lysis buffer:** 1M Tris pH 8/DEPC: 10ml (100mM), LiCl: 2.12g (500mM), 0.5M EDTA pH 8/DEPC: 2ml (10mM), 10% sodium dodecyl sulphate (SDS): 10ml (1%), 1M DTT/DEPC: 500µl (5Mm) in a final volume of 100ml.

**RNasin:** Promega, N2115.

**Washing buffer:** 1M Tris pH 8/DEPC: 1ml (10mM), LiCl: 0.63g (0.15M), 0.5M EDTA/DEPC: 200µl (1mM), +/- 10% SDS: +/-1ml (0.1%) in a final volume of 100ml.

### 2.1.5.9 Polymerase Chain Reaction

**AJ buffer (10x):** Tris-HCl (45mM, pH 8.8), NH<sub>4</sub>SO<sub>4</sub> (11mM), MgCl<sub>2</sub> (4.5mM), dNTP (200µM each), Bovine serum albumin (110µg/ml), β-mercaptoethanol (6.7mM), EDTA (4.4µM, pH 8.0).

**Taq polymerase:** Invitrogen, 18038-042.

### 2.1.5.10 Agarose Gel Electrophoresis

**Bioline ladder:** Hyperladder I (Bioline Catalogue Number 33025).

**DNA ladder (100bp):** Invitrogen, 15628-050.

**Ethidium bromide:** Made up to 10mg/ml stock in UP-water (Sigma, E-1385).

**Polymerase chain reaction (PCR) loading buffer (5x):** Bromophenol blue (20mg), Xylene-cyanol Ff (20mg), dH<sub>2</sub>O (8ml), T.A.E (50x) (2ml), Glycerol (10ml).

**Sea kem:** Cambrex Bio Science, 50005.

**Tris acetate EDTA (TAE) buffer:** Tris (40mM), Glacial acetic acid (20mM), EDTA (0.1mM) pH 8.0.

### 2.1.6 PCR Primer sequences

All primers were designed using the Primer3 website ([http://frodo.wi.mit.edu/cgi-bin/primer3/primer3\\_www.cgi](http://frodo.wi.mit.edu/cgi-bin/primer3/primer3_www.cgi)) using sequences taken from the National Center for Biotechnology Information (NCBI) database (<http://www.ncbi.nlm.nih.gov/>), with the exception of the P-cadherin and glyseraldehyde-3-phosphate dehydrogenase (GAPDH) genotyping primers, which were developed by a previous student (Table 2.4, primer sets 1 and 2).

Primer Set	Gene Symbol	Forward Primer	Reverse Primer	Amplicon Size (bp)	Annealing Temperature (°C)	Cycles	Accession Number	Application
1	P-cadherin	CCCATTCTGATTTTGAT TTTTATCGTT	CTCGGAGACCACGCT GCGTAG	350	61	30	NM_001037 809	Genotyping Transformation
2	GAPDH	GGGTGGAGCCAAACGG GTC	GGAGTTGCTGTTGAA GTCGCA	550	64	30/35	BC_095932	Genotyping
3	Pcad-into-promoter	ATGAAGCCCGCTCGGT AG	-	-	50	35	-	Sequencing
4	Pcad-into-vector	AGGTGCTAGGGGAGTG GATT	-	-	50	35	-	Sequencing
5	Pcad-into-vector2	GGCCCTGGTACATTTCT CTG	-	-	50	35	-	Sequencing
6	FABP-Pcad	CTGTTGTGGTCAGGGG GAT	-	-	50	35	-	Sequencing
7	Native P-cadherin	TGGAGGTGGAAGGAAC TGAC	GGACGAATATTGGTG GCATC	207	60	35	NM_001037 809	RT-PCR
8	Transgene P-cadherin	GCAGACAGAGCTGTTG TGGT	GGACGAATATTGGTG GCATC	450	60	35	-	RT-PCR
9	L-FABP	CATCCAGAAAGGGAAG GACA	TTTTCCCCAGTCATGG TCTC	150	60	35	BC_009812	RT-PCR

**Table 2.4 - Mouse genotyping, sequencing and reverse transcriptase polymerase chain reaction (RT-PCR) primers.** This table provides information on all primers utilised in this study such as the gene symbol, sequence, amplicon size, annealing temperature, the PCR cycle number, the accession number and the application for which they were used.

## 2.2 Methods

### 2.2.1 Tissue Processing

#### 2.2.1.1 *Human Tissue*

Depending on availability, fresh tissue samples were subjected to analysis by a pathologist and subsequently verified as being; normal oesophagus, normal stomach, BM or oesophagitis. These were collected at time of endoscopy and immediately either; (i) fixed in 10% (v/v) NBF, processed through graded alcohols and embedded in paraffin wax following standard protocols, and/or (ii) placed into explant media for use in primary culture. Prior to use of the tissue, a 6µm section was cut and stained with H&E to ensure that the tissue morphology and histology were sufficient.

#### 2.2.1.2 *Clinical Trial Tissue*

Resection material was collected from theatre and transported to the Histopathology Unit at Leicester Royal Infirmary. Here a trained pathologist processed the specimen for both routine pathology and also obtained experimental specimen blocks for this clinical trial, an example of the tissue sample preparation can be seen in Appendix 1, page 214. These tissue samples were cut perpendicular to the mucosal surface. The samples were fixed in 10% formalin, processed through graded alcohols and embedded in paraffin wax following standard protocols. Histological sections were taken from the normal squamous oesophagus, normal gastric tissue, BM tissue, tumour (if present) and the GOJ. Serial tissue sections were cut at a thickness of 4µm and IHC studies undertaken.

#### 2.2.1.3 *Mouse Tissue*

Homozygous, heterozygous or wild type mice were generated and then sacrificed using a CO<sub>2</sub> chamber followed by a cervical dislocation. The entire GI tract was then dissected; including the stomach through to the rectum, trying to dissect away the excess fat and mesentery, and this was then placed in cold PBS and placed on ice. Whilst on ice, this was roughly divided into three sections of small intestine (up to the caecum) and one section of large bowel (after the caecum to the rectum). The sections were then cut and flushed with cold PBS to remove contents and debris.

The tissue was processed for fixation by threading each section onto a metal rod and a piece of blotting paper was placed into the base of the rod holder and the rods were then inserted into the slots in the holder in the correct order. The cover was placed onto the holder and using a sharp scalpel each section was cut down the entire length of the metal rods. The cover

was then removed and the blotting paper carefully lifted out and placed on a flat surface, ensuring that the rods stayed in place. Each rod was then gently rolled backwards and forwards to allow the gut to flatten and adhere to the blotting paper, ensuring that the villi were not damaged. The blotting paper was then gently lowered into 10% (v/v) NBF. At the same time the oesophagus was washed with PBS and the stomach, liver, and caecum bisected, washed with cold PBS and then all were also placed into the NBF along with the other sections and allowed to fix for a minimum of 6 hours at room temperature and a maximum of 48 hours at 4°C.

The tissue was washed once with PBS and transferred to 70% ethanol for less than a week at room temperature. The tissue sections were processed along with the bisected organ samples and were formalin fixed paraffin embedded (FFPE) following a standard protocol. As previously mentioned the intestines were divided into four sections; small bowel 1 (SB1) was the piece directly after the stomach and first 0.5cm of duodenum; small bowel 2 (SB2) was the next section and small bowel 3 (SB3) was the final section from the small intestine, ending at the caecum; large bowel 1 (LB1), the fourth and final section, was from the end of the caecum up to the anus. After fixation these sections were rolled up, using the method described by Moolenbeek and Ruitenberg (1981) processed and then embedded so that the tissue appeared as a circle on the cut surface.

The oesophagus was cut into two or three sections (depending on the length) and all pieces were embedded cut side down in one block. The bisected stomach, caecum and liver were washed with PBS and each half embedded (cut side down) into separate blocks (A and B). For each block that was sectioned (except the oesophagus there were 15 serial slides; slide 1, 8 and 15 were stained with H&E; with slides 2-7 and 9-14 being used for experimental work and each having two sections of oesophagus at the top of the slide and two sections of the relevant block in serial order, these being either SB1, SB2, SB3, LB1, stomach, caecum or liver.

If the tissue was being processed for snap freezing then the tissue was taken using a similar method although in this case after the samples were washed in cold PBS the oesophageal, SB1, SB2, SB3 or LB1 sample was placed into a universal, proximally to distally orientated, and then placed straight into liquid nitrogen. Again the stomach, liver, and caecum were all bisected, washed with cold PBS and then all were also placed into liquid nitrogen before long term storage at -80°C until experimental work was undertaken.

To assess proliferation and fission the tissue was processed in a different manor. Mice were injected with 1mg/kg vincristine (to arrest cells as they enter metaphase) and killed 2 hours later (Goodlad, 1994). The small bowel and colon were isolated, rinsed and weighed and fixed in Carnoy's fixative for 3 hours before being transferred to 70% ethanol.

Representative samples of tissue from the proximal, mid and distal small bowel and colon (taken from positions 10, 50 and 90% of the total length of the small bowel or colon) were hydrated, hydrolysed and stained with the Feulgen reaction. The mucosal crypts were gently teased apart under a dissection microscope and the numbers of mitoses per crypt (mean of 20 crypts) and crypt fission events per 200 crypts were then determined (Alferez and Goodlad, 2006). All samples were counted in a blinded fashion as detailed by Goodlad (1994).

#### 2.2.1.4 *Zebrafish Tissue*

Zebrafish that were 3-4d.p.f. were sacrificed using 4mg/ml of tricaine. The fish were then fixed in either NBF or 4% paraformaldehyde in PBS for several hours at room temperature or overnight at 4°C. Following 2 x 5 minute washes in PBS the samples were then dehydrated in increasing concentrations of ethanol (30%, 50%, 70%, 87%, 95%, 100%, 100%) for 30 minutes each, followed by a 30 minute wash in a 1:1 ethanol/histoclear mixture. The samples were then washed in histoclear for 30 minutes followed by a second histoclear wash in a 60°C oven. Half the volume of histoclear was then replaced with molten wax in a 1:1 final mixture for a 30 minute wash, followed by two 30 minute molten wax washes. The samples were then prepared for embedding by transferring a single sample at a time into plastic moulds, using a heated glass pipette, and orientating the samples accordingly while the wax cooled. Each well was then labelled with sample number and orientation of specimen and the wax was allowed to cool at room temperature for 12 hours. The wax blocks were removed from the moulds and stored upright at 4°C until the mounting and sectioning processes occurred.

To mount the wax block, containing the sample, each block was carefully removed from the plastic mould, (these were stored at +4 or -20°C for 30 minutes to loosen the blocks if required). Then using a razor blade the excess wax was trimmed from each of the four sides to make square. Some of this excess wax was then melted and poured onto the surface of a wooden block. The wax tissue block was then laid onto the melted wax and allowed to set, fixing the block to the wood. Each block was labelled accordingly with experiment number, treatment, sample number and orientation and they were then stored at room temperature or in the fridge until sectioning occurred.

The sectioning process that was employed for the zebrafish material differed slightly from a standard sectioning protocol. This was mainly due to the small size of the sample material and also because a special microtome attachment, for holding the wooden blocks, was needed. As such it is described here in detail. Firstly, a slide drying bench was set to between 30 and 33°C. A plastic backed piece of paper was cleaned with 70% ethanol and the microtome was also cleaned appropriately and it was ensured that the cutting handle was locked before screwing the tissue block into place on the block holder above the blade. The tissue block was aligned parallel to the cutting blade and excess wax was trimmed from the block with a razor blade to aid the ribboning process and to minimise the space between sections. The top and bottom edges were trimmed to make them smooth and parallel and the left hand edge was made perpendicular to the top and bottom, while the right hand edge was angled to allow for later orientation.

The tissue block was advanced towards the cutting blade and 10µm sections were cut to quickly section through the front of the block and to allow the ribboning of the sections to start. When the sample came into view, 7µm sections were then taken and the emerging ribbon was held with a small paint brush and forceps. Once the ribbon was of sufficient length, (ideally after the whole fish has been sectioned), the ribbon was carefully lifted and placed on the plastic backed sheet. The ribbon was then cut with a razor blade into equal lengths, of roughly 10 sections per length, however it was important that the length was shorter than the length of the coverslip once the ribbon had fully expanded.

A clean microscope slide was placed on the slide drying bench and labelled before a pool of deionised water was pipetted onto the slide surface. The strips of wax ribbon were then carefully placed on the surface of the water ensuring that no air bubbles were trapped underneath. Three lengths of sections were placed on each slide and these were laid from bottom to top and from right to left to ensure that orientation and order of sections was clear (Figure 2.1). The slides were left for approximately 30 minutes on the slide bench, ensuring that the water did not evaporate and to allow sufficient time for the tissue sections to fully expand. The water was carefully removed from each slide with a fine tip Pasteur pipette, ensuring that the strips stuck to the slide in the correct location and orientation. Each slide was left to dry overnight at 33°C and the quality of the sectioning was checked on a dissecting microscope before storing the slides at room temperature prior to IHC analysis.

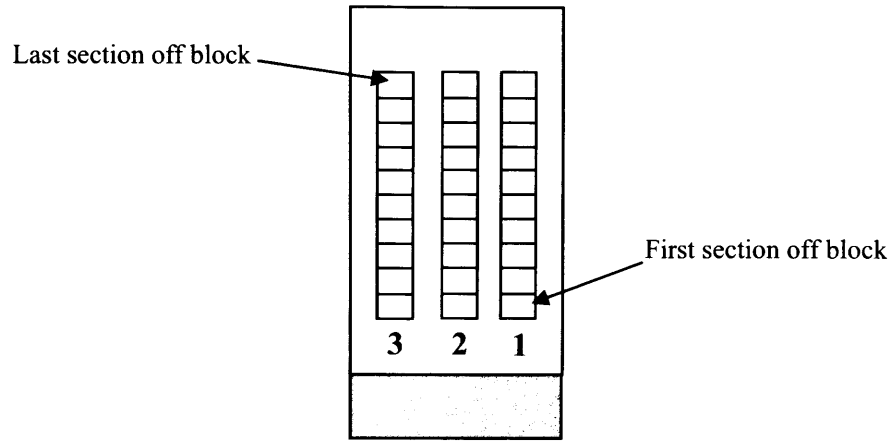


**Figure 2.1:** - Layout of zebrafish sections on slide. This image illustrates the method that was used to place serial zebrafish sections on slides before further analysis.

## 2.2.2 Cell Culture

### 2.2.2.1 *Routine Cell Culture*

All cell culture procedures were performed in a laminar flow tissue culture cabinet using an aseptic technique and cells were incubated in a Sanyo MCO 175 incubator at 37°C in a 5% CO<sub>2</sub> atmosphere. Cell lines were grown in DMEM with Glutamax-1, pyridoxine and 4500mg/L glucose supplemented with 10% (v/v) FCS, 50U/ml penicillin and 50µg/ml streptomycin (TE-7) or RPMI medium supplemented with FCS, penicillin and streptomycin at the same concentrations as in DMEM (OE-21). Cell lines were typically passaged at 80% confluence by aspirating the culture medium, washing in sterile PBS and incubating with 3ml of 0.05% (w/v) trypsin until cells had detached. 5ml of culture media was added and cells were disaggregated by trituration and then centrifuged at 1000rpm for 5 minutes. The cell pellet was either re-suspended in culture media and reseeded or was re-suspended in 1ml of 10% (v/v) DMSO in FCS and placed in a cryovial for cryopreservation. The freezing process was slowed by placing the cryovial in a -80°C freezer within a cryo freezing chamber (Nalgene) containing isopropanol. After 3 days the cryovials were transferred to liquid nitrogen for long term storage. Frozen cells were resurrected by rapid warming of the cryovial in a 37°C water bath and the cells were then washed and suspended in pre-warmed culture media. Cells were then seeded into tissue culture flasks and grown in the standard manner.

### 2.2.2.2 *Deoxycholic Acid Zebrafish Stimulation*

After an initial experiment to assess the toxicity of deoxycholic acid (DCA) to zebrafish 3 repeat experiments were set up with 6 animals in each treatment group under sterile conditions. Animals were 3-4d.p.f. on initiation of the experiment and the experiment ran for 4 days until animals were 7-8d.p.f. DCA was prepared and animals were exposed to either

0 $\mu$ M DCA, where embryo media acted as a control, or 10 $\mu$ M and 100 $\mu$ M of DCA in the treatment animals. The zebrafish were placed into an incubator at 37°C in a 5% CO<sub>2</sub> atmosphere for 4 days. Treatment solutions were replaced half way through each experiment and daily health scores were recorded. The animals were sacrificed, fixed in NBF and processed for embedding and sectioning according to the methods previously discussed in section 2.2.1.4.

#### 2.2.2.3 *IUdR Reconstitution*

Each sterile vial contained 200mg of dry white powder cake. This was reconstituted with sterile water for injection to pH 10.4 (osmolarity of 100 mosmol/Kg) and used within 8 hours.

All IUdR reconstitution for use in the clinical trial subjects was performed by the pharmacy at Leicester Royal Infirmary Hospital. This was all in accordance with LREC guidelines and was performed under aseptic techniques. Each 200mg vial was reconstituted with 10ml of water and the resultant solution was then added to 250ml of 0.9% sodium chloride to generate the infusion solution. This was infused at a dose of 200mg per m<sup>2</sup> body surface with a maximum dose of 400mg per individual patient. Each patient had the correct drug dosage calculated to ensure that the maximum dose was not reached; an example of the drug dosage chart can be seen in Appendix 1, page 212.

‘SAINT’ clinical trial patients were infused with no more than 400mg of the IUdR per subject. To recreate these conditions in the cell lines it was ensured that this dose was not exceeded relative to the size of the tissue. The IUdR was reconstituted with 10ml of sterile water in aseptic conditions to make up a working concentration of 200mg/ml. 1ml of this solution was added to 24ml of sterile PBS to give a 0.8mg/ml working concentration. 1ml of this 0.8mg/ml was taken and added to 20ml of each RPMI, DMEM and Medium-199 supplemented media to make up a working concentration of 40 $\mu$ g/ml.

#### 2.2.2.4 *In Vitro Culture of TE-7 and OE-21 cell lines*

Cell lines derived from oesophageal squamous carcinoma (OE-21), or OAs (TE-7) were maintained as previously described in section 2.2.2.1. On reaching 70-80% confluence, cell lines were stimulated with growth media containing 40 $\mu$ g/ml of IUdR. Cells grown in normal growth media were used as controls. Cells were stimulated continuously over a 24-hour time period. A concentration of 40 $\mu$ g/ml was used, as this was equivalent to the *in vivo* dose used

in the 'SAINT' Clinical Trial setting. The 24 hour time was chosen, as this time interval was considered sufficient to allow optimal diffusion of the IUdR.

#### 2.2.2.5 Preparation of TE-7 and OE-21 cell lines

The 'Shandon Cytoblock Cell Block Preparation System' was used and each flask was removed from the incubator after the 24 hour diffusion time and cells removed by trypsinisation. The cells were centrifuged for 5 minutes at 1000rpm, and the media discarded before the pellets were fixed in 15ml of 10% formalin for approximately 1 hour. Cytoblocks were made up for each cell line according to the manufacture's instructions. The assembled Cytoclip was then placed into the Cytospin Sealed Head and the mixed cell suspension added to each Cytofunnel. The Cytospin was centrifuged for 5 minutes at 1500rpm. The Cytofunnel assemblies were removed, following the manufacture's instructions, and fixed in 10% formalin before processing occurred. The following day the cell button was dislodged from the base mould and embedded into a paraffin block. These samples were then stored before being sectioned using a microtome to a thickness of 6µm and used for ICC work.

### 2.2.3 Primary Explants

#### 2.2.3.1 Ex Vivo Culture of Barrett's Mucosal Biopsies

*Ex vivo* tissue culture was performed according to previously published methods (Haigh *et al.* 2003). In brief, fresh biopsy tissue of BM and matched squamous and gastric mucosa were obtained during routine endoscopy and immediately placed into ice cold Medium-199 with Glutamax-1, Earles salts and NaHCO<sub>3</sub>, supplemented with 10% FCS, 50U/ml penicillin, 50µg/ml streptomycin, and 500U/ml insulin for explant cell culture. Samples were made anonymous according to good clinical research practice guidelines and were collected after approval from Leicestershire National Health Service Ethical Committee guidelines.

Biopsy specimens were washed in fresh media and bisected, each half acting as an internal control. Halved biopsy specimens were divided into 2 groups and each group stimulated with growth media containing 40µg/ml of IUdR, which was reconstituted according to methods previously stated (section 2.2.2.3), or normal growth media without IUdR, to act as a control. The biopsy tissues were placed onto a sterile aluminium mesh grid, in a 6 well plate with 1ml of media. This was placed into a sealable hypoxic chamber, which was flushed with 100% O<sub>2</sub>, to provide a high oxygen environment. The gas ports were closed and the chamber incubated for 24 hours at 37°C.

### 2.2.3.2 *Preparation of Primary Explant Mucosal Biopsies*

Once the 24 hours had elapsed the samples were taken from the incubator and removed from the hypoxic chamber. The samples were then prepared for cryostat sectioning using the following method. 25ml of isopentene was placed into a beaker, which was placed inside a small amount of liquid nitrogen, ensuring that the beaker would remain upright, but also so that the liquid nitrogen was covering a substantial portion of the beaker. Each biopsy was added to a small piece of cork using some OCT embedding medium and placed into the isopentene until the OCT embedding medium had turned completely white and the biopsy was attached to the cork. Each sample was placed inside a fully labelled cryotube and then placed into liquid nitrogen. This was repeated for each sample. These samples were then stored in the tissue bank until they were ready for cryostat sectioning and IHC work.

## 2.2.4 Immunostaining of Human Tissue Sections

### 2.2.4.1 *Dewaxing and Rehydrating*

Tissue was fixed in 10% (v/v) NBF prior to embedding in paraffin, sections were cut at a thickness of 6-7 $\mu$ m and these were mounted onto vectabond coated slides and air dried overnight at 37°C to prevent tissue loss during antigen retrieval. The slides were placed into a 60°C incubator for 10 minutes to allow the wax to melt. Sections were de-waxed in xylene for 6 minutes and then rehydrated by equilibrating the sections in decreasing concentrations of IMS (99%, 99%, 95%) for 1 minute each, followed by a 5 minute equilibration in running tap water.

### 2.2.4.2 *Haematoxylin and Eosin Staining of FFPE Sections*

Following dewaxing and rehydration the sections were stained in haematoxylin for 5 minutes, after which they were washed in running tap water for 2-5 minutes. The sections were then immersed in eosin for 1 minute, and afterwards rinsed in tap water. The sections were then dehydrated through increasing concentrations of IMS, and cleared in xylene before being mounted using DPX mountant with an appropriately sized cover slip. All tissues were analysed on a Leitz Laborlux 12 light microscope prior to experimental work being carried out.

### 2.2.4.3 *Microwave antigen retrieval*

Dewaxed and rehydrated slides (section 2.2.4.1) were submerged in citrate buffer and heated on full power (750W) for 20 minutes. The sections were then left to stand in the buffer and allowed to cool at room temperature for 45 minutes.

#### 2.2.4.4 *Proteinase K digestion antigen retrieval*

Following dewaxing and rehydration (section 2.2.4.1) a 10µg/ml solution of PK was made up by adding 10µl of the stock 1mg/ml PK solution to 990µl of 0.05M Tris, and mixed using a vortex. The PK was pipetted onto slides in a humidity chamber and after adding a cover slip (to minimize evaporation) they were incubated at 37°C for 1 hour. Following this enzymatic antigen retrieval, the coverslips were removed and each slide was rinsed with running tap water and equilibrated in TBS for 5 minutes.

#### 2.2.4.5 *Pressure cooking antigen retrieval*

Following dewaxing and rehydration (section 2.2.4.1) the citrate buffer was prepared by mixing 75ml of 20x citrate buffer in 1.5L of UP water. This was placed into a pressure cooker (Prestige, 6189), and left to boil. Once boiling the sections were fully submerged and the lid was secured. The slides were left to boil in citrate buffer ( $\approx 126^\circ\text{C}$ ) for 2 minutes at full pressure and the slides then removed and quickly cooled by equilibrating them in running tap water.

#### 2.2.4.6 *Non-specific antigen and hydrogen peroxidase blocking*

Following antigen retrieval, slides were immersed in either 2 or 10% hydrogen peroxide for 10 minutes if a HRP based detection method was employed. This was to block any endogenous peroxidase activity in the tissue, which could later interfere with staining. Slides were washed in TBS for 2 x 5 minutes before incubation for 20 minutes with 100µl of normal rabbit serum (1:5 dilution with blocking solution).

#### 2.2.4.7 *Streptavidin-Biotin-Horseradish Peroxidase Detection (ABC-HRP)*

This system was used in the detection of the following antibodies – E-cadherin,  $\beta$ -catenin, Ki-67, PCNA and Bromodeoxyuridine (BrdU). After each step the sections were washed in TBS for 2 x 5 minutes in order to wash any unbound reagent from the previous step from the tissue.

After primary antibody incubation, (overnight at 4°C), sections were washed and incubated for 30 minutes at room temperature with a biotinylated rabbit anti mouse secondary antibody. The slides were then washed again in TBS (2 x 5 minutes) and the ABC-HRP complex applied. This is a kit reagent, and was prepared by mixing 9µl of reagent A (streptavidin) with 9µl of reagent B (biotinylated peroxidase) in 982µl of blocking solution to give a 1:100 dilution or by mixing 1µl of reagent A (streptavidin) with 1µl of reagent B (biotinylated

peroxidase) in 1ml of blocking solution to give a 1:1000 dilution. The 1:100 dilution was used for all microwave antigen retrievals and the 1:1000 for all pressure cooker antigen retrievals. This was prepared 30 minutes prior to use, to allow the complex to form, and the slides were then incubated in 100 $\mu$ l of the solution for 30 minutes at room temperature.

After this incubation, the slides were washed for 2 x 5 minutes in TBS and developed using DAB. This was either prepared with 500 $\mu$ l of liquid DAB, 9.5ml of TBS and 100 $\mu$ l of 3% hydrogen peroxidase or by using the DAB Sigma Fast Tablet Sets, where one urea tablet was dissolved in 5ml of dH<sub>2</sub>O and then the DAB tablet added and also dissolved. Each was mixed by vortexing prior to the addition of 100 $\mu$ l to each slide for an incubation of 10 minutes at room temperature. The slides were washed in tap water for 5 minutes and counterstained in haematoxylin for 15 seconds.

#### 2.2.4.8 *Streptavidin-Biotin- Alkaline Phosphatase Detection (ABC-AP)*

This system was used in detection of the following antibodies – P-cadherin and  $\beta$ 1-integrin. After each step the sections were washed in TBS for 2 x 5 minutes in order to wash any unbound reagent from the previous step off the tissue.

After primary antibody incubation, (overnight at 4°C), sections were washed and incubated for 30 minutes at room temperature with the appropriate biotinylated rabbit anti-mouse secondary antibody. The slides were then washed again in TBS (2 x 5 minutes) and the ABC-AP complex was applied as described previously in section 2.2.4.7.

After this incubation, the slides were washed for 2 x 5 minutes in TBS and then rinsed in UP-water twice before being washed in VAB for 5 minutes. To prepare the Red Developer 25mg of Fast Red TR salt was added to 50ml of VAB and mixed well. To this 12mg of Levamisole was added and mixed well. Finally, 25mg of Naphthol ASBI phosphate dissolved in 250 $\mu$ l of dimethylformamide was added. The solution was filtered into a Coplin jar and the slides were immersed for 1 hour before being washed in tap water for 5 minutes and counterstained in haematoxylin for 15 seconds.

#### 2.2.4.9 *IHC for Bromodeoxyuridine (BrdU)*

For this antibody both explant and FFPE sections were used and each needed a different method to initiate the immunological process. As previously described in section 2.2.4.1, the FFPE sections were de-waxed, rehydrated, and equilibrated in running tap water. The explant

slides were brought to room temperature for 10 minutes and then fixed in 70% ethanol for 20 minutes. All slides were then washed in tap water and incubated in 2 molar HCl acid for 30 minutes at room temperature; this was to make the DNA single stranded in order that the antibody could bind. The slides were washed in UP-water for 2 x 5 minutes before being washed in 0.1% sodium tetraborate (pH 8.5) for 2 x 5 minutes, which was used to neutralise the HCl step so that the antibody was not destroyed when applied. Following this, each section was washed in TBS for 2 x 5 minutes and then incubated in normal rabbit serum (1:5 diluted in blocking solution) for 10-30 minutes at room temperature to block non-specific binding. The negative controls were left in rabbit serum, whereas the test slides had primary antibody applied and were incubated for 2 hours at room temperature. The subsequent detection was performed using the ABC-HRP detection kit as detailed in section 2.2.4.7.

#### *2.2.4.10 Double Staining*

This technique was used to detect LRCs and proliferating cells in the same specimen. The method used the ABC-HRP detection system with two different chromogens. Essentially the steps involved were the same as in any other ABC-HRP detection, except that they were repeated twice. As previously described in section 2.2.4.1, the sections were de-waxed, rehydrated, and equilibrated in running tap water. Antigen retrieval was achieved by microwaving the sections in citrate buffer (section 2.2.4.3), and then after a TBS wash for 5 minutes the endogenous peroxidase activity in the tissue was blocked in 10% hydrogen peroxidase for 10 minutes, (section 2.2.4.6).

Sections were washed in TBS for 2 x 5 minutes before blocking non-specific binding by incubating the sections in normal rabbit serum for 10 minutes at room temperature. The negative controls were left in rabbit serum (1:5 dilution in blocking solution) while the test slides had the BrdU primary antibody applied and were incubated overnight at 4°C.

After this incubation, the slides were washed for 2 x 5 minutes in TBS and the secondary biotinylated rabbit anti-mouse antibody was applied (1:400 diluted in blocking solution) for 30 minutes at room temperature. After the 30 minute incubation the secondary antibody was washed off with TBS (2 x 5 minutes) and the tertiary ABC-HRP was applied for 30 minutes at room temperature. The slides were then washed for 2 x 5 minutes in TBS and the subsequent detection was performed with DAB enhanced nickel for 15 minutes, which blocks any active peroxidase sites from the first ABC-HRP complex.

The DAB enhanced nickel was prepared by dissolving 30mg of ammonium nickel sulphate into 10ml of 0.2M Tris solution, pH 7.6, using a vortex. 9.5ml of this solution was added to 500µl of liquid DAB and 70µl of 3% hydrogen peroxidase, which was filtered and applied to the slides for an incubation of 15 minutes at room temperature. After washing for 2 x 5 minutes in TBS the second set of primary antibodies, Ki-67 or PCNA, were applied for 1 hour at room temperature.

Sections were rinsed in tap water and washed in TBS for 2 x 5 minutes and the secondary biotinylated rabbit anti-mouse antibody applied (1:400 diluted in BS) for 30 minutes at room temperature. After the 30 minute incubation the secondary antibody was washed off with TBS (2 x 5 minutes) and the tertiary ABC-HRP applied for 30 minutes at room temperature. After this incubation, the slides were washed for 2 x 5 minutes in TBS and the ABC-HRP complex incubated with nova red.

Nova red is kit reagent and was prepared by adding three drops of reagent 1 to 5ml of distilled water (dH<sub>2</sub>O). Two drops of reagent 2 were added and the solution vortexed before adding 2 drops of reagent 3, which was followed by a second vortex. Finally 2 drops of hydrogen peroxidase solution (kit supplied) were added and the solution was mixed and filtered before adding to the slides for an incubation of 15 minutes at room temperature. The slides were washed in water and a light counterstain of Fast Red applied for 1 minute before sections were washed in running tap water until clear.

#### *2.2.4.11 Dehydrating and Mounting*

Once counterstaining had occurred, and the sections had been washed in tap water until clear, mounting could occur. For the ABC-HRP detection method the sections were dehydrated and cleared by passing the slide rack through a series of staining dishes containing increasing concentrations of IMS. Firstly, they were placed in 95% IMS for 15 seconds and then into 2 separate dishes of 99% IMS for 1 minute each. The slides were placed in xylene for 3 minutes prior to mounting and mounted by placing DPX mountant onto each coverslip and lowering the slide onto coverslip, allowing the DPX to spread out. Air bubbles were removed by applying gentle pressure. The slides were left to dry before putting them away.

If the ABC-AP detection method was employed then sections were taken straight from the water after the counterstaining step and mounted by placing Aquamount onto each coverslip and lowering the slide onto coverslip, allowing the Aquamount to spread out. Any air bubbles

were removed by applying gentle pressure and the slides were left to dry before putting them away.

Antibody	Antigen Retrieval	Endogenous Peroxidase Block	Non-Specific Block	Secondary Antibody	Tertiary	Chromogen
<b>P-cadherin</b> Clone 56	Microwave	N/A	NRS	Bt R $\alpha$ M	ABC-AP: 1:100	Fast Red
<b>E-cadherin</b> Clone HECD-1	Pressure Cooker	2% H <sub>2</sub> O <sub>2</sub>	NRS	Bt R $\alpha$ M	ABC-HRP: 1:1000	DAB
<b><math>\beta</math>1-integrin</b> Clone $\beta$ 1-4B7	Proteinase K	N/A	NRS	Bt R $\alpha$ M	ABC-AP: 1:100	Fast Red
<b><math>\beta</math>-catenin</b> Clone 14	Pressure Cooker	2% H <sub>2</sub> O <sub>2</sub>	NRS	Bt R $\alpha$ M	ABC-HRP: 1:1000	DAB
<b>Ki-67</b> Clone NCL-Ki67	Pressure Cooker	2% H <sub>2</sub> O <sub>2</sub>	NRS	Bt R $\alpha$ M	ABC-HRP: 1:1000	Nova red
<b>PCNA</b> Clone PC10	Microwave	10% H <sub>2</sub> O <sub>2</sub>	NRS	Bt R $\alpha$ M	ABC-HRP: 1:100	Nova red
<b>BrdU</b> Clone Bu20a	Microwave	10% H <sub>2</sub> O <sub>2</sub>	NRS	Bt R $\alpha$ M	ABC-HRP: 1:100	DAB/DAB Enhanced Nickel

**Table 2.5 – Antibody details and conditions for IHC.** This table details all antibodies and the methods utilised in the immunostaining of human tissue sections.

#### 2.2.4.12 Human IHC Tissue Controls

Negative controls were included in every case, where the primary antibody was replaced with 100 $\mu$ l of blocking solution. An IgG<sub>1</sub> primary antibody, (DakoCytomation), was used as an isotype-matched control for all mouse IgG<sub>1</sub> antibodies on tissue sections. Positive tissue controls were also employed and were either tissue positive controls, known to show expression of the particular antibody or were experimental control cytocontrols created for use as a positive control (Table 2.3).

#### 2.2.4.13 Evaluation of Immunostained Sections

The immunostained material was scored by two independent observers – Lea-Anne Harrison and Janusz Jankowski, (who examined a subset of cases). These results were compared and are described in Chapter 3. In brief the staining intensity was scored on a scale of 1 to 5 (1 = absent, 5 = very strong). Where the staining was focal the strongest area of expression was used for scoring intensity and the site specificity of the staining noted e.g. in different mucosal compartments – superficial, mid or basal, and for different types staining such as cellular, membranous or nuclear.

## 2.2.5 Immunostaining of Mouse Tissue Sections

### 2.2.5.1 *Mouse IHC for P-cadherin, Clone 56*

As previously described in section 2.2.4.1, the sections were de-waxed, rehydrated, and equilibrated in running tap water. Slides were prepared for the antigen retrieval which was achieved by pressure cooking as described in section 2.2.4.5. Endogenous peroxidase activity was eliminated by immersing the slides into 3% hydrogen peroxidase for 5 minutes.

After this incubation, the slides were washed for 2 x 5 minutes in TBS. The Vector Labs mouse on mouse (M.O.M) kit was used, following the manufacturer's instructions. The sections were incubated in M.O.M Mouse Ig Blocking Reagent at room temperature for 1 hour. Sections were washed in TBS for 2 x 5 minutes and the M.O.M diluent added for 5 minutes at room temperature. The negative controls were left in M.O.M diluent, whereas the test slides had primary antibody applied and were incubated overnight at 4°C.

Following this incubation the sections were washed in TBS 2 x 2 minutes and incubated in M.O.M biotinylated anti-mouse IgG reagent (kit supplied) for 10 minutes at room temperature. The slides were washed for 2 x 2 minutes in TBS and the tertiary Vectastain ABC reagent (kit supplied), prepared 30 minutes in advance, was applied for 5 minutes. After 2 x 2 minutes washes in TBS the slides were developed using DAB. This was prepared using the DAB Sigma Fast Tablet Sets where one urea tablet was dissolved in 5ml of dH<sub>2</sub>O and then the DAB tablet added and also dissolved. Each was mixed by vortexing prior to the addition of 100µl to each slide for an incubation of 10 minutes at room temperature. Slides were washed in tap water for 5 minutes and counterstained in haematoxylin for 15 seconds. The slides were then be dehydrated and mounted as detailed in section 2.2.4.11.

### 2.2.5.2 *Mouse IHC for P-cadherin, Clone PCD-1*

As previously described in section 2.2.4.1, the sections were de-waxed, rehydrated, and equilibrated in running tap water. Slides were prepared for the antigen retrieval which was achieved by pressure cooking as described in section 2.2.4.5. Endogenous peroxidase activity was eliminated by immersing the slides into 3% hydrogen peroxidase for 5 minutes. After this incubation, the slides were washed for 5 minutes in TBS and incubated in normal rabbit serum (1:5 dilution in blocking solution) for 10 minutes at room temperature. The negative controls were left in rabbit serum, whereas the experimental slides had primary antibody applied and were incubated overnight at 4°C.

After this incubation, the slides were washed for 2 x 5 minutes in TBS. The sections were incubated in a biotinylated rabbit anti-mouse antibody (1:400 diluted in BS) for 30 minutes at room temperature. The slides were washed for 2 x 5 minutes in TBS and the ABC-HRP complex applied. This is a kit reagent and was prepared by mixing 2µl of reagent A (streptavidin) with 2µl of reagent B (biotinylated peroxidase) in 2ml of blocking solution to give a 1:1000 dilution. This was prepared 30 minutes prior to use, to allow the complex to form, and the slides then incubated in 100µl for 30 minutes at room temperature.

After this incubation, the slides were washed for 2 x 5 minutes in TBS and then developed using DAB. This was prepared using the DAB Sigma Fast Tablet Sets where one urea tablet was dissolved in 5ml of dH<sub>2</sub>O and the DAB tablet added and also dissolved. Each was mixed by vortexing prior to the addition of 100µl to each slide for an incubation of 10 minutes at room temperature. Slides were washed in tap water for 5 minutes and counterstained in haematoxylin for 15 seconds. The slides could then be dehydrated and mounted as detailed in section 2.2.4.11.

### 2.2.5.3 IHC for Phospho-Histone (H3)

As previously described in section 2.2.4.1, the sections were de-waxed, rehydrated, and equilibrated in running tap water. Slides were then rinsed in PBS for 2 x 3 minutes before the antigen retrieval was achieved by microwaving the sections as described in section 2.2.4.3. The sections were washed in PBS for 5 minutes before blocking endogenous peroxidase activity by immersing the slides into 1.6% (v/v) hydrogen peroxide for 10 minutes. After washing in running water for 5 minutes, and rinsing the slides in PBS, the slides were incubated in normal goat serum (1:10 diluted in 1% BSA/PBS) for 30 minutes at room temperature. The negative controls were left in goat serum, whereas the experimental slides had primary antibody applied and were incubated for 1 hour at room temperature.

After this incubation, the slides were washed for 2 x 5 minutes in PBS. The sections were incubated in a biotinylated goat anti-rabbit antibody (1:300 diluted in BS) for 30 minutes at room temperature. The slides were washed for 2 x 5 minutes in PBS and the ABC-HRP complex was applied. This is a kit reagent and was prepared by mixing 9µl of reagent A (streptavidin) with 9µl of reagent B (biotinylated peroxidase) in 982µl of blocking solution to give a 1:100 dilution. This was prepared 30 minutes prior to use, to allow the complex to form, and the slides then incubated in 100µl for 30 minutes at room temperature.

After this incubation, the slides were washed for 2 x 5 minutes in PBS and then developed using DAB. This was prepared using the DAB Sigma Fast Tablet Sets where one urea tablet was dissolved in 5ml of dH<sub>2</sub>O and the DAB tablet added and also dissolved. Each was mixed by vortexing prior to the addition of 100µl to each slide for an incubation of 10 minutes at room temperature. Slides were washed in tap water for 5 minutes and counterstained in light haematoxylin (dilution of 1:5 with dH<sub>2</sub>O) for 15 seconds. The slides could then be dehydrated and mounted as detailed in section 2.2.4.11.

#### 2.2.5.4 *Mouse Tissue IHC Controls*

Negative controls were included in every case, where the primary antibody was replaced with 100µl of blocking solution. Positive tissue controls were also employed in each experiment these being; mouse embryo (Phospho-Histone H3), normal human squamous oesophagus (P-cadherin, clone 56) and wild type mouse oesophagus and large bowel (P-cadherin, clone PCD-1) (Table 2.3).

#### 2.2.6 Immunostaining of Zebrafish Tissue Sections

Sections were dewaxed in histoclear for 10 minutes and then rehydrated by equilibrating the sections in decreasing concentrations of ethanol (100%, 95%, 70%, 50% and 30%) for 5 minutes each, followed by two 5 minute washes in PBS. Endogenous peroxidase activity was blocked by immersing the sections in 3% hydrogen peroxide for 5 minutes at room temperature. After washing in PBT (PBS, 0.1% Tween 20) for 2 x 5 minutes, non-specific binding was blocked by incubating the sections in PBT plus 10% FBS for 20 minutes at room temperature. The negative controls were left in PBT, whereas the test slides had primary antibody applied and were incubated overnight at 4°C.

Following this incubation the sections were washed in PBT for 3 x 5 minutes and then incubated in PBT plus 10% FBS for 20 minutes as an additional blocking step between primary and secondary antibodies. The secondary antibody utilised was dependent on the primary antibody used. If the primary antibody was a mouse monoclonal a biotinylated rabbit anti-mouse (1:100) was used, however if the primary antibody was a rabbit polyclonal a biotinylated swine anti-rabbit (1:1000) or HRP-conjugated goat anti-rabbit (1:300) secondary antibody was used. The secondary antibody was incubated for 1 hour at room temperature, after which each section was washed in PBT for 3 x 10 minutes. During this washing step the tertiary antibody Vectastain Elite ABC Kit was prepared and 100µl applied to each slide for 30 minutes at room temperature. After 3 x 5 minutes washes in PBS and a 5 minute wash in

dH<sub>2</sub>O, DAB was applied to the sections for an incubation time of 10 minutes. The sections were washed in water and counterstained using either toluidine blue (0.1% solution in 0.1% sodium borax) for 5 seconds, or a H&E counterstain which was used following the same method employed in section 2.2.4.2. The sections were washed in water and then dehydrated in increasing concentrations of ethanol (30%, 50%, 70%, 95% and 100%) for 5 minutes each, followed by two 5 minute washes in histoclear. The sections were mounted with a glass cover slip using DPX mountant.

### 2.2.7 Competent Cell Transformation

Commercially available DH5 $\alpha$  competent cells were used in transformations. 50 $\mu$ l of the competent cells were thawed on ice, and 2ng of the P-cadherin transgene was added to the cells, mixed by pipetting, and then placed on ice for 30 minutes. Uptake of DNA was accomplished by incubating the cells for 20 seconds at 37°C, the samples were then placed on ice for 2 minutes, and 950 $\mu$ l of LB medium added. The cells were incubated at 37°C with constant shaking at 200rpm for 1 hour.

100 $\mu$ l of the transformed cell suspensions were added to agar plates plus 100 $\mu$ g/ml ampicillin, which were spread across the plate. Plates were inverted in the incubator at 37°C overnight. White colonies were picked using a pipette tip and placed into 200 $\mu$ l of PBS. 10 $\mu$ l of this was then placed on a GeneAmp PCR System 9700 to boil for 10 minutes at 95°C. PCR was carried out for 35 cycles of denaturation at 94°C for 30 seconds, annealing at 61°C for 30 seconds and extension at 72°C for 30 seconds using 10pmol P-cadherin primers. 3% TAE gels were run at 100V for 45-60 minutes to see which colonies were positive.

### 2.2.8 Plasmid Preparation

Plasmids were grown in transformed *E. Coli* in LB medium supplemented with ampicillin (50 $\mu$ g/ml). Plasmids were stored in 100 $\mu$ l of 10mM MgSO<sub>4</sub> and 300 $\mu$ l of 70% glycerol at -20°C. 'Mini' prep cultures were grown 5ml LB medium. Cultures were grown by shaking at 200rpm in a 37°C incubator overnight using a Rapidpure Plasmid Mini Kit (Cat No. 2066-400) method according to the manufacture's instructions.

#### 2.2.8.1 *'Mini' Plasmid Preparations*

This purification method was used to produce small volumes of low purity plasmid for the purpose of restriction digest analysis of colonies derived from DNA sub-cloning. In brief 1.5ml of the overnight culture was transferred to an eppendorf and centrifuged for 5 minutes

at maximum speed and the supernatant was then discarded. 50µl of pre-lysis buffer (kit supplied) was added to the cell pellet and mixed by vortexing or pipetting up and down until the cells were completely resuspended. 100µl of alkaline solution (kit supplied) was added and mixed by inverting the tubes several times, and then incubated at room temperature for 3 minutes. 100µl neutralising solution (kit supplied) was added and incubated for 1 minute at room temperature, mixing or vortexing gently several times. Samples were then centrifuged for 2 minutes at maximum speed and the supernatant transferred to clean eppendorfs. 250µl of RapidPURE mini salt solution (kit supplied) was added to each sample and this was then inverted several times.

The DNA/Salt mixture was then transferred to an assembled RapidPURE turbo cartridge and centrifuged for 30 seconds at maximum speed. 350µl of wash solution (kit supplied) was added to each RapidPURE turbo cartridge and these were centrifuged for 30 seconds at maximum speed. The lower catch tubes were emptied by removing them from the centrifuge and discarding the contents. The RapidPURE turbo filters were returned to the same catch tubes and samples centrifuged for an additional 2 minutes at maximum speed to drive the last of the wash solution from the turbo filters. The lower catch tubes were then discarded and the RapidPURE turbo filters, containing the bound DNA, were transferred to RapidPURE turbo recovery tubes (kit supplied).

As a final step 100µl of dH<sub>2</sub>O was added directly onto the GLASSMILK embedded membrane and incubated for 5 minutes at room temperature. Samples were centrifuged for 1 minute at maximum speed to collect the plasmid DNA at the bottom of the RapidPURE turbo recovery tubes. The turbo filters were discarded and the recovery tubes capped and stored at 4°C. 2µl of the resuspended 'mini' prep DNA was used in each sequencing reaction (section 2.2.9) and 10µl of resuspended 'mini' prep DNA was used in each restriction digest to determine vector map (section 2.2.10).

### 2.2.9 Sequencing

PCR reactions were purified using the QIAquick PCR purification kit according to the manufacturer's instructions. 20µl BigDye sequencing reactions were set up containing 2µl 'mini' prep DNA, 8µl BigDye Mix, and 1pM of the appropriate primer. Samples were then amplified by PCR for 35 cycles with 96°C denaturation, 10 seconds, 50°C annealing, 5 seconds and 60°C extension, 4 minutes. Unincorporated DyeDeoxy terminators were removed

using centri-sep spin columns and the sequence analysed by the Protein and Nucleic Acid Chemistry Laboratory (PNAACL), University of Leicester.

#### 2.2.10 DNA Restriction

Following the manufacturer's guidelines, 10µl of high molecular weight DNA was diluted with the manufacturer's reaction buffer, sterile water and 1U of restriction enzyme with or without BSA to a volume of 20µl. In the negative controls, the restriction enzymes were replaced with sterile water. This was incubated at 37°C for up to 16 hours to ensure complete digestion of the DNA. The double digest reactions were incubated at 25°C throughout the day and then at 37°C for up to 16 hours overnight. To inactivate the enzyme the temperature was raised to 94°C for 5 minutes before cooling and storing at 4°C. To ensure complete digestion an aliquot was run on a low percentage (0.8%) TAE agarose gel. High quality DNA has a high molecular weight and this is demonstrated on a TAE gel by low mobility, while DNA that is of lower quality (or had been previously digested) shows a smear on a TAE gel because DNA fragments have a variety of sizes and therefore varying mobility.

#### 2.2.11 DNA Extraction

DNA was extracted from samples of mouse tail tissue (n=505) which had been stored in a -80°C tissue bank, using a tail lysis buffer. Tissue was thawed on ice and 0.5-1cm of tissue was placed into 100µl of tail lysis buffer containing 4% (10mg/ml) PK and incubated at 60°C overnight. Samples were placed on a 95°C heat block for 10 minutes and centrifuged for 1 minute at 10,000rpm. Optical Density (OD) of the DNA was measured at 260nm on a spectrophotometer and the concentration of DNA calculated using the equation 1 OD unit = 50µg/ml DNA. The supernatant was used in PCR and DNA stored at -20°C.

#### 2.2.12 RNA Extraction

Total RNA was extracted using Sigma TRI Reagent™, where 1ml of TRI Reagent was used for between 15-20 snap frozen tissue sections, cut to 7µm, depending on the tissue size. Tissue was dispersed by vortexing and samples incubated for 5 minutes at room temperature to allow complete dissociation of nucleoprotein complexes. 200µl of chloroform was added, and the tube vigorously shaken for 15 seconds to form an emulsion. After standing at room temperature for 15 minutes the partially separated suspension was fully separated by centrifugation (12,000rpm) for 15 minutes at 4°C. A red organic phase contained the protein; the cloudy interface contained DNA; and a colourless aqueous phase contained the RNA.

The aqueous layer was transferred to a fresh eppendorf, and the organic phase retained in case later isolation of DNA or protein was desired, (stored at  $-20^{\circ}\text{C}$ ). A double extraction was then undertaken and so  $500\mu\text{l}$  of TRI Reagent™ was added to each eppendorf along with  $100\mu\text{l}$  of chloroform. Samples were inverted 15 times and incubated at room temperature for 3 minutes. Samples were then separated, for a second time, with centrifugation ( $12,000\text{rpm}$ ) for 15 minutes at  $4^{\circ}\text{C}$ . Again the colourless aqueous phase containing the RNA was removed to a fresh eppendorf and the second organic phase retained in case later isolation of DNA or protein was desired, (stored at  $-20^{\circ}\text{C}$ ).

The RNA was precipitated from the aqueous phase by mixing with  $500\mu\text{l}$  isopropanol and  $1\mu\text{l}$  ( $20\mu\text{g}$ ) of glycogen was added to act as a carrier to precipitate all of the RNA. Samples were then incubated for 10 minutes at room temperature and centrifuged ( $12,000\text{rpm}$ ) for 10 minutes at  $4^{\circ}\text{C}$ . The RNA pellets were washed twice in  $1\text{ml}$  of 70% ethanol and centrifuged ( $7,000\text{rpm}$ ) for 6 minutes at  $4^{\circ}\text{C}$ . The ethanol was removed, the RNA pellet allowed to air dry with inversion for 2-5 minutes at room temperature, and then dissolved in an appropriate volume of RNase/DNase free water; this was usually  $50\mu\text{l}$ . RNA concentrations were determined using a Nano Drop Spectrophotometer and the concentration of RNA calculated using the equation  $1\text{ OD unit} = 40\mu\text{g/ml RNA}$ . Samples were then split into small aliquots and snap frozen on dry ice before being stored at  $-80^{\circ}\text{C}$ .

### 2.2.13 Reverse Transcription

All reverse transcription (RT) reactions were carried out using AMV reverse transcriptase on  $10\mu\text{g}$  total RNA using the Dynabeads Oligo(dT)25 method according to the manufacture's guidelines. In brief  $10\mu\text{g}$  of total RNA was added to RNase/DNase free water to a final volume of between  $30\text{-}50\mu\text{l}$ . The Dynabeads were then pre-conditioned for later use; this was achieved by mixing them thoroughly ( $30\mu\text{l}$  for each reaction) and then washing them twice in binding buffer. To do this the Dynabeads were placed in a magnetic rack and once the beads had been attracted to the magnet the supernatant was removed and discarded. The beads were then resuspended in binding buffer (this was always the same amount as the original volume of beads needed). Ensuring that the beads were well washed they were once again placed into the magnetic rack, and the supernatant removed and discarded. The beads were resuspended in the same volume of binding buffer and washed well. As a final step the beads were separated magnetically and then resuspended for a final time in the same volume of binding buffer.

The eppendorfs containing only the total RNA and RNase/DNase free water were heated for 2 minutes at 65°C. Once the 2 minutes had elapsed the beads were thoroughly mixed and 30µl of the beads were resuspended in 10µg of the RNA for each reaction. This was repeated for each sample and followed by a thorough vortex. Samples were incubated for 5 minutes at room temperature to allow the polyA tail of the mRNA molecules to hybridise with the oligo(dT) on the beads. During this incubation each sample was transferred from 0.5ml eppendorfs to 1.5ml eppendorfs. Once the 5 minute incubation was over the beads/mRNA complexes were collected using the magnet and the supernatant removed and discarded. The beads/mRNA complexes were washed twice in 60µl of washing buffer. For this they were resuspended in 60µl of washing buffer and mixed thoroughly. Each sample was placed in the magnetic rack once again and the supernatant removed and discarded. The beads were resuspended in 60µl of washing buffer and mixed. As a final step the beads were separated magnetically and the mRNA resuspended for a final time in 30µl of sterile UP-water.

For each sample two positive and one negative RT reactions, (excluding the AMV-Enzyme), were set up with 10µl of bead linked mRNA for each reaction. The RT reaction mixture was prepared as described in Table 2.6. Once each reaction was prepared the RT reactions were incubated at 42°C for one hour. The resulting cDNA was stored at 4°C.

Component	Concentration
AMV RT - Buffer	5x
dNTP mix	10mM
RNasin®	40U
AMV-RT Enzyme	5U
Total RNA	10µg
Dynabeads	10µl
RNase/DNase free water to final volume	25µl

**Table 2.6 – RT reaction mix composition.** This table details the components and concentrations in the RT reaction mix.

#### 2.2.14 Polymerase Chain Reaction

To minimise variation a master mix was created when performing PCR reactions. This would be specific for each primer set used, requiring only the addition of a template, be that DNA or cDNA, and the *Taq* polymerase. The composition of the final PCR reaction mixture is given in Table 2.7.

Component	Amount
AJ buffer (10x)	5 $\mu$ l (1x)
Forward primer	100pmol
Reverse Primer	100pmol
<i>Taq</i> polymerase	1U
Template	1-5 $\mu$ l
Total Volume	50 $\mu$ l

**Table 2.7 – The composition of a PCR reaction.** This table details the components and concentrations in the PCR reaction multi mix.

Once the master mix had been created the correct volume was aliquoted into a PCR reaction tube. To this the template DNA was then added. The thermal cycling was then started; at the first annealing point the reaction was paused to allow the addition of *Taq* polymerase. Once the PCR reaction had finished the product was stored at 4°C prior to analysis.

Most reverse transcriptase polymerase chain reaction (RT-PCR) reactions have a very similar cycle structure with an initial denaturing step, followed by the cyclic denaturing, annealing and extension phases and finishing with a final extension step. The annealing temperature of the reaction was optimised by running parallel reactions at a number of different temperatures and using gel electrophoresis to determine which gave the most specific product. The temperatures assessed were based on the melting point of the primers ( $T_m$ ), with the temperatures ( $T_m$ )°C, ( $T_m$ -1)°C and ( $T_m$ -2)°C being used.

For each set of PCR amplifications a positive and negative control was used in each experiment. The positive control was determined depending on the experiment and the negative control consisted of water blank which would not contain any template DNA. This was used to ensure that there was no contamination in the PCR reaction. A PCR for the GAPDH house-keeping gene was also analysed in each PCR experiment to validate expression levels.

#### 2.2.15 Agarose Gel Electrophoresis

PCR products were run on agarose gels to determine the size of the products; it was also possible to semi-quantify levels of expression by band intensity. The gels used were 1% agarose dissolved in 1 x TAE buffer and run at 100V in a bath of 1 x TAE for approximately 1 hour. Ethidium bromide was added to visualise the double stranded DNA (5 $\mu$ l/100ml). 10 $\mu$ l of PCR product was added to 2.5 $\mu$ l of 5x PCR loading buffer prior to loading and mixed by

pipetting. For each gel a 100bp DNA size ladder was also run (20µl/lane). Once the gel had finalised the PCR products were visualised on a UV transilluminator.

#### 2.2.16 Statistical Analysis

All statistical analysis was performed using the SPSS statistical software package. Normal distribution of data was not assumed and therefore non-parametric tests were employed. Significance of results was assessed by performing a Fishers Exact Test, a Wilcoxon's Rank Test or a one-way Analysis of Variance (ANOVA). The significant differences between data were calculated from either the positive or vehicle controls where by a value of  $p < 0.05$  was classed as significant.

**Chapter 3: Stem Cell Compartment Identification and Mapping  
of LRC Location in Human Tissue**

### 3.1 Introduction

Cancer is a stem cell disease – although this seems to be a rather definitive statement and will no doubt have its exceptions, it would seem to be intuitive, because only stem cells have the ability to self-renew and neoplasia is essentially dysregulated self-renewal (Garcia *et al.*, 1999; Radtke and Clevers, 2005).

Malignant tissue formation requires epithelial remodelling, implying that cell-cell and cell-matrix adhesion must be modified such that cells alter their physical relationship with one another and with adjacent extracellular matrix. Studies have shown that over expression of E-cadherin in the intestine of transgenic mice leads to a reduction in cell migration and altered differentiation patterns (Hermiston *et al.*, 1996). Conversely, silencing E-cadherin expression in the intestine of transgenic mice leads to a disruption of cell-cell adhesion, colitis and adenoma formation (Hermiston and Gordon, 1995a; Hermiston and Gordon, 1995b).

Several studies analysing colorectal adenomas from human subjects have also shown that there is a reduction in E-cadherin protein expression compared to normal colonic mucosa, which persists into invasive colorectal cancer (Dorudi *et al.*, 1993; Dorudi *et al.*, 1995; Gagliardi *et al.*, 1995; Ghadimi *et al.*, 1999; Hao *et al.*, 1997; Hiscox and Jiang, 1997; Karatzas *et al.*, 1999; Sloncova *et al.*, 2001).

Reduction in E-cadherin protein levels in colonic cells undergoing neoplastic transformation begs the question as to whether expression of other cell adhesion molecules is altered in such lesions. Evidence of widespread dysregulation is seen in ulcerative colitis and Crohn's disease, where downregulation of E-cadherin is accompanied by aberrant expression of the stratified epithelium associated cadherin, P-cadherin (Jankowski *et al.*, 1998).

The condition known as BM, whereby the normal squamous epithelium of the oesophagus is replaced by the columnar intestinal mucosa, has been associated with chronic GOR and predisposes to OA. The cancer is thought to evolve from a multistep process whereby the normal oesophageal squamous epithelium is replaced by the columnar epithelium in BO, followed in some individuals by progression through dysplasia to an invasive stage (Jankowski *et al.*, 1999). The prognosis in patients with established OA remains very poor (Jankowski *et al.*, 2000a). Little is known about signalling pathways or cell lineage which give rise to BM (Bailey *et al.*, 1998; Jankowski *et al.*, 2000a) although it is currently the commonest pre-malignant lesion in the UK (1% population) (Jankowski *et al.*, 2002).

Within the GI tract an epithelial cells normal lifespan culminates in being shed from the epithelial surface into the lumen, and being replaced from below by the action of a replicating somatic stem cell and its progeny TA cells. The GI tract is one of the most common sites of carcinogenesis (Kayahara *et al.*, 2003) and as stem cells are the only long-residing cells they are the most likely target for mutations that lead to aberrant epithelial biology such as BM and to an increase in malignancy. It is for this reason that the identification and physical isolation of epithelial stem cells is critical to the understanding of their growth regulation during homeostasis, wound healing and carcinogenesis.

Our group has previously shown that putative squamous stem cells are located in the basal compartment of the normal squamous epithelium, especially at the tips of the papillae (Jankowski *et al.*, 2000a). To date however, the identification of the putative BM stem cell, the pre-malignant condition leading to OA, has not been clearly defined.

Stem cells can not be identified morphologically or distinguished from their progeny, the TA cells, or from any other epithelial cells (Marshman *et al.*, 2002; Tani *et al.*, 2000). Stem cells can be localised by specialised function, but as yet there are no definitive markers of stem cells (Jankowski and Dover, 1993). As a result stem cells remain poorly characterised and most interpretations of stem cell behaviour are based upon monitoring cohorts of cells before and after perturbation of the tissue (Booth and Potten, 2000).

There have been many molecules suggested to be upregulated in stem cells and as such they are implicated as possible stem cell markers due mainly to the fact that they are preferentially expressed in metaplastic rather than normal or inflamed squamous oesophageal mucosa (Jankowski and Anderson, 2004). In this study the changing expression patterns of Ki-67,  $\beta 1$  integrin, P-cadherin, and its associated binding partner  $\beta$ -catenin, were examined in oesophageal mucosa from normal through to invasive carcinoma. In this manner temporal patterns of expression of these molecules could be studied. Normal stomach mucosa was also studied, in order to contrast expression of these molecules in a control set of tissue, thought to have low malignant potential.

IUdR is a molecule needed for nucleic acid synthesis and will incorporate into dividing cells only. The stem cells are likely to divide much more slowly and hence would retain the IUdR label for longer thus allowing for the differentiation between the normal faster proliferating cells and the stem cells. In this study IUdR will be utilised to identify those cells which divide

slowly and remain in the epithelium, these are thought to be the putative stem cells, as opposed to those which label and are lost into the lumen, the TA cells. This will be investigated in human subjects attending for surgical resection. Where IHC will then identify labelled cells in normal and abnormal tissue sections and these data used to characterise the oesophageal stem cell compartment.

This research is focused on putative oesophageal stem cells and may help to identify the earliest molecular processes and stages of neoplastic transformation related to the MDCS in the human oesophagus. Identification of some of these mechanisms, including those, which determine their fate, regulation of proliferation and differentiation pattern, might have a broader, general relevance to the understanding of biological processes that play a role in the generation of a neoplastic cell population in a chronic inflammatory environment.

In addition, the results might be further used to develop more specific early markers of neoplastic progression in surveillance or identify targets for early interventions. We therefore assume that the research will yield both new data important for basic science and practical implications for clinical use.

### **3.2 Aims**

The aim of this Chapter was to test the hypothesis that the location of the stem cell compartment and LRCs could be mapped in oesophageal epithelium using molecular targets.

The specific objectives were:

- 1) To carry out H&E analysis on all experimental tissues prior to optimisation of commercially available antibodies and use these for IHC studies.
- 2) To use primary explant culture in an *ex vivo* model for LRC proof of concept.
- 3) To identify the location of LRC, the putative stem cells, in normal human oesophagus, BM, gastric and tumour sites for a sub-group of resection patients *in vivo*.
- 4) To carry out double labelling IHC on experimental tissue from a sub-group of resection clinical trial patients to determine proliferation dynamics and location of LRCs.

### **3.3 Materials and Methods**

Human fresh tissue samples and clinical trial tissue samples used in this Chapter are described in sections 2.1.1.1 and 2.1.2 respectively. Processing details for each tissue type can be found in section 2.2.1.1 and 2.2.1.2 respectively. General reagents used are described in section

2.1.5. H&E staining of FFPE sections was performed as detailed in section 2.2.4.2. Expression and localisation of molecules studied was achieved by IHC as described in section 2.2.4. Primary antibodies used are described in section 2.1.4 and in Table 2.3. Cell line details can be found in section 2.1.3 and Table 2.2 with cell culture information outlined in section 2.2.2 with routine cell culture details in section 2.2.2.1, IUdR reconstitution in section 2.2.2.3, *in vitro* culture of TE-7 and OE-21 cell lines in section 2.2.2.4 and preparation of these cell lines in section 2.2.2.5. Primary explant culture and preparation of mucosal biopsies are outlined in section 2.2.3. Statistical analysis information can be found in section 2.2.16.

### **3.4 Results**

#### **3.4.1 Tissue Morphology**

The histological appearance of all fresh tissue was assessed by H&E staining prior to immunostaining, which allowed for elimination of poorly preserved tissues. Figure 3.1 shows examples of H&E staining of all experimental tissues which were included as representative samples from the six case studies investigated.

The *ex vivo* model experimental tissue and clinical trial tissue was also assessed by H&E staining prior to immunostaining. This allowed each tissue to be examined for morphological appearance which was especially helpful in the primary explant cases where the nature of processing meant that the quality of tissue was poor. The tissue for the patients recruited to the 'SAINT' clinical trial was also examined prior to any experimental work being carried out. Figure 3.2 shows examples of H&E staining for both the control OE-21 and TE-7 cell lines, along with examples of the oesophageal endoscopy primary explants after 24 hours of culture. The primary explants were taken from normal gastric tissue, normal squamous mucosa and BM mucosa. Figure 3.3 shows examples of H&E staining for the patients recruited onto the 'SAINT' clinical trial. Each image was taken from tissue that had received IUdR infusion 7 days prior to surgery and shows examples of normal gastric tissue, normal squamous mucosa, intestinal metaplasia (IM) tissue and OA tissue.

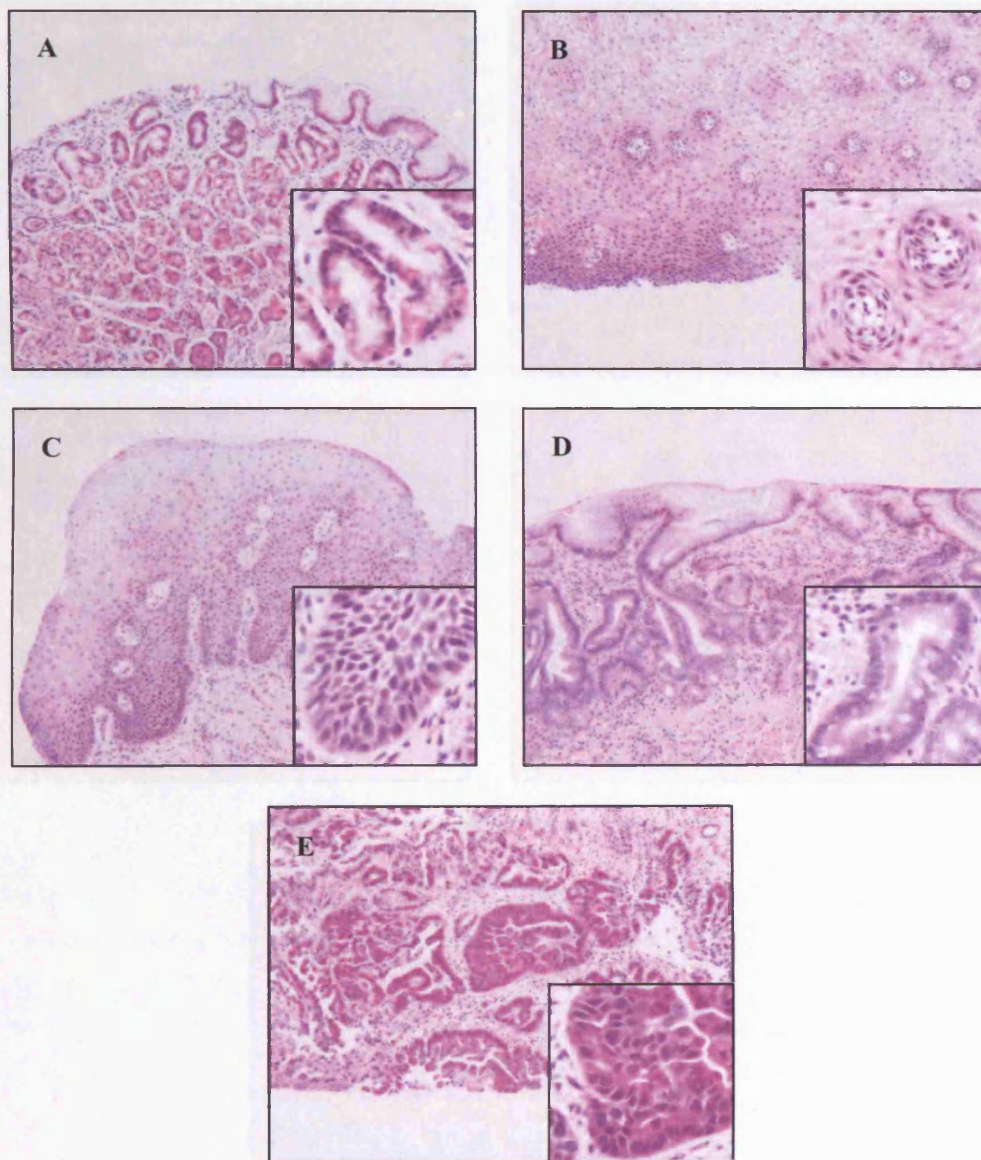


**Figure 3.1 - H&E staining of a sample of clinical cases.** (A) Normal stomach tissue. (B) Stratified squamous oesophageal mucosa. (C) Oesophagitis tissue showing inflammation. (D) BM oesophageal mucosa with a mixture of cell types and architectural pattern resembling intestinal mucosa. The epithelium shown is a specialised intestinal epithelium with goblet cells. (E) Moderately differentiated OA with poorly formed glands. Magnification is x10 for all main images and x40 for all higher powered inserts.

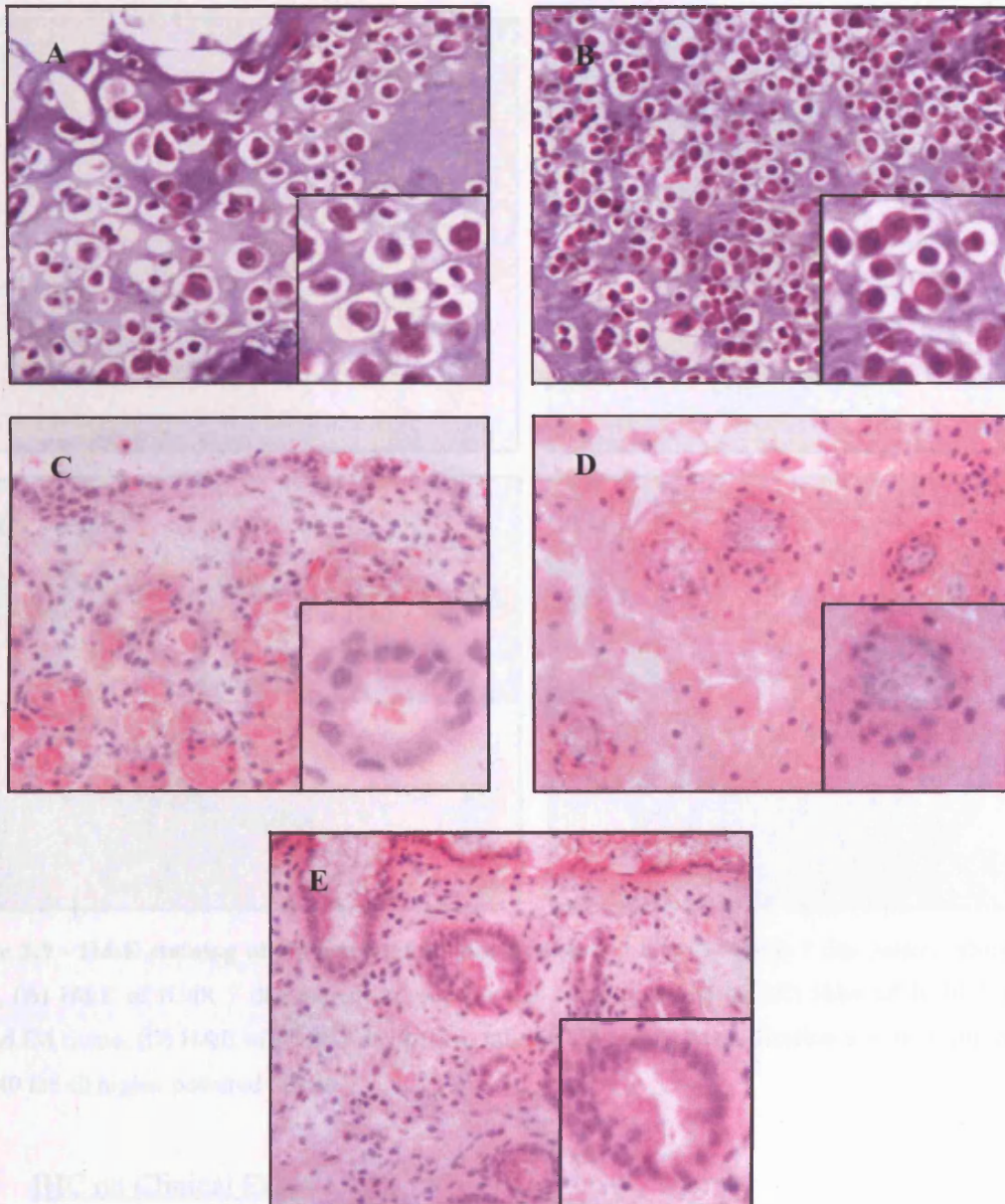


**Figure 3.2 - H&E staining of control cells and tissues.** (A) H&E of control cytocontrol for the OE-21 cell line, (B) H&E of control cytocontrol for the TE-7 cell line, (C) H&E of control primary explant from normal gastric mucosa after 24 hours of culture, (D) H&E of control primary explant from normal squamous mucosa after 24 hours of culture, (E) H&E of control primary explant from BM mucosa after 24 hours of culture. Magnification is x25 for all main images and x40 for all higher powered inserts.

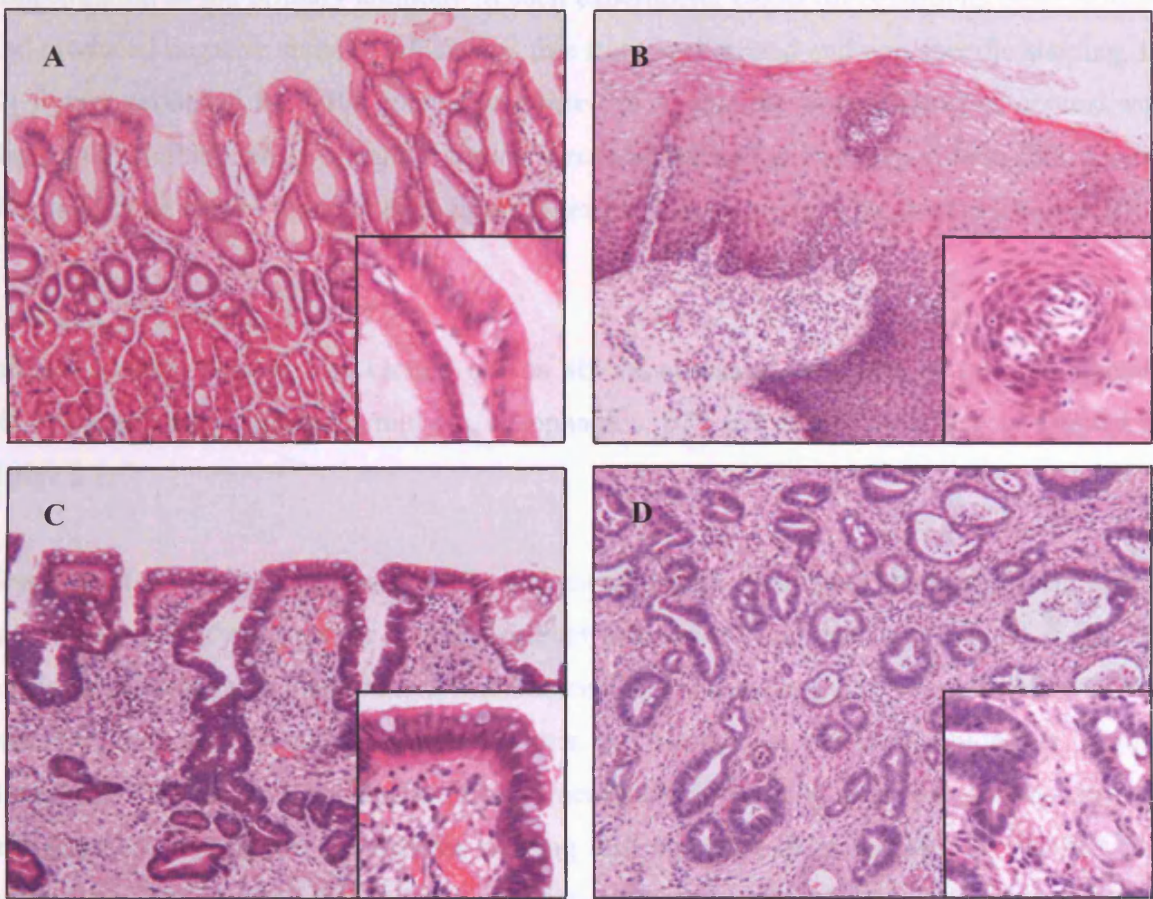


**Figure 3.3 - H&E staining of clinical trial patient tissues.** (A) H&E of IUdR 7 day patient infused stomach tissue, (B) H&E of IUdR 7 day patient infused normal oesophageal tissue, (C) H&E of IUdR 7 day patient infused IM tissue, (D) H&E of IUdR 7 day patient infused OA tissue. Magnification is x10 for all main images and x40 for all higher powered inserts.

### 3.4.2 IHC on Clinical Cases

IHC studies were conducted on six clinical cases of human tissue for gastric, normal squamous, oesophagitis, BM and OA, as detailed in section 2.1.1.1. Four different antibodies were utilised, as detailed in Table 2.3. All of these antibodies were endorsed by the manufacturers for immunohistochemical use in human tissue. All had associated methods for antigen retrieval apart from the  $\beta$ 1-integrin, 4B7, which required some optimisation work before initial experiments were conducted.

#### 3.4.2.1 Immunoreactivity Controls

In each of the IHC experiments undertaken in this Chapter no primary antibody (NPA) and isotype-matched controls were employed. The isotype-matched control was the DakoCytomation IgG<sub>1</sub> (catalogue number: X0931), which was adjusted to the same

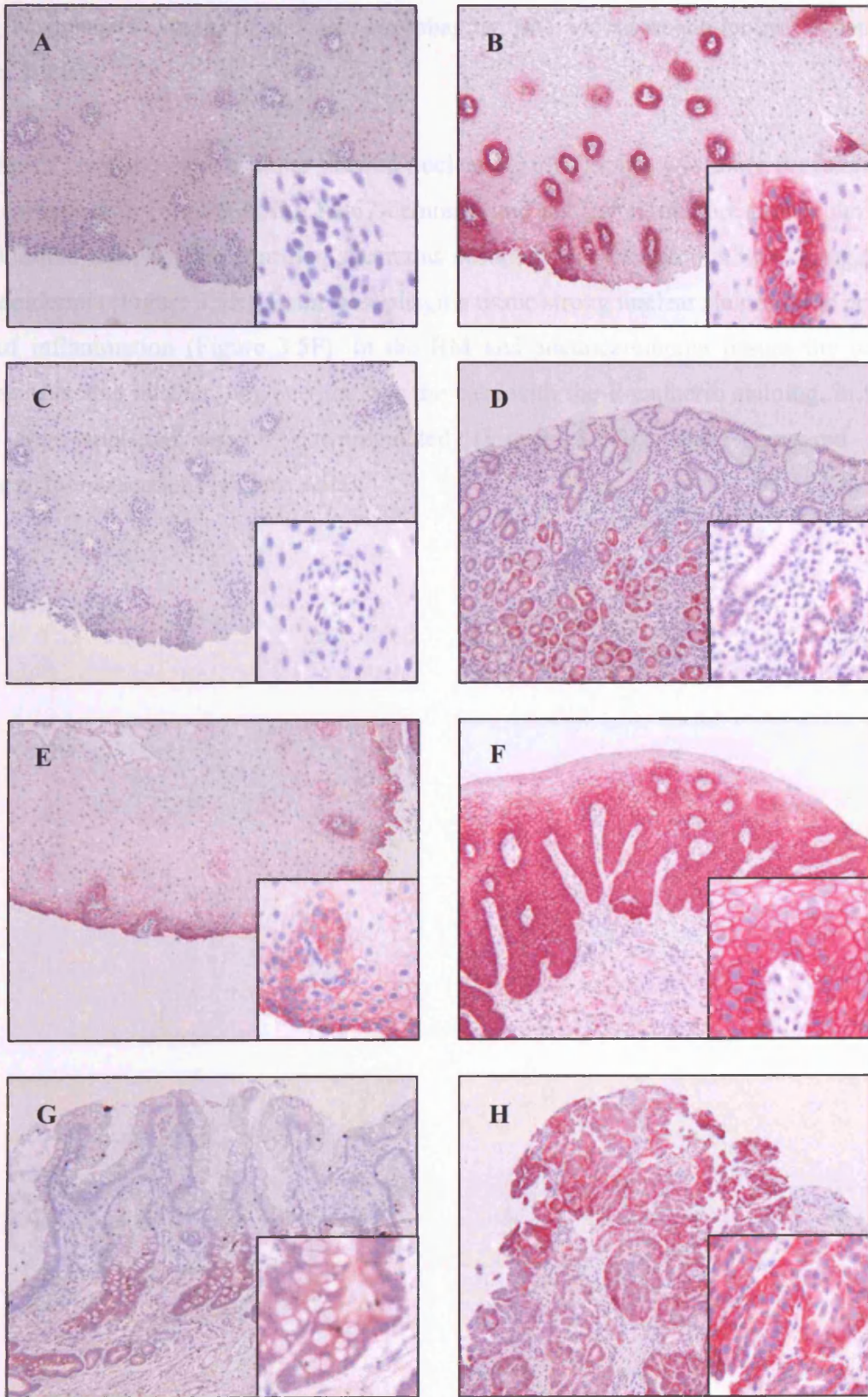
concentration as the primary antibody in each experiment. Under all conditions these worked and produced negative staining which was free from background and non-specific staining. In all figures produced the NPA control was listed as A, and the isotype-matched control was listed as C. Suitable positive control tissues were also utilised in each experiment and specific details of these can be found in each figure legend and in each figure these were listed as B.

#### 3.4.2.2 *P-cadherin, 610227*

Immunological staining was carried out on six experimental case sets of normal stomach tissue, oesophageal squamous mucosa, oesophagitis, BM and adenocarcinoma, as detailed in Table 2.1.

Staining of normal stomach tissue showed membranous P-cadherin staining in the apical layers with a slightly stronger staining present in the basal parietal cells (Figure 3.4D). P-cadherin demonstrated membranous immunoreactivity throughout all epidermal layers of the stratified squamous oesophagus although this was stronger at the basal epidermis (Figure 3.4E). In the oesophagitis tissue strong membranous staining was present at sites of inflammation with some cytoplasmic staining also observed (Figure 3.4F). In the BM and adenocarcinoma tissues the observed staining was more cytoplasmic than membranous, however in the BM tissue this appeared to be downregulated (Figure 3.4G) when compared to the adenocarcinoma sections (Figure 3.4H).

**Figure 3.4 – P-cadherin IHC analysis on experimental tissues.** The primary antibody was clone 56, 610227 used at a final concentration of 2.5µg/ml with a 20 minute microwave antigen retrieval step. AP conjugated St-ABC was used as the tertiary detection system with Fast Red as the chromogen. A) Normal squamous negative control, B) Normal squamous with membranous expression of P-cadherin, C) Normal squamous isotype matched control, D) Normal stomach tissue with expression of P-cadherin, E) Normal squamous tissue with membranous expression of P-cadherin, F) Oesophagitis tissue with membranous expression of P-cadherin, G) BO tissue with expression of P-cadherin, H) Adenocarcinoma tissue with expression of P-cadherin. Magnification is x10 for all main images and x40 for all higher powered inserts.



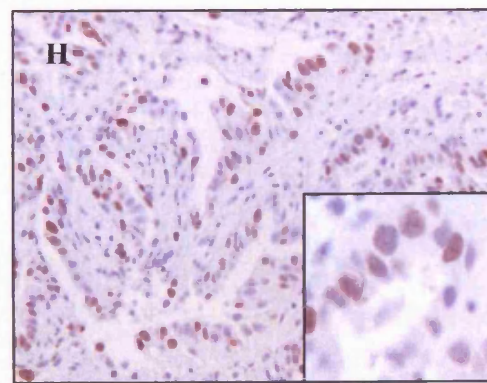
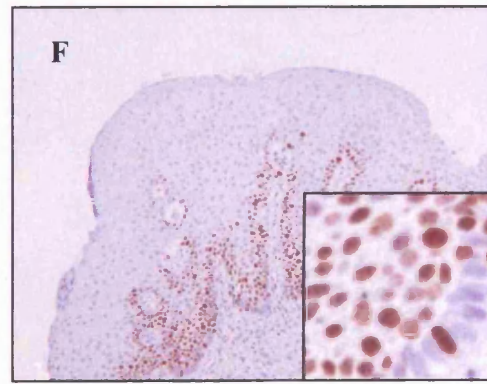
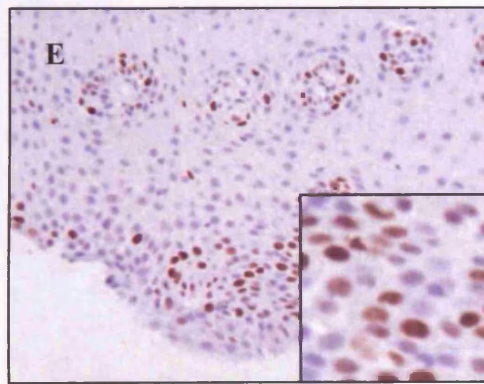
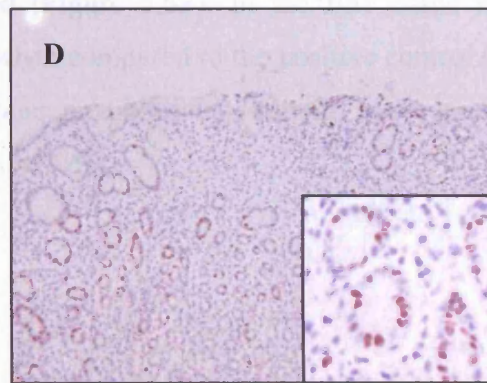
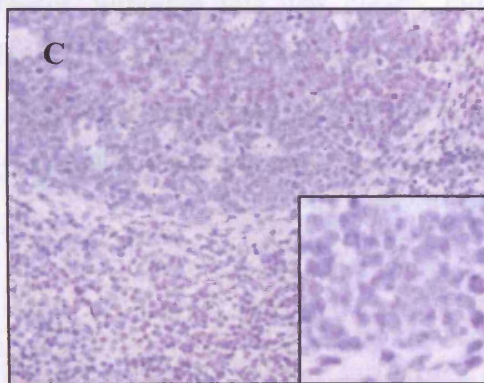
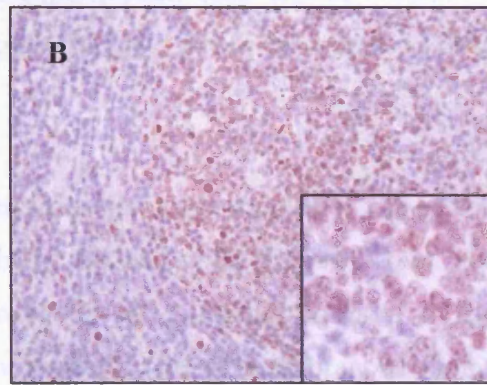
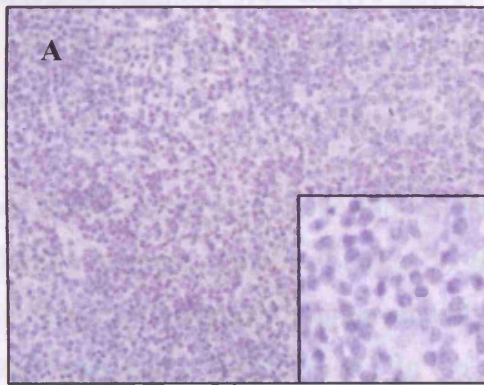
### 3.4.2.3 *Ki-67, NCL-Ki67*

Immunological staining was carried out on six experimental case sets of normal stomach tissue, oesophageal squamous mucosa, oesophagitis, BM and adenocarcinoma, as detailed in section 2.1.1.1.

Staining of normal stomach tissue showed nuclear Ki-67 staining was more prevalent in the basal parietal cells (Figure 3.5D). Ki-67 demonstrated nuclear immunoreactivity throughout all epidermal layers of the stratified squamous oesophagus although this was stronger in the basal epidermis (Figure 3.5E). In the oesophagitis tissue strong nuclear staining was present at sites of inflammation (Figure 3.5F). In the BM and adenocarcinoma tissues the observed staining was also nuclear, however, as was the case with the P-cadherin staining, in the BM tissue this appeared to be downregulated (Figure 3.5G) when compared to the adenocarcinoma sections (Figure 3.5H).

**Figure 3.5 – Ki-67 IHC analysis on experimental tissues.** The primary antibody was clone MM1, NCL-Ki67 used at a final concentration of 0.5µg/ml with a 2 minute pressure cooker antigen retrieval step. HRP conjugated St-ABC was used as the tertiary detection system with DAB as the chromogen. A) Normal tonsil negative control, B) Normal tonsil with expression of Ki-67, C) Normal tonsil isotype matched control, D) Normal stomach tissue with expression of Ki-67, E) Normal squamous tissue with expression of Ki-67, F) Oesophagitis tissue with expression of Ki-67, G) BO tissue with expression of Ki-67, H) Adenocarcinoma tissue with expression of Ki-67. Magnification is x25 for images A, B, C and H, x10 for images D, E, F and G and x40 for all higher powered inserts.

3.4.24 *β-carrubin*, 610153

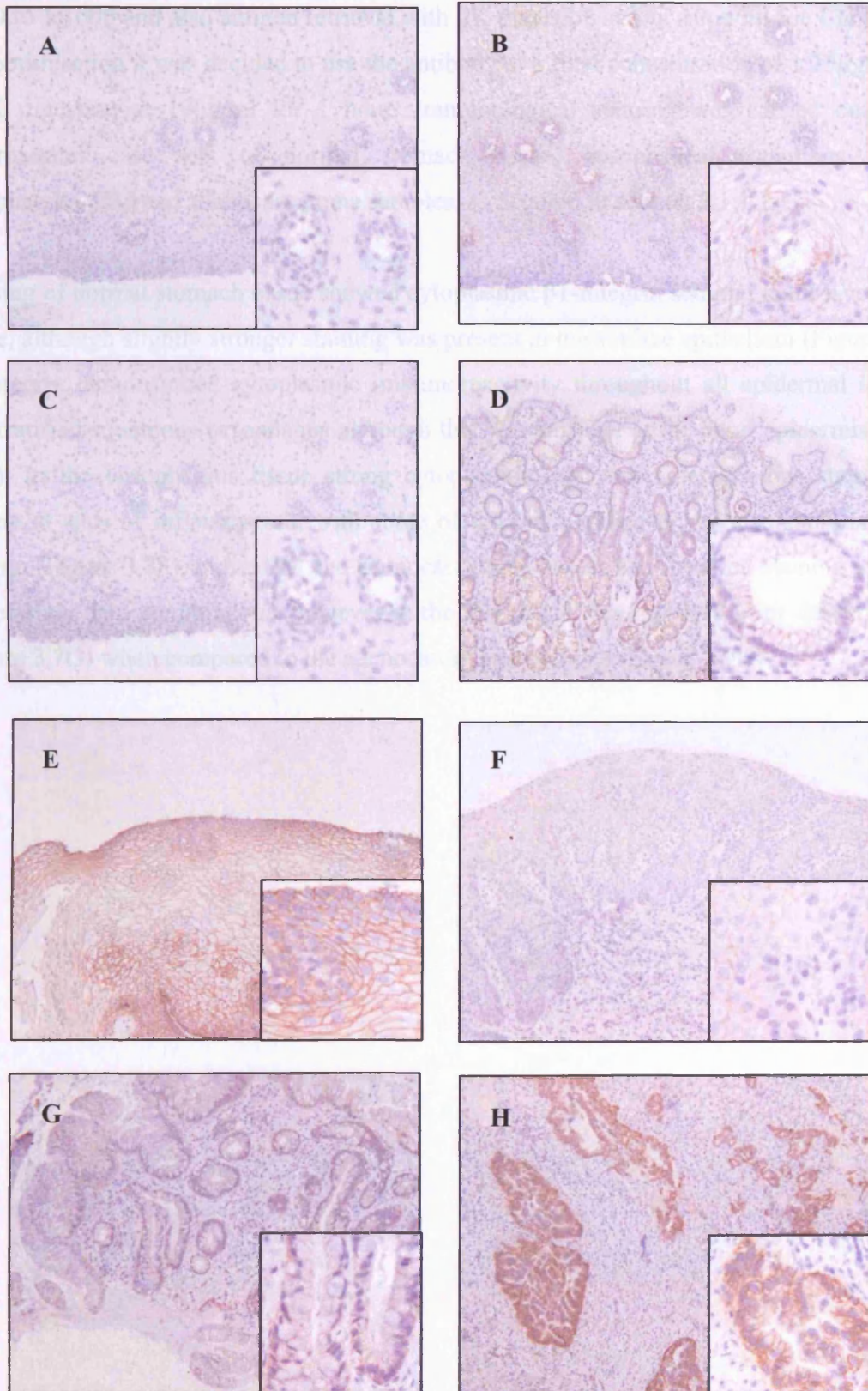


#### 3.4.2.4 *β-catenin, 610153*

Immunological staining was carried out on six experimental case sets of normal stomach tissue, oesophageal squamous mucosa, oesophagitis, BM and adenocarcinoma, as detailed in section 2.1.1.1.

Staining of normal stomach tissue showed membranous  $\beta$ -catenin staining in the apical layers with slightly stronger staining present in the basal parietal cells (Figure 3.6D).  $\beta$ -catenin demonstrated membranous immunoreactivity throughout all epidermal layers of the stratified squamous oesophagus (Figure 3.6E). In the oesophagitis tissue the membranous staining was still present, although this was clearly reduced (Figure 3.6F). In the BM tissue again a reduction in the membranous staining was seen when compared to the positive control (Figure 3.6G). The adenocarcinoma section showed some membranous staining, however nuclear staining was also observed in these sections (Figure 3.6H).

**Figure 3.6 –  $\beta$ -catenin IHC analysis on experimental tissues.** The primary antibody was clone 14, 610153 used at a final concentration of 0.5 $\mu$ g/ml with a 2 minute pressure cooker antigen retrieval step. HRP conjugated St-ABC was used as the tertiary detection system with DAB as the chromogen. A) Normal squamous negative control, B) Normal squamous with expression of  $\beta$ -catenin, C) Normal squamous isotype matched control, D) Normal stomach tissue with expression of  $\beta$ -catenin, E) Normal squamous tissue with expression of  $\beta$ -catenin, F) Oesophagitis tissue with expression of  $\beta$ -catenin, G) BO tissue with expression of  $\beta$ -catenin, H) Adenocarcinoma tissue with expression of  $\beta$ -catenin. Magnification is x10 for all main images and x40 for all higher powered inserts.



#### 3.4.2.5 *β1-integrin, 4B7*

The optimisation of antibody β1-4B7 involved a serial dilution of antibody, ranging from 1:100 to 1:1000 and also antigen retrieval with PK digestion at 5 or 10µg/ml for 1 hour. After this optimisation it was decided to use the antibody at a final concentration of 1.25µg/ml with a PK digestion at 10µg/ml for 1 hour. Immunological staining was carried out on six experimental case sets of normal stomach tissue, oesophageal squamous mucosa, oesophagitis, BM and adenocarcinoma samples, as detailed in section 2.1.1.1.

Staining of normal stomach tissue showed cytoplasmic β1-integrin staining in all layers of the tissue, although slightly stronger staining was present in the surface epithelium (Figure 3.7D). β1-integrin demonstrated cytoplasmic immunoreactivity throughout all epidermal layers of the stratified squamous oesophagus although this was stronger at the basal epidermis (Figure 3.7E). In the oesophagitis tissue strong cytoplasmic and some membranous staining was present at sites of inflammation, with some of the interpapillae layers also staining for β1-integrin (Figure 3.7F). In the BM and adenocarcinoma tissues the observed staining was more cytoplasmic than membranous, however in the BM tissue this appeared to be downregulated (Figure 3.7G) when compared to the adenocarcinoma sections (Figure 3.7H).

**Figure 3.7 –  $\beta$ 1-integrin IHC analysis on experimental tissues.** The primary antibody was clone 4B7R,  $\beta$ 1-4B7 used at a final dilution of 1:200 with a PK digestion at 10 $\mu$ g/ml for 1 hour. AP conjugated St-ABC was used as the tertiary detection system with Fast Red as the chromogen. A) Normal breast negative control, B) Normal breast with expression of  $\beta$ 1-integrin, C) Normal breast isotype matched control, D) Normal stomach tissue with expression of  $\beta$ 1-integrin, E) Normal squamous tissue with expression of  $\beta$ 1-integrin, F) Oesophagitis tissue with expression of  $\beta$ 1-integrin, G) BO tissue with expression of  $\beta$ 1-integrin, H) Adenocarcinoma tissue with expression of  $\beta$ 1-integrin. Magnification is x10 for all main images and x40 for all higher powered inserts.

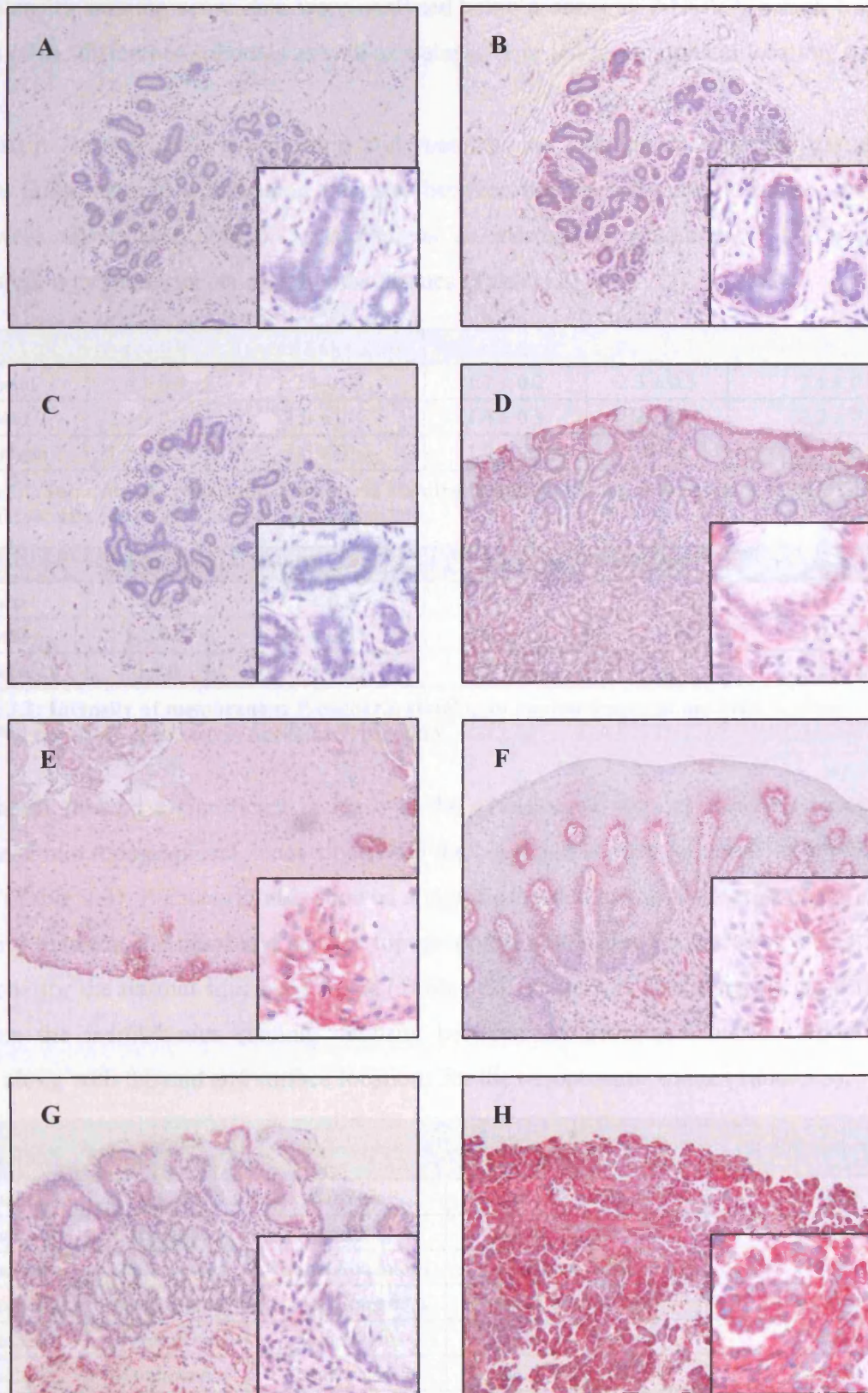


Table 3.1: Results of statistical analysis...  
investigate the significant difference when comparing...  
micrograph... with different...  
0.01 level... analysis...

## 3.4.2.6 Statistical Analysis for IHC Data

The intensity staining score data were analysed using a one way ANOVA, which tested for effects of the different antibodies as well as staining type and topographical location.

P-cadherin showed both cytoplasmic and membranous staining in different tissues, and notable differences in the staining intensity between the topographical locations and tissue type were observed (Table 3.1), as well as an increase in membranous staining when compared to cytoplasmic staining in most tissues (Table 3.2).

	Stomach	Normal Squamous	Oesophagitis	Barrett's	Adenocarcinoma
<b>Basal</b>	2.4 ± 0.4	1.2 ± 0.2	1.7 ± 0.2	2.3 ± 0.3	2.1 ± 0.5
<b>Mid</b>	2.1 ± 0.3	1.0 ± 0	1.4 ± 0.3	1.5 ± 0.27	2.2 ± 0.5
<b>Surface</b>	1.5 ± 0.3	1.0 ± 0	1.2 ± 0.2	1.0 ± 0	2.4 ± 0.5

**Table 3.1: Intensity of cytoplasmic P-cadherin staining in human tissues of the MDCS.** Mean ± SEM; n = 6. Full raw data can be seen in Appendix 7, page 254.

	Stomach	Normal Squamous	Oesophagitis	Barrett's	Adenocarcinoma
<b>Basal</b>	1.1 ± 0.2	3.1 ± 0.3	3.5 ± 0.6	1.2 ± 0.3	3.2 ± 0.7
<b>Mid</b>	1.1 ± 0.2	2.6 ± 0.3	2.5 ± 0.4	1.0 ± 0	3.2 ± 0.5
<b>Surface</b>	1.0 ± 0	1.2 ± 0.2	1.5 ± 0.4	1.0 ± 0	3.2 ± 0.7

**Table 3.2: Intensity of membranous P-cadherin staining in human tissues of the MDCS.** Mean ± SEM; n = 6. Full raw data can be seen in Appendix 7, page 255.

P-cadherin showed a significant increase in the cytoplasmic staining intensity between the basal and mid topographical zones along with the basal and surface locations for the Barrett's tissue (Table 3.3). P-cadherin also showed a significant increase in the membranous staining intensity between the basal and surface topographical zones along with the mid and surface locations for the normal squamous tissue (Table 3.3). There was also a significant difference between the membranous staining intensity between the basal and surface topographical zones along with the mid and surface locations for the oesophagitis tissue (Table 3.3).

Antibody	Staining Type	Tissue Type	Comparison Between Topographical Location	Significance Value
P-cadherin	Cytoplasmic	Barrett's	Basal vs. Mid	<b>P&lt;0.05</b>
P-cadherin	Cytoplasmic	Barrett's	Basal vs. Surface	<b>P&lt;0.01</b>
P-cadherin	Membranous	Normal Squamous	Basal vs. Surface	<b>P&lt;0.01</b>
P-cadherin	Membranous	Normal Squamous	Mid vs. Surface	<b>P&lt;0.01</b>
P-cadherin	Membranous	Oesophagitis	Basal vs. Surface	<b>P&lt;0.01</b>
P-cadherin	Membranous	Oesophagitis	Mid vs. Surface	<b>P&lt;0.01</b>

**Table 3.3: P-cadherin statistical analysis.** A one way ANOVA with Tukey's post hoc test was used to investigate the significant difference when comparing the P-cadherin intensity staining scores between the topographical locations, within different tissue types. The mean difference was either significant at the 0.05 or 0.01 level, n = 6. Full statistical analysis can be seen in Appendix 7, pages 254 and 255.

Ki-67 was the only nuclear marker investigated in this study and several differences in the staining intensity between the topographical locations and tissue type were seen (Table 3.4).

	Stomach	Normal Squamous	Oesophagitis	Barrett's	Adenocarcinoma
<b>Basal</b>	3.8 ± 0.4	4.5 ± 0.3	3.3 ± 0.3	3.3 ± 0.6	2.8 ± 0.5
<b>Mid</b>	2.3 ± 0.5	3.8 ± 0.4	3.5 ± 0.2	2.5 ± 0.6	4.3 ± 0.3
<b>Surface</b>	1.0 ± 0	1.0 ± 0	3.2 ± 0.2	1.2 ± 0.2	3.0 ± 0.5

**Table 3.4: Intensity of nuclear Ki-67 staining in human tissues of the MDCS.** Mean ± SEM; n = 6. Full raw data can be seen in Appendix 7, page 256.

Ki-67 showed a significant increase in the nuclear staining intensity between the basal and surface locations for stomach tissue (Table 3.5). Ki-67 also showed a significant increase in the nuclear staining intensity between the basal and surface topographical zones along with the mid and surface locations for the normal squamous tissue (Table 3.5). The Barrett's tissue showed that there was a significant increase in nuclear staining between the basal and surface locations (Table 3.5) while the adenocarcinoma tissue produced significant differences between the basal and mid topographical zones along with the mid and surface locations (Table 3.5).

Antibody	Staining Type	Tissue Type	Comparison Between Topographical Location	Significance Value
Ki-67	Nuclear	Stomach	Basal vs. Surface	<b>P&lt;0.01</b>
Ki-67	Nuclear	Normal Squamous	Basal vs. Surface	<b>P&lt;0.01</b>
Ki-67	Nuclear	Normal Squamous	Mid vs. Surface	<b>P&lt;0.01</b>
Ki-67	Nuclear	Barrett's	Basal vs. Surface	<b>P&lt;0.05</b>
Ki-67	Nuclear	Adenocarcinoma	Basal vs. Mid	<b>P&lt;0.05</b>
Ki-67	Nuclear	Adenocarcinoma	Mid vs. Surface	<b>P&lt;0.05</b>

**Table 3.5: Ki-67 statistical analysis.** A one way ANOVA with Tukey's post hoc test was used to investigate the significant difference when comparing the Ki-67 intensity staining scores between the topographical locations, within different tissue types. The mean difference was either significant at the 0.05 or 0.01 level, n = 6. Full statistical analysis can be seen in Appendix 7, page 256.

$\beta$ -catenin showed membranous staining only in the various tissues examined, however it showed no significant difference in the staining intensity between any of the topographical locations for each tissue studied (Table 3.6).

	Stomach	Normal Squamous	Oesophagitis	Barrett's	Adenocarcinoma
<b>Basal</b>	3.7 ± 0.3	3.2 ± 0.6	3.3 ± 0.5	2.8 ± 0.7	2.0 ± 0.3
<b>Mid</b>	3.3 ± 0.4	3.2 ± 0.6	3.2 ± 0.5	2.7 ± 0.7	2.8 ± 0.7
<b>Surface</b>	2.2 ± 0.7	3.2 ± 0.7	3.2 ± 0.5	2.3 ± 0.8	2.0 ± 0.5

**Table 3.6: Intensity of membranous  $\beta$ -catenin staining in human tissues of the MDCS.** Mean ± SEM; n = 6. Full raw data can be seen in Appendix 7, page 257.

$\beta$ 1-integrin showed both cytoplasmic and membranous staining in different tissues, and notable differences in the staining intensity between the topographical locations and tissue type were observed (Table 3.7), as well as an increase in cytoplasmic staining when compared to membranous staining in all tissues (Table 3.8).

	Stomach	Normal Squamous	Oesophagitis	Barrett's	Adenocarcinoma
<b>Basal</b>	3.0 $\pm$ 0.5	3.2 $\pm$ 0.5	3.0 $\pm$ 0.3	3.2 $\pm$ 0.4	4.3 $\pm$ 0.4
<b>Mid</b>	3.0 $\pm$ 0.5	2.7 $\pm$ 0.3	3.3 $\pm$ 0.3	3.0 $\pm$ 0	4.0 $\pm$ 0.3
<b>Surface</b>	3.2 $\pm$ 0.5	1.2 $\pm$ 0.2	3.3 $\pm$ 0.4	2.8 $\pm$ 0.4	4.7 $\pm$ 0.3

**Table 3.7: Intensity of cytoplasmic  $\beta$ 1-integrin staining in human tissues of the MDCS.** Mean  $\pm$  SEM; n = 6. Full raw data can be seen in Appendix 7, page 268.

	Stomach	Normal Squamous	Oesophagitis	Barrett's	Adenocarcinoma
<b>Basal</b>	1.8 $\pm$ 0.4	1.5 $\pm$ 0.6	1.5 $\pm$ 0.6	1.2 $\pm$ 0.2	3.0 $\pm$ 0.8
<b>Mid</b>	1.5 $\pm$ 0.3	1.5 $\pm$ 0.6	1.5 $\pm$ 0.6	1.5 $\pm$ 0.6	3.2 $\pm$ 0.9
<b>Surface</b>	1.7 $\pm$ 0.4	1.0 $\pm$ 0	1.5 $\pm$ 0.6	1.5 $\pm$ 0.6	3.3 $\pm$ 0.9

**Table 3.8: Intensity of membranous  $\beta$ 1-integrin staining in human tissues of the MDCS.** Mean  $\pm$  SEM; n = 6. Full raw data can be seen in Appendix 7, page 259.

$\beta$ 1-integrin showed a significant increase in the cytoplasmic staining intensity between the basal and surface topographical zones along with the mid and surface locations for the normal squamous tissue (Table 3.9).

Antibody	Staining Type	Tissue Type	Comparison Between Topographical Location	Significance Value
$\beta$ 1-integrin	Cytoplasmic	Normal Squamous	Basal vs. Surface	<b>P&lt;0.01</b>
$\beta$ 1-integrin	Cytoplasmic	Normal Squamous	Mid vs. Surface	<b>P&lt;0.01</b>

**Table 3.9:  $\beta$ 1-integrin statistical analysis.** A one way ANOVA with Tukey's post hoc test was used to investigate the significant difference when comparing the  $\beta$ 1-integrin intensity staining scores between the topographical locations, within different tissue types. The mean difference was either significant at the 0.01 level, n = 6. Full statistical analysis can be seen in Appendix 7, pages 258 and 259.

Within the IHC data it was also possible to look at other trends in the staining intensity data for each antibody under investigation. However, this was not executed in this study as it was felt that 6 patients was not a large enough sample size to perform such detailed statistical analysis. Investigation into areas such as the comparison of staining type and intensity staining scores within the same topographical locations between separate tissues for the same antibody or even different antibodies, may be worthy of future investigation.

### 3.4.3 BrdU IHC on Control Cells and Tissues

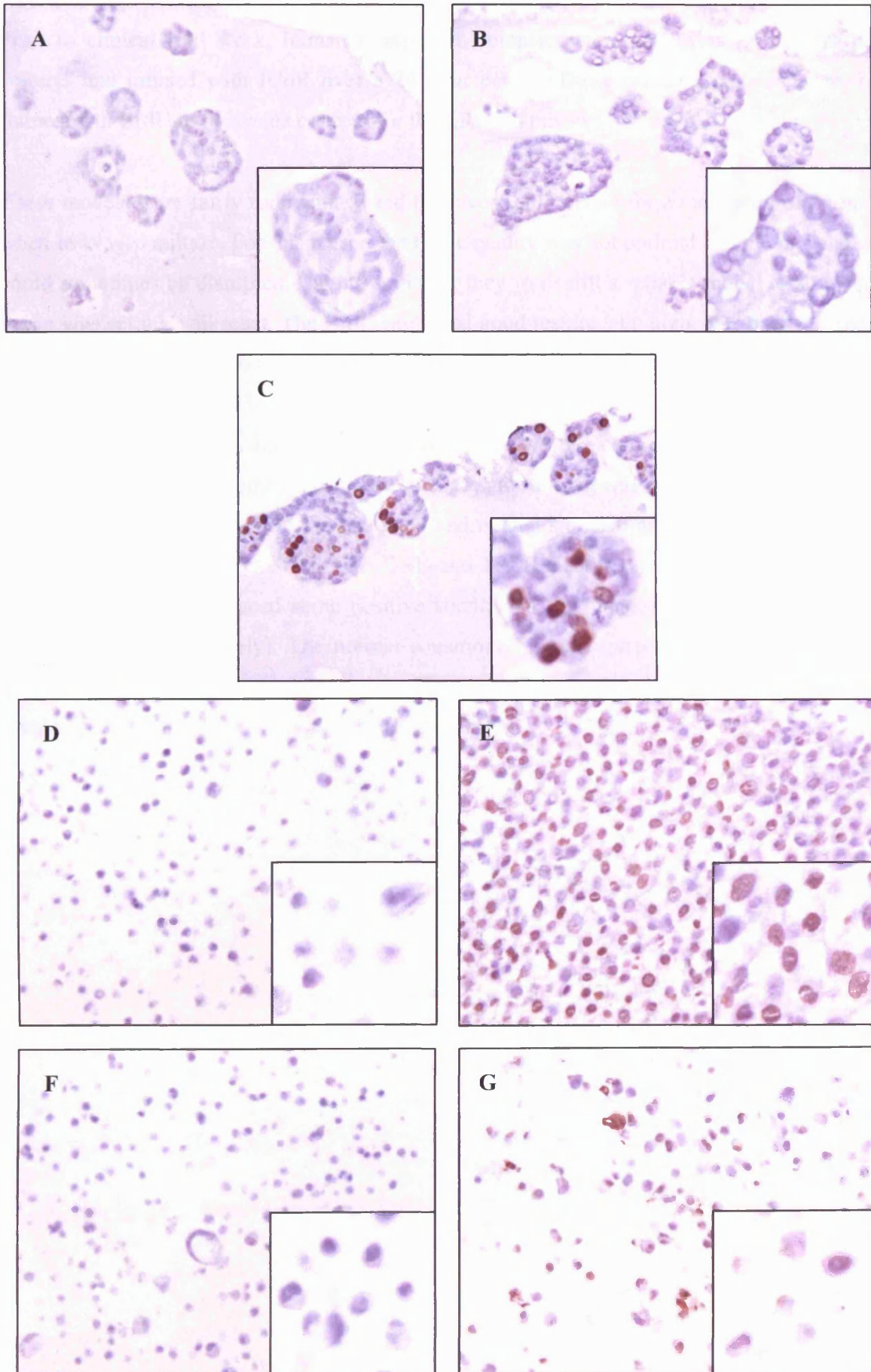
#### 3.4.3.1 *Cytoblock Immunoreactivity Controls*

In each of the cytochrome immunoreactivity experiments undertaken in this Chapter a breast carcinoma cell line, kindly provided by J. Luckett, was utilised as both the positive and negative experimental controls. This consisted of MCF-7 cells which had been grown in matrigel for 7 days and infused with a 5mM solution of BrdU for 3 hours prior to fixation. To act as a negative control this was incubated with either a NPA control or an isotype-matched control. The isotype-matched control was the DakoCytomation IgG<sub>1</sub> (catalogue number: X0931), which was adjusted to the same concentration as the primary antibody in each experiment. To act as a positive control it was incubated with the appropriate concentration of the BrdU DakoCytomation IgG<sub>1</sub> (catalogue number: MO744).

As IUdR is not found naturally in any tissue or organ it was also necessary to produce internal tissue controls. OE-21 and TE-7 cell lines were stimulated with either growth media containing 40µg/ml of IUdR for the positive controls or grown in normal growth media to act as internal negative controls, as detailed in section 2.2.2.4.

In this Chapter full details of when and where these controls were utilised can be found in the figure legends. However, it should be noted that under all conditions these worked and produced the expected staining, as can be seen from Figure 3.8, which has been put together as an example. When used as a negative control, using either the NPA or isotype-matched antibody, all sections of the MCF-7 cytochrome were free from background and non-specific staining (Figures 3.8A and 3.8B respectively). When used as a positive control strong staining was seen throughout the section (Figure 3.8C). The OE-21 and TE-7 cytochromes also worked when incubated with the appropriate concentration of the BrdU DakoCytomation IgG<sub>1</sub> (catalogue number: MO744) with the non-infused cytochromes showing no positive staining for both OE-21 cells (Figure 3.8D), and TE-7 cells (Figure 3.8F), and the infused cytochromes produced strong staining which was free from any background staining for both OE-21 cells (Figure 3.8E) and TE-7 cells (Figure 3.8G). Where appropriate suitable positive control tissues were also utilised in each experiment and specific details of these can be found in each figure legend.

**Figure 3.8 - BrdU immunohistochemical analysis on experimental control cells.** The primary antibody was clone Bu20a used at a final concentration of 6.3µg/ml. HRP conjugated St-ABC was used as the tertiary detection system with DAB as the chromogen. (A) MCF-7 cell line negative control, (B) MCF-7 isotype matched negative control, (C) MCF-7 positive control, (D) OE-21 control cell line with no expression of IUdR, (E) IUdR treated OE-21 cell line with expression of IUdR, (F) TE-7 control cell line with no expression of IUdR, (G) IUdR treated TE-7 cell line with expression of IUdR. Magnification is x25 for all main images and x40 for all higher powered inserts.



#### 3.4.3.2 Primary Explant Immunoreactivity Controls

Prior to clinical trial work, human oesophageal biopsies were set up as primary explant cultures and infused with IUdR over a 24 hour period. These primary explants were then stained with BrdU to prove the concept for the LRCs in this *ex vivo* model.

These models were fairly rudimentary and they were only viable for a maximum of 24 hours when in *ex vivo* culture. For this reason the tissue quality was not optimal and the morphology could sometimes be disrupted. Having said this, they were still a reliable model to show how the *in vivo* setting will react. The BrdU produced good results, although as expected some of the tissue morphology was compromised. The NPA negative controls and isotype matched controls worked well and were free from any background staining when DAB was used as the chromogen (Figures 3.9A and 3.9C respectively). The positive control showed strong positive staining (Figure 3.9B). Some non-specific background staining was observed for this antibody at a 6.3 $\mu$ g/ml concentration in the untreated and treated stomach and also the untreated and treated BM tissues (Figures 3.9D, 3.9E, 3.9H and 3.9I respectively). The treated stomach and treated BM tissues produced some positive staining in the glandular surface cells (Figures 3.9E, and 3.9I respectively). The normal squamous explants gave the best results with the untreated giving no background staining (Figures 3.9F) and the treated producing positive staining in the cells of the basal papillae (Figure 3.9G).

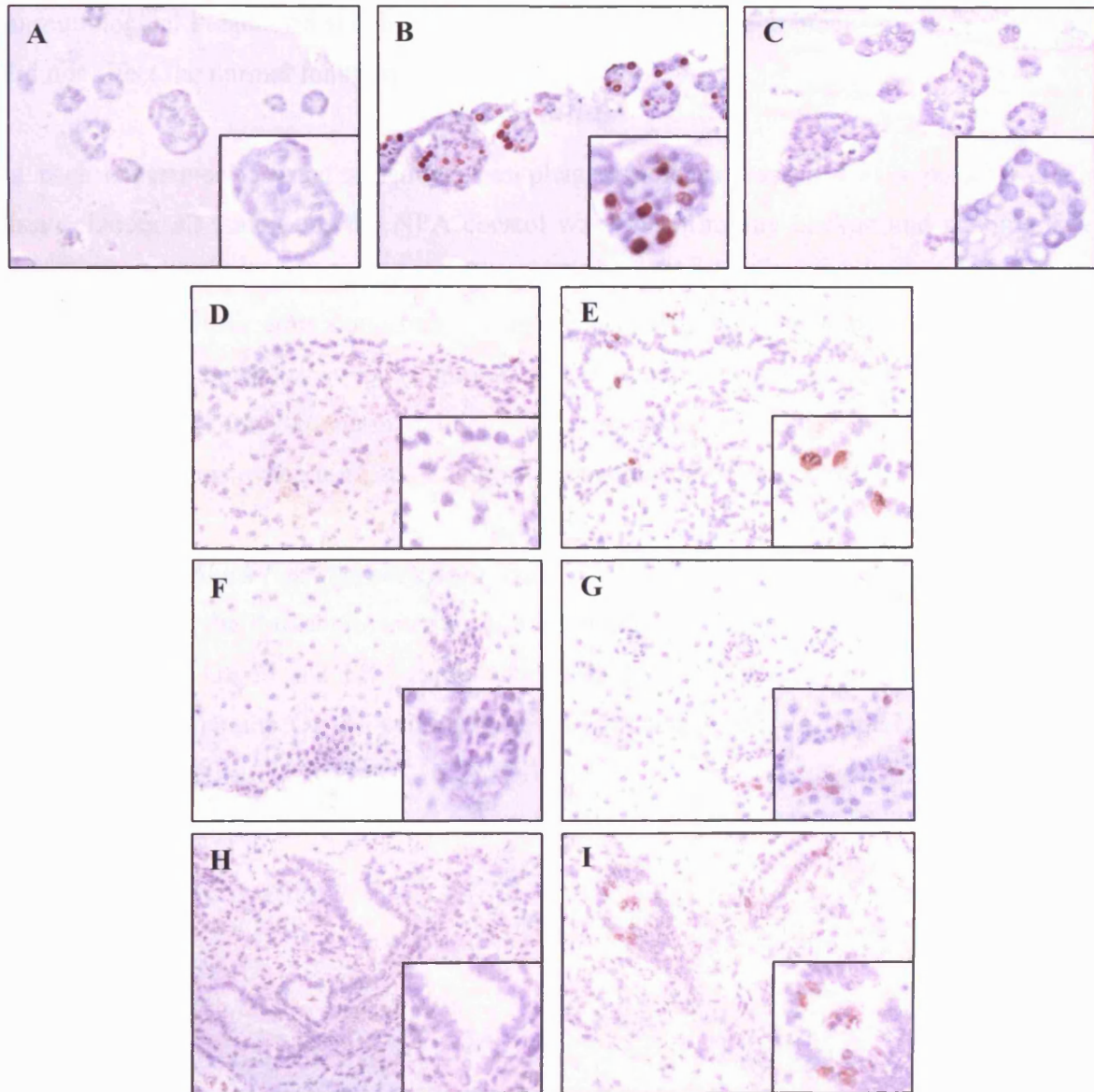


**Figure 3.9 - BrdU immunohistochemical analysis on primary explant control tissues.** The primary antibody was clone Bu20a used at a final concentration of 6.3 $\mu$ g/ml. HRP conjugated St-ABC was used as the tertiary detection system with DAB as the chromogen. (A) MCF-7 cell line negative control, (B) MCF-7 positive control, (C) MCF-7 isotype matched negative control, (D) Untreated primary stomach explant with no expression of IUdR, (E) IUdR treated primary stomach explant with expression of IUdR, (F) Untreated primary squamous explant with no expression of IUdR, (G) IUdR treated primary squamous explant with expression of IUdR, (H) Untreated primary BM explant with no expression of IUdR, (I) IUdR treated primary BM explant with expression of IUdR. Magnification is x25 for all main images and x40 for all higher powered inserts.

### 3.4.4 P-cadherin IHC on Cytoblock Control Cells

#### 3.4.4.1 *Cytoblock Immunoreactivity Controls*

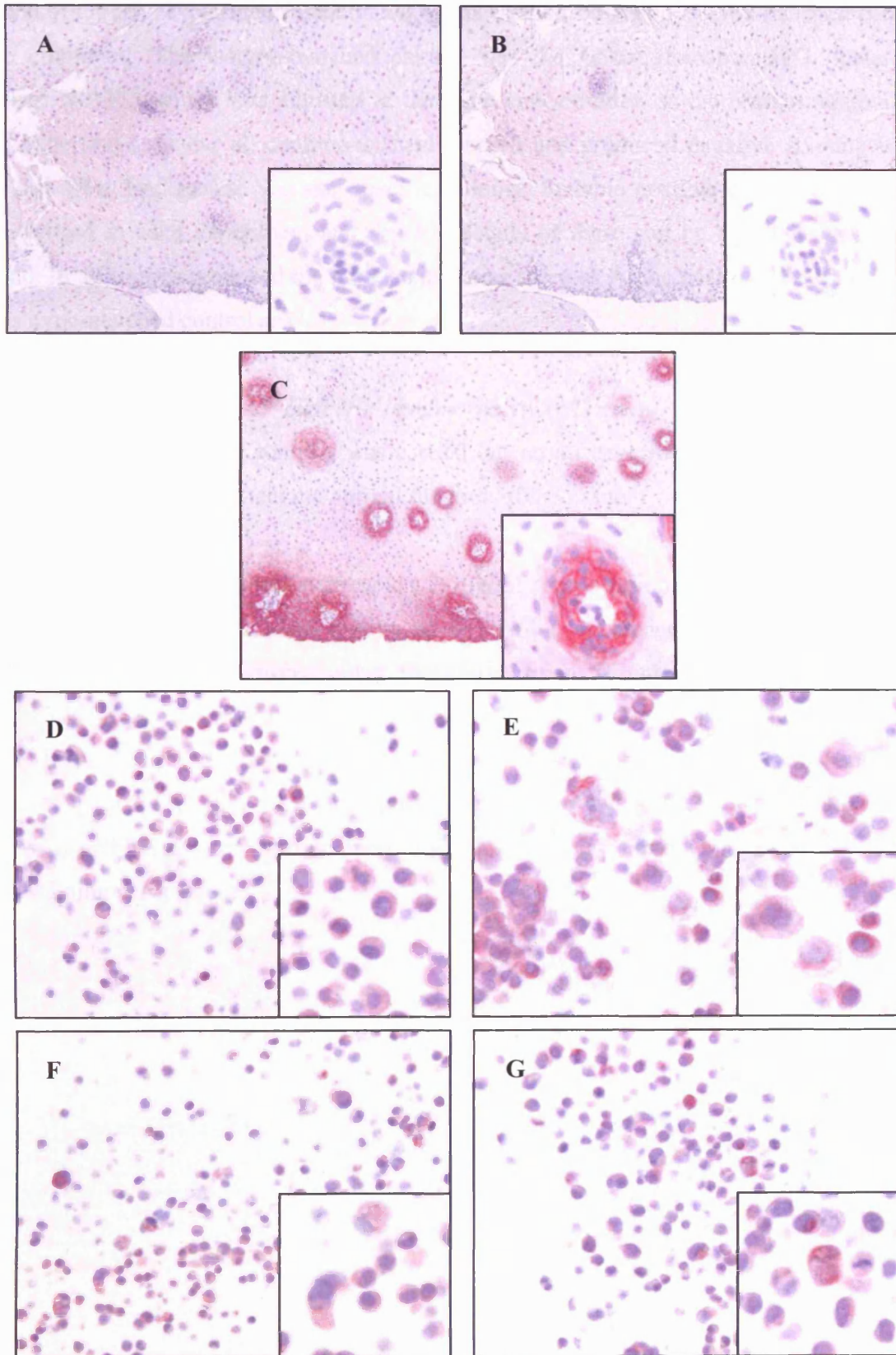
Immunological P-cadherin staining was carried out on control cytoblocks to ensure that IUdR did not affect the normal function of the tissue.

In each experiment normal squamous oesophageal mucosa was used as a positive control tissue. Under all conditions the NPA control was free from any background staining when Fast Red was used as the chromogen (Figure 3.10A). The isotype matched negative control was adjusted to the same concentration as the primary antibody and also produced good results with no staining observed (Figure 3.10B). Squamous oesophageal mucosa was used as a positive control for P-cadherin staining. Membranous P-cadherin staining was confined to the basal epidermis, when used at a 2.5µg/ml concentration (Figure 3.10C).

#### 3.4.4.2 *Cytoblock Immunoreactivity Tissues*

When observing the P-cadherin staining at a 2.5µg/ml concentration in both the IUdR infused and non-infused OE-21 and TE-7 cytoblocks no observable difference in expression was seen between either the OE-21 cells (Figures 3.10D and 3.10E) or the TE-7 cells (Figures 3.10F and 3.10G).

**Figure 3.10 – P-cadherin IHC analysis on cytoblock experimental controls and cytoblock control cells.** The primary antibody was clone 56, 610227 used at a final concentration of 2.5µg/ml with a 20 minute microwave antigen retrieval step. AP conjugated St-ABC was used as the tertiary detection system with Fast Red as the chromogen. (A) NPA normal squamous negative control, (B) Isotype matched normal squamous negative control, (C) Normal squamous positive control with expression of P-cadherin, (D) OE-21 control cytoblock with expression of P-cadherin, (E) IUdR treated OE-21 cytoblock with expression of P-cadherin, (F) TE-7 control cytoblock with expression of P-cadherin, (G) IUdR treated TE-7 cytoblock with expression of P-cadherin. Magnification is x25 for all main images and x40 for all higher powered inserts.



### 3.4.5 IHC on Experimental Cells and Tissues

#### 3.4.5.1 *Immunoreactivity Controls*

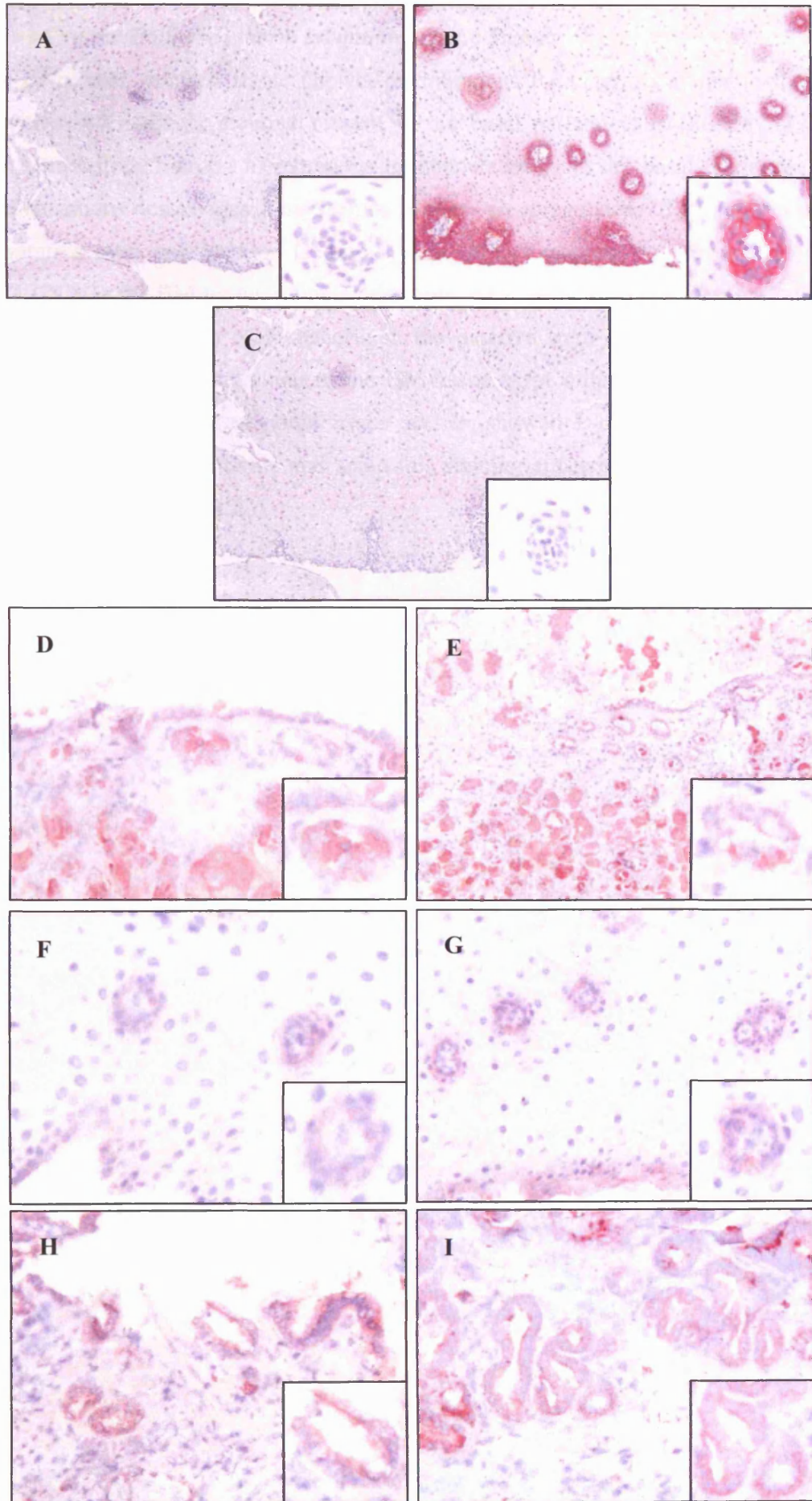
In each of the IHC experiments undertaken in this Chapter NPA and isotype-matched controls were employed. The isotype-matched control was the DakoCytomation IgG<sub>1</sub> (catalogue number: X0931), which was adjusted to the same concentration as the primary antibody in each experiment. Under all conditions these worked and produced negative staining which was free from background and non-specific staining. Suitable positive control tissues were also utilised in each experiment and specific details of these can be found in each figure legend. In all figures produced the NPA control was listed as A, the positive control as B and the isotype-matched control as C.

#### 3.4.5.2 *Primary Explant P-cadherin Immunoreactivity Tissues*

Immunological P-cadherin staining was carried out on all experimental cells and tissues to ensure that IUdR did not affect the normal function of the tissue.

When observing the P-cadherin staining at a 2.5µg/ml concentration, in both the IUdR infused and non-infused primary explant tissues, no observable difference to the expression of P-cadherin could be seen between either the gastric tissue (Figures 3.11D and 3.11E), the normal squamous tissue (Figures 3.11F and 3.11G), or the BM tissue (Figures 3.11H and 3.11I). It should be noted that there was some loss of staining between the normal squamous control (Figure 3.11B) and the explant normal squamous models (Figures 3.11F and 3.11G). The tissue architecture was fairly compromised in these tissues and while the model was not ideal, staining was present.

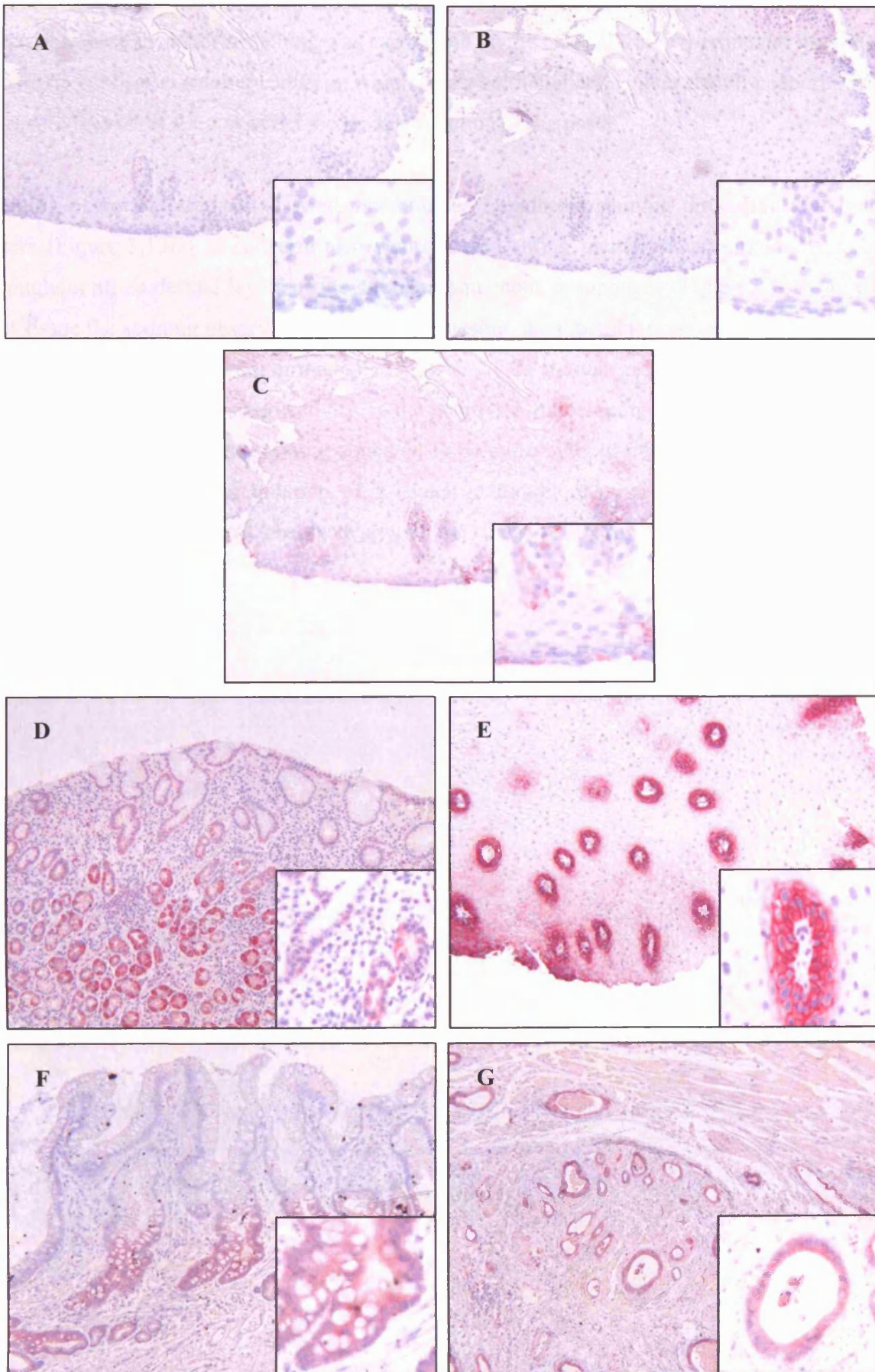
**Figure 3.11 – P-cadherin IHC analysis on primary explant tissues.** The primary antibody was clone 56, 610227 used at a final concentration of 2.5µg/ml with a 20 minute microwave antigen retrieval step. AP conjugated St-ABC was used as the tertiary detection system with Fast Red as the chromogen. (A) NPA normal squamous negative control, (B) Isotype matched normal squamous negative control, (C) Normal squamous positive control, (D) IUdR untreated primary stomach explant with expression of P-cadherin, (E) IUdR treated primary stomach explant with expression of P-cadherin, (F) IUdR untreated primary normal squamous explant with expression of P-cadherin, (G) IUdR treated primary normal squamous explant with expression of P-cadherin, (H) IUdR untreated primary BM explant with expression of P-cadherin, (I) IUdR treated primary BM explant with expression of P-cadherin. Magnification is x25 for all main images and x40 for all higher powered inserts.



#### 3.4.5.3 *Clinical Trial P-cadherin Immunoreactivity Tissues*

Staining of normal stomach tissue showed membranous P-cadherin staining in the apical layers with much stronger staining present in the basal parietal cells (Figure 3.12D). P-cadherin demonstrated strong membranous immunoreactivity at the basal epidermis of the stratified squamous oesophagus. This seemed to show an upregulation of P-cadherin staining in the putative stem cell location (Figure 3.12E), when compared to the positive control (Figure 3.12C). In the BM tissue, staining was more cytoplasmic than membranous, and there was clearly an upregulation of P-cadherin in the putative stem cell compartment. This is where most proliferation occurs and in the BM tissue crypt bifurcation could also be seen (Figure 3.12F). The adenocarcinoma tissue section showed P-cadherin immunoreactivity throughout all layers of the tissue and again this staining appeared to be more cytoplasmic than membranous (Figure 3.12G).

**Figure 3.12 – P-cadherin IHC analysis on clinical trial tissues.** The primary antibody was clone 56, 610227 used at a final concentration of 2.5µg/ml with a 20 minute microwave antigen retrieval step. AP conjugated St-ABC was used as the tertiary detection system with Fast Red as the chromogen. (A) NPA normal squamous negative control, (B) Isotype matched normal squamous negative control, (C) Normal squamous positive control, (D) ST001 patient recruit with 7 day IUdR infusion on gastric tissue with expression of P-cadherin, (E) ST001 patient recruit with 7 day IUdR infusion on normal squamous tissue with expression of P-cadherin, (F) ST002 patient recruit with 7 day IUdR infusion on IM tissue with expression of P-cadherin, (G) ST002 patient recruit with 7 day IUdR infusion on adenocarcinoma tissue with expression of P-cadherin. Magnification is x10 for all main images and x40 for all higher powered inserts.

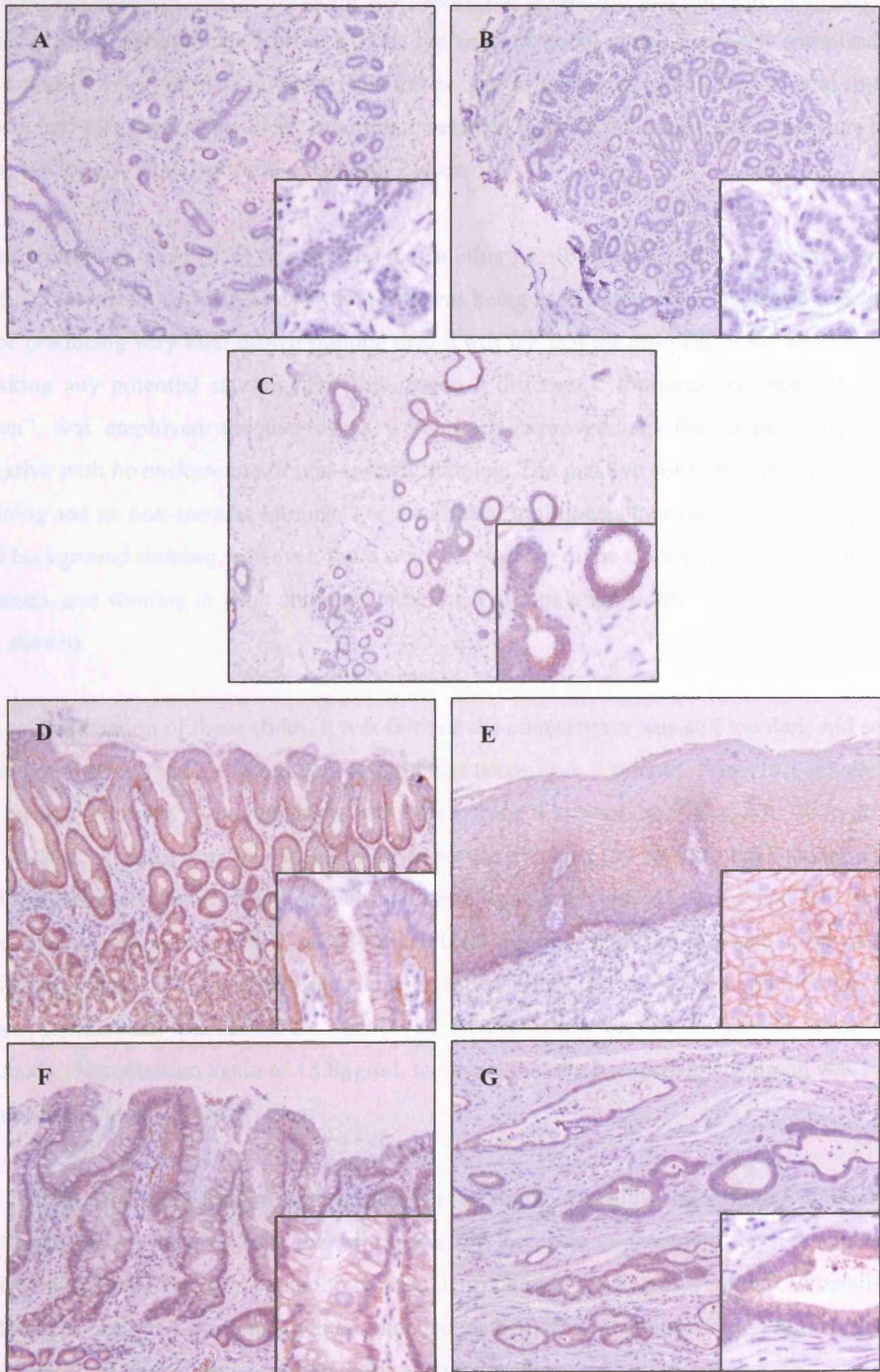


#### 3.4.5.4 *Clinical Trial E-cadherin Immunoreactivity Tissues*

Immunological E-cadherin staining was carried out on the clinical trial experimental tissues to enable us to observe another cadherin, which labels epithelial cells, other than P-cadherin, and to ensure that IUdR did not affect the normal function of the tissue.

Staining of normal stomach showed membranous E-cadherin staining throughout all tissue layers (Figure 3.13D). E-cadherin also demonstrated strong membranous immunoreactivity throughout all epidermal layers of the stratified squamous oesophagus (Figure 3.13E). In the BM tissue the staining observed was more cytoplasmic than membranous, and again this was expressed to the same degree throughout all tissue layers and was not upregulated, unlike the case with P-cadherin immunoreactivity, in the putative stem cell compartment (Figure 3.13F). The adenocarcinoma tissue staining appeared to be more cytoplasmic than membranous and seemed to show a downregulation of E-cadherin immunoreactivity throughout the tissue however, staining was still observed around the areas of highly dysplastic tissue (Figure 3.13G).

**Figure 3.13 – E-cadherin IHC analysis on clinical trial tissues.** The primary antibody was clone HECD-1, Ab1416 used at a final concentration of 13.3µg/ml with a 2 minute pressure cooker antigen retrieval step. HRP conjugated St-ABC was used as the tertiary detection system with DAB as the chromogen. (A) NPA normal breast negative control, (B) Isotype matched normal breast negative control, (C) Normal breast positive control, (D) ST001 patient recruit with 7 day IUdR infusion on gastric tissue with expression of E-cadherin, (E) ST001 patient recruit with 7 day IUdR infusion on normal squamous tissue with expression of E-cadherin, (F) ST002 patient recruit with 7 day IUdR infusion on IM tissue with expression of E-cadherin, (G) ST002 patient recruit with 7 day IUdR infusion on adenocarcinoma tissue with expression of E-cadherin. Magnification is x10 for all main images and x40 for all higher powered inserts.



#### 3.4.6 Method Development for BrdU IHC on Clinical Trial Tissues

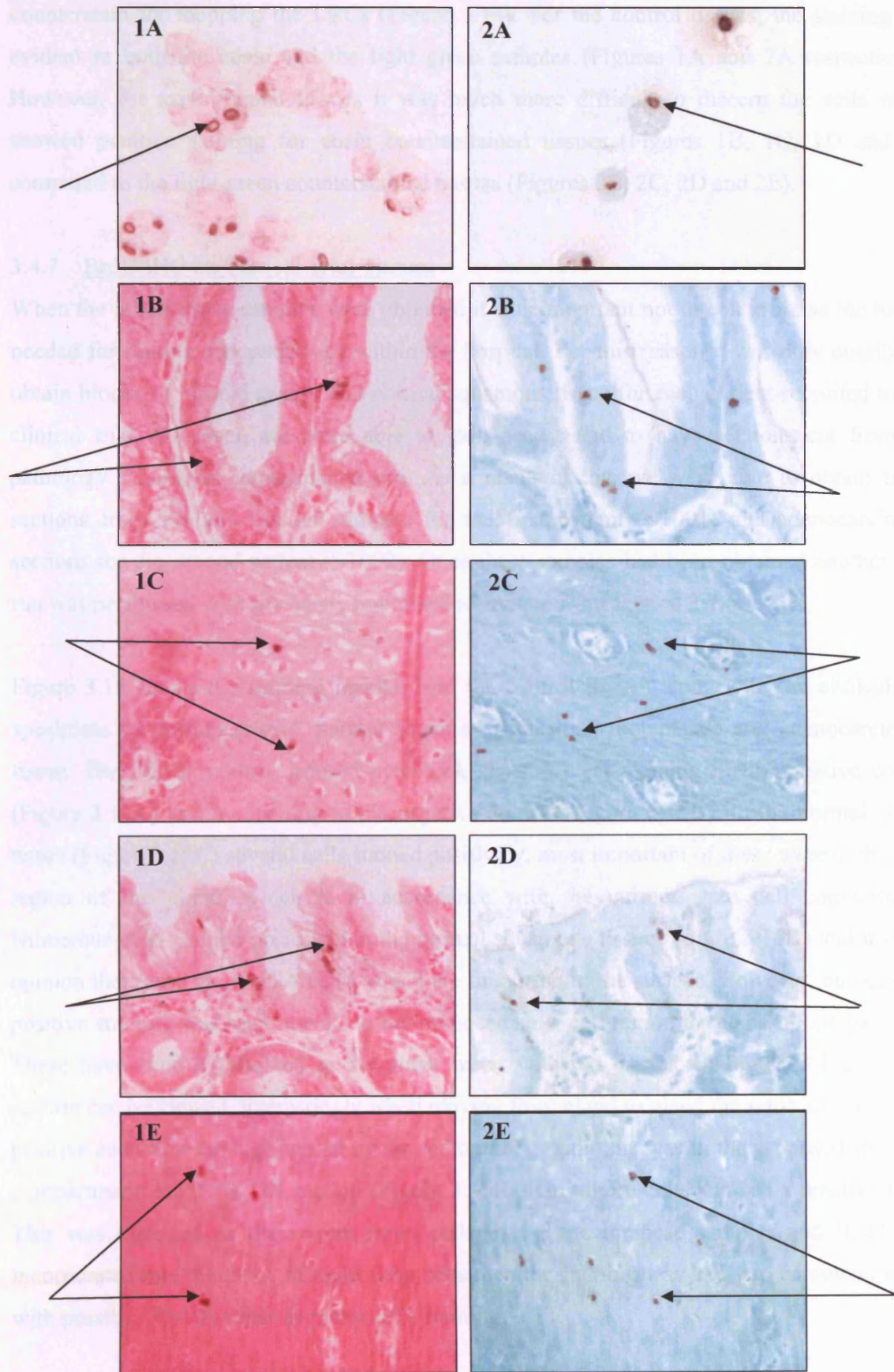
Method development and optimisation was carried out to confirm that the BrdU antibody was working to its optimal capabilities. Firstly, the same protocol which had been optimised for the controls was employed however; this did not produce staining in the clinical trial tissues. It was first thought that the 7 day time frame between infusion and tissue collection may have been too long to show LRCs in a tissue specimen.

After looking at the slides it was decided that another possible factor could be the use of eosin as the counterstain. Due to the fact that DAB was being used as the chromogen and was likely to be producing very faint brown staining then it was felt that the red/pink of the eosin may be masking any potential staining. For this reason a different cytoplasmic counterstain “light green”, was employed and the results were much improved. All the control slides were negative with no background or non-specific staining. The positive controls also showed good staining and no non-specific staining. For the clinical trial tissues there was some non-specific and background staining, however, there was also staining in the stem cell area of the stomach sections, and staining in what appeared to be the TA population in the squamous tissue (data not shown).

On re-examination of these slides, it was felt that the counterstain was still too dark and so the emersion time in the light green counterstain was taken from 4 minutes down to 1 minute and the primary antibody concentration was taken from 6.3 $\mu$ g/ml to 9.43 $\mu$ g/ml. A hydrogen peroxidase blocking step was added to try to reduce non-specific background staining due to endogenous peroxidase activity, which had been present in some of the tissues. The results from these slides indicated that this additional blocking step should be included in the method as this eliminated the previously seen background staining. It was also decided that the ‘light green’ counterstain was now at the right level, however it was decided to increase the primary antibody concentration again to 18.8 $\mu$ g/ml, to ensure that the best possible staining was being achieved (data not shown).

As a final IHC optimisation slides were run in duplicate using the primary antibody at 18.8 $\mu$ g/ml and comparing both the light green and the eosin counterstain for 1 minute each. This would enable the best method to be used in all future experiments. Figure 3.14 details the differences observed when using either an eosin or light green counterstain on normal gastric and normal squamous tissue for both clinical trial patients.

**Figure 3.14 - BrdU IHC comparison analysis on experimental control tissues using different counterstains.** The primary antibody was clone Bu20a used at a final concentration of 18.8 $\mu$ g/ml. HRP conjugated St-ABC was used as the tertiary detection system with DAB as the chromogen. (1A) MCF-7 positive control using an eosin counterstain, (1B) ST001 patient recruit with 7 day IUdR infusion on normal gastric tissue using an eosin counterstain, (1C) ST001 patient recruit with 7 day IUdR infusion on normal squamous tissue using an eosin counterstain, (1D) ST002 patient recruit with 7 day IUdR infusion on normal gastric tissue using an eosin counterstain, (1E) ST002 patient recruit with 7 day IUdR infusion on normal squamous tissue using an eosin counterstain, (2A) MCF-7 positive control using a light green counterstain, (2B) ST001 patient recruit with 7 day IUdR infusion on normal gastric tissue using a light green counterstain, (2C) ST001 patient recruit with 7 day IUdR infusion on normal squamous tissue using a light green counterstain, (2D) ST002 patient recruit with 7 day IUdR infusion on normal gastric tissue using a light green counterstain, (2E) ST002 patient recruit with 7 day IUdR infusion on normal squamous tissue using a light green counterstain. Magnification is x40 for all main images. Arrows indicate examples of positive staining in each tissue section.



These data revealed that the use of a light green counterstain was superior to the eosin counterstain for mapping the LRCs (Figure 3.14). For the control tissues, the staining was evident in both the eosin and the light green samples (Figures 1A and 2A respectively). However, for experimental tissues it was much more difficult to discern the cells which showed positive staining for eosin counterstained tissues (Figures 1B, 1C, 1D and 1E) compared to the light green counterstained tissues (Figures 2B, 2C, 2D and 2E).

#### 3.4.7 BrdU IHC on Clinical Trial Tissues

When the initial tissue samples were obtained it was important not to compromise the tissues needed for routine histopathology within the hospital. For this reason it was only possible to obtain blocks of normal gastric and normal squamous tissue for each patient recruited to this clinical trial. However, we were able to gain access and to have sections cut from the pathology blocks for experimental use. As a result of this we were able to obtain tissue sections from IM and tumour samples for the first patient (ST001) and adenocarcinoma sections for the second patient (ST002). Once these samples had been obtained another IHC run was performed with the newly optimised technique from section 3.4.6.

Figure 3.15 shows the staining results from the control tissues along with the clinical trial specimens of normal gastric, normal squamous, intestinal metaplastic and adenocarcinoma tissue. The OE-21 control infused cyto block showed clear staining in the positive control (Figure 3.15A) and no staining in the negative control (Figure 3.15B). In the normal gastric tissue (Figure 3.15C) several cells stained positively, most important of these were in the neck region of the gland, which is in accordance with the current stem cell compartment. Numerous cells stained positively in the normal squamous tissue (Figure 3.15D) and it is our opinion that these are the TA cells, which are migrating to the surface. However, on occasion positive staining was seen in cells in the proposed stem cell region in the basal compartment. These have been highlighted in the upper insert with red circles. In Figure 3.15E the IM section can be viewed, interestingly when moving from gland to gland the same area appeared positive each time (as highlighted by the red circles), again this was in the proposed stem cell compartment. With the OA section (Figure 3.15F) many more cells showed a positive label. This was expected as there were more cells in s-phase in these samples and IUdR was incorporated into the DNA of replicating cells then the staining was likely to be much higher, with possibly 30-100 times as many cells staining.

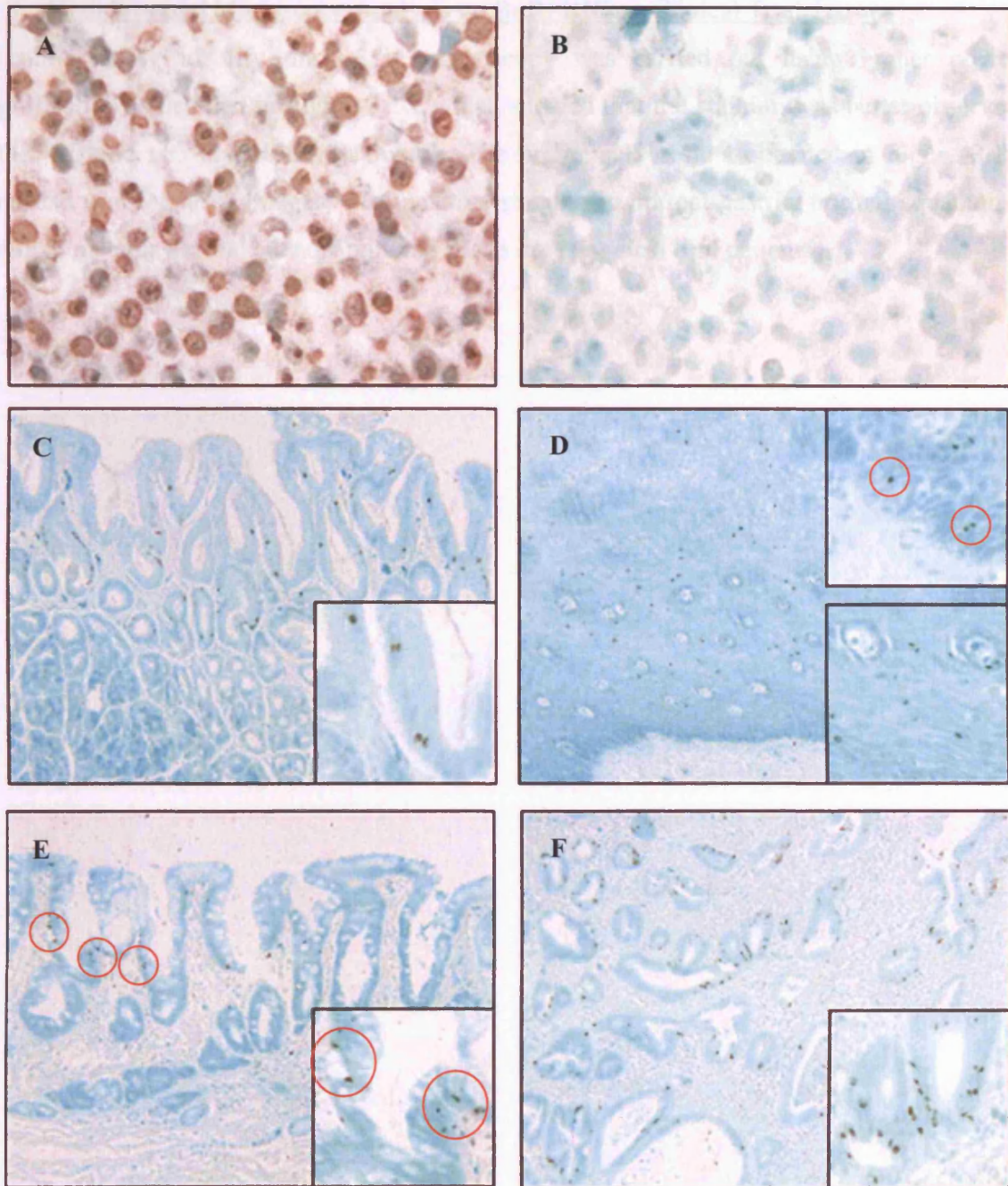


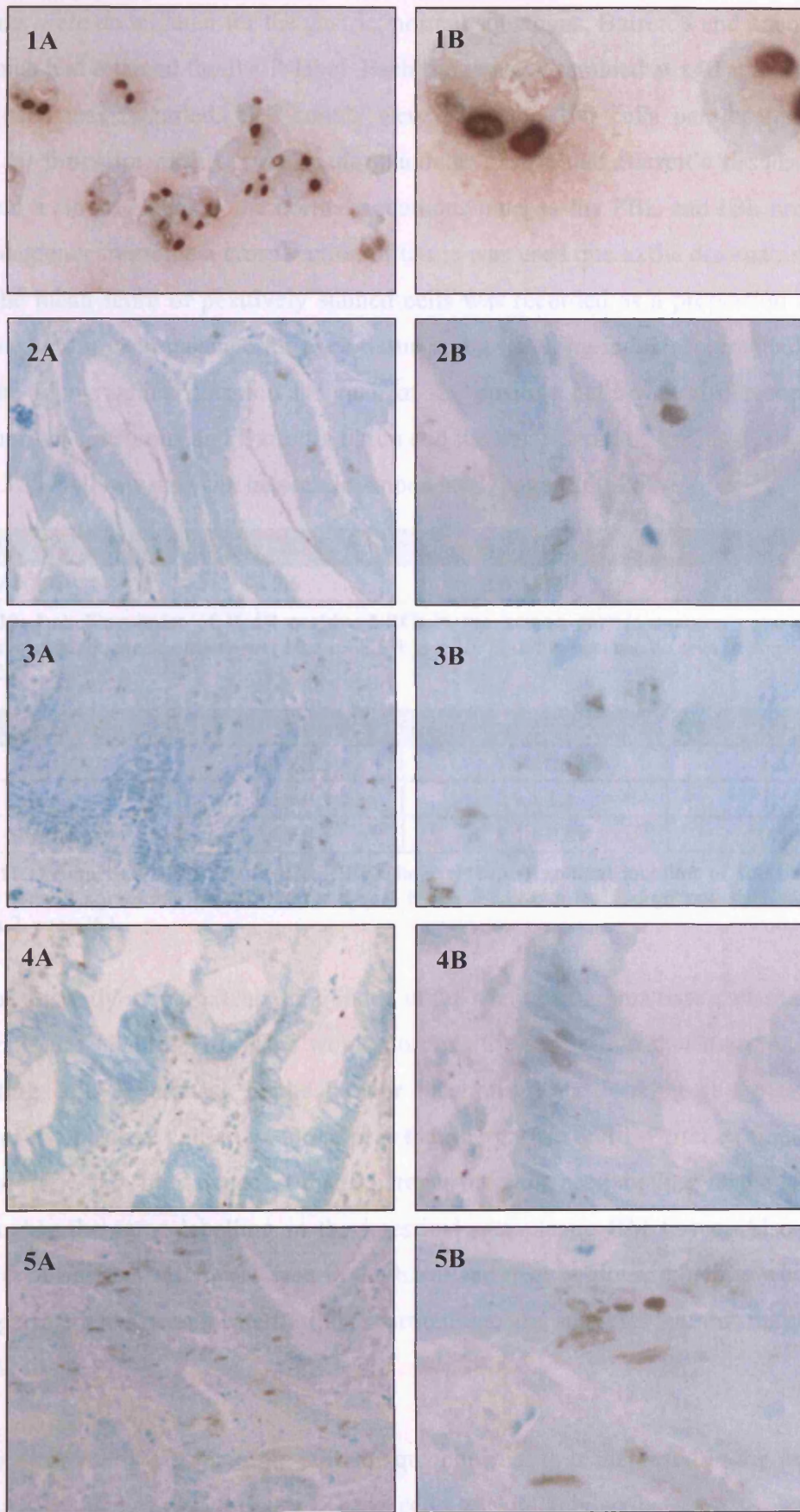
**Figure 3.15 – BrdU IHC analysis on clinical trial tissues.** The primary antibody was clone Bu20a used at a final concentration of 18.8 $\mu$ g/ml. HRP conjugated St-ABC was used as the tertiary detection system with DAB as the chromogen. (A) OE-21 positive control using a light green counterstain, (B) NPA OE-21 positive control using a light green counterstain, (C) ST001 patient recruit with 7 day IUdR infusion on normal stomach tissue using a light green counterstain, (D) ST001 patient recruit with 7 day IUdR infusion on normal squamous tissue using a light green counterstain, (E) ST002 patient recruit with 7 day IUdR infusion on IM tissue using a light green counterstain, (F) ST002 recruit with 7 day IUdR infusion on OA tissue using a light green counterstain. Magnification is x25 for images A and B and x10 for all other main images. All higher powered inserts are at x40.

#### 3.4.8 High Powered Microscope Analysis on BrdU IHC on Clinical Trial Tissues

To more clearly identify the LRCs, microscopy was carried out using higher power magnification as detailed in Figure 3.16, which showed that the staining was better observed in the x20 and x63 magnification images. The preliminary results obtained in Figure 3.15 were also true for these images, with positive staining in normal gastric, normal squamous, intestinal metaplastic and adenocarcinoma tissue in the clinical trial patients.

**Figure 3.16 – High powered BrdU IHC analysis on clinical trial tissues.** The primary antibody was clone Bu20a used at a final concentration of 18.8µg/ml. HRP conjugated St-ABC was used as the tertiary detection system with DAB as the chromogen. (1A and 1B) MCF-7 positive control using a light green counterstain, (2A and 2B) ST001 patient recruit with 7 day IUdR infusion on normal gastric tissue using a light green counterstain, (3A and 3B) ST001 patient recruit with 7 day IUdR infusion on normal squamous tissue using a light green counterstain, (4A and 4B) ST002 patient recruit with 7 day IUdR infusion on intestinal metaplastic tissue using a light green counterstain, (5A and 5B) ST002 patient recruit with 7 day IUdR infusion on adenocarcinoma tissue using a light green counterstain. Magnification is x20 for all primary images, i.e. those listed as A and x63 for all secondary images, i.e. those listed as B.

3.4.4. Localization of IDH1 LRC in Clinical Tissue



### 3.4.9 Labelling Index of IUdR LRC's in Clinical Trial Tissues

Cell counts were undertaken for the gastric, normal squamous, Barrett's and adenocarcinoma tissue which had retained the IUdR label. Each tissue was examined at x40 and the number of positive cells was recorded. Cell counts were based on 100 cells per location and were repeated 10 times for each tissue. In the glandular gastric and Barrett's tissues each count focused on a single gland, in the normal squamous mucosa the PBL and IBL area was used and in the adenocarcinoma a cross section of tissue was used due to the disorganisation of the tissue. The mean score of positively stained cells was recorded as a proportion of the 1000 cell total count in each instance for each tissue and a labelling index score calculated (Table 3.10). The topographical location for each of the positive cells was also recorded for the gastric, normal squamous and Barrett's tissue and the mean score of this analysis can be seen in Table 3.11. All raw data can be seen in Appendix 7, pages 260-262.

Gastric	Normal Squamous	Intestinal Metaplasia	Adenocarcinoma
3.8 ± 1.0	5.9 ± 2.6	3.5 ± 1.1	23.7 ± 4.3

**Table 3.10: Labelling index of IUdR positive LRCs in the human gastric mucosa, normal squamous, Barrett's and adenocarcinoma tissue.** Mean ± SEM; n = 10. Full raw data can be seen in Appendix 7, pages 260 and 261.

Topographical Location	Gastric	Normal Squamous	Intestinal Metaplasia
Basal	1.8 ± 0.5	1.6 ± 0.9	1.5 ± 0.6
Mid	1.6 ± 0.5	2.9 ± 1.3	1.3 ± 0.4
Surface	0.4 ± 0.7	1.4 ± 0.8	0.7 ± 0.4

**Table 3.11: Proportion of IUdR positive LRCs in each topographical location of the human gastric mucosa, normal squamous and Barrett's tissue.** Mean ± SEM; n = 10. Full raw data can be seen in Appendix 7, page 262.

There was a greatly increased labelling index in the adenocarcinoma tissue when compared to the other tissues (Table 3.10). This would confirm the suggestion that there are a lot more proliferating cells in s-phase in the tumour location. When looking at the topographical location of the positive cells it would appear that the gastric and IM tissue mimic each other fairly closely, which might suggest that wherever the cells are labelling in the stomach they show roughly the same labelling in the intestinal metaplastic BM tissue. Also the highest proportion of positive cells were seen in the basal and neck regions, which is where the stem cell compartment has been located for the gastric tissue and suggests that this may also be true of the BM tissue.

The number of positive cells in the normal squamous tissue is increased in the mid zone and relatively high in the surface layer. These cells are unlikely to be stem cells, due to the location, and what is much more likely that most of these are TA cells which are residing in

the mucosa for more than 7 days. The positive cells in the basal zone of the squamous mucosa are the potential stem cells (Table 3.11).

#### 3.4.10 Double Labelling IHC on Clinical Trial Tissues

Double labelling analysis was attempted to compare BrdU with one of each of the following proliferation markers, either proliferating cell nuclear antigen (PCNA), or Ki-67, on serial sections of the clinical trial experimental tissues. For this method DAB enhanced nickel was used as the chromogen for the BrdU staining, and then nova red was used as the chromogen for detecting either the Ki-67 or PCNA respectively (see methods section 2.2.4.10).

BrdU was used as it would detect cells which had retained the IUdR label for 7 days after the infusion. The Ki-67 will detect cells in the S phase, however the label is technically a week younger than the IUdR and so it was of interest to compare the staining patterns seen in these antibodies to enable us to see what this tissue is like 7 days later. The PCNA antibody is a marker for cells in early G1 phase as well as S phase of the cell cycle. Therefore positive staining should indicate which cells have been cycling in the last 24 hours and still have the proliferative mechanics. As such more cells should show a positive label here.

##### 3.4.10.1 *Experimental Tissue Controls*

In each experiment TE-7 IUdR infused cytoblocks were used as a control. Under all conditions the NPA control was free from any background staining and showed only the Fast Red counterstain (Figure 3.17A). TE-7 infused cytoblocks were double stained with BrdU using a DAB enhanced nickel chromogen followed by either Ki-67 or PCNA using a nova red chromogen. In the BrdU and Ki-67 double stained control (Figure 3.17B) nuclear staining could be observed for both antibodies although the amount of Ki-67 staining was reduced when compared to the PCNA staining seen in the BrdU and PCNA double staining control tissue (Figure 3.17C).

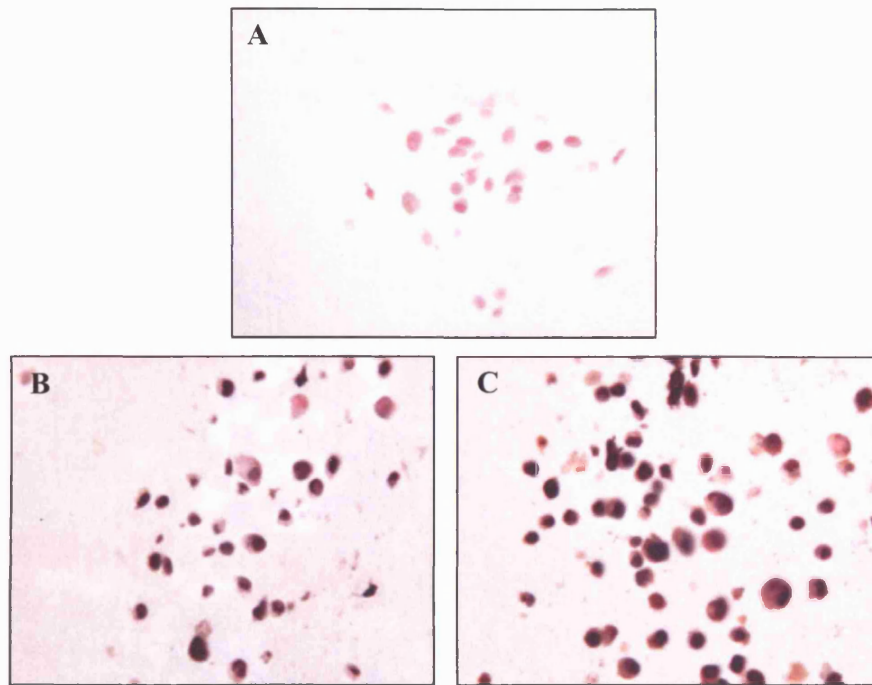


**Figure 3.17 – Double labelling IHC analysis on cytoblock control tissues.** The method used the ABC-HRP detection system and two different chromogens with Fast Red as the counterstain. The first primary antibody was BrdU, clone Bu20a, used at a final concentration of  $18.8\mu\text{g/ml}$  with a DAB enhanced nickel chromogen, and the second primary antibody was either Ki-67, clone MM1, used at a final concentration of  $0.5\mu\text{g/ml}$ ; or PCNA, clone PC10, used at a final concentration of  $0.8\mu\text{g/ml}$ , with a nova red chromogen. A microwave antigen retrieval step of 20 minutes was utilised. (A) NPA TE-7 IUdR infused cytoblock, (B) BrdU and Ki-67 double staining on TE-7 IUdR infused cytoblock showing expression of both IUdR and Ki-67, (C) BrdU and PCNA double staining on TE-7 IUdR infused cytoblock showing expression of both IUdR and PCNA. Magnification is  $\times 40$  for all images.

#### 3.4.10.2 Clinical Trial Experimental Tissues

Double staining was carried out for either BrdU and Ki-67 or BrdU and PCNA on serial sections of experimental control tissue from one of the patient recruits (ST002) enrolled on the SAINT clinical trial. Staining of matched normal oesophagus, gastric mucosa, Barrett's mucosa and adenocarcinoma tissue was undertaken. The results of this staining can be found in Figure 3.18 which has been split into 4 panels to allow images to be seen in the best conditions.

**Figure 3.18 – Double labelling IHC analysis on clinical trial experimental tissues.** The method used the ABC-HRP detection system and two different chromogens with Fast Red as the counterstain. The first primary antibody was BrdU, clone Bu20a, used at a final concentration of 18.8µg/ml with a DAB enhanced nickel chromogen, and the second primary antibody was either Ki-67, clone MM1, used at a final concentration of 0.5µg/ml; or PCNA, clone PC10, used at a final concentration of 0.8µg/ml, with a nova red chromogen. A microwave antigen retrieval step of 20 minutes was utilised. Panel One: (1A and 1B) BrdU and Ki-67 double staining on normal squamous mucosa showing expression of both IUDR and Ki-67, (2A and 2B) BrdU and PCNA double staining on normal squamous mucosa showing expression of both IUDR and PCNA. Panel Two: (3A and 3B) BrdU and Ki-67 double staining on normal gastric mucosa showing expression of both IUDR and Ki-67, (4A and 4B) BrdU and PCNA double staining on normal gastric mucosa showing expression of both IUDR and PCNA. Panel Three: (5A and 5B) BrdU and Ki-67 double staining on Barrett’s mucosa showing expression of both IUDR and Ki-67, (6A and 6B) BrdU and PCNA double staining on Barrett’s mucosa showing expression of both IUDR and PCNA. Panel Four: (7A and 7B) BrdU and Ki-67 double staining on adenocarcinoma tissue showing expression of both IUDR and Ki-67, (8A and 8B) BrdU and PCNA double staining on adenocarcinoma tissue showing expression of both IUDR and PCNA. Magnification is x25 for all images in A and x40 for all images in B.

Figure 3.18 - Panel One:

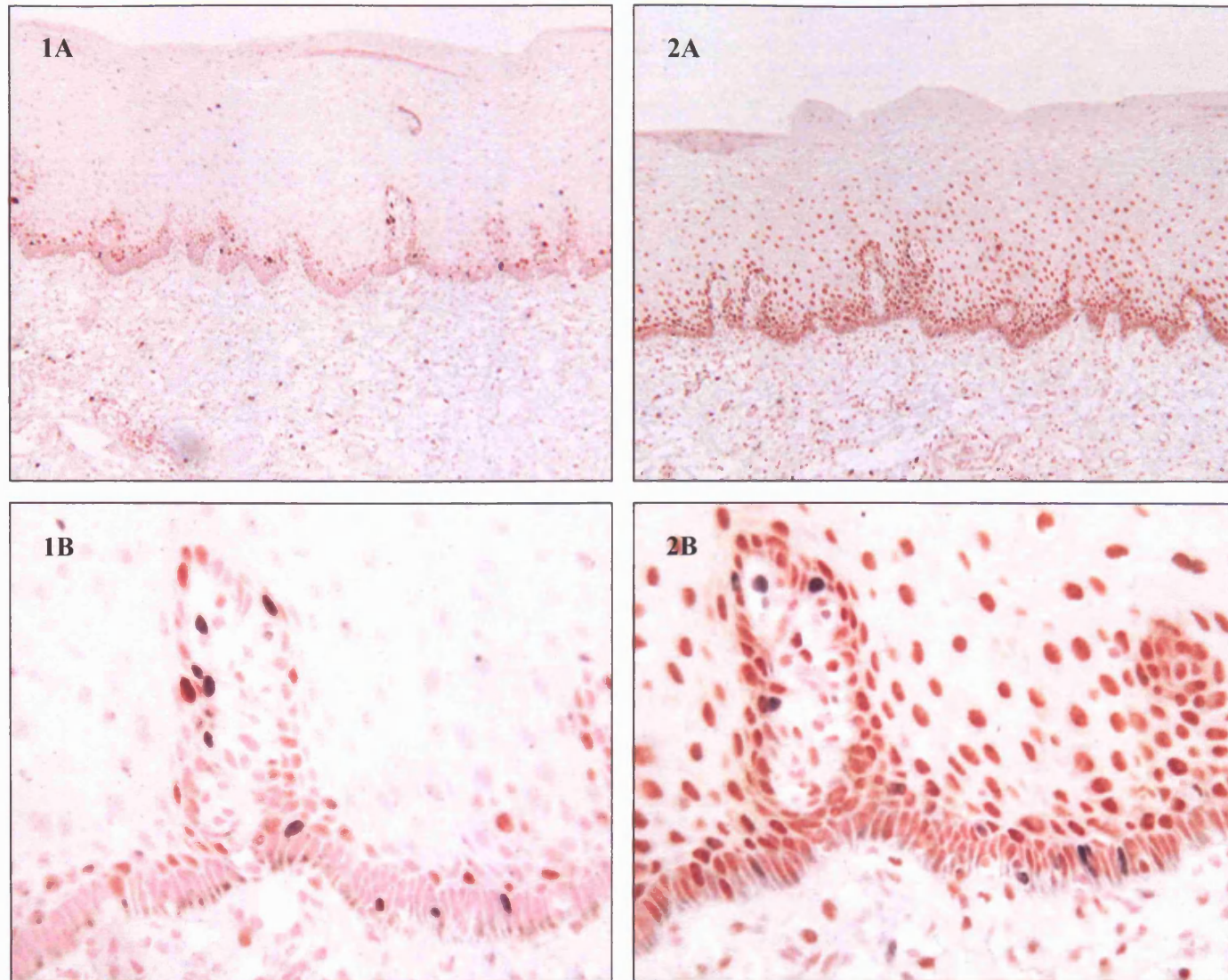


Figure 3.18 - Panel Two:

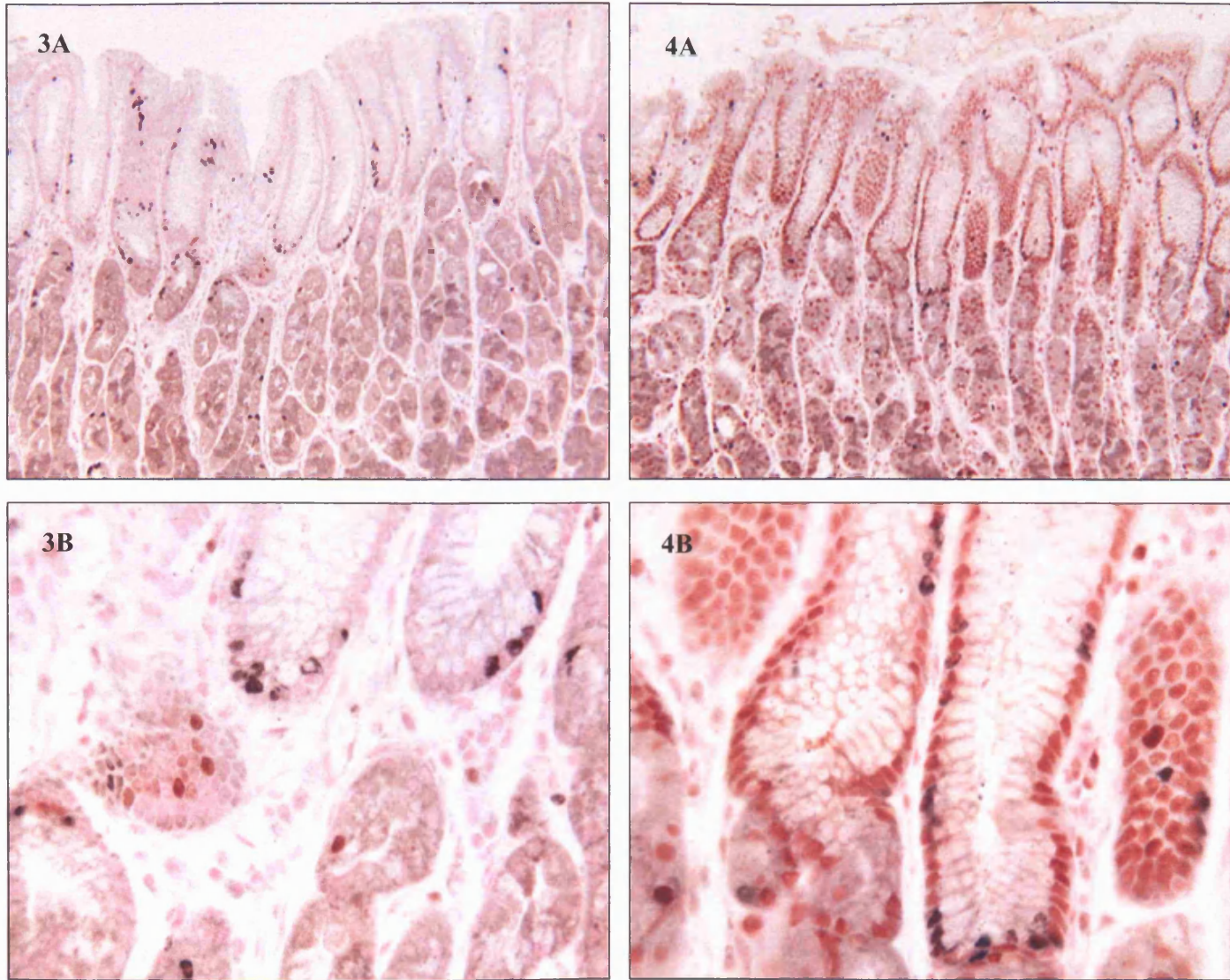


Figure 3.18 - Panel Three:

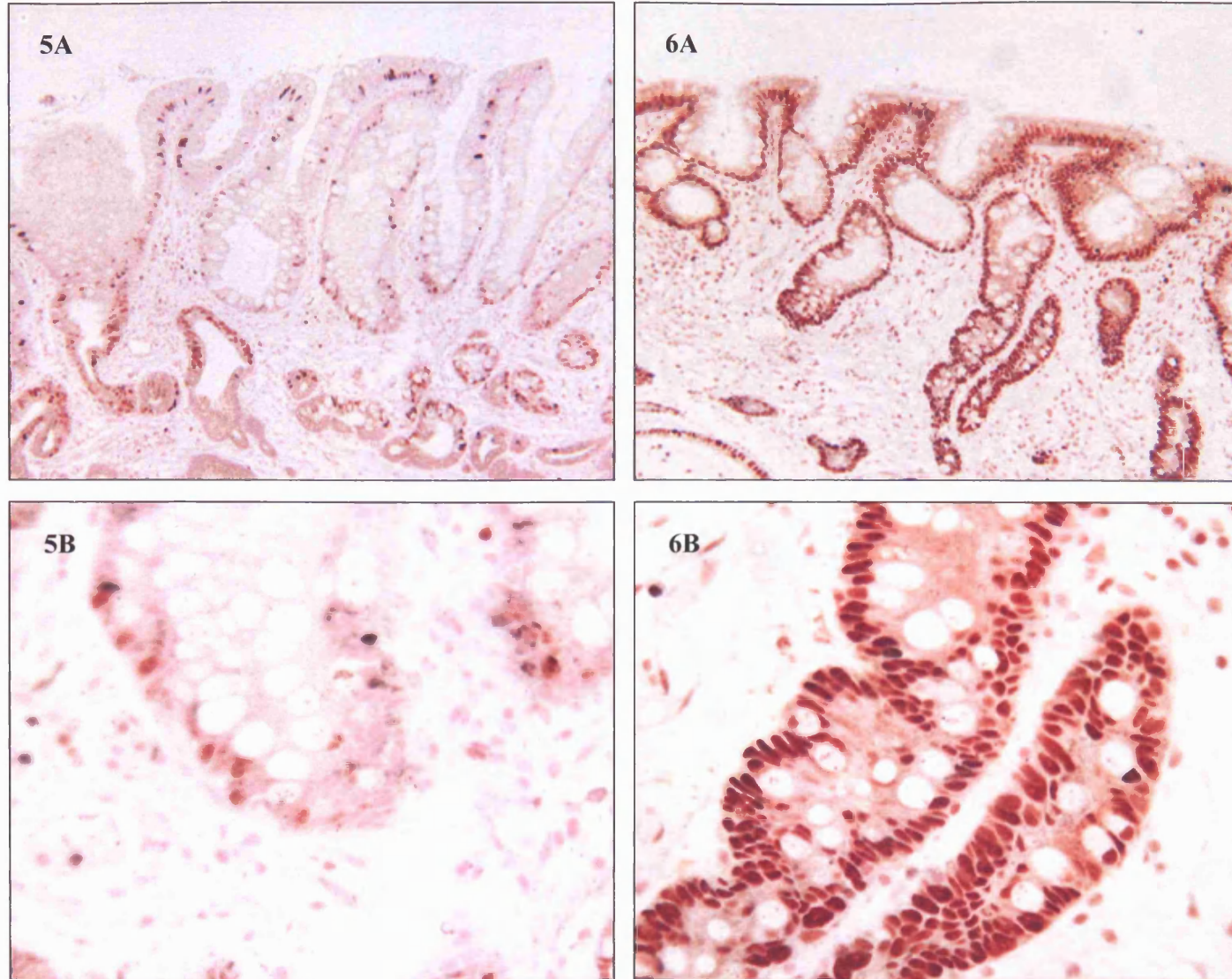
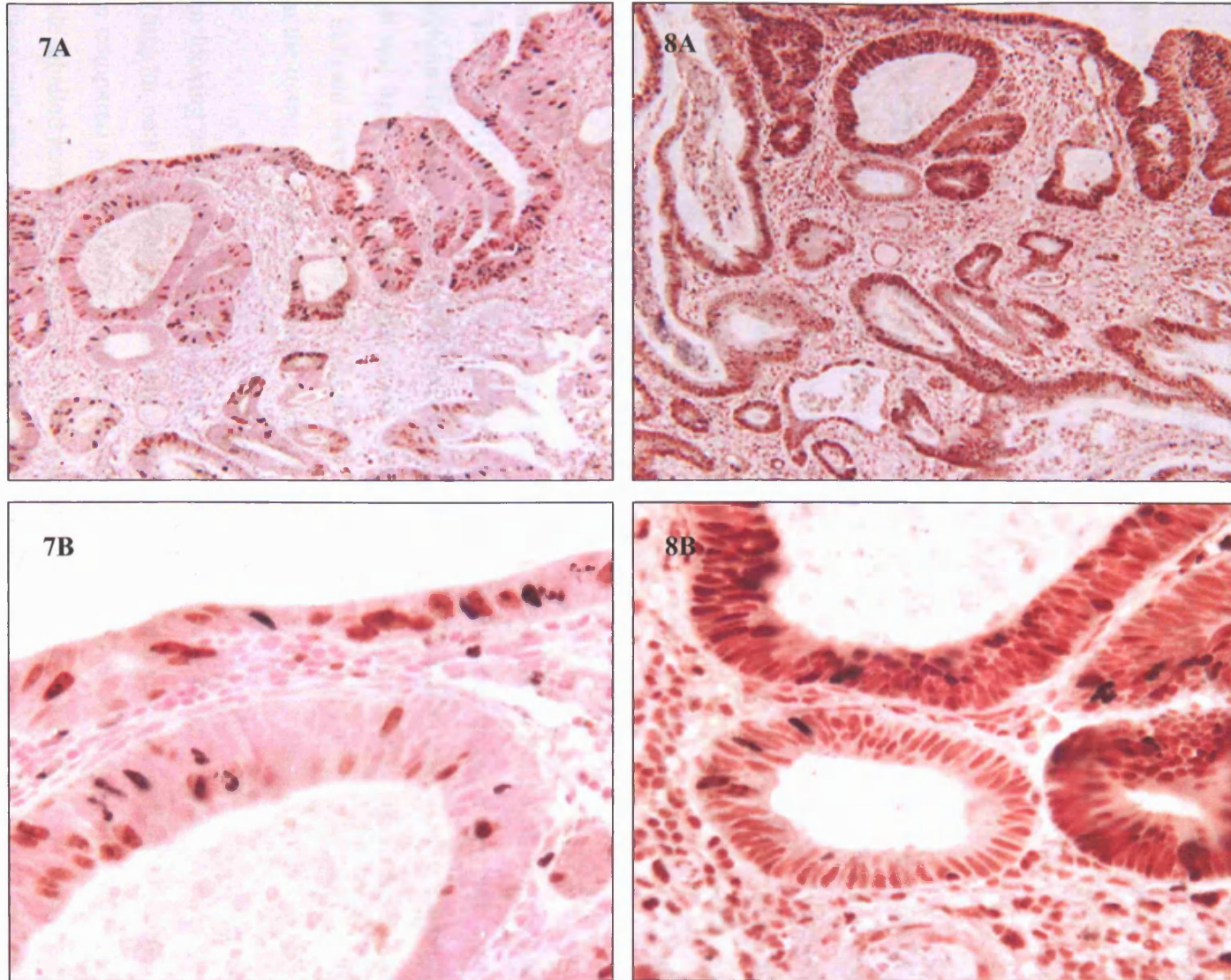


Figure 3.18 - Panel Four:



In the normal squamous oesophagus sections (Figure 3.18 – Panel One) the IUDR labelled cells were mainly present in the basal and parabasal compartment, for both BrdU/Ki-67 (1A and 1B) and BrdU/PCNA (2A and 2B) and were rarely observed in the superficial compartment of the mucosa. By contrast the Ki-67 and PCNA proliferative antibodies showed more widespread staining throughout all layers of the epidermis, although as expected the Ki-67 proportion of labelled cells was less than the PCNA fraction of labelled cells.

The gastric mucosa sections (Figure 3.18 – Panel Two) showed that the IUDR labelling cells were fairly widespread in the parietal cells and in the basal, mid crypt and surface crypt regions, for both the BrdU/Ki-67 (3A and 3B) and BrdU/PCNA (4A and 4B). By contrast the Ki-67 proliferative antibody showed more localised staining in the basal crypt region while the PCNA proliferative index was upregulated throughout all tissue layers, but preferentially in the basal, mid and surface of the crypt regions. Again in these sections the Ki-67 proportion of labelled cells was less than the PCNA fraction of labelled cells.

In the Barrett's mucosa sections (Figure 3.18 – Panel Three) the proliferative compartment seen with the Ki-67 staining (5A and 5B) was at the base of the image rather than spread throughout the whole tissue section as observed with the PCNA labelling index (6A and 6B), which was again greatly increased when compared to that of the Ki-67. The Ki-67 staining may indicate where the stem cell zone is for Barrett's tissue, which appears to be further down the tissue, on a par with what is known to occur in the colon.

When looking at the OA tissue sections (Figure 3.18 – Panel Four) a lot more cells were labelling for both the IUDR labelled cells and for the proliferative markers Ki-67 and PCNA when compared to the other experimental tissue sections. When looking at the BrdU/Ki-67 double labelled sections (7A and 7B) there appeared to be an almost equal proportion of cells labelling with each antibody. We know that the cells showing positive IUDR staining were labelled a week ago and are still very prevalent in the tissue. The same can be said for the BrdU/PCNA double labelled sections (8A and 8B), although the proportion of cells showing positive staining for PCNA was greatly increased when compared to the Ki-67 proportion of labelled cells.

### 3.4.10.3 Statistical Analysis for Double Labelling IHC

In the double labelled normal oesophageal tissue a cell count was undertaken for the number of positive cells which had retained the BrdU or the Ki-67 label, along with those that had not shown any positive staining in the PBL and IBL compartments.

The normal squamous mucosa was examined microscopically under a magnification of x40 and then 10 separate fields of view were chosen, each detailing the PBL and IBL areas. The number of positively stained cells was then recorded for the BrdU and Ki-67 antibodies, and also a count of the negative cells which were present in the same population. A mean score of the number of cells (Table 3.12), and also a cell population percentage (Table 3.13) was then calculated for each location and staining type. All raw data can be seen in Appendix 7, page 263.

Staining Type	Papillary basal layer	Interpapillary basal layer
IUdR	7.6 ± 1.6	11 ± 2.5
Ki-67	24.4 ± 3.0	25.8 ± 5.7
Negative	35.6 ± 6.0	46.8 ± 8.2
Total	67.6 ± 7.2	83.6 ± 14.7

**Table 3.12: Proportion of IUdR, Ki-67 and negative cells in the human normal oesophageal mucosa.** Mean ± SEM; n = 10. Full raw data can be seen in Appendix 7, page 263.

Staining Type	Papillary basal layer	Interpapillary basal layer
IUdR	11.3 ± 2.0	13.2 ± 1.7
Ki-67	37.1 ± 5.7	30.1 ± 3.5
Negative	51.6 ± 6.0	56.7 ± 4.4

**Table 3.13: Percentage of IUdR, Ki-67 and negative cells in the human normal oesophageal mucosa.** Mean ± SEM; n = 10. Full raw data can be seen in Appendix 7, page 263.

When looking at the mean labelling score data there was an increase in the amount of IUdR LRCs within the IBL when compared to the PBL, while the proportion of the Ki-67 proliferative population was fairly static between the two compartments. A higher total cell count was seen in the IBL when compared to the PBL compartment.

The mean score of positive cells was analysed using the non-parametric Wilcoxon's test to see if there was a significant difference in the proportion of positive cells seen for each staining type and the topographical location. There was a significant increase in the number of positively labelled BrdU cells within the IBL when compared to the PBL ( $P = 0.05$ ). When looking at the Ki-67 labelled cell population there was no significant difference observed in the proportion of cells when comparing the PBL to the IBL.

### 3.5 Discussion

The rapid rate of cell turnover in the GI tract makes the stem cells of this tissue amongst the most diligent in the body, although they remain elusive due to their immature, undifferentiated phenotype. Our knowledge of the mechanisms regulating GI stem cell function is evolving, along with the identification of putative cellular markers and the clarification of signalling pathways which regulate cell behaviour in the normal and neoplastic GI tract (Brittan and Wright, 2003).

As already stated cancer is most likely a stem cell disease, and thus if the stem cell population can be defined then there is more chance of determining the genetic alterations responsible for malignancy. It is generally considered that the basal zone, adjacent to the basal lamina, contains the stem cell and their progeny while the parabasal layers contain the TA cells (Jankowski and Wright, 1992). However, conflicting opinions are present in the literature as to the exact location of the stem cells in the basal zone. While some workers believe that the stem cells are found only within the IBL (Seery, 2002) others have the understanding that they are found in both the IBL and PBL of the oesophagus within the papillae themselves, and that there is a mixed population of dividing cells here (Janusz Jankowski, personal communication). For this reason it was decided that the examination of the IBL and the PBL in the basal compartment of the human oesophageal tissue was of major importance for this study.

Firstly, tissue specimens were analysed by IHC for several markers of interest. It was decided that patient tissues would be investigated for 6 tissue sets from areas of stomach, normal oesophagus, oesophagitis, BM and OA. Where possible these tissues were matched specimens from the same patient for the stomach, normal oesophagus, oesophagitis, and BM tissue. However, due to the nature of the way these tissues were obtained it was not possible to obtain adenocarcinoma tissue and so these 6 tissues were taken from a separate subset of patients. While our preferential interest was the oesophageal mucosa it was decided that control stomach tissue would also be useful to include, as well as looking at how the gene expression changed from the normal oesophagus to oesophagitis, BM and OA tissues of the MDCS. Full details of the tissues used in this study, along with primary characterisation details can be found in section 2.1.1.1 and Table 2.1.

While potential biomarkers of malignant progression in OA have been reported (Bani-Hani *et al.*, 2000; Hofler *et al.*, 2003), in this study it was decided to focus on only a limited number

of markers. This was because it was felt that there was not enough time to go on a trawling exercise through a large number of markers and this Chapter was more hypotheses testing, looking at other literature in the field, rather than hypotheses generating. This Chapter aimed to examine markers which had existing literature highlighting them as potential stem cell markers and which were preferentially expressed in the human oesophageal stem cell compartment. It was hoped that they would be able to serve as biomarkers in the risk of malignant progression in the oesophagus. Ki-67,  $\beta$ -catenin,  $\beta$ 1-integrin and P-cadherin were chosen as the markers of interest and their protein levels were assessed by IHC.

Our group and others have shown that in colorectal tumourigenesis, altered patterns of cadherin expression are associated with neoplastic progression (Hardy *et al.*, 2002b). Specifically, P-cadherin, normally expressed only in stratified epithelia (and not normal colon), is intimately associated with early aberrant crypt foci and subsequent colorectal carcinoma development (Hardy *et al.*, 2002b). Activating mutations in P-cadherin have not been identified, and chromosome 16q, where P-cadherin is located, is not a common region of chromosomal amplification in colorectal cancer (Bardi *et al.*, 1993; Hardy *et al.*, 2002b). The mechanism underlying aberrant P-cadherin expression in colorectal neoplasia is thus uncertain but may involve demethylation (Janusz Jankowski, personal communication).

P-cadherin showed significantly increased staining throughout the basal and mid topographical locations for normal oesophageal and oesophagitis tissue when compared to the surface locations in these tissues, and to the stomach control tissue. A significant increase in staining was also seen in the basal zone in the Barrett's metaplastic tissue. This would suggest that P-cadherin is upregulated in the stem cell compartment of the human oesophageal basal compartment and also in oesophagitis tissue following inflammation. The maximal expression seen in the basal Barrett's tissue would suggest that this is the location of the stem cell compartment. Therefore it can be concluded that P-cadherin overexpression could prove to be useful as a predictive biomarker of risk for the development of OA.

E-cadherin showed no localisation of staining intensity and was expressed throughout all tissue layers in each sample studied, however a decrease in staining intensity was seen when moving from normal squamous tissue to Barrett's, and then to adenocarcinoma tissue. These findings are in accordance with the literature where analysis of OA has shown that tumour stage and invasiveness are associated with a reduction of E-cadherin expression (Richards *et al.*, 1999).

Studies by Watt (2002) suggest that  $\beta 1$ -integrin staining is confined to the basal zone, in the stem cell compartment. The data gained here showed an increase in intensity of staining in the adenocarcinoma tissue sections and also in the basal location of the normal squamous mucosa; however staining was seen consistently throughout all tissue layers with no difference in expression being determined for any of the other tissues or topographical locations. High  $\beta 1$ -integrin expression in the stem cell compartment would be of functional significance for two reasons. Firstly, if  $\beta 1$  expression and function are downregulated via a dominant-negative integrin mutation, the cells would behave like TA cells, differentiating in a few rounds of division.  $\beta 1$ -integrins and MAP kinase cooperate to maintain the epidermal stem cell compartment *in vitro*. Secondly, high  $\beta 1$ -integrin expression helps to maintain the patterned distribution of stem cells; stem cells are less motile than TA cells and thus tend to remain clustered in the epidermal basal layer (Watt, 2002).

Integrins are expressed throughout the immune system and are therefore not exclusive to GI stem cells. As such integrin subunits have been identified as stem cell markers in the epidermis (Hotchin *et al.*, 1995; Jones and Watt, 1993; Li *et al.*, 1998) and testes (Shinohara *et al.*, 1999), and have recently been suggested as markers of intestinal clonogenic cells, based upon observations of a restricted expression of the  $\beta 1$ -integrin subunit in proliferating epithelial cells in the lower third of the human colonic crypts, and the expression of the  $\alpha 2\beta 1$  integrin in epithelial cells in the base of the crypts in the human small intestine (Beaulieu, 1992). However, our results did not provide conclusive evidence as to the use  $\beta 1$ -integrin as a marker of oesophageal stem cells.

The findings for the  $\beta$ -catenin IHC analysis were not as expected, as no statistical significant difference was found in the membranous staining intensity observed for any of the topographical locations in any of the tissues studied. However, observational analysis appeared to show a decrease in intensity in the oesophagitis and Barrett's tissues when compared to the normal squamous mucosa.

A hallmark of colon carcinoma is transient localisation of  $\beta$ -catenin to the nucleus and it has been shown that mutations in adenomatous polyposis coli (APC) or  $\beta$ -catenin initiate the vast majority of colorectal neoplasms (Shih *et al.*, 2001). APC binds to  $\beta$ -catenin, stimulating  $\beta$ -catenin degradation and thereby inhibiting transcriptional activation of  $\beta$ -catenin/Tcf4 transcription complexes (Kinzler and Vogelstein, 1996; Polakis, 2000). One way of evaluating the APC pathway is through IHC staining with a monoclonal antibody for  $\beta$ -

catenin. In non-neoplastic epithelial cells most  $\beta$ -catenin should be bound to E-cadherin at the cell membranes. In contrast, in neoplastic tissue,  $\beta$ -catenin staining should be localised in the nucleus as well as showing some staining in the cytoplasm and cell membranes. This would support the evidence that a loss of function of one of the genes in the *Wnt* pathway, most likely APC, had occurred with a subsequent translocation of  $\beta$ -catenin to the nucleus in these dysplastic cells. Studies by Hao *et al.*, (2002) and Preston *et al.*, (2003) confirm this to be the case in colorectal adenomas and carcinomas. In this study however no nuclear  $\beta$ -catenin staining was observed in the 6 OA tissue sections and the possible reasons for this may be that only a small sample size containing low grades of dysplasia, which were poorly defined, were examined.

Changes related to dysplastic tissue formation are frequently associated with increased cell proliferation. The monoclonal antibody Ki-67 was employed to detect a nuclear antigen that is present in the nuclei of replicating but not quiescent cells (Gerdes *et al.*, 1984). This study revealed that Ki-67 staining showed a similar staining pattern to P-cadherin and  $\beta$ 1-integrin, in that it was also upregulated in the basal oesophageal and Barrett's tissue compartments and in areas of inflammation, such as the oesophagitis and adenocarcinoma sections. This would indicate that it is labelling a similar cell population as the other antibodies and suggests that it can be used as a reliable means of rapidly evaluating the growth fraction of normal and neoplastic human cell populations.

A high degree of non-specific staining of parietal cells or oxyntic cells was also seen in the stomach experimental tissues in this study. This was most likely due to the fact the parietal cells contain an extensive secretory network and as such they contain numerous mitochondria whose granules will take up the label non-specifically.

A major problem of this work is that the tissues were not matched for all tissue samples studied and the OA sections came from separate patients to the rest of the matched samples. It was felt that this was something that was difficult to overcome as once OA had been determined treatment steps are likely to be put into place, and therefore those attending for routine endoscopy are very unlikely to have OA. Another potential flaw in this Chapter was that it was retrospective and only patients with matched tissue specimens were recruited, therefore there was a potential problem of selection bias. This was due to the fact that the patients studied are, by definition, those that have already developed BO. Obtaining representative samples by endoscopic biopsy could also be viewed as a potential problem of

this study. This is because samples were taken by different consultants, at different times and so would not all be judged by the same criteria, this may reduce the sensitivity of any biomarker. The sensitivity of these markers could be improved if they are used in combination with other biomarkers that indicate early events in the progression of BO to OA. Thus it is likely that development of a panel of biomarkers will hold the key to refining the identification of BM patients whose disease is at high risk of progression to malignancy.

Carcinomas of the upper GI tract have been intensively studied for decades in order to identify markers for a) design of simple blood tests to detect presence or recurrence of the disease, b) prediction of therapy response, c) identification of molecular targets for novel therapies. These aims have not yet been fully reached by analysing single genes (Hofler *et al.*, 2003). For this reason it was decided that this study would focus not only on single genes but also on the potential of LRCs to highlight stem cell location.

To meet this aim clinical trial tissue was utilised for patients who had received an intravenous infusion of the labelling thymidine analogue IUdR. Firstly, it was important to create IUdR control tissues to make sure that the IUdR was being taken up by each tissue and then retained. IUdR is not expressed naturally in any tissue or organism and so a control tissue had to be created. In each experiment if we had not used these controls, and no positive staining was observed, then it would not have been possible to say to say that the experiment had failed, or just that that all the cells with the IUdR label had been lost to differentiation or proliferation.

From all of the data obtained for the BrdU staining the results showed that infusion at three days or less in the *in vivo* primary explants revealed abundant staining of the proliferative compartments. However, *ex vivo* IUdR labelling at 7 days showed positive discrete staining of LRCs in various GI tissue types in both patients studied. These LRCs were seen in both the IBL and PBL basal layers of the squamous epithelium. LRCs were also seen at several locations in Barrett's metaplastic tissue, both at the base of the gland and in the neck region, suggesting that this tissue may have two stem cell compartments.

The two patients recruited to the SAINT clinical trial each received an infusion of IUdR 7 days prior to resection surgery. Only a fraction of the originally labelled cell population at the time of infusion was still present at resection as the turnover time of the GI tract is between 3-10 days. It is important to understand that the suggestion is not that all of the positively

stained cells present at 7 days post infusion are stem cells, only that they have a longer labelling index. Certainly any cells present in the apical layers of the tissues are not stem cells and to eliminate these cells the time period needs to be increased, to perhaps 14 days, between infusion and resection. This way it would be possible to exclude some of the LRCs as TA cells and to determine a more focused review of the potential stem cell location.

The double labelling analysis also provided some important results. When looking at the squamous oesophageal tissue the same population of cells showed positive staining for IUdR and Ki-67 in both the IBL and the PBL. This is very interesting as previous workers have indicated that stem cells are located only in the IBL of the oesophageal mucosa (Watt and Hogan, 2000). The findings here challenge this believe and suggest that while the LRCs have a propensity to be in the IBL, the fact remains that LRCs were seen with uniform regularity in the PBL as well IBL. What we would expect and was indeed true of the observed results is that the LRCs were present in the basal layer or just above in the lower parabasal or prickle cell layer. What is not so clear however, is if the stem cell is at the base and divides laterally, or if it is sitting slightly higher up and then pushes its cells downwards.

In the gastric tissue the LRCs were fairly widespread however, cells were positive in the purported stem cell compartment, the neck region of the gland. In the Barrett's metaplastic tissue there is still a lot of controversy trying to ascertain where the proliferative compartment is located. It has been suggested that this could be similar to the gastric situation and be at the neck region of the gland or more like the colonic situation where the stem cell compartment has been determined at the base of the crypt. The double labelling experiments showed that the proliferative Ki-67 label was preferentially expressed at the base of the Barrett's tissue and so these findings would suggest that the Barrett's stem cell compartment is more "colonic" than "gastric" in nature. The IUdR staining showed comparable staining in the basal region, although staining was also seen in the neck region, which could indicate the possibility that two types of metaplasia are seen in BO. The first being an intestinal metaplastic form, which would show a colonic stem cell compartment phenotype, and the other being a gastric metaplastic form, which would show a gastric stem cell compartment phenotype.

The most interesting observation in the double labelled IM sections was that there appeared to be a failure of migration at the tissue surface. This phenomenon was more apparent in the BrdU/Ki-67 double labelling section where an increased cell population of IUdR labelled

cells were seen at the surface. If these surface cells were proliferating then they would also show positive Ki-67 staining, although this was not the case. This suggests that these cells were labelled a week ago, at the infusion of IUdR, when they were in the proliferative compartment. After they were labelled they began to migrate to the tissue surface, but now seemed to be stuck there, almost like a bottleneck, with certain areas showing many cells backed up behind each other. If they can not go anywhere then this would indicate a failure of migration and may indicate something about the TA population and the proliferative flux. This was less clear on the BrdU/PCNA double labelled section, although it was still possible to see a high proportion of IUdR labelled cells at the tissue surface.

Unfortunately, in the clinical trial samples it was not possible to obtain oesophagitis tissue for experimental analysis. The reason why this would have been of interest would be to document whether the amount of LRCs increased from the normal oesophageal population to the stressed environment of the oesophagitis tissue. It is anticipated that the stem cell compartment in the oesophagitis tissue would not be greater than the normal squamous stem cell compartment and so in theory the proportion of LRCs should be comparable in each population. There is an argument that the amount of stem cells can be increased at times of injury or stress and in this situation dormant potential stem cells could start to proliferate.

In the OA tissue there was a much increased labelling index for both the IUdR labelled cells and for the proliferative markers Ki-67 and PCNA when compared to the other experimental tissue sections. This indicates that these cells have a greater longevity in the adenocarcinoma tissue when compared to the other tissues examined. This would indicate that these tumour cells have a prolonged existence and provides information about tumour mechanics in oesophageal cancer, in that it suggests that a lot of the cells are remaining in the tissue for at least a week, and are not dying with necrosis or apoptosis.

Currently, malignancies of the upper GI tract are often diagnosed at an advanced stage and are generally associated with a poor patient prognosis. With an improved understanding of the molecular biology of these tumours, there is hope that new targets for diagnosis, chemoprevention, and therapy will be developed (Lin and Beerm, 2004). The possibility of using molecular markers to identify high-risk individuals, and then targeting these with more frequent surveillance, would represent a valuable advance in the clinical management of BO and provide an opportunity to improve prognosis of OA, a disease that is continuing to increase in public health relevance (Bani-Hani *et al.*, 2000).

In conclusion, work in this Chapter has demonstrated expression and localisation of adhesion; signalling and proliferative biomarkers in a subset of patient's matched tissues. In particular, P-cadherin expression was seen in the basal oesophageal stem cell compartment, was upregulated in oesophagitis, and also present in areas where stem cells have been implicated in BM tissue. Also LRC analysis has provided many insights into stem cell dynamics in the tissues studied although, as is often the case, many more questions have been asked rather than answered. Studies such as these can provide insight into the characteristics of stem cells, in normal and regenerating circumstances and demonstrate why a thorough understanding of these cells is an essential pre-requisite for stem cell based therapeutic approaches.

**Chapter 4: The Role of Bile Acid Stimulation and Suppression in  
the Normal *in Vivo* System of the Zebrafish**

## 4.1 Introduction

There have been a number of animal models, which have demonstrated that severe and chronic exposure of the distal oesophageal mucosa to acid reflux can induce metaplasia. Most existing models are post operative rodents, some requiring the addition of exogenous carcinogens, or prior mucosal injury, with none reliably mimicking what we currently know of the MDCS. Buskens *et al.*, (2006) state that some detailed histopathological studies of the MDCS have found similarities in the reflux-induced oesophageal metaplasia, but some of the resulting adenocarcinomas have been significantly different between humans and rodents, usually occurring alongside squamous cell tumours.

The difficulty in inducing oesophageal metaplasia in animal models most likely reflects multifactorial pathogenesis. Whilst in humans, exposure to acid reflux almost certainly plays a role in the development of BO; it has to also be seen in the context of genetic susceptibility and the oesophageal microenvironment (Fitzgerald, 2005). Complex gene to gene and gene to environmental interactions may explain why only a small proportion of people with GORD go on to develop BO (Mann *et al.*, 1989; Winters, Jr. *et al.*, 1987).

Evidence suggests that bile acids alone could be highly important in BM, especially since most bile acids are active in the refluxate (Sharma and Sampliner, 1997). Garewal and colleagues have shown that conjugated bile acids might exacerbate oesophageal mucosal injury either alone or in combination with acid, both *in vitro* and in animals (Garewal *et al.*, 1996). Bile acids have also been implicated in the promotion of goblet-cell-containing metaplasia in other GI epithelia, including the stomach, duodenum, intestine, bile ducts, and the oesophagus (Tselepis *et al.*, 1999). All evidence suggests that bile acids may have a much greater role in the progression of Barrett's dysplasia and the development of cancer than previously thought (Jankowski *et al.*, 2000a).

Duodeno-GOR results in altered bile acid metabolism causing dehydrogenation of cholic acid to form DCA. Moreover, bile acids may be physiologically more cytotoxic at a neutral pH, and it is therefore theoretically possible that DCA could promote oesophageal metaplasia and cancer in humans. This suggests that in animal models of duodenogastric reflux there may be an enhanced metaplasia development and cancer risk.

In this Chapter zebrafish were used as a novel model to study the effects of acid exposure. Zebrafish are becoming an increasingly useful model for scientific research and recent studies

have demonstrated that they function similarly to humans in terms of toxicity levels of known human toxic compounds (Rubinstein, 2006). For this reason zebrafish were examined in this study as a high throughput system to look at potential pharmacological targets to measure bile acid exposure and effect in the GI tract. It was our hypothesis that the zebrafish oesophageal mucosa would have similar changes in exposure to chronic bile acid as that seen in the human.

## 4.2 Aims

The aim of this Chapter was to examine the role of bile acid stimulation and suppression in the normal zebrafish *in vivo*, and to see which environmental factors may have a causative role.

The specific objectives were:

- 1) To carry out H&E analysis on zebrafish tissue sections to allow for tissue architecture to be studied.
- 2) To optimise  $\beta$ 1-integrin,  $\beta$ -catenin, and Pan-cadherin commercially available antibodies and use these for IHC studies in normal zebrafish tissue and control tissues.
- 3) To carry out an exposure experiment for DCA stimulation in experimental zebrafish.
- 4) To examine DCA stimulation animals using electron microscopy (EM).

## 4.3 Materials and Methods

All zebrafish tissue was obtained from a collaborative project involving Daniolabs, Cambridge. General reagents used are described in section 2.1.5. Primary antibodies used are described in section 2.1.4 in Table 2.3. Tissue samples used in this Chapter are described in section 2.1.1.3 and processing details can be found in section 2.2.1.4. H&E staining of FFPE sections was performed as detailed in section 2.2.4.2. Expression and localisation of molecules studied was achieved by IHC as described in section 2.2.6. The DCA stimulation experiment was carried out as detailed in section 2.2.2.2. EM work was also carried out on the experimental DCA stimulated Zebrafish although as this work was carried out by Angeleen Fleming at Daniolabs, Cambridge, there is no method listed. Statistical analysis information can be found in section 2.2.16.

## 4.4 Results

### 4.4.1 Tissue Morphology

Prior to any experimental investigation the assessment of tissue morphology and histological appearance of various tissues throughout the zebrafish was performed. This was prudent as the zebrafish was a new investigation model and as such it was vital that key factors such as basic anatomy, tissue type and orientation could be determined. Several fish were sectioned from head to tail, as detailed in section 2.2.1.4, and firstly the overall appearance of a cross section through a zebrafish was observed. Figure 4.1 details the main histological features in a one-month old zebrafish.

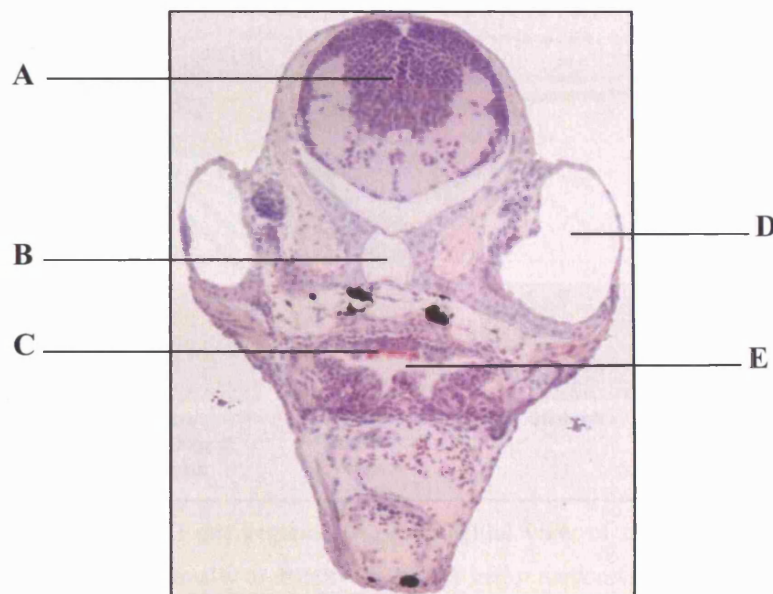


**Figure 4.1 – Cross section through a one month old zebrafish.** H&E stained cross section view of a whole mount zebrafish to highlight tissue morphology and phenotype of the zebrafish. The main anatomical features have been labelled and are as follows: (A) Brain. (B) Notochord. (C) Pharyngeal ‘Teeth’. (D) Otolith. (E) Opening of Gut. Magnification is x10.

Thereafter particular attention was focused on the mid oesophageal, to open intestinal bulb regions, and this was where examination took place for any induced change in experimental phenotype. Figure 4.2 highlights the areas which were examined and details their histological appearance.

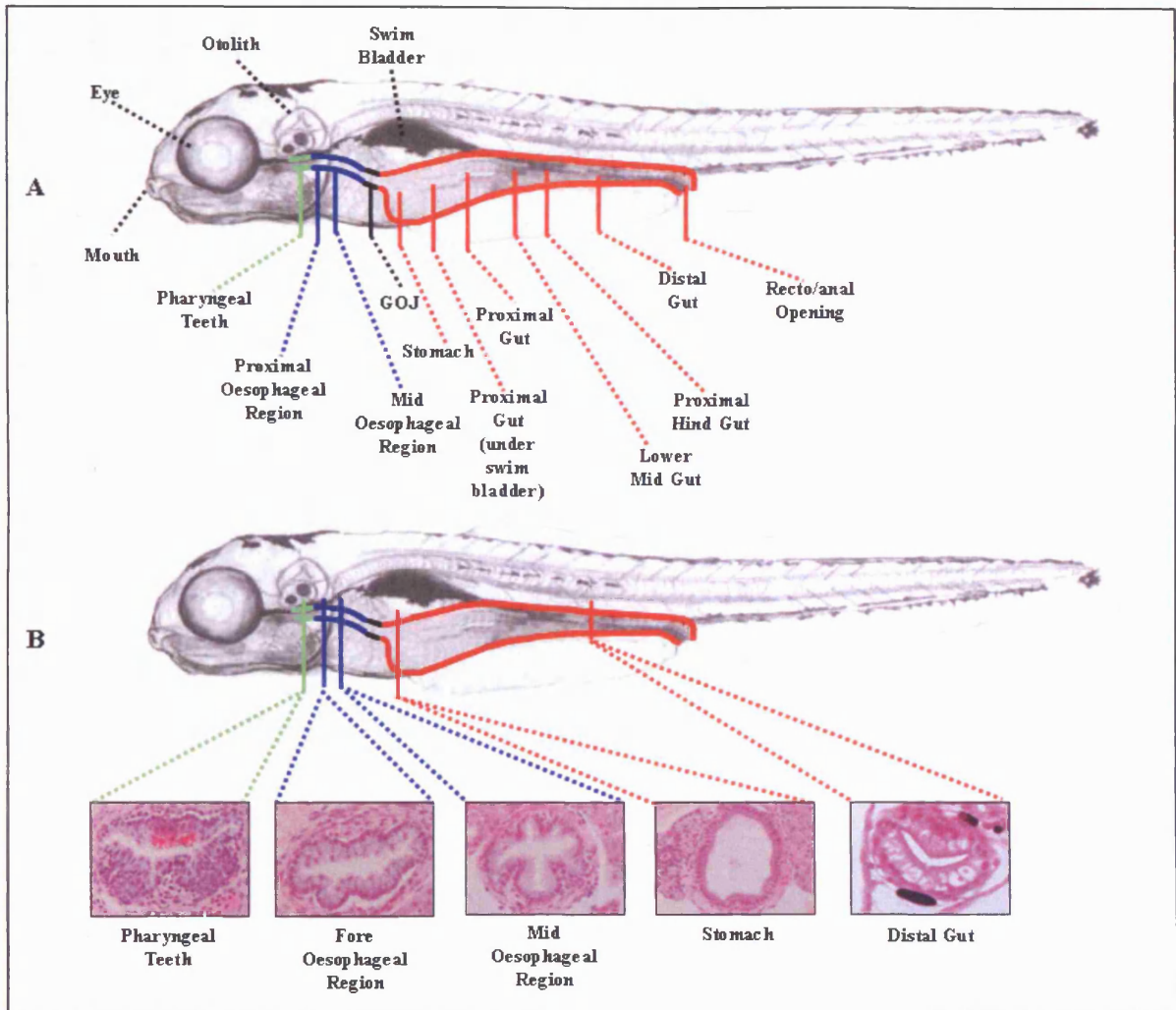


**Figure 4.2 - Zebrafish (7d.p.f.) gut regions.** (A) Parasagittal view of a zebrafish detailing all main areas throughout the gut, running proximally to distally, and other major anatomical features. (B) Parasagittal view of a zebrafish complete with histological H&E stained cross sections of the areas that underwent investigation in this study, (shown in high power in Figure 4.3), along with a section of distal gut, for information. This highlights the histopathology and phenotype that was examined in all experimental animals. [This is an original figure and has been created using Dahm's (2002) parasagittal diagram found in "Zebrafish – A Practical Approach". All H&E images were taken at a magnification of x25 and are authors own, Lea-Anne Harrison © (2006)].

When processing experimental animals it was decided that each individual animal would be sectioned from head to tail and that all sections would be mounted onto slides, as it was difficult when dealing with such small sections, to examine the histopathology and determine the areas of interest prior to each section being mounted and stained for H&E. Once each section had been processed it was then possible to see which slides contained the sections of interest, which were then examined more closely. To facilitate analysis certain key features were used as a starting point and it was decided that the pharyngeal 'teeth' would be used as a marker of where the examination should start. The pharyngeal 'teeth', seen in Figure 4.3A, lie

beneath the otoliths and are the best guide as to whether you are in the pharynx. Therefore if you are further back than the teeth then you are in the oesophagus and so they were used to determine the beginning of the digestive tract. It should be noted that these are not real teeth in the true sense of the word although this is the accepted terminology. The opening of the gut into the 'stomach' region would determine where examination should terminate (Figure 4.3D). Again this is not a true stomach but will be the terminology employed throughout this text to indicate the opening out of the intestinal bulb after the oesophageal region. Figure 4.3 highlights these areas and demonstrate which features dictated the sections which underwent closer observation and analysis.

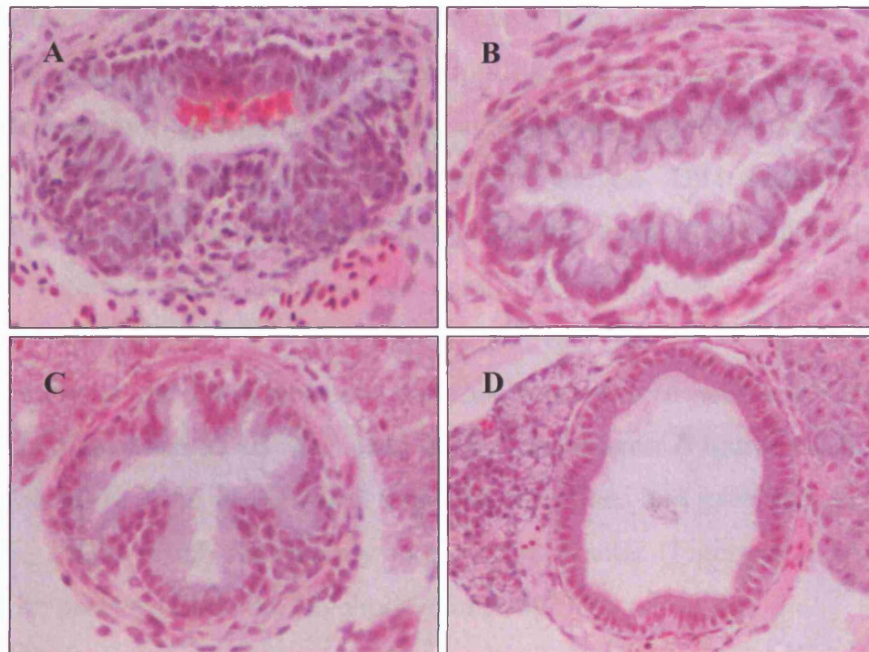


**Figure 4.3 – Cross section at four key sites showing major anatomical features of the zebrafish digestive tract.** H&E stained cross section views of several sections of a 7d.p.f. zebrafish to highlight histopathology and phenotype which were examined in all experimental animals. (A) The pharyngeal 'teeth' which are clearly visible with strong pink staining. (B) The proximal oesophagus is characterised by this distinct shape, where the cell walls are surrounded by smooth muscle and have minimal folding. (C) The mid oesophageal region is characterised by distinctive cell wall invaginations, which form a 'clover leaf' shape. (D) The 'stomach' region can be seen very distinctly as a large open area which replaces the 'clover leaf' shape seen previously. Magnification is x25 for all images.

#### 4.4.2 Zebrafish IHC

The antibodies chosen for investigation were highlighted in the human tissue study. However, as the zebrafish is a relatively new scientific model there were a limited number of commercially available antibodies which were zebrafish specific. This meant that finding suitable antibodies was challenging.

Three different antibodies were used in zebrafish IHC evaluation. However, only one of these was endorsed by the manufacturer for immunohistochemical use on zebrafish tissue (Ab6302). The other two were chosen due to the manufacturers recommendation that they could be employed for IHC across a variety of species, or that they had a high identity with zebrafish. All antibodies required method optimisation.

#### 4.4.2.1 *Experimental Controls*

To examine which of these antibodies worked on zebrafish tissue it was decided that an experimental antibody control be used rather than an experimental tissue positive control. For this a ZnS5 antibody was utilised which had previously been optimised in zebrafish tissue by Daniolabs, Cambridge and was known to label dorsal and ventral spinal neurons in the spinal cord or central nervous system (CNS). This antibody was obtained from the Zebrafish International Resource Center (ZFIN), University of Oregon. This would ensure that the zebrafish tissue was appropriately fixed and preserved, even if the antibodies were not suitable. For a negative control the usual NPA control was employed.

Under all conditions the NPA negative controls worked well and were free from any background staining when DAB was used as the chromogen (Figure 4.4D). The control experimental antibody ZnS5 worked well under all conditions and gave expected dark brown staining in the brain, which was mainly in the white matter (Figure 4.4A) which was in accordance with previous literature (Svoboda *et al.*, 2002).

#### 4.4.2.2 *$\beta$ 1-integrin, Ab89918*

The optimisation of the  $\beta$ 1-integrin 2B1 antibody involved a series of antibody concentrations, ranging from 0.25 $\mu$ g/ml to 1.25 $\mu$ g/ml. This antibody did not produce the expected staining. Some non-specific staining was observed at a concentration of 1.25 $\mu$ g/ml dilution; however there was no positive staining observed (Figure 4.4B). At 0.25 $\mu$ g/ml no staining, non-specific or otherwise was seen and the section was completely negative (data not shown).

#### 4.4.2.3 *$\beta$ -catenin, Ab6302*

This was the only primary antibody that was reported to be suitable for IHC in zebrafish. For all zebrafish tissues examined the staining was very strong and occurred most predominately in the white matter of the brain, which gave very intense dark brown staining at a

concentration of 10 $\mu$ g/ml. Positive staining was also observed in the brachial bars (the gills) and around the surface membranes, although this staining was less intense (Figure 4.4C).

4.4.2.4 *Fun-coelurus*, 1519507

This antibody was reported as having a 91% identity with zebrafish by the manufacturer and it was in this report that it was proven. Work was carried out by the University of Cambridge. 7d.p.f. zebrafish was treated with either DMSO or with a solution of DSA at 4

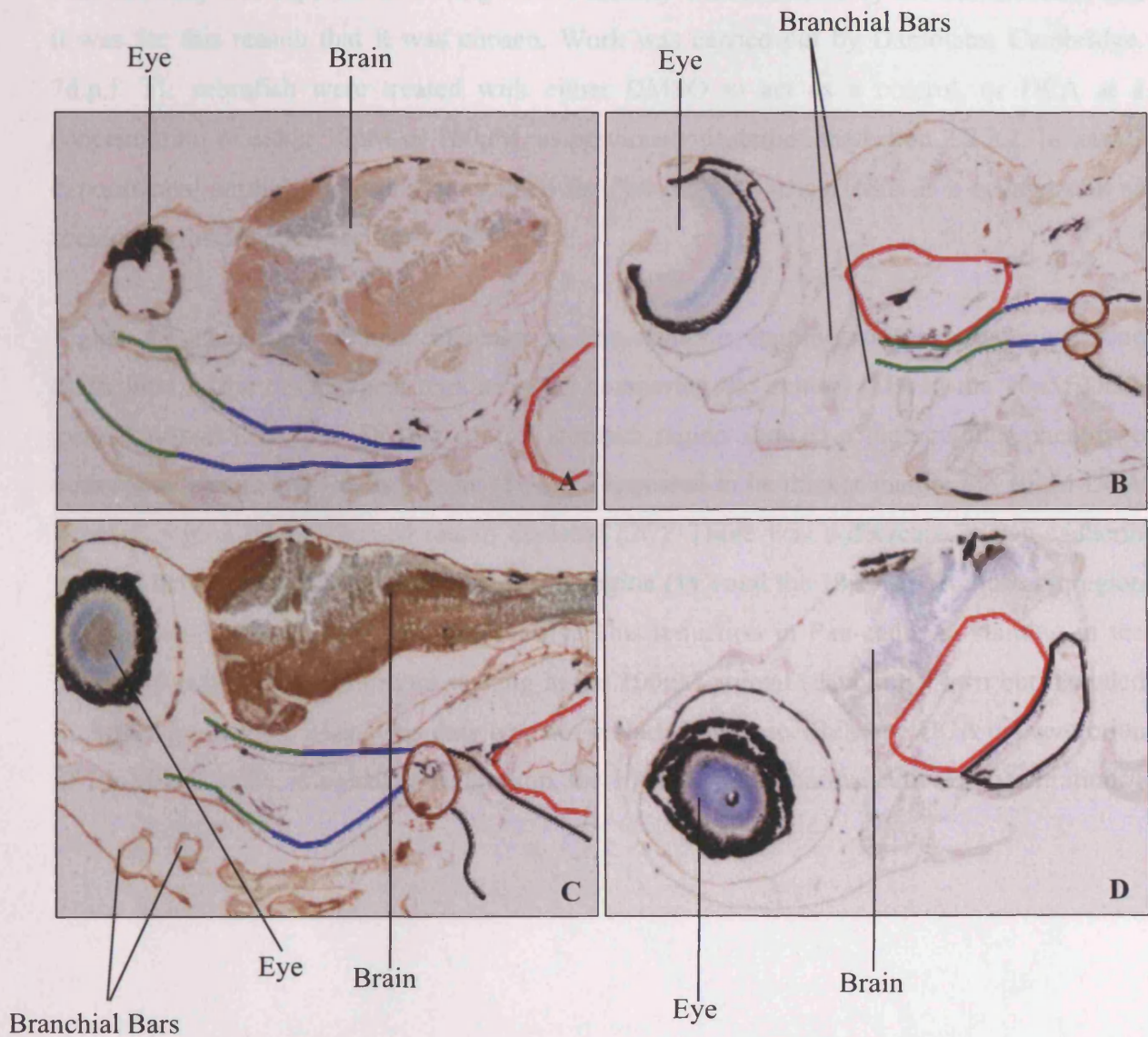


**Figure 4.4 – IHC analysis of antibodies used in zebrafish tissue.** All images are parasagittal views of several sections of a 7d.p.f. zebrafish used in various IHC methods. In each picture the sections are positioned so that the head to tail runs from left to right and that the dorsal to ventral surfaces run from top to bottom respectively. (A) Positive control showing ZnS5 staining at a concentration of 110 $\mu$ g/ml. (B) 1.25 $\mu$ g/ml  $\beta 1$ -integrin staining. (C) 10 $\mu$ g/ml  $\beta$ -catenin staining. (D) NPA negative control. Magnification is x10 for all images.

- = Oesophageal Junction
- = Pharynx
- = Oesophagus
- = Stomach
- = Swim Bladder



#### 4.4.2.4 *Pan-cadherin, Ab16505*

This antibody was reported as having a 91% identity with zebrafish by the manufacturer and it was for this reason that it was chosen. Work was carried out by Daniolabs, Cambridge. 7d.p.f. TL zebrafish were treated with either DMSO to act as a control, or DCA at a concentration of either 10 $\mu$ M or 100 $\mu$ M, as previously described in section 2.2.2.2. In total 3 experimental animals were immunostained for Pan-cadherin using H&E as a counterstain as previously described in section 2.2.4.11.

Figure 4.5 showed a definite increase in Pan-cadherin staining in the transitional zone epithelium in the oesophageal regions when comparing the control (1B) to the 10 $\mu$ M DCA treated animal (2B). The DMSO control stomach region showed a multicellular phenotype with some 'mucin type' cells present (1C) and appeared to be thicker than in the 10 $\mu$ M DCA stomach region which seemed mucin depleted (2C). There was a decrease in Pan-cadherin staining between the DMSO control stomach region (1C) and the 10 $\mu$ M DCA stomach region (2C) although this was difficult to quantify. This reduction in Pan-cadherin staining in the 'stomach' region was even more striking in the 100 $\mu$ M animal (data not shown but included in Appendix 3, page 241). This data was not included because while the DCA concentration of 10 $\mu$ M was a physiological concentration, the 100 $\mu$ M was a pharmaceutical concentration.

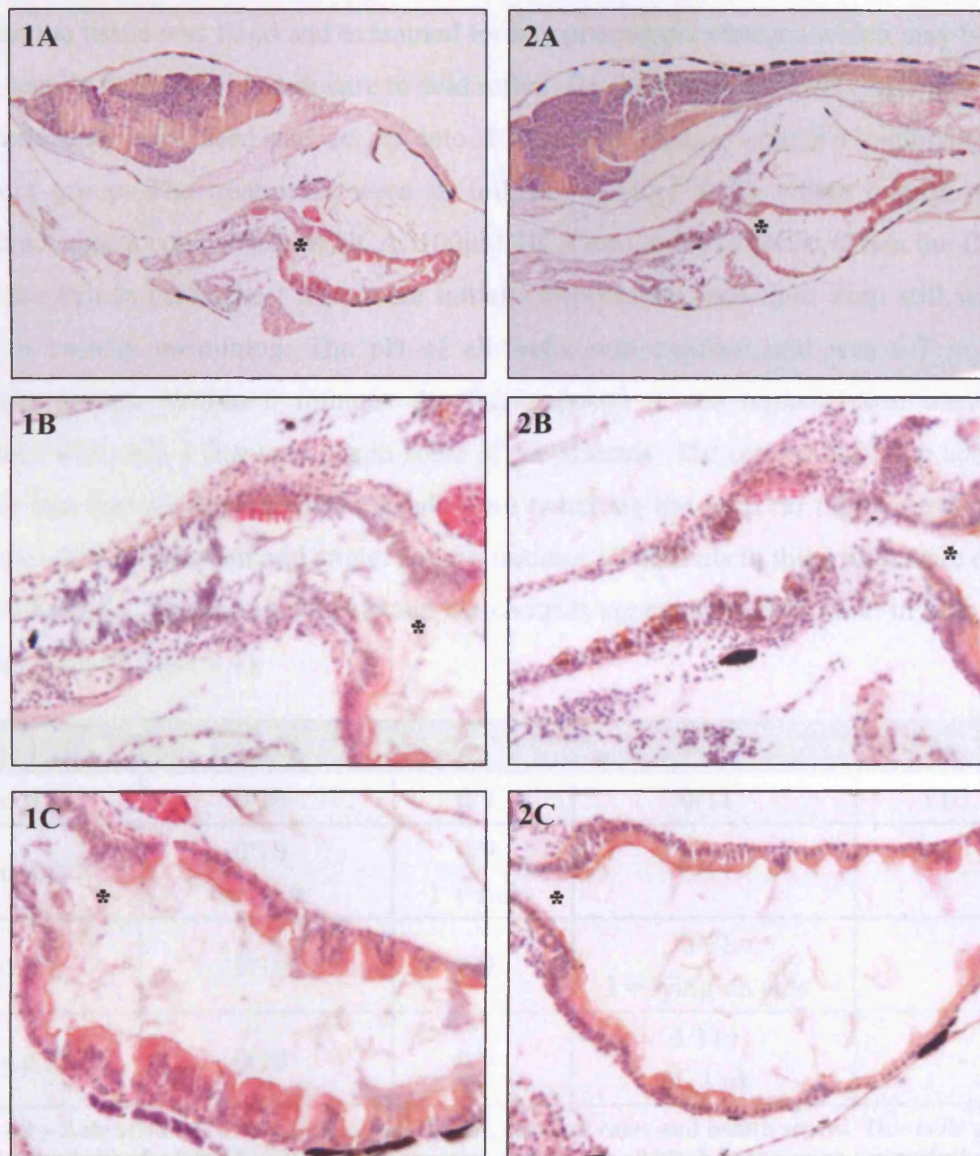


**Figure 4.5 – Pan-cadherin IHC analysis on zebrafish tissue.** The primary antibody is the Pan-cadherin rabbit polyclonal (Ab16505) used at a final concentration of 2µg/ml. HRP conjugated St-ABC was used as the tertiary detection system with DAB as the chromogen, using H&E as the counterstain. All images are parasagittal views of 7d.p.f. zebrafish. In each picture the sections are positioned so that head to tail runs from left to right and that the dorsal to ventral surfaces run from top to bottom respectively. These images are taken from the region oesophagus where it opens into the intestinal bulb or ‘stomach’, (as indicated by an \* in each figure). (1A) Whole section of DMSO control animal. (1B) Oesophageal region of DMSO control animal. (1C) ‘Stomach’ region of DMSO control animal. (2A) Whole section of 10µM DCA treated animal. (2B) Oesophageal region of 10µM DCA treated animal. (2C) ‘Stomach’ region of 10µM DCA treated animal. Magnification is x10 for primary images, i.e. those listed as A and x40 for all higher powered shots, i.e. those listed as B and C.

#### 4.4.3 DCA Zebrafish Stimulation Experiment

This was achieved by exposing 3 or 4d.p.f. zebrafish to DCA for 4 days continuously. After this time the tissue was fixed and examined for any phenotypic changes which may be similar to that seen in humans with exposure to acid reflux. On the first run of this experiment, 4d.p.f. LWT zebrafish were used and set up into 4 treatment groups, with 9-11 animals in each treatment group. The treatments were as follows: 0 $\mu$ M of DCA where embryo media + DMSO acted as a control; 10 $\mu$ M DCA, 100 $\mu$ M DCA and 1mM of DCA. When the DCA was added the fish in the highest dose were initially hyperactive, and then went still with short spells of twitchy swimming. The pH of all wells was checked and was 6-7 in all four treatment groups. Within 5 minutes the fish exposed to the highest dose were mainly stationary with only a few twitches in some of the animals. The interesting thing about these animals was that while some of the heads were twitching the pectoral fins were not moving and were sticking out at an odd angle. After 8 minutes all animals in this group were dead. All other animals for both the treatments and the controls appeared to be normal in both motility and appearance (Table 4.1).

Time Point	Control	10 $\mu$ M	100 $\mu$ M	1mM
4d.p.f.	0/10	0/9	0/11	11/11+
5d.p.f.	0/10 1 = sick	0/9 1 = sick	0/11	-
6d.p.f.	0/10	0/9	0/11 3 = lying on side	-
7d.p.f.	0/10	0/9	3/11+ 8/11 ok	-

**Table 4.1 – Zebrafish DCA stimulation experiment, survival rates and health scores.** This table details all animals enrolled in the first DCA stimulation experiment. Animals which did not survive are marked with +.

From this first experiment it would appear that DCA was toxic to the animals at a 1mM concentration, and for that reason it was no longer used. It was hypothesised that a concentration of 100 $\mu$ M may also have reached a toxic level due to 3 of the animals failing to survive. However, it was decided to do several dose response repeats due to clutch variability observed in zebrafish assays (Angleen Fleming, personal communication).

When conducting the first repeat of this experiment 3d.p.f. TL zebrafish were used and set up into 3 treatment groups, with 6 animals in each treatment group. The treatments were as follows: 0 $\mu$ M of DCA where embryo media + DMSO acted as a control; 10 $\mu$ M DCA, and

100 $\mu$ M of DCA. All animals survived this experiment and when checked on a daily basis, throughout the course of the experiment, all animals showed normal behaviour.

It was decided to do an exact repeat of this experiment so that the results were in triplicate and to enable statistical analysis. During the course of this experiment all the animals in the 100 $\mu$ M concentration of DCA died at 6d.p.f. prior to the completion of the experiment. Due to this variability in survival it was decided that another repeat should be set up, this time looking again at the dose response by using several more concentrations. This was decided as there had been a time gap between repeating the experiments which may have an effect on survival. In this repeat 6 animals were set up in each of the following treatment groups 0 $\mu$ M of DCA where embryo media + DMSO acted as a control; 10 $\mu$ M DCA, 25 $\mu$ M DCA, 50 $\mu$ M DCA, 75 $\mu$ M DCA, and 100 $\mu$ M of DCA. Again the results varied; there was high toxicity in the 75 $\mu$ M and 100 $\mu$ M with no surviving animals. There were only a few survivors in the 50 $\mu$ M group and all experimental animals in the 10 $\mu$ M and 25 $\mu$ M survived with no observed toxicity.

These conflicting results presented a challenge but by reviewing the experimental method it was noted that on the first experiment, when limited toxicity was seen in the 100 $\mu$ M, the experimental animals were 4d.p.f. at the start of the experiment and not 3d.p.f. as had been used in the subsequent repeats. It was felt that the DCA must be much more toxic to these animals when given a day earlier. To confirm these results an exact repeat was run of the primary experiment, however the 1mM group was excluded due to its original toxicity. As expected when the DCA was given to animals a day later at 4d.p.f. all animals in the 100 $\mu$ M group survived and no toxicity was seen.

When all of these experiments were completed the surviving animals in each treatment group were processed and H&E analysis undertaken to examine the effects of DCA stimulation. An interesting phenotype was seen when comparing control animals to the 100 $\mu$ M exposure group. In Figure 4.6 this has been highlighted whereby the sections highlighting the pharyngeal 'teeth' and proximal oesophagus, (images A and B respectively), in both the control and the 100 $\mu$ M DCA exposed animal, (images 1 and 2 respectively), appeared to have a similar appearance. However, when looking at the mid oesophageal section in each animal, (image C), there was a marked phenotypic difference in some of the experimental animals, where a vacuolated cell type was observed. This can be seen in more detail in Figure 4.7.

In the first DCA stimulation experiment there was another phenotype which was also observed in the 100 $\mu$ M stimulated animals. The site of interest was where the oesophagus and the intestinal bulb meet and then open out into the 'stomach' area. Here a marked thinning of the intestinal wall was observed and a thin flattened epithelium was seen in the DCA exposed animals when compared to the control (data not shown). This phenotype was however, only observed on one occasion and it was felt that this was probably more due to the toxicity of the DCA than any metaplastic changes that had occurred, as it was not found to be reproducible on subsequent experiments.

H&E analysis was undertaken to examine the effects of DCA stimulation at 10 $\mu$ M. Interestingly the same vacuole cell types were observed in the mid oesophageal region of some of these experimental animals. This phenotype can clearly be seen in Figure 4.8 when looking at the mid oesophageal section in each animal, where 1A is the control animal and 1B is the animal exposed to 10 $\mu$ M of DCA.

The control animals were also closely examined and in some of the animals it was felt that a similar phenotype was seen. It appeared that while there were some control animals, which showed this vacuole cell phenotype it was not as exaggerated and occurred much less frequently than in the DCA treated animals.

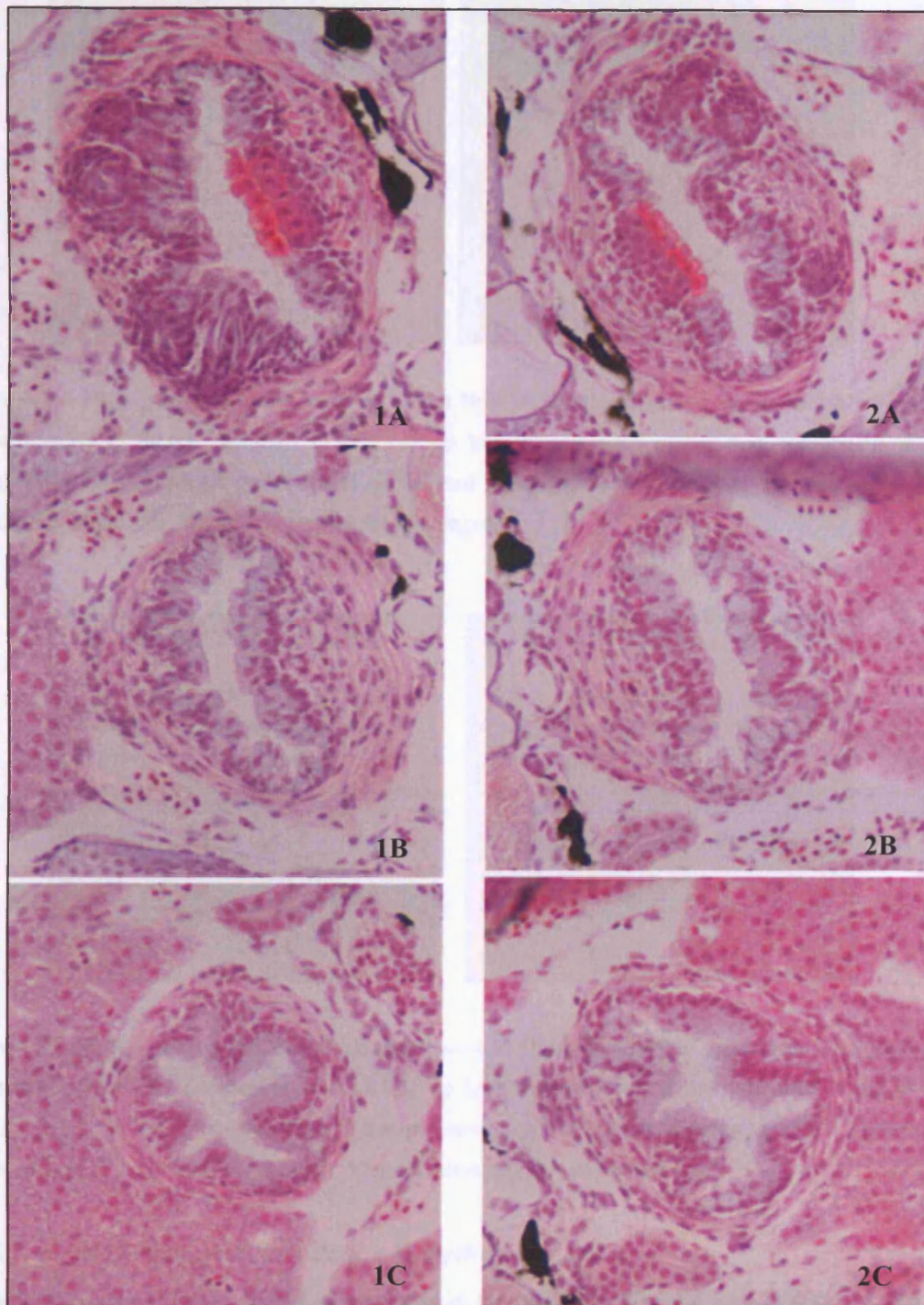


**Figure 4.6 – H&E analysis of first DCA stimulation experiment.** All images are cross sectional views of 8d.p.f. zebrafish. (1A) Pharyngeal ‘teeth’ are clearly seen by strong pink staining in the control animal. (1B) Proximal oesophagus in the control animal. (1C) Mid oesophagus in the control animal, seen in high power in Figure 4.7, 1A. (2A) Pharyngeal ‘teeth’ are clearly seen by strong pink staining in the 100µM exposed animal. (2B) Proximal oesophagus in the 100µM exposed animal. (2C) Mid oesophagus in the 100µM exposed animal seen in high power in Figure 4.7, 2A. Magnification x25 for all images.

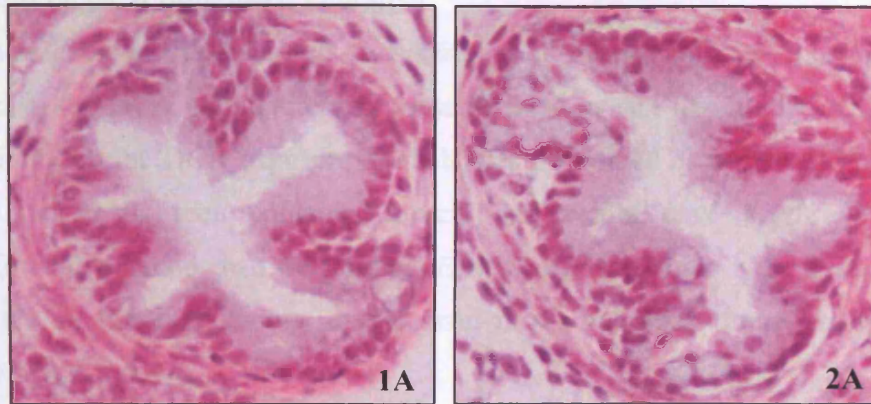


**Figure 4.7 – High powered H&E analysis of the first DCA stimulation experiment.** All images are cross sectional views of 8d.p.f. zebrafish. (1A) Close up high power insert of the mid oesophagus in the control animal. (2A) Close up high power insert of the mid oesophagus in the 100µM exposed animal, showing a vacuole cell phenotype. Magnification x25 for all images.

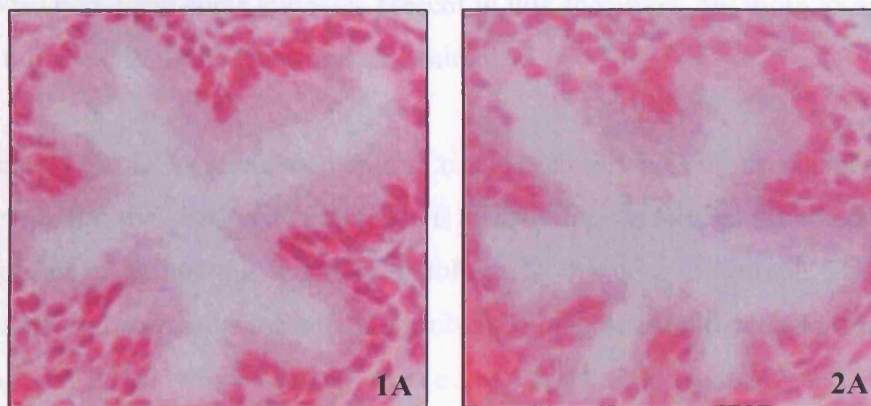


**Figure 4.8 – High powered H&E analysis of the second DCA stimulation experiment.** All images are cross sectional views of 7d.p.f. zebrafish. (1A) Close up high power insert of the mid oesophagus in the control animal. (2A) Close up high power insert of the mid oesophagus in the 10µM exposed animal, showing a vacuole cell phenotype in the top left hand corner. Magnification x25 for all images.

#### 4.4.3.1 DCA Zebrafish Stimulation Statistics

Statistical analysis was carried out to see if there was a significant difference between the DCA stimulated animals versus the control groups when showing a vacuole cell phenotype. The Fishers exact test looked at 19 animals in the DCA group (11 = positive, 8 = negative) and 20 animals in the control group (5 = positive, 15 = negative). A two-tailed probability value of  $P = 0.05$  for the DCA versus control animal group was observed. Full statistical analysis and raw data can be seen in Appendix 7, page 264.

#### 4.4.4 EM on DCA Stimulated Zebrafish

Electron microscopy was carried to determine if the vacuole cell phenotype which was observed in the DCA stimulation experiments were in fact like goblet cells. Initially alcian blue staining on the DCA exposure animals was performed as this would have shown if the vacuole type cells seen contained mucin and would have been a faster and more straightforward method than performing EM work. The alcian blue worked in the human control tissues however, it was unsuccessful in the zebrafish tissues, and as such did not produce any useful data.

EM work was carried out with support from Angleen Fleming and the analysis with guidance from David Hopwood. The EM of the control animal revealed an epithelium in which the villi were more regularly organised at the cellular apex (Figure 4.9A). The cells were regular in form and while there was some debris in the intracellular space, the specimen could clearly be examined. There were some vacuoles present in this specimen, but these looked very different to those observed in the DCA stimulated animal.

Unfortunately the DCA stimulated animal tissue quality was slightly decreased and therefore the image quality has suffered (Figure 4.9B). However, there was a marked difference in the phenotype when comparing it to the histology of the control animal. The epithelium was recognisable and numerous lucent and semilucent vacuoles could be seen throughout the cells from base to apex, which looked markedly different to anything seen in the previous specimen. The villi at the surface, and possibly also on the sides, were irregularly arranged. There were some intracellular canaliculi visible and the lamina propria and smooth muscle fibres were also recognisable.

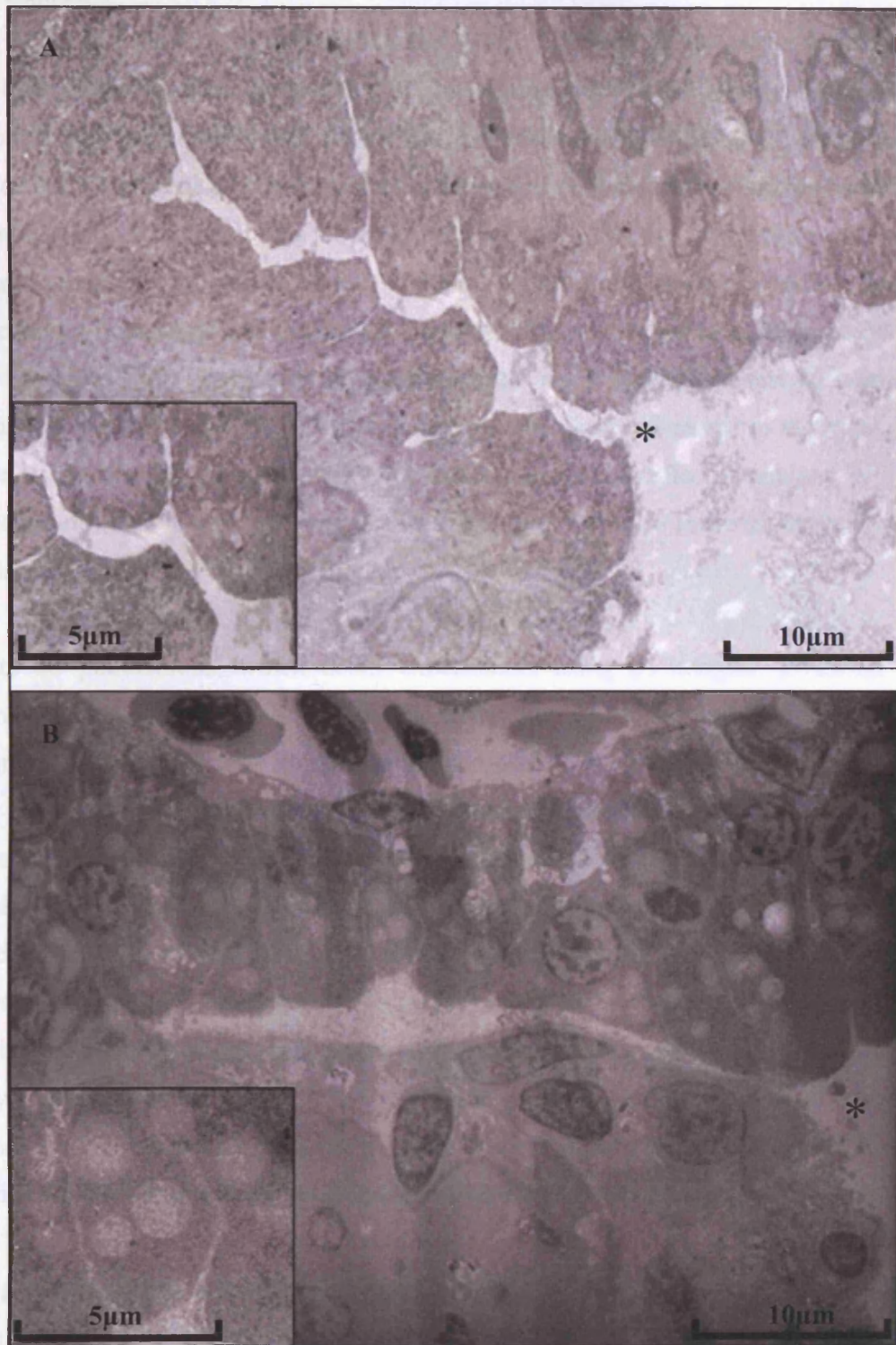


**Figure 4.9 – Zebrafish EM analysis.** All images are parasagittal views of 8d.p.f. zebrafish. In each picture the sections are positioned so that head to tail runs from left to right and that the dorsal to ventral surfaces run from top to bottom respectively. These images are increased magnification shots of the region of the oesophagus where it meets the junction with the intestinal bulb (as indicated by an \* in each figure). (A) Control exposure animal. (B) 100uM DCA exposure animal. In each picture scale bars are representative of size.

## 4.5 Discussion

IHC is difficult to perform in zebrafish as they have only recently become a widely used and recognised scientific research model. For this reason there is a scarcity of commercially available antibodies optimised for their use and even less available which are zebrafish specific. While only one of the antibodies utilised was endorsed by the manufacturer for use in zebrafish IHC, it was felt that the other two antibodies should be investigated due to the fact that they were endorsed as being functional across a wide range of species and/or had high sequence homology with zebrafish. The antibodies were chosen as the proteins were of major importance throughout this body of research and it was of interest to examine their function in zebrafish and to see if this was comparable to that observed in the human setting. Despite trying several different antibodies under a range of different antigen retrieval and detection conditions it was not possible to satisfactorily optimise these to perform successful zebrafish IHC.

To date no publications, which detail experiments using  $\beta$ 1-integrin,  $\beta$ -catenin or Pan-cadherin for zebrafish IHC in the GI tract have been published. For this reason it is difficult to compare any of our findings with other published work. Whilst the  $\beta$ 1-integrin antibody could not be endorsed for zebrafish IHC, both the  $\beta$ -catenin and Pan-cadherin antibody produced good staining and would be endorsed for future use. In the DCA treated animals an upregulation of Pan-cadherin was seen in the oesophageal region. Anti-pan-cadherin antibodies can cross-react with virtually all members of the cadherin family, such as neuronal cadherin (N-cadherin), E-cadherin, P-cadherin, and others (Lee *et al.*, 2003) and display a broad cross reactivity with other members of the cadherin family (Geiger *et al.*, 1990). As already mentioned E-cadherin is decreased in poorly differentiated tissue in all other models, therefore the upregulation seen here is likely to be P-cadherin, as this is one of the only cadherins which is known to increase in differentiated tissues (Muller *et al.*, 2002).

It was also noted that there was an experimental phenotype showing a thinning of the mucosal wall in the Pan-cadherin sections. As mentioned this was observed in a previous experiment where zebrafish were exposed to 100 $\mu$ M of DCA. However as this phenotype was only seen twice it would suggest that it may be a disease induced phenotype. This is in accordance with the findings by Fleming *et al.*, (2007), where picryl sulfonic acid (PSA) was used to induce inflammatory bowel disease in zebrafish. Although this work focussed more on the loss of the convolutions in the gut wall rather than the mucosal thickness, they do state that a thinning of the gut wall in the region below the swim bladder ('stomach' area) was observed.

IHC is a powerful technique for determining both the presence of and the sub-cellular location of proteins in tissues. Zebrafish are particularly amenable to this technique and it is possible to localise proteins both in whole embryos and larvae, as well as sectioned material. For this reason it is felt that zebrafish specific antibodies will continue to be developed and become much more commercially prevalent, this will in turn lead to a greater scientific appreciation of how valuable studies, such as those seen here, can be.

When looking at the DCA stimulation experiments there were some interesting, if confounding, results. Initially, it was noted that the 100 $\mu$ M DCA exposure stimulation experiments produced inconsistent results. Data varied from either all test animals surviving with no noxious effects, or all test animals becoming sick with no survival in treatment groups, or even a variation of both extremes. This variability in survival was confounding but on closer examination of the experimental conditions several factors could be taken into account.

Firstly, it was noted that when the exposure experiment was set up with 4d.p.f. animals their chance of survival was greatly increased than if 3d.p.f. animals were utilised. As no other experimental conditions had changed it was felt that the toxicity had not occurred due to a longer exposure, but purely that the DCA must be much more toxic to animals if exposure occurred a day earlier (confirmed by Angleen Fleming, personal communication).

Secondly there were also some problems with variability in clutch survival, during the course of these experiments, when repeats were undertaken. Initially it was felt that the results may not be reproducible and therefore limit their scientific validity. However, it should be noted that when working with zebrafish there are many factors that can alter the outcome of a particular experiment. The most likely cause for the clutch variability observed here is that the aquarium was running at a different temperature when the initial assays were run and so the larvae were able to tolerate higher doses of compound. There could be two possible explanations for this; firstly, if the aquarium was running at a cooler temperature then all processes in the animals would slow down such as; swallowing, absorption, and metabolism. This would mean that the animals could tolerate toxic compounds for much longer. Paradoxically, if the aquarium was running at a higher temperature then the DCA could have degraded more quickly and therefore would not have shown such toxicity within the animals (Angleen Fleming, personal communication). It is for this reason dose/response studies are normally repeated if there is a time gap between experiments.

When examining the DCA stimulation assay test animals a distinct phenotype was observed in both the 100 $\mu$ M and 10 $\mu$ M exposed animals. When looking at the mid oesophageal section in each animal a vacuole cell type phenotype was observed. On some occasions however, another phenotype was noted in the 100 $\mu$ M stimulated animals, where a thinning of the cell wall was seen and a flattened epithelium surrounded the 'stomach'. As already mentioned this was only seen once and the 100 $\mu$ M exposure produced varied results, which indicates that a DCA concentration of 100 $\mu$ M is in the toxic range for zebrafish. For this reason the inclination for future work would be to suggest exposures under the 100 $\mu$ M dosage as this appears to be below the toxic dose and still produces the main phenotype of interest.

When examining the statistical findings of the stimulation experiment two main conclusions could be drawn. Firstly, while there were some control animals which exhibited the phenotype, this was not as exaggerated and was a milder phenotype, than those seen in the DCA exposed animals. If this were to be repeated it may be beneficial to grade the animals into mild, strong or no phenotype and stage them according to these criteria for analysis. This would mean that statistics could be carried out to see if there were significant values between controls having a mild phenotype, if at all, and the DCA exposures showing only the more exaggerated phenotype. The fact that the phenotype was also observed in some of the controls may seem to discredit the findings; however this may accurately suggest that these models are even better mimics of the human setting. The results show that when looking at the control animals the phenotype was induced in 5 out of 20 animals. However, when looking at the DCA treated animals this increased by over 2 fold to 11 animals out of 19 showing the phenotype. This could suggest that the phenotype is a naturally occurring phenomenon, due to natural physiology of acid within the animal, as with the human environment, and that all we are doing by adding the DCA is exaggerating this phenotype pathologically. Also it is important to note that in a human setting there would not be 100 $\mu$ M of DCA present in the oesophagus. There may be 100-200 $\mu$ M of bile acids present but the DCA would only constitute a small proportion of this in the normal setting (Janusz Jankowski, personal communication). Therefore, we can say that the 100 $\mu$ M concentration of DCA is a pharmaceutical level while the physiological level of DCA is closer to 10 $\mu$ M. For this reason the 10 $\mu$ M DCA results reflect the human setting more accurately.

Secondly, when looking at the experimental animals it was obvious that not all animals exposed to the DCA showed a metaplastic phenotype. The reason why this did not develop in all animals is unclear; however it may be comparable to BO in man, where only a proportion

of people with GORD go on to develop BM and subsequently onto OA. In humans roughly 30% of the population have GORD of which only 10% suffer with chronic reflux disease, and BO is only seen in 10-15% of cases (Jankowski *et al.*, 1999; Jankowski *et al.*, 2000a; Scott and Jankowski, 2001). These preliminary findings show that the phenotype observed in these assays appear to be comparable to that of human GORD, although it should be taken into account that this was only a three day exposure. It would be of interest to repeat assays with a different time course, and see if this produced a proportion of animals with a phenotype similar to that seen in OA. These results suggest that the zebrafish is not only an excellent high throughput model system to employ for research but that it may also be accurately mimicking what occurs in the human setting, at least for the disease physiology associated with some people where GORD has been attributed to causing BO and finally to adenocarcinoma pathogenesis.

The EM data suggested that the DCA treated animals had a marked phenotypic change to those animals without DCA exposure. In the DCA stimulated animals the tissue was not as organised and showed less uniformity. In the tissue numerous vacuoles were observed throughout the cells from base to apex which appear to be mucin cells with a goblet like cell phenotype. However, it is difficult to say if this experimental animal has been induced to show a “BM phenotype”.

In 1979 Hopwood *et al.*, documented human oesophageal prickle cells having a ruffling of the cell membrane, on these intraepithelial cells which possibly formed after the passage of an intrusive cell. This corresponded to an appearance seen in normal human oesophageal EM which had previously been defined as ‘villous fields’ which could be induced by a variety of substances. By culturing the biopsy for several hours ruffling was apparently more common in inflamed biopsies (David Hopwood, personal communication). Hopwood *et al.*, (1979) also observed intracellular conalculi in gastric parietal cells along with changes in the lysosomes, Golgi apparatus and multi-vesicular bodies. It is possible that the DCA stimulation experiment has induced a similar phenomenon to that observed by these workers, albeit by a different route.

In conclusion, the data presented in this Chapter suggests that any IHC studies carried out on this model system without employing zebrafish specific antibodies should be interpreted with caution. Moreover it was not possible to draw any firm conclusions about DCA pathogenic effects in the zebrafish animal model, despite repeated investigations. However, both 10 $\mu$ M

and 100 $\mu$ M DCA treatments produced findings comparable with that observed during the pathogenesis of human GORD. As a result of this preliminary evidence showing a phenotypic change it would seem prudent to repeat this work with longer time points and a greater range of concentrations. Hopefully, with more robust animal models and further investigation into potential model systems, combined with a molecular epidemiological approach, the contribution of genetic and environmental factors in the development of BM can be clarified.

## **Chapter 5: P-cadherin Transgenic Mouse Model**

## 5.1 Introduction

Since 1980, when the first successful gene-transfer experiment using DNA microinjection on a mouse was reported (Gordon *et al.*, 1980), a method has been established that allows the transfer of a single isolated gene. Gene transfer is the transfer of *in vitro* recombined gene constructs into animals. When a gene construct is integrated into the genome of the animal it is described as a transgene. The coded protein produced by this transgene is the transgenic product. Animals that contain transgenes are transgenic and, if the transgene is passed onto the offspring, transgenic lines or populations will be created (Brem and Wagner, 1991).

The use of animals, especially mice, in biomedical research has become more established due mainly to the improved techniques to create novel designer mutant mice. Transgenic techniques are designed to stably introduce isolated genetic elements (transgenes) into the genome of an organism (Gassmann *et al.*, 2000). There are over 1000 transgenic mice models, and a significant number of these serve as models for genetic disease, accelerating the understanding of diseases and leading towards cures (Hardouin and Nagy, 2000).

In this study an *in vivo* model was designed consisting of transgenic mice and a transgene incorporating the fatty acid binding protein (FABP) promoter to force the expression of P-cadherin in a site of the GI tract where it is not normally expressed. It was hoped that this “knock-in” P-cadherin transgenic mouse would help to explicate the normal and potential pathological roles of P-cadherin expression in the intestine.

E, N and P-cadherin isoforms belong to a highly conserved superfamily of cellular adhesion molecules, which have been implicated in the development and homeostasis of normal tissue function (Takeichi, 1995). Being cell surface proteins, cadherins are glycosylated (Gahmberg and Tolvenen, 1996). Protein-linked carbohydrates determine protein stability, activity and specificity of interaction, and they are also involved in cell-cell and cell-matrix recognition (Varki, 1993). The homophilic binding of cadherins is regulated by extracellular and intracellular signals, which modulate cadherin activity without concomitant changes in cadherin expression (Williams, 1997). Nevertheless, the signals that modulate cadherin activity are not completely characterised.

The recognition of key roles for cadherins in the determination of epithelial cell phenotype, migration, differentiation, and tumour dissemination have stimulated much interest in this family of adhesion molecules (Sanders *et al.*, 2000). In the normal squamous mucosa of the

oesophagus there is membranous co-expression of E- and P-cadherin in the basal compartment whereas suprabasal stratification is associated with preservation of E-cadherin expression but loss of P-cadherin (Sanders *et al.*, 1998).

In the GI tract, alteration of the expression of classical cadherins with aberrant P-cadherin upregulation, associated with co-expression or loss of E-cadherin expression, is seen in neoplastic transformation of oral and oesophageal squamous mucosa and in lesions representing early neoplastic transformation of glandular mucosa, such as aberrant crypt foci and metaplastic and adenomatous polyps. This same phenotype is seen in enterocytes adjacent to foci of ulceration in the intestine in colitis, including inflammatory bowel disease, and in colitis-associated dysplasia. In coeliac disease, reversible E-cadherin downregulation correlates with the degree of villous atrophy, but in contrast with colitis, aberrant P-cadherin expression is not a feature. Aberrant epithelial P-cadherin expression is thus associated with a proliferative phenotype related to ulceration and neoplastic transformation in the GI tract, which may confer a survival advantage on these cells (Sanders *et al.*, 2000). At present very little is known about the phenotypic effects of anomalous P-cadherin expression in the intestine, and the functional roles of P-cadherin and E-cadherin along with the molecular mechanisms underlying P-cadherin/catenin interactions have yet to be elucidated. The current understanding is that P-cadherin expression is elevated in several carcinomas, and mainly associated with well-differentiated tumours (Muller *et al.*, 2002).

There have been various mouse models involving changes in cadherin biology along with their related molecules. N-cadherin and E-cadherin are critical in mouse development and knock-out mice show early embryonic lethality (Luo *et al.*, 2001; Shanahan, 1996).

There is only one main study by Radice (1997) of a P-cadherin knock-out mice showing no embryonic lethality, whereby the P-cadherin gene was mutated to establish the effect of mice deficient in P-cadherin on mammary development. Heterozygous and homozygous progeny did not display any obvious developmental abnormalities compared to their wild type littermates. However, an unexpected phenotype was observed, and the P-cadherin deficient mice displayed precocious alveolar differentiation resembling an early pregnant gland. Also after two years the mice developed alveolar hyperplasia and ductile dysplasia. These findings suggest that P-cadherin appears to act as a negative regulator of mammary cell growth and differentiation.

Many techniques have been developed to overcome embryonic lethality. Hermiston *et al.*, (1996) used an intestine specific promoter (a rat intestinal FABP gene) so that a mutant cadherin was not expressed during foetal development. FABPs are members of a superfamily of cytosolic proteins that participate in lipid transport and metabolism and in intracellular signalling within vertebrates and invertebrates (Wang *et al.*, 2005). Differences in tissue expression, and sometimes co-expression in single cell types suggest that FABPs have specialised functions.

The small intestine is lined by a continuously regenerating epithelium and is the initial site of dietary fatty acid uptake. The proximal intestinal enterocytes contain two FABPs, namely liver FABP (L-FABP) and intestinal FABP (I-FABP), at relatively high concentrations (0.1-0.3mM) and the intestine maintains gradients in L-FABP gene expression throughout the small and large intestine (Bass, 1985; Sweetser *et al.*, 1988). For this reason the L-FABP gene represents a useful tool for analysing the molecular basis for intestinal epithelial differentiation since it exhibits cell-specific, region-specific, as well as developmental stage specific expression (Roth *et al.*, 1990).

## 5.2 Aims

The aim of this Chapter was to investigate the phenotypic changes resulting from P-cadherin neoexpression in the mouse GI tract.

The specific objectives were:

- 1) To characterise the P-cadherin transgene construct, and confirm sequence identity.
- 2) To induce the expression of P-cadherin in a site of the murine GI tract where it is not normally expressed, using a FABP promoter.
- 3) To investigate the association of native P-cadherin expression and disease status.
- 4) To investigate both native and transgene P-cadherin expression throughout the GI tract.

## 5.3 Materials and Methods

General reagents are described in section 2.1.5. Primary antibodies are described in section 2.1.4 in Table 2.3. Oligonucleotides are described in section 2.1.6 in Table 2.4. Tissue samples are described in section 2.1.1.2 and processing details found in section 2.2.1.3. H&E staining of FFPE sections was performed as detailed in section 2.2.4.2. Expression and localization of molecules studied was achieved by IHC as described in section 2.2.5. Competent cell transformation and colony selection was carried out as detailed in 2.2.7.

Plasmids were propagated and DNA extracted and purified as described in sections 2.2.8 and 2.2.8.1. Characterisation of the P-cadherin plasmid was achieved by sequencing work and restriction analysis as described in sections 2.2.9 and 2.2.10. DNA and RNA extraction from tissues was performed as described in sections 2.2.11 and 2.2.12. cDNA was generated as detailed in section 2.2.13. PCR was carried out according to the protocol in section 2.2.14. Statistical analysis information can be found in section 2.2.16.

## 5.4 Results

### 5.4.1 Characterisation of P-cadherin Transgene Plasmid Construct

As previously described the P-cadherin transgenic mice were utilised in accordance with the project licence of Dr. R.A. Goodlad (PPL 70/5134, 19b1). These transgenic mice were initially involved in another project and all original information, relating to both the generation of these transgenic mice and any construct information was not available. For this reason it was considered important that prior to any experimental analysis conducted for the purposes of this thesis some basic characterisation of the construct should be performed to confirm sequence identity for P-cadherin and to identify the promoter specificity.

Initially DH5- $\alpha$  competent cells were transformed with the given P-cadherin transgene clone. 20 colonies were picked and screened by PCR, (primer set 1; Table 2.4), to see which colonies were positive for the P-cadherin transgene. From Figure 5.1A it can be observed that from this initial screening process five samples were positive for the P-cadherin transgene (lanes 3, 4, 7, 9 and 14) although two were much stronger than the others (lanes 7 and 9) and it was decided to use colony number 9 in all future experiments.

Colony number 9 was streaked out onto agar and grown to gain single colonies. The plasmid DNA was isolated using mini prep cultures and glycerol stocks were prepared and stored. Figure 5.1B shows the agarose gel which was run from the mini prep DNA samples obtained after processing which clearly shows that all mini prep samples had DNA present (lanes 1-6). This plasmid DNA was then pooled and used in all future experimental work.

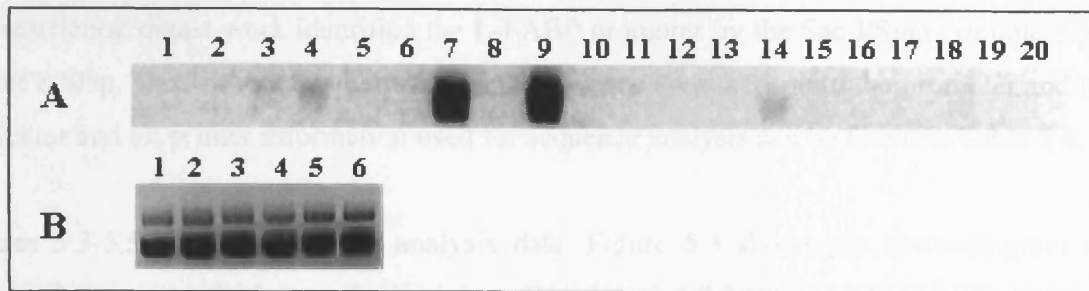


**Figure 5.1 – Colony screen PCR of P-cadherin transformed DH5- $\alpha$  competent cells and mini prep DNA agarose gel.** (A) 20 colonies were picked and examined for the presence of the P-cadherin gene following transformation with DH5- $\alpha$  competent cells. The band represents the P-cadherin transgene. (B) P-cadherin transgene mini preps from 6 daughter colonies from colony number 9. Lanes 1-6 contain the mini prep samples.

Restriction digest work was carried out on pooled plasmid DNA, to determine the P-cadherin transgene plasmid map. The restriction enzymes used were Sac I, Sma I, Hind III, EcoRV along with a Sac I/Sma I double digest, which were based on information given to me regarding the original cloning vector and cloning sites. Figure 5.2A details the restriction analysis when the digests were run on a 1% agarose gel. The uncut DNA shows the total size of the vector (lane 2) and each separate digest can then be seen in the subsequent lanes (lanes 3-7). Figure 5.2B provides information on the Bioline Hyperladder I marker which was used, giving a detailed molecular weight for each product band size.

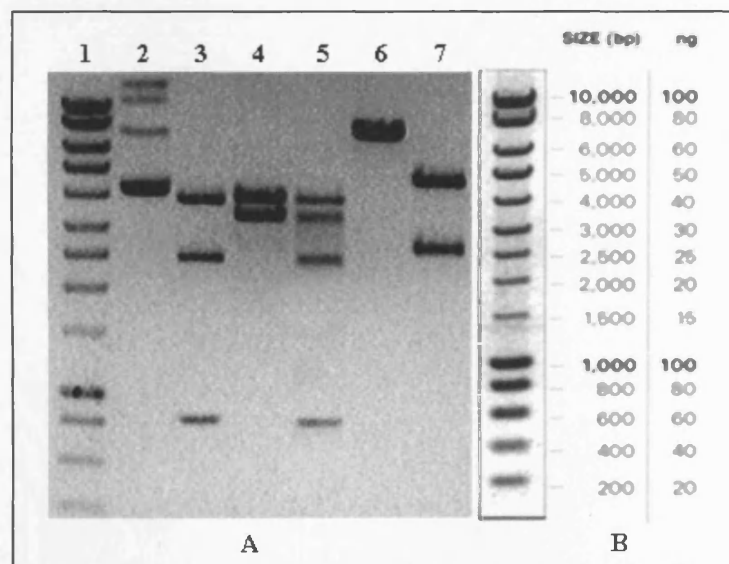


**Figure 5.2 – Restriction digest analysis.** Five restriction enzymes were used to perform digests on pooled mini prep plasmid DNA, as previously described. 10 $\mu$ l of the resulting restriction digest was run out on a 1% agarose gel. (A) Lane 1 represents the site standard (5 $\mu$ l of the Bioline Hyperladder I); lane 2 represents a sample of 5 $\mu$ l of uncut DNA. Lanes 3-7 detail the restriction digest analysis where; lane 3 contains the Sac I digest; lane 4 contains the Sma I digest; lane 5 contains the Sac I/Sma I double digest; lane 6 contains the Hind III digest and; lane 7 contains the EcoRV Digest. (B) Provides information on the Bioline Hyperladder I marker which was used, giving molecular weight for each marker band size.

The restriction digest work identified the L-FABP promoter by the Sac I/Sma I double digest size of 800bp. Next primers were designed to sequence P-cadherin into the promoter and into the vector and all primer information used for sequence analysis can be found in Table 2.4.

Figures 5.3-5.5 show sequencing analysis data. Figure 5.3 shows the chromatogram and 640bp of sequence which was obtained from the analysis of the primer designed to sequence the promoter region of the P-cadherin transgene plasmid DNA. Figure 5.4 shows the chromatogram and 745bp of sequence which was obtained from the analysis of the primer designed to sequence the vector region of the P-cadherin transgene plasmid DNA. Figure 5.5 shows the chromatogram and 896bp of sequence which was obtained from the analysis of the primer designed to sequence the FABP promoter region of the P-cadherin transgene vector. Blast database searches using the NCBI database (<http://www.ncbi.nlm.nih.gov/>) were then performed to check sequence identity, which can be found in Appendix 4.

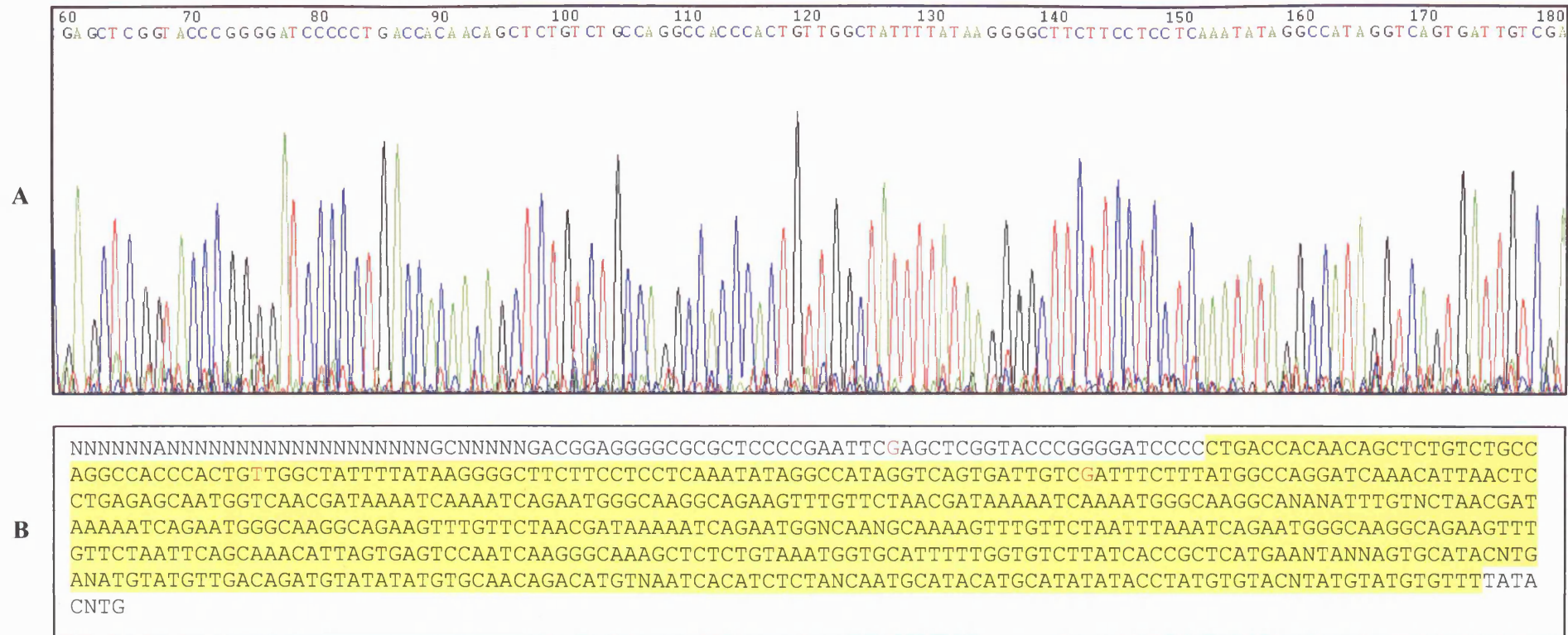


**Figure 5.3 – 5' end region of P-cadherin transgene plasmid DNA sequence analysis for the primer into the promoter region.** (A) A selected region of the chromas trace file for the primer designed to sequence the promoter region. This was exported from chromatogram file obtained from the PNAFL, Leicester. (B) A complete sequence for the analysis of the primer designed to sequence the promoter region. In total 640bp of good quality sequence was obtained and base numbers 60, 120 and 180 have been highlighted in red to correspond with the selected region of the chromas trace in A. The area highlighted in yellow relates to the sequence which corresponded to rat L-FABP.

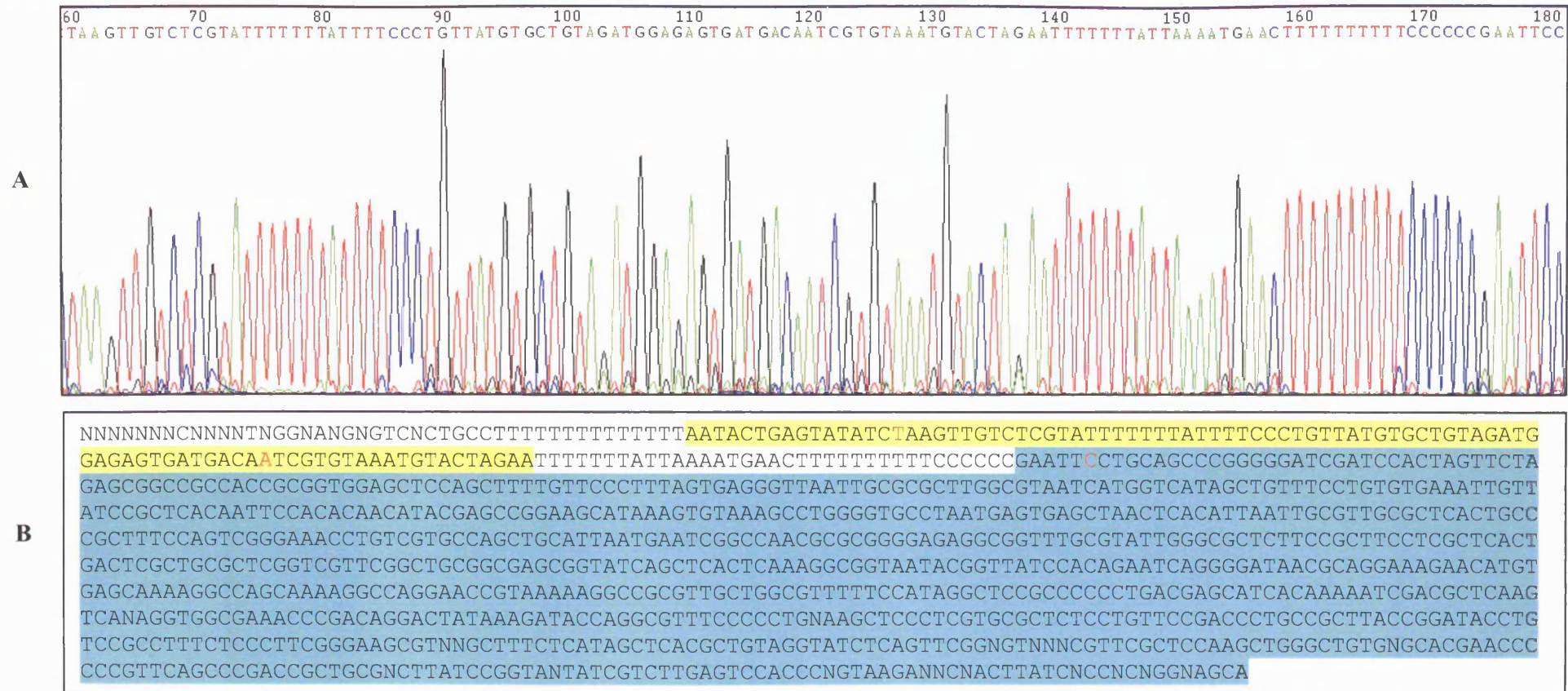


**Figure 5.4 – P-cadherin transgene plasmid DNA sequence analysis for the primer into the vector 3' end region.** (A) A selected region of the chromas trace file for the primer designed to sequence the vector region. This was exported from chromatogram file obtained from the PNAFL, Leicester. (B) A complete sequence for the analysis of the primer designed to sequence the vector region. In total 745bp of good quality sequence was obtained and base numbers 60, 120 and 180 have been highlighted in red to correspond with the selected region of the chromas trace in A. The area highlighted in yellow relates to the sequence which corresponded to mouse mRNA for P-cadherin and those in blue to the pBluescript cloning vector.

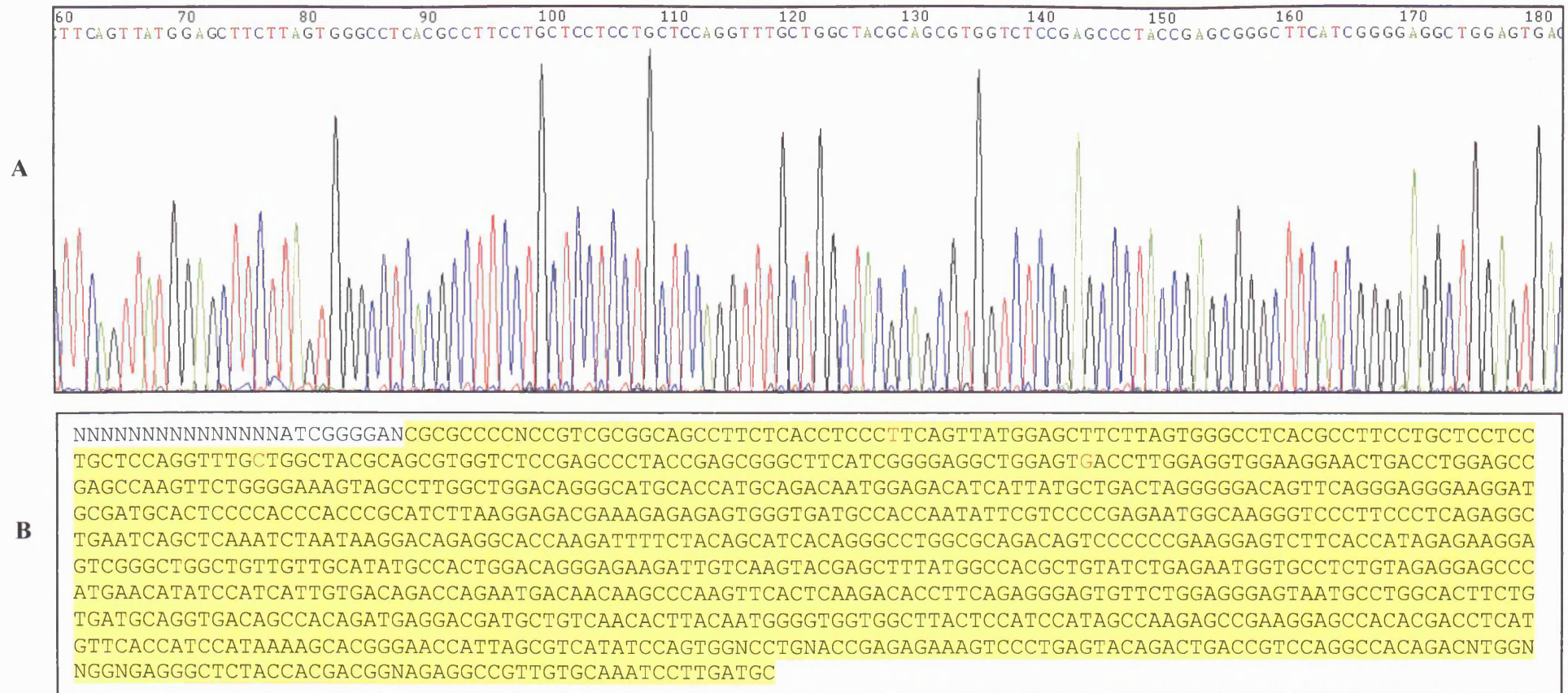


**Figure 5.5 – P-cadherin transgene plasmid DNA sequence analysis for the primer into the fatty acid binding promoter region.** (A) A selected region of the chromas trace file for the primer designed to sequence the FABP promoter region. This was exported from chromatogram file obtained from the PNACL, Leicester. (B) A complete sequence for the analysis of the primer designed to sequence the promoter region. In total 896bp of good quality sequence was obtained and base numbers 60, 120 and 180 have been highlighted in red to correspond with the selected region of the chromas trace in A. The area highlighted in yellow relates to the sequence which corresponded to mouse P-cadherin.

The sequencing plot for the trace into the promoter showed that the sequence was a match to rat L-FABP where 227 out of 235 nucleotides matched and created a 96% identity and there were no gaps in the sequence. These bases have been highlighted in yellow in Figure 5.3 and the NCBI blast data can be seen in Appendix 4, page 243, where bases 398 to 632 of the sequencing plot aligned to bases 464 to 230 of the rat L-FABP sequence. This result was very interesting as from the original sequence we were not sure if we had liver or intestinal FABP.

The sequencing plot for the trace into the vector showed two things. Firstly, the start of the sequence was a match to mouse mRNA for P-cadherin and there were 95 bases of exact matched sequence. These bases have been highlighted in yellow in Figure 5.4 and the NCBI blast data can be seen in Appendix 4, page 243, where bases 45 to 139 line up with 100% identity to bases 3062 to 3156 in the mouse mRNA for P-cadherin and 95 out of 95 nucleotides match.

The second part of the trace into the vector showed a match to the pBluescript cloning vector where 843 out of 870 nucleotides matched and created a 96% identity and there were 8 gaps in the sequence. These bases have been highlighted in blue in Figure 5.4 and the NCBI blast data can be seen in Appendix 4, page 244, where bases 174 to 1039 of the sequencing plot aligned to bases 700 to 1565 of the cloning vector sequence.

The sequencing plot for the trace into the FABP promoter region showed that the sequence was a match to mouse mRNA for P-cadherin where 972 out of 981 nucleotides matched and created a 99% identity and there were 2 gaps in the sequence. These bases have been highlighted in yellow in Figure 5.5 and the NCBI blast data can be seen in Appendix 4, page 245, where bases 25 to 1005 of the sequencing plot aligned to bases 5 to 983 of the mouse mRNA for P-cadherin sequence.

Following the restriction digest analysis and sequencing work it was possible to construct a plasmid map for the P-cadherin transgene. Figure 5.6 shows the plasmid map characterisation with confirmation that the expression vector was L-FABP, not I-FABP, as originally suggested. The P-cadherin cDNA is clone 29 which was sub-cloned in an EcoRV fragment and taken from Nose *et al* (1987). Our sequence from the 3' end of P-cadherin shows the vector to be pBluescript SK+, or derived from this vector, and our sequence from the 5' end of P-cadherin shows  $\geq 800$ bp of L-FABP sequence to be included.

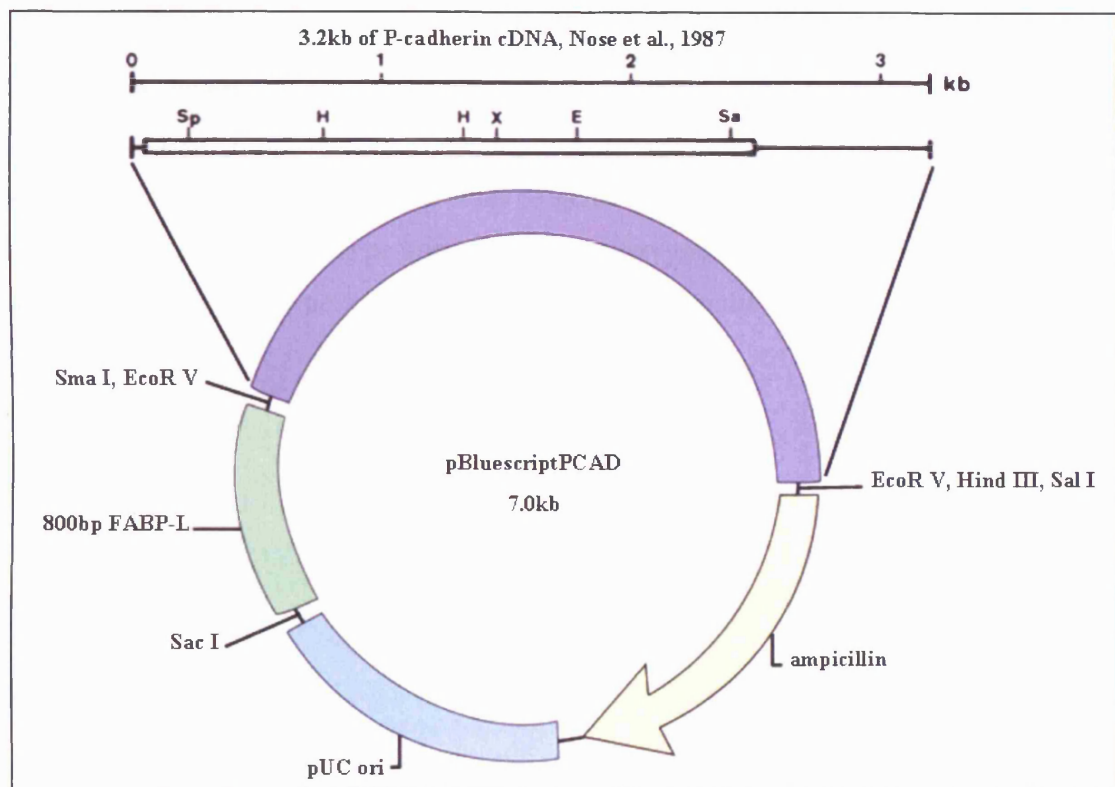


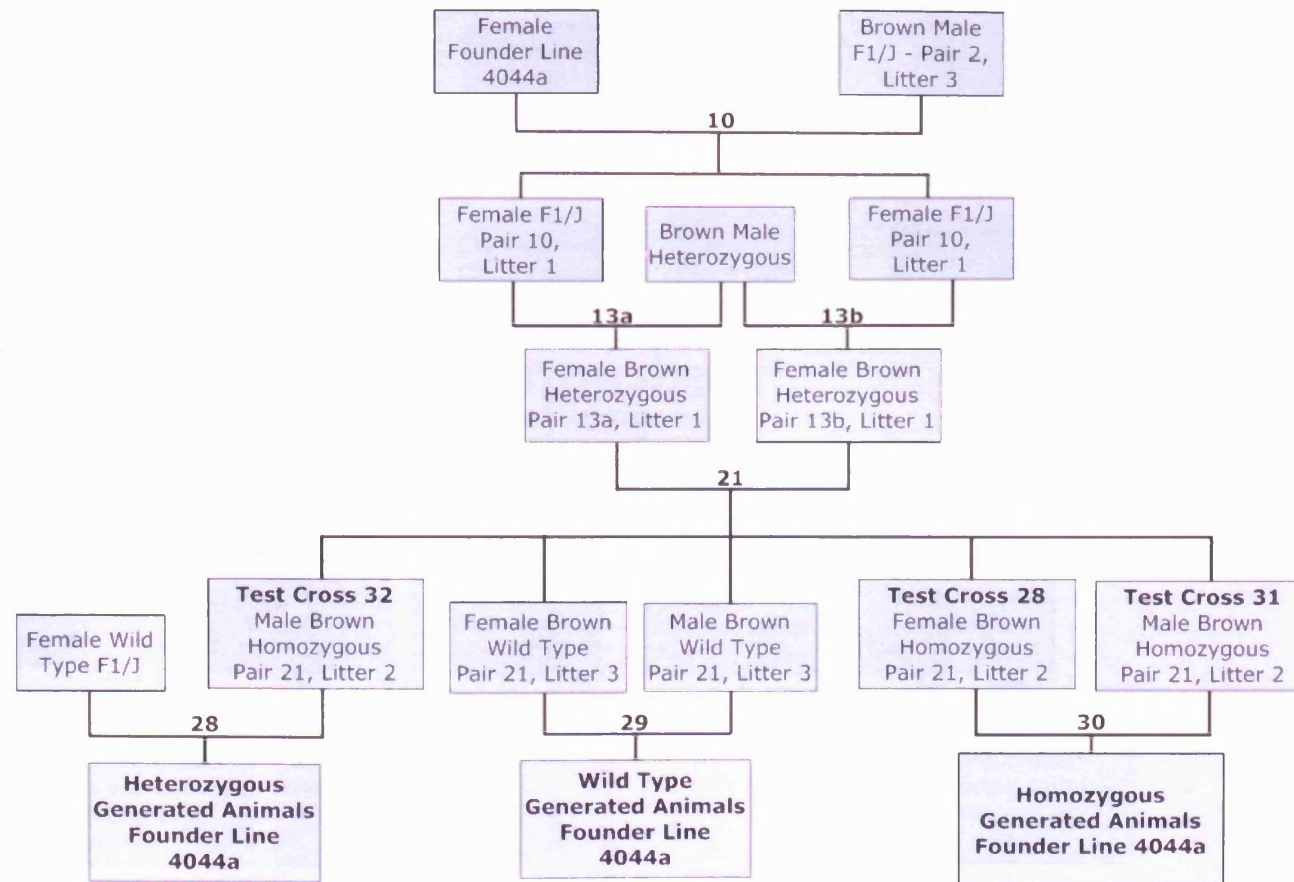
**Figure 5.6 – pBluescriptPCAD plasmid map.** After restriction analysis and sequencing a plasmid map was constructed for the P-cadherin transgene plasmid construct. Sequencing showed the vector to be pBluescript SK+ or a sub-clone derived from this vector. Sequencing also confirmed the presence of an 800bp sequence of L-FABP promoter. The P-cadherin cDNA was confirmed to be 3.2kb of clone 29 which was sub-cloned in an EcoRV fragment (Nose *et al.*, 1987). The open reading frame is shown as an open box. Sp, SphI; H, HincH; X, XAol; E, EcoRV; Sa, SacI. Various restriction sites have also been included.

#### 5.4.2 Generation of Experimental Animals

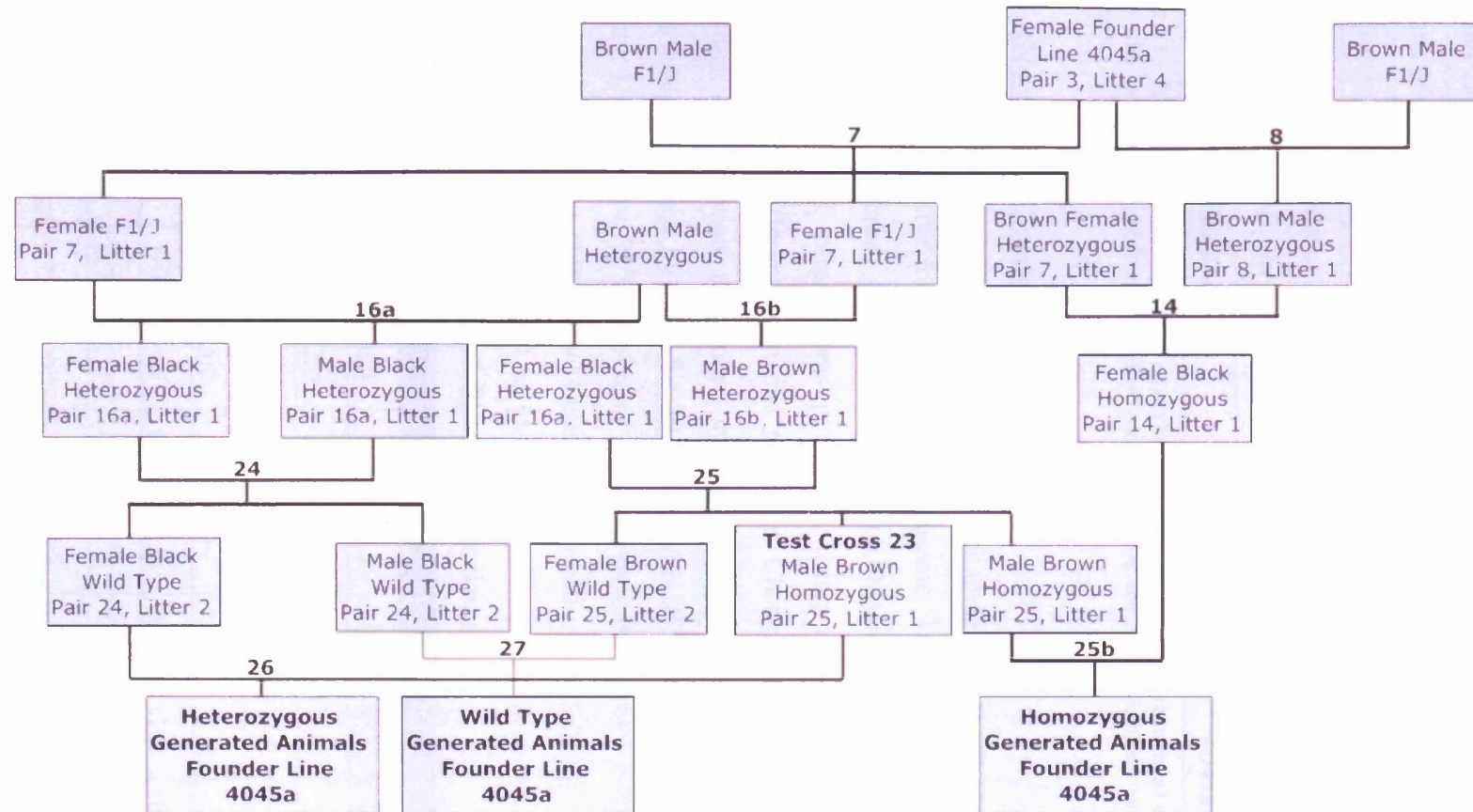
All experimental animals for the wild type, homozygous and heterozygous genotypes were generated using a similar breeding strategy. Experimental animals were generated from two founder female animals which were either from the 4044a female = line 1 or the 4045a female = line 2. The line description will now be used in all subsequent experimental data. All generated animals are listed in Appendix 3, pages 250-252.

Figure 5.7 details the breeding strategy that was performed to generate the heterozygous, wild type and homozygous 4044a (line 1) experimental animals. Figure 5.8 details the breeding strategy that was performed to generate the heterozygous, wild type and homozygous 4045a (line 2) experimental animals. As can be seen from Table 5.1 the experimental animals were produced after four generations of breeding and originated from either the 4044a female

founder animal or the 4045a female founder animal. These females were initially crossed with a F1/J male animal. To create the second generation a female animal from this first cross was mated with a heterozygous male. The third generation consisted of a heterozygous-heterozygous cross from a second generation animal. The fourth and final generation consisted of homozygous-wild type crosses to generate heterozygous animals, wild type-wild type crosses to generate wild type animals and homozygous-homozygous crosses to generate homozygous animals. The genotype of each animal was analyzed using PCR as described in section 5.4.3.



**Figure 5.7 – Founder line 4044a (line 1) breeding strategy and family tree.** This is an abbreviated family tree diagram to show the breeding strategy undertaken to generate the heterozygous, wild type and homozygous line 1 experimental animals. These animals were bred from the 4044a female founder animal, and were generated after four generations of breeding.



**Figure 5.8 – Founder line 4045a (line 2) breeding strategy and family tree.** This is an abbreviated family tree diagram to show the breeding strategy undertaken to generate the heterozygous, wild type and homozygous line 2 experimental animals. These animals were bred from the 4045a female founder animal, and were generated after four generations of breeding.

Experiment Animal	Genotype	Number of Breeding Generations	Founder Animal	Line
Litter 28	Heterozygous	4	4044a	1
Litter 29	Wild Type	4	4044a	1
Litter 30	Homozygous	4	4044a	1
Litter 26	Heterozygous	4	4045a	2
Litter 27	Wild Type	4	4045a	2
Litter 25b	Homozygous	4	4045a	2

**Table 5.1 – Information on transgenic experimental animals used in subsequent experiments.** This table details the genotype, number of breeding generations and the initial founder animal from which they originated.

#### 5.4.3 Genotyping of Transgenic Animals

Genotyping of all generated transgenic animals was undertaken by PCR to determine if they were positive or negative for the P-cadherin transgene. This information enabled a breeding strategy to be undertaken to generate wild type, heterozygous or homozygous animals. Optimisation of PCR primers was performed using the P-cadherin transgene plasmid construct using 10 different multi mix reactions. Changes were made to the PCR buffer, magnesium concentration, and primer concentration. All reaction volumes were 25 $\mu$ l and samples were amplified by PCR for 30 cycles with 95 $^{\circ}$ C denaturation, 30 seconds, 61 $^{\circ}$ C annealing, 1 minute and 72 $^{\circ}$ C extension, 1 minute. In multi mixes 1-6 the Promega GoTaq<sup>TM</sup> Flexi DNA Polymerase (M8305) was used and in multi mixes 7-10 the Invitrogen Taq DNA Polymerase (18038-042) was used, as indicated by the \*. All varied PCR conditions utilised can be seen in detail in Table 5.2; all figures are stated in  $\mu$ l.

	1	2	3	4	5	6	7	8	9	10
Taq	0.2	0.2	0.2	0.2	0.2	0.2	0.2*	0.2*	0.2*	0.2*
PCR Buffer	2.0	2.0	2.0	2.0	~	~	2.0	2.0	~	~
dNTPs	2.0	2.0	2.0	2.0	~	~	2.0	2.0	~	~
MgCl <sub>2</sub>	3.0	3.0	5.0	5.0	~	~	3.0	3.0	~	~
PCADR	1.5	0.75	1.5	0.75	1.5	0.75	1.5	0.75	1.5	0.75
PCADR	1.5	0.75	1.5	0.75	1.5	0.75	1.5	0.75	1.5	0.75
AI Buffer	~	~	~	~	2.5	2.5	~	~	2.5	2.5
H <sub>2</sub> O	13.8	15.3	11.8	13.3	18.3	19.8	13.8	15.3	18.3	19.8
Construct	1.0	1.0	1.0	1.0	1.0	1.0	1.0	1.0	1.0	1.0

**Table 5.2 – Genotyping PCR optimisation conditions.** This table details the PCR optimisation conditions with various amounts of the PCR components in each multi mix in order to optimise the conditions for batch analysis of mouse genotyping.

Experimental Animal	Genotype	Number of Breeding Generations	Founder Animal	Line
Litter 28	Heterozygous	4	4044a	1
Litter 29	Wild Type	4	4044a	1
Litter 30	Homozygous	4	4044a	1
Litter 26	Heterozygous	4	4045a	2
Litter 27	Wild Type	4	4045a	2
Litter 25b	Homozygous	4	4045a	2

**Table 5.1 – Information on transgenic experimental animals used in subsequent experiments.** This table details the genotype, number of breeding generations and the initial founder animal from which they originated.

#### 5.4.3 Genotyping of Transgenic Animals

Genotyping of all generated transgenic animals was undertaken by PCR to determine if they were positive or negative for the P-cadherin transgene. This information enabled a breeding strategy to be undertaken to generate wild type, heterozygous or homozygous animals. Optimisation of PCR primers was performed using the P-cadherin transgene plasmid construct using 10 different multi mix reactions. Changes were made to the PCR buffer, magnesium concentration, and primer concentration. All reaction volumes were 25µl and samples were amplified by PCR for 30 cycles with 95°C denaturation, 30 seconds, 61°C annealing, 1 minute and 72°C extension, 1 minute. In multi mixes 1-6 the Promega GoTaq™ Flexi DNA Polymerase (M8305) was used and in multi mixes 7-10 the Invitrogen Taq DNA Polymerase (18038-042) was used, as indicated by the \*. All varied PCR conditions utilised can be seen in detail in Table 5.2; all figures are stated in µl.

	1	2	3	4	5	6	7	8	9	10
<b>Taq</b>	0.2	0.2	0.2	0.2	0.2	0.2	0.2*	0.2*	0.2*	0.2*
<b>PCR Buffer</b>	2.0	2.0	2.0	2.0	~	~	2.0	2.0	~	~
<b>dNTPs</b>	2.0	2.0	2.0	2.0	~	~	2.0	2.0	~	~
<b>MgCl</b>	3.0	3.0	5.0	5.0	~	~	3.0	3.0	~	~
<b>PCADF</b>	1.5	0.75	1.5	0.75	1.5	0.75	1.5	0.75	1.5	0.75
<b>PCADR</b>	1.5	0.75	1.5	0.75	1.5	0.75	1.5	0.75	1.5	0.75
<b>AJ Buffer</b>	~	~	~	~	2.5	2.5	~	~	2.5	2.5
<b>H2O</b>	13.8	15.3	11.8	13.3	18.3	19.8	13.8	15.3	18.3	19.8
<b>Construct</b>	1.0	1.0	1.0	1.0	1.0	1.0	1.0	1.0	1.0	1.0

**Table 5.2 – Genotyping PCR optimisation conditions.** This table details the PCR optimisation conditions with various amounts of the PCR components in each multi mix in order to optimise the conditions for batch analysis of mouse genotyping.

Following this optimisation, PCR products were run on a 1.5% TBE agarose gel (Figure 5.9) and multi mix 8 was chosen as optimal for further genotyping analyses.

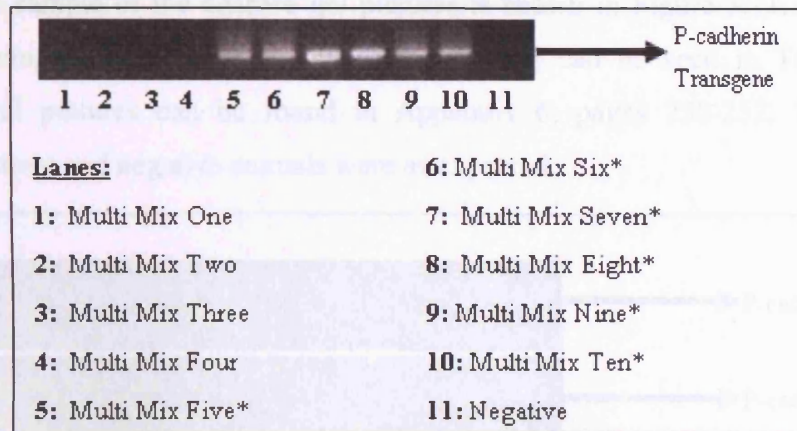


**Figure 5.9 – Optimisation of the genotyping PCR method prior to batch analysis.** The P-cadherin transgene plasmid construct was used as the template in 8 different PCR multi mixes to determine the best PCR reaction (Table 5.2). The band representing the P-cadherin transgene plasmid construct is marked with an arrow and represents 350bp. All positive samples are indicated by an \*.

Once these conditions had been optimised, and three positive and three negative animals had been identified by genotyping, a control PCR was run. This was to determine the most optimal dilution for which to use the P-cadherin transgene plasmid construct which would act as the experimental control. From Figure 5.10 it can be seen that the 1/1000 P-cadherin transgene plasmid construct dilution (lane 9) was the most optimal as the 1/100 dilution (lane 8) produced streaking due to too much DNA being present. It is also possible to see that all of the negative animals showed no product band (lanes 2-4) while the positive animals produced clear bands at the correct 350bp product size (lanes 5-7). Lane 10 was the water blank negative control and showed no band as expected.

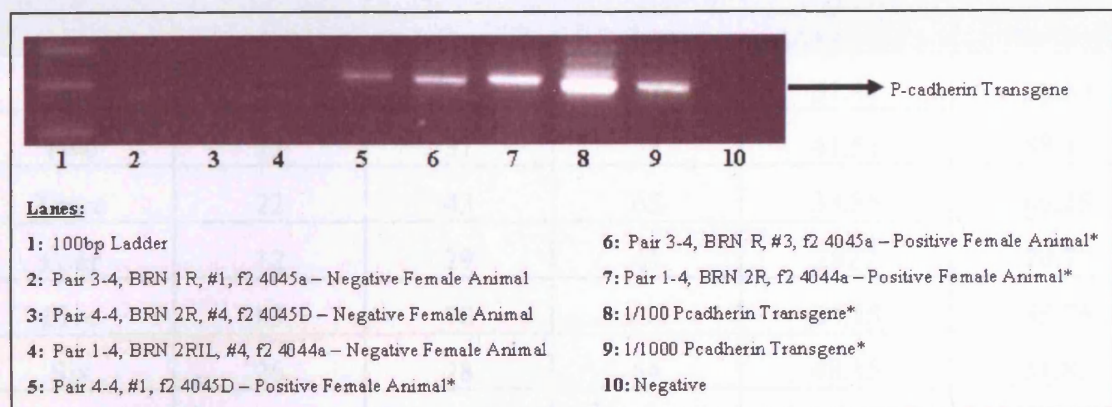


**Figure 5.10 – Optimised PCR method trial prior to batch analysis.** Three negative and three positive animals were used in analysis, along with two dilutions of the P-cadherin transgene. The band representing the P-cadherin transgene is marked with an arrow and represents 350bp.

Genotyping was carried out using the optimal PCR conditions. In total 505 animals were genotyped and 251 of these were positive for the P-cadherin transgene plasmid construct. A representative sample of the agarose gel pictures is shown in Figure 5.11. A more detailed analysis showing all results for the batch genotyping can be seen in Table 5.3 and all genotyping gel pictures can be found in Appendix 6, pages 250-252. The numbers of generated positive and negative animals were as expected.

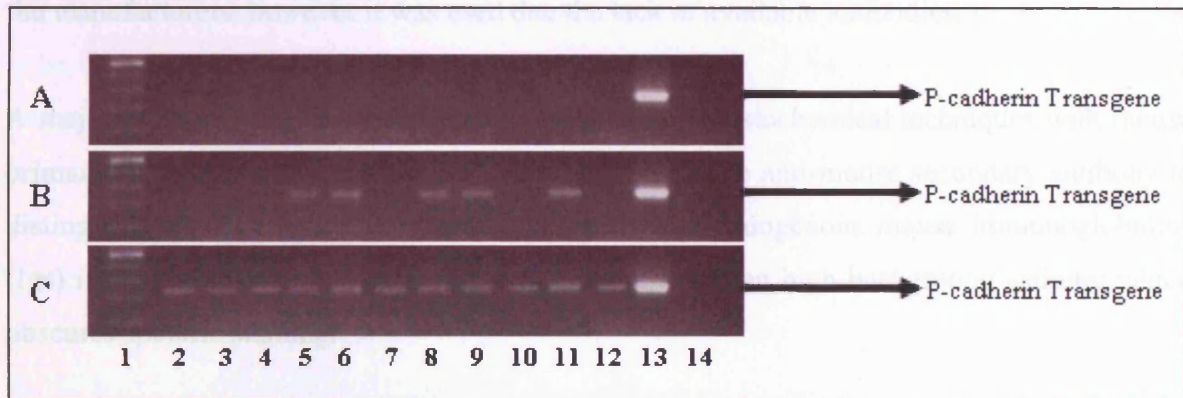


**Figure 5.11 – A representative sample of genotyping analysis for 33 experimental animals.** This batch genotyping was performed in order to breed and generate experimental animals. (A) A representative gel showing wild type animals where no P-cadherin transgene plasmid construct has been detected in the experimental samples. (B) A representative gel showing animals heterozygous for the P-cadherin transgene plasmid construct, where a mixed proportion of the experimental samples show expression of the transgene. (C) A representative gel showing animals homozygous for the P-cadherin transgene plasmid construct where all the experimental samples show expression of the P-cadherin transgene. In each gel, lane 1 represents a 100bp ladder, lanes 2-12 detail the experimental samples, lane 13 represents the positive P-cadherin transgene plasmid construct control at a 1/1000 dilution and lane 14 represents the water blank negative control. The band representing the P-cadherin transgene is marked with an arrow and represents 350bp.

Genotyping Experiment	Number of Negative Animals	Number of Positive Animals	Total Number of Animals	Percentage of Negative Animals	Percentage of Positive Animals
One	35	22	57	61.41	<b>38.59</b>
Two	22	31	53	41.51	<b>58.49</b>
Three	22	43	65	33.85	<b>66.15</b>
Four	12	29	41	29.27	<b>70.73</b>
Five	83	70	153	54.25	<b>45.75</b>
Six	26	28	54	48.15	<b>51.85</b>
Seven	56	27	83	67.47	<b>32.53</b>

**Table 5.3 – Genotyping results for all experimental animals investigated in the batch analysis.** This table represents results obtained from seven independent genotyping experiments which were undertaken for the P-cadherin transgenic animals.

#### 5.4.4 Mouse IHC

Two antibodies were used for P-cadherin immunoreactivity in the mice tissue. The Invitrogen P-cadherin antibody clone PCD-1 IgG<sub>2a</sub> raised in rat had been reported to be suitable for immunohistochemical use on mouse tissue (Nose and Takeichi, 1986; Radice *et al.*, 1997). The Transduction Laboratories P-cadherin antibody clone 56 was a mouse monoclonal antibody and its species reactivity was reported to be limited to human and rat according to the manufacturers; however it was used due the lack of available antibodies.

A major problem faced by investigators to use immunohistochemical techniques with mouse primary antibodies on mouse tissues is the inability of the anti-mouse secondary antibody to distinguish between the mouse primary antibody and endogenous mouse immunoglobulins (Igs) in the tissue. A consequence of this problem has been high background staining which obscures specific staining.

This background problem can be essentially eliminated by using the Vector® M.O.M.<sup>™</sup> immunodetection kit which utilises a novel blocking agent and special labelling methodology to significantly reduce undesired binding of the secondary antibody to endogenous tissue immunoglobulin. The M.O.M. kit is designed specifically to localise mouse primary monoclonal antibodies on mouse tissues. These kits have previously been reported to be useful in specialised areas of research, such as studies in genetically engineered mice, including transgenic and knock-out models, as well as mouse xenografts (Pow *et al.*, 2000).

##### 5.4.4.1 *Immunoreactivity Controls*

In each of the IHC experiments undertaken in this Chapter NPA controls were employed. Under all conditions these worked and produced negative staining which was free from background and non-specific staining. In all figures produced the NPA control was listed as A. Suitable positive control tissues were also utilised in each experiment and specific details of these can be found in each figure legend and in each figure these are listed as B.

##### 5.4.4.2 *P-cadherin, Clone 56*

Immunological staining was carried out on three experimental case sets of caecum tissue and oesophageal squamous mucosa for matched samples of wild type, heterozygous and homozygous mouse transgenic animals.

Using the DAB detection system and Vector® M.O.M.™ immunodetection kit there was no staining present in either the caecum or the oesophageal tissue of any of the experimental animals for either the wild type animal (Figures 5.12C and 5.12D), the heterozygous animal (Figures 5.12E and 5.12F), or the homozygous animal (Figures 5.12G and 5.12H). It was decided that this method was not suitable and therefore not pursued.

#### 5.4.4.3 *P-cadherin, Clone PCD-1*

Immunological staining was carried out on three experimental case sets of caecum tissue and oesophageal squamous mucosa for matched samples of wild type, heterozygous and homozygous mouse transgenic animals.

Using the DAB detection system there was no staining present in either the caecum or the oesophageal tissue of any of the experimental animals for either the wild type animal (Figures 5.13C and 5.13D), the heterozygous animal (Figures 5.13E and 5.13F), or the homozygous animal (Figures 5.13G and 5.13H). It was decided that this method was not suitable and therefore not pursued.

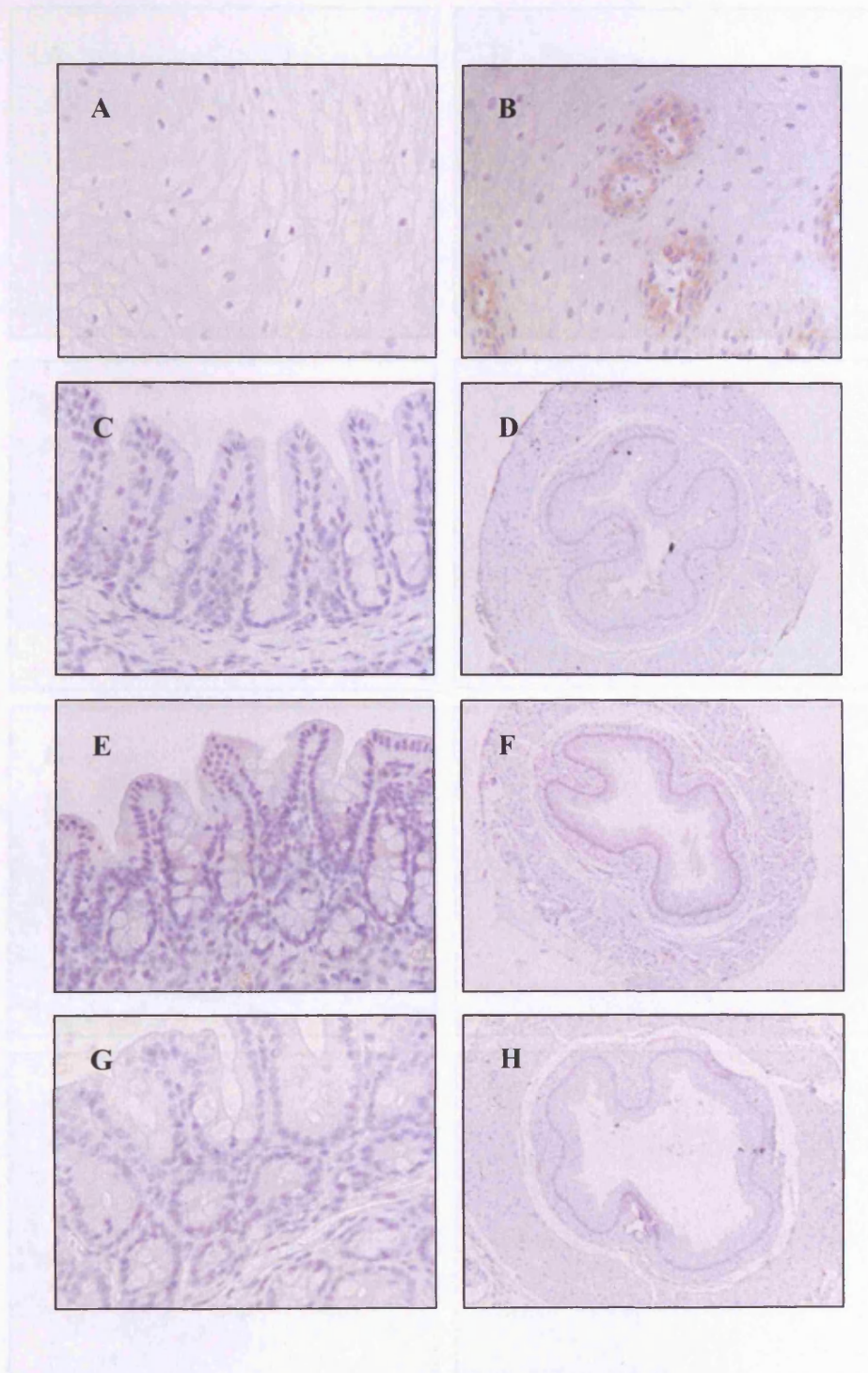


**Figure 5.12 – P-cadherin IHC analysis on mouse experimental control tissues.** The primary antibody is clone 56, 610227 used at a final concentration of  $5\mu\text{g/ml}$  in all tissue with a 20 minute microwave antigen retrieval step. ABC-HRP was used as the tertiary detection system with DAB as the chromogen. (A) Normal squamous negative control, (B) Normal squamous with expression of P-cadherin, (C) Wild type mouse caecum, (D) Wild type mouse oesophagus, (E) Heterozygous mouse caecum, (F) Heterozygous mouse oesophagus, (G) Homozygous mouse caecum, (H) Homozygous mouse oesophagus. Magnification x40 for images A, B, C, E and G and x10 for images D, F and H.

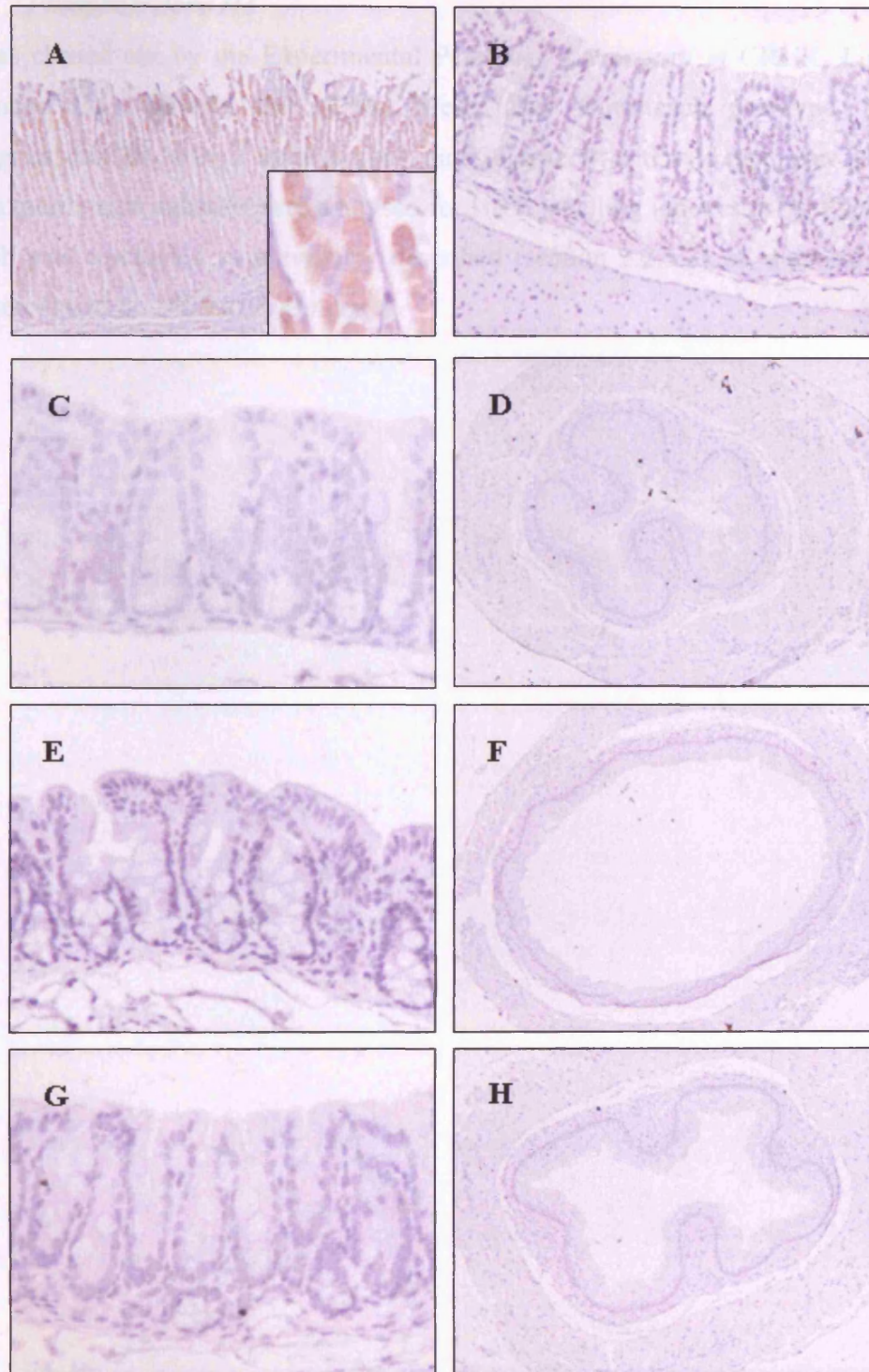
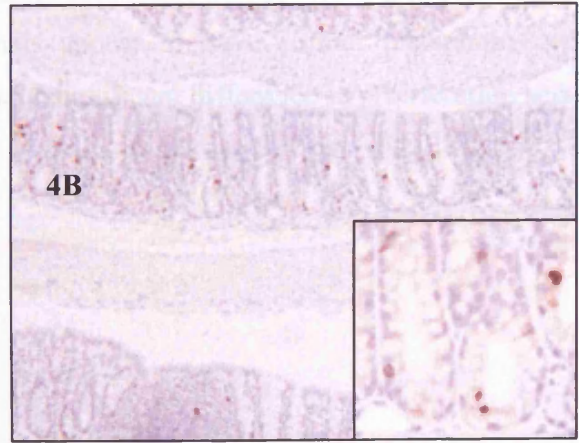
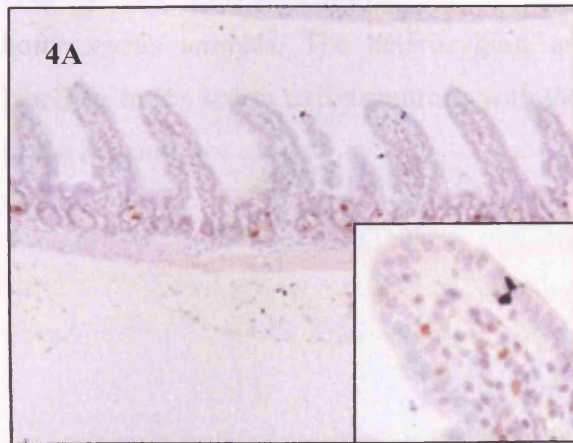
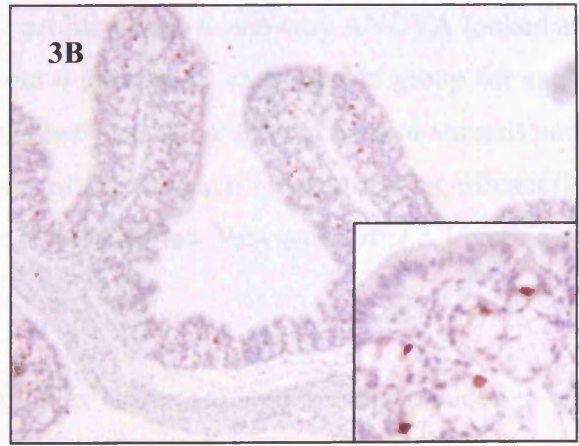
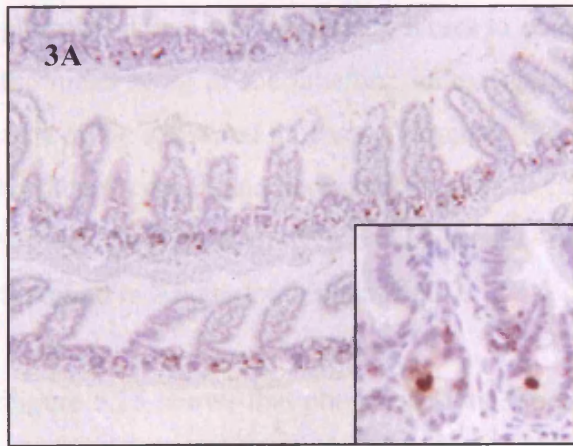
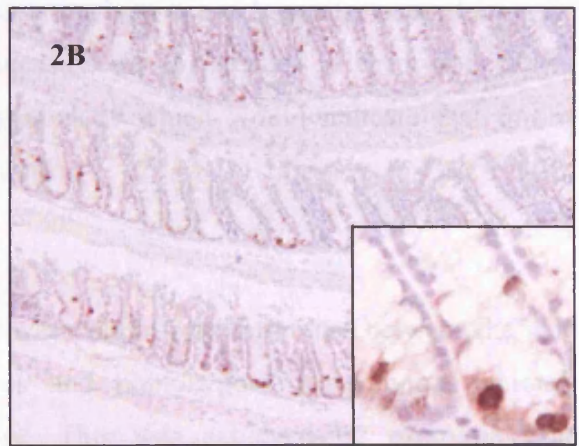
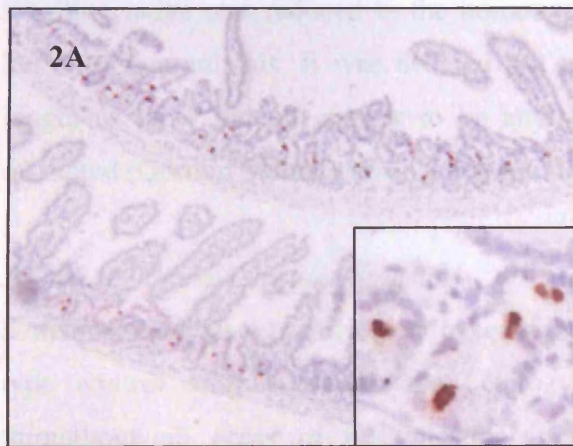
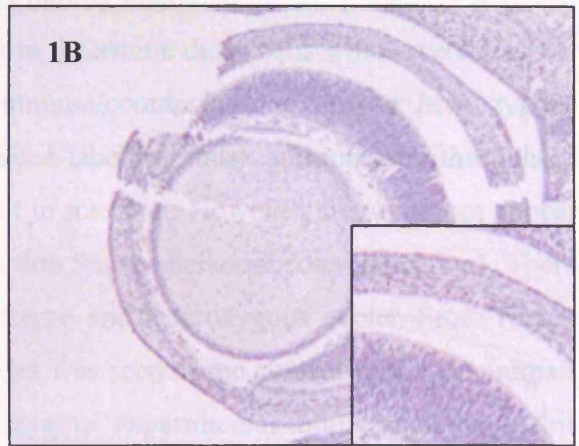
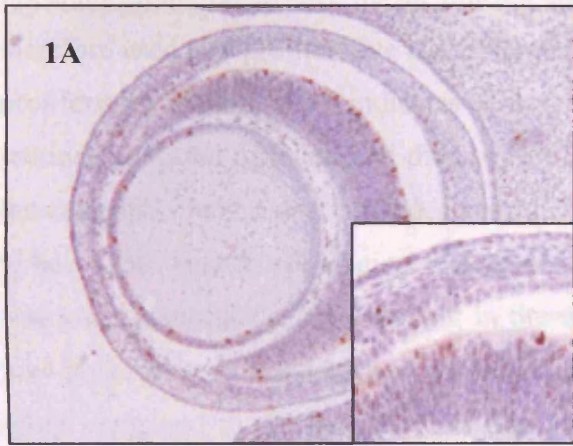


**Figure 5.13 – P-cadherin IHC analysis on mouse experimental control tissues.** The primary antibody is clone PCD-1, 132000Z used at a final concentration of  $10\mu\text{g/ml}$  in all tissues with a 2 minute pressure cooker antigen retrieval step. ABC-HRP was used as the tertiary detection system with DAB as the chromogen. (A) Homozygous mouse stomach, (B) Homozygous mouse LB, (C) Wild type mouse caecum, (D) Wild type mouse oesophagus, (E) Heterozygous mouse caecum, (F) Heterozygous mouse oesophagus, (G) Homozygous mouse caecum, (H) Homozygous mouse oesophagus. Magnification  $\times 10$  for images A, D, F and H,  $\times 25$  for image B, and  $\times 40$  for the high powered insert in A and for images C, E and G.

#### 5.4.4.4 *Phosphohistone H3*

Work was carried out by the Experimental Pathology Laboratory at CRUK, London. Four female mice from founder line 4044A were taken from each genotype, these being heterozygous, pair 28, litter 2; homozygous, pair 30, litter 4; and wild type, pair 29, litter 5. In total 12 experimental animals were analysed for H&E labelling indexes using Phosphohistone H3 which was conducted as previously described (section 2.2.5.3) on mucosal tissue. The counts were based on 1000 cells per crypt.

**Figure 5.14 – Phosphohistone H3 IHC analysis on mouse experimental control tissues.** The primary antibody is polyclonal, 06-570 used at a final concentration of 4 $\mu$ g/ml with a 15 minute microwave antigen retrieval step. ABC-HRP was used as the tertiary detection system with DAB as the chromogen. (1A) Normal mouse embryo eye positive control, (1B) Normal mouse embryo eye negative control, (2A) Wild type mouse SB3, (2B) Wild type mouse LB1, (3A) Heterozygous mouse SB3, (3B) Heterozygous mouse LB1, (4A) Homozygous mouse SB3, (4B) Homozygous mouse LB1. Magnification x10 for all main images and x40 for all high powered inserts.



Phosphohistone H3 is specific for mitosis and is rapidly degraded on entry into G1 and was therefore used as a proliferative labelling marker to determine those cells which were actively proliferating. Figure 5.14 indicates that the immuno/counterstaining on the homozygous sections appeared different and there was a reduced labelling index and intensity throughout the controls, which made the slides very difficult to interpret. However, there did not appear to be a significant morphological difference (Gordon Stamp, personal communication). There was more granular nuclear labelling in the wild type and heterozygous nuclei. From Figure 5.14 it can be seen that a higher proliferative index was seen in the control wild type animals when compared to the heterozygous and homozygous experimental animals, although this labelling index was reduced in the homozygous animals to a much greater extent than the heterozygous animals. It was decided not to measure the differences in crypt and villous length as there did not appear to be anything obvious which would indicate that this is disrupted (Gordon Stamp, personal communication).

#### 5.4.4.5 *Phosphohistone Statistics*

Statistical analysis was carried out to see if there was a significant difference between the wild type control animals versus the heterozygous and homozygous experimental animals throughout all areas of the intestinal mucosa. This was achieved by examining the phosphohistone labelling index scores to observe proliferation. A one-way ANOVA looked at the mean score of the labelling index figures from 4 animals in each sample group for each area of the intestinal mucosa. The mean difference between the wild type control animals and the heterozygous and homozygous animals in areas of the intestinal mucosa was significant ( $P = 0.05$ ). Statistical analysis can be seen in Table 5.4 and all raw data and statistical work can be found in Appendix 7, page 265.

Figure 5.15 shows that phosphohistone labelling index scores are significantly reduced in all areas of the intestinal mucosa when comparing the control wild type animals to the homozygous animals. The heterozygous animals appear to have similar phosphohistone labelling index scores to the controls, with the only significant difference in proliferation seen in the caecum.

Area of Intestinal Mucosa	Comparison Between Animals	Significance Value
SB1	Wild Type vs. Homozygous	0.037
SB1	Wild Type vs. Heterozygous	0.950
SB2	Wild Type vs. Homozygous	0.001
SB2	Wild Type vs. Heterozygous	0.899
SB3	Wild Type vs. Homozygous	0.010
SB3	Wild Type vs. Heterozygous	0.482
LB1	Wild Type vs. Homozygous	0.009
LB1	Wild Type vs. Heterozygous	0.477
Caecum	Wild Type vs. Homozygous	0.001
Caecum	Wild Type vs. Heterozygous	0.009

**Table 5.4: Phosphohistone statistical analysis.** A one way ANOVA with Tukey's post hoc test was used to investigate the significant difference when comparing the phosphohistone labelling index scores between the wild type control animal, and either the homozygous or heterozygous experimental animals, within areas of intestinal mucosa. The mean difference is significant at the 0.05 level, where figures in blue reach statistical significance and those in purple do not, n = 4. Full statistical analysis can be seen in Appendix 7, page 265.

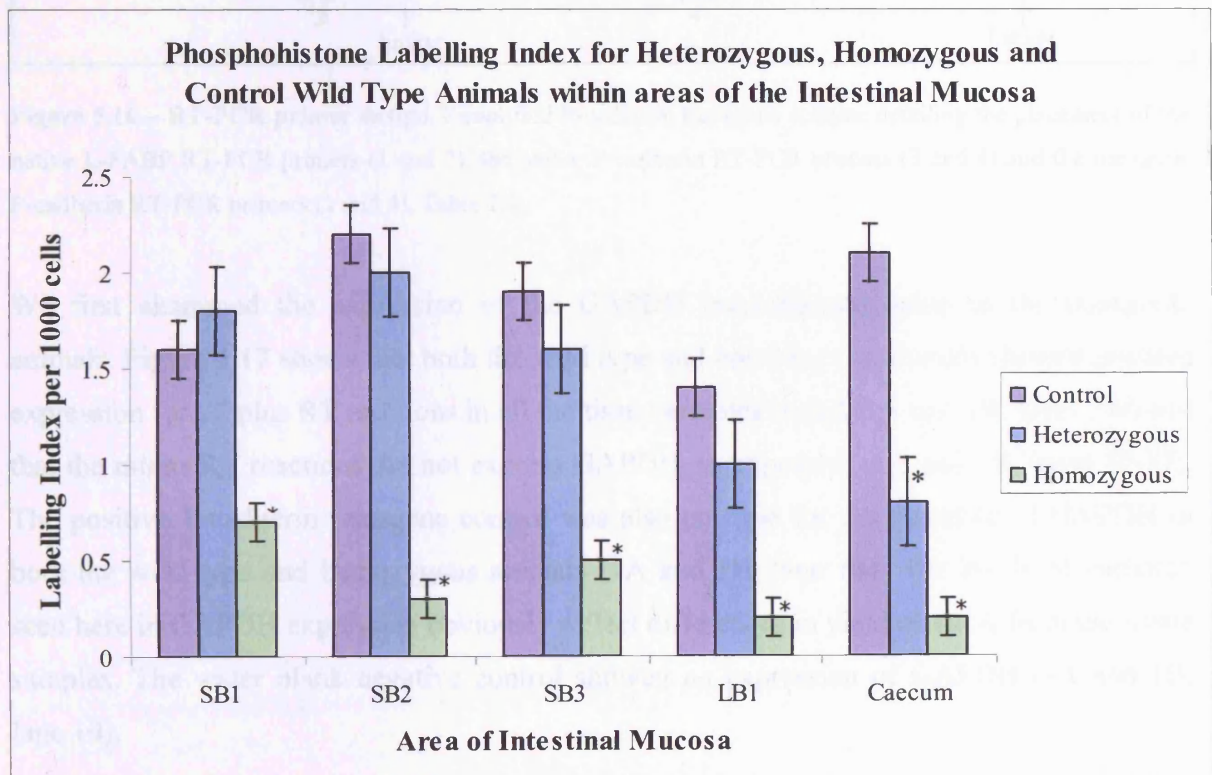


**Figure 5.15 – Phosphohistone labelling index scores for control wild type, heterozygous and homozygous animals in the areas of SB1, SB2, SB3, LB1 and caecum intestinal mucosa.** Each group represents the average labelling index in 1000 cells per crypt taken from 4 female experimental animals from founder line 4044A, where the control wild type animals were from pair 29, litter 5, the heterozygous animals were from pair 28, litter 2; the homozygous animals were from pair 30, litter 4. Error bars represent two standard errors of the mean (SEM). Statistical significance between the wild type control animal and the heterozygous and homozygous animals in areas of the intestinal mucosa is indicated by \* where the mean difference is significant at the 0.05 level.

#### 5.4.5 Expression of P-cadherin Transgene mRNA in Transgenic Mouse Tissues

Animal tissues from line 1, 4044a were examined for P-cadherin transgene plasmid construct expression by RT-PCR. Primers were designed that were specific to native P-cadherin, transgenic P-cadherin and native L-FABP, (Table 2.4, primer sets 7, 8 and 9 respectively). As detailed above the plasmid map for the P-cadherin transgene had been determined and contained the L-FABP promoter and had mouse native P-cadherin inserted into the vector. Using this information primers were designed so that they mapped to either L-FABP cDNA sequence, P-cadherin cDNA sequence or both. Figure 5.16 shows a simplified linear version of the plasmid map, and the position of the RT designed primers.

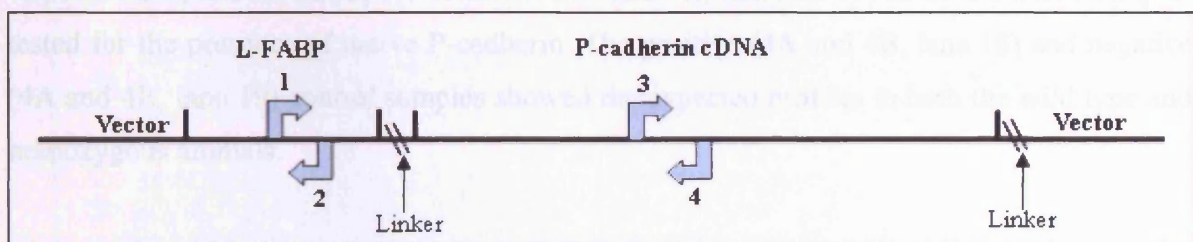


**Figure 5.16 – RT-PCR primer design.** Simplified P-cadherin transgene scheme detailing the placement of the native L-FABP RT-PCR primers (1 and 2), the native P-cadherin RT-PCR primers (3 and 4) and the transgene P-cadherin RT-PCR primers (1 and 4), Table 2.4.

We first examined the expression of the GAPDH housekeeping gene in the transgenic animals. Figure 5.17 shows that both the wild type and homozygous animals showed positive expression for all plus RT reactions in all the tissue samples tested (1A and 1B, lanes 2-9) and that the minus RT reactions did not express GAPDH, as expected, (1A and 1B, lanes 10-17). The positive P-cadherin transgene control was also positive for the presence of GAPDH in both the wild type and homozygous animals (1A and 1B, lane 18). The levels of variation seen here in GAPDH expression obviously reflect differences in yield of RNA from the tissue samples. The water blank negative control showed no expression of GAPDH (1A and 1B, lane 19).

There was no expression throughout all tissue samples tested for the presence of transgene P-cadherin in either the plus or minus RT reactions from the wild type animal (2A, lanes 1-17). The homozygous animal showed weak positive expression of P-cadherin in the plus RT reactions for SB1, SB2, SB3 and colon (2B, lanes 4-7). However, no positive expression was observed in the oesophageal, stomach, liver or caecum (2B, lanes 2-3, 8-9). The positive (2A and 2B, lane 18) and negative (2A and 2B, lane 19) control samples showed the expected profiles in both the wild type and homozygous animals.

Analysis of the expression of the native L-FABP gene (Figure 5.17) showed that both the wild type and homozygous animals expressed L-FABP for all plus RT reactions in all tissue samples (3A and 3B, lanes 2-9), with a definite upregulation of L-FABP in the liver tissues for each animal (3A and 3B, lane 8). The minus RT reactions (3A and 3B, lanes 10-17) and the water blank negative control samples (3A and 3B, lane 18) showed the expected profiles in both the wild type and homozygous animals.

The expression of the native P-cadherin gene observed in Figure 5.17 showed that both the wild type and homozygous animals showed no expression for all plus RT reactions (4A and 4B, lanes 2-9) and all minus RT reactions (4A and 4B, lanes 10-17) in all the tissue samples tested for the presence of native P-cadherin. The positive (4A and 4B, lane 18) and negative (4A and 4B, lane 19) control samples showed the expected profiles in both the wild type and homozygous animals.

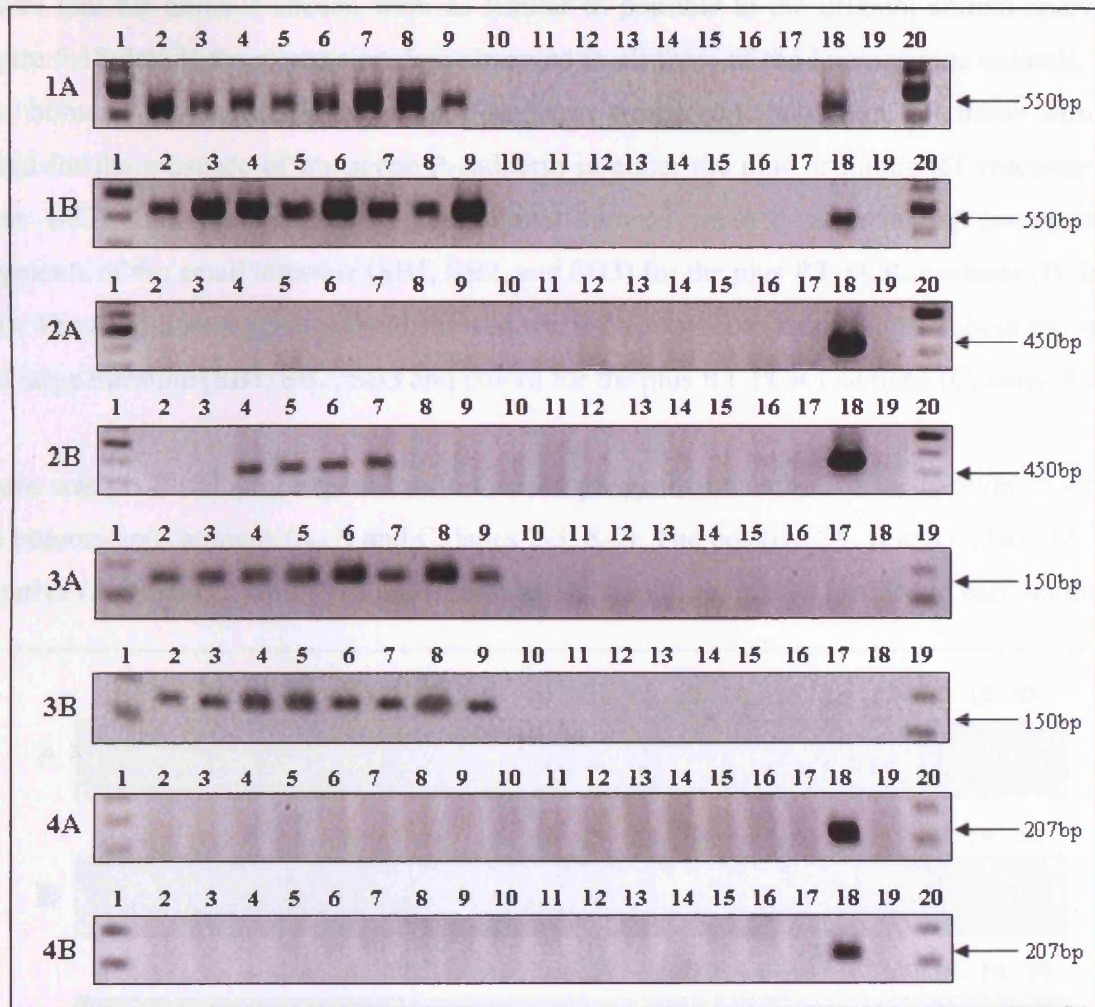


**Figure 5.17 – Expression of P-cadherin transgene mRNA in RT-PCR for wild type and homozygous animals from line 1, 4044a.** (1A) ♂ Wild type animal 3, 4044a 29-6 showing GAPDH expression. (1B) ♂ Homozygous animal 6, 4044a 30-5 showing GAPDH expression. (2A) ♂ Wild type animal 3, 4044a 29-6 showing transgene P-cadherin expression. (2B) ♂ Homozygous animal 6, 4044a 30-5 showing transgene P-cadherin expression. (3A) ♂ Wild type animal 3, 4044a 29-6 showing native L-FABP expression. (3B) ♂ Homozygous animal 6, 4044a 30-5 showing native L-FABP expression. (4A) ♂ Wild type animal 3, 4044a 30-5 showing native P-cadherin expression. (4B) ♂ Homozygous animal 6, 4044a 30-5 showing native P-cadherin expression. In each gel, lanes 1 and 19/20 represent a 100bp ladder, lanes 2-9 represent the plus RT reactions for oesophagus (2), stomach (3), SB1 (4), SB2 (5), SB3 (6), colon (7), liver (8) and caecum (9) respectively. Lanes 10-17 represent the minus RT reactions for oesophagus, stomach, SB1, SB2, SB3, colon, liver and caecum respectively. Lane 18 represents the positive P-cadherin transgene control at a 1/1000 dilution in figure 1, 2 and 4. The water blank negative control in is represented by lane 19 in figures 1, 2 and 4 and by lane 18 in figure 3. Each band has been marked with an arrow and labelled with the appropriate product size.

In order to confirm these findings two more homozygous animals were analysed by RT-PCR. Animals were chosen that were of the same founder line, same sex, the same litter and pair number, and as similar as possible with the weight and tissue sample detail. This was to

ensure that the animals chosen were as similar as possible to the original animal analysed. Figure 5.18 details the expression data observed in all three of the homozygous animals. The first homozygous animal showed no P-cadherin expression throughout all tissue samples tested for the presence of transgene P-cadherin in either the plus or minus RT reactions (A, lanes 1-17). The second homozygous animal showed weak P-cadherin expression in all fragments of the small intestine (SB1, SB2, and SB3) for the plus RT-PCR reactions (B, lanes 4-6). The third homozygous animal showed weak P-cadherin expression throughout the small and large intestine (SB1, SB2, SB3 and colon) for the plus RT-PCR reactions (C, lanes 4-7).

There was no P-cadherin expression in the oesophageal, stomach, liver or caecum in any of the homozygous animals (A, B and C, lanes 2-3, 8-9). The positive (A, B and C, lane 18) and negative (A, B and C, lane 19) control samples showed the expected profiles in each animal.

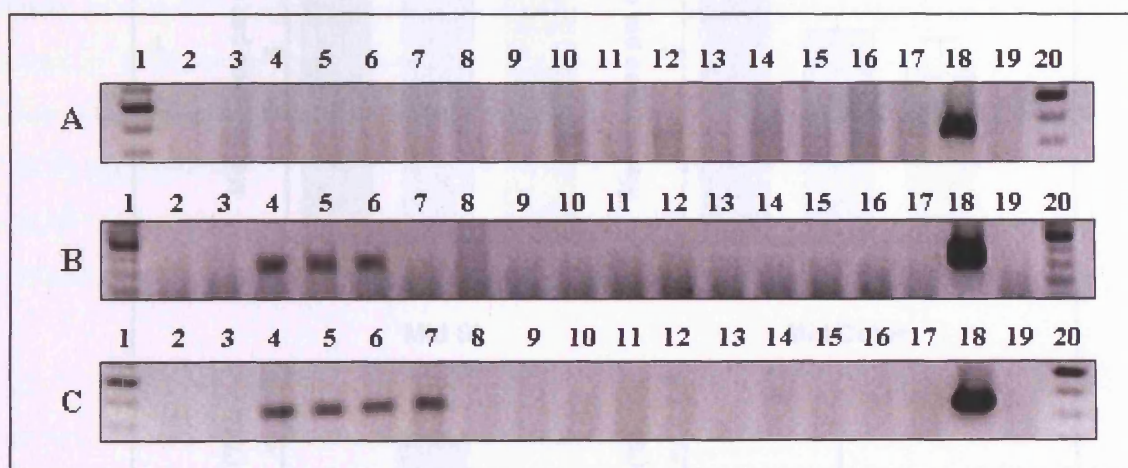


**Figure 5.18 – RT-PCR transgene P-cadherin expression data for three separate homozygous animals from line 1, 4044a.** (A) ♂ Homozygous animal 4, 4044a 30-5. (B) ♂ Homozygous animal 5, 4044a 30-5. (C) ♂ Homozygous animal 6, 4044a 30-5. In each gel, lanes 1 and 20 represent a 100bp ladder. Lanes 2-9 represent the plus RT reactions for oesophagus, stomach, SB1, SB2, SB3, colon, liver and caecum respectively. Lanes 10-17 represent the minus RT reactions for oesophagus, stomach, SB1, SB2, SB3, colon, liver and caecum respectively. Lane 18 is the positive P-cadherin transgene control at a 1/1000 dilution. The water blank negative control in is lane 19. The band representing the P-cadherin transgene represents 450bp.

#### 5.4.6 Protein Analysis

Animals from line 1, 4044a were examined for the presence of the P-cadherin protein by Western blot analysis. The animals which were examined were both heterozygous and homozygous in genotype. Homozygous Animal number 6 was chosen principally as this was the animal which had shown the maximum expression of transgene P-cadherin by RT-PCR investigation. Unfortunately this work has yielded no conclusive results so far and attempts to resolve this are ongoing in Professor Jankowski's research group.

### 5.4.7 Assessment of Proliferation and Fission

Work was carried out by the Histopathology Unit at CRUK, London. Animals from the line 1, 4044a founder line and the line 2, 4045a founder line were examined. Assessment of proliferation and fission thought the gut was performed using the 'crypt microdissection' method as previously described by Goodlad (1994) and in detail in section 2.2.1.3. Figure 5.19A details cell proliferations, assessed by the two-hour accumulation of vincristine-arrested metaphases in the mid small intestine and colon. Figure 5.19B details crypt fission in the mid small intestine and colon.

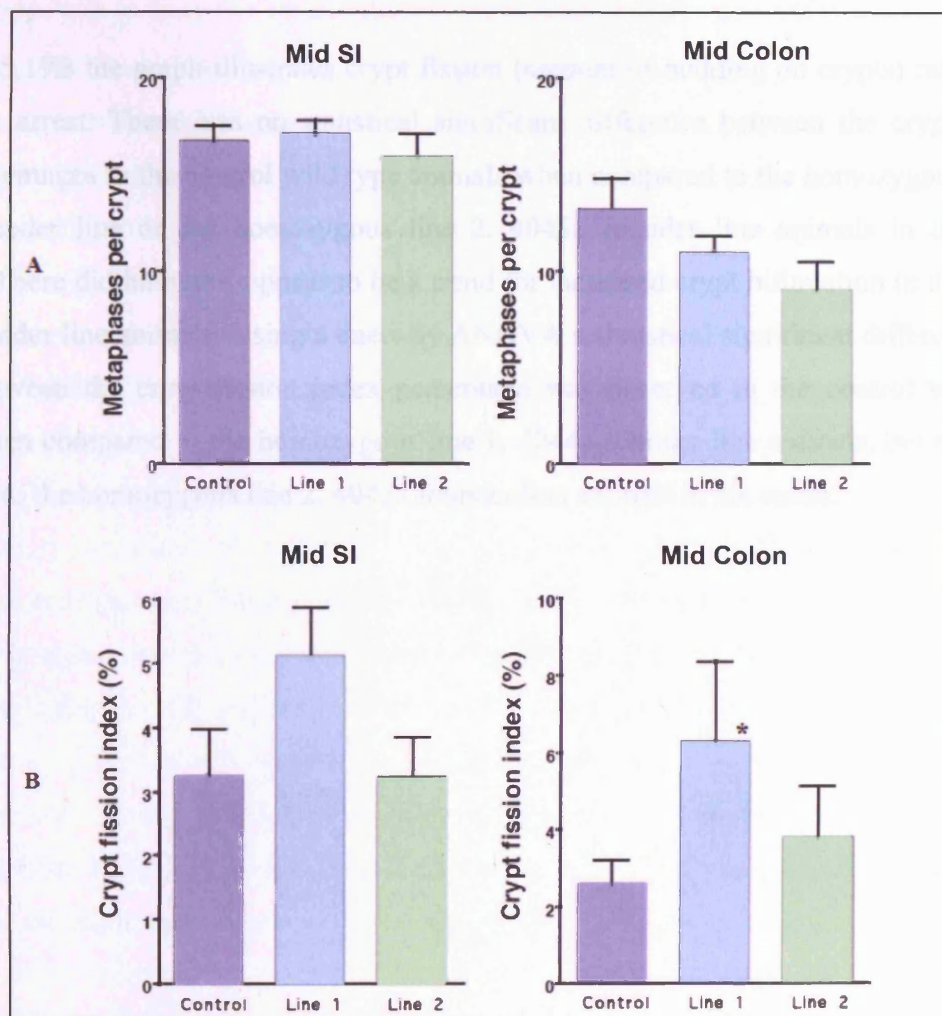


**Figure 5.19 – Cell proliferations and crypt fission in the mid small intestine and colon.** (A) Cell proliferations, assessed by the two-hour accumulation of vincristine-arrested metaphases in the mid small intestine and colon. Each group represents the numbers of mitoses per crypt (mean of 20 crypts). (B) Crypt fission in the mid small intestine and colon. Each group represents the number of crypt fission events per 200 crypts. Error bars represent two standard errors of the mean (SEM). Statistical significance between the wild type control animal and the homozygous line 1, 4044a founder line and the homozygous line 2, 4045a founder line animals in areas of the intestinal mucosa is indicated by \* where the mean difference is significant at the 0.05 level.

From Figure 5.19A it can be determined that there was no significant difference between the number of metaphases per crypt in the control wild type animals when compared to the homozygous line 1, 4044a founder line or the homozygous line 2, 4045a founder line animals when examining either the small intestine or colon intestinal mucosa. The normal proliferation in the small intestine was higher than that observed in the colon. Also it can be assumed that the addition of P-cadherin had not changed the physiology or altered the normal proliferative biology as the number of metaphases per crypt was maintained between both control and experimental animals in each case.

In Figure 5.19B the graph illustrates crypt fission (amount of budding on crypts) rather than metaphase arrest. There was no statistical significant difference between the crypt fission index percentages in the control wild type animals when compared to the homozygous line 1, 4044a founder line or the homozygous line 2, 4045a founder line animals in the small intestine. There did however, appear to be a trend for increased crypt bifurcation in the line 2, 4045a founder line animals. Using a one way ANOVA a statistical significant difference ( $P = 0.047$ ) between the crypt fission index percentage was observed in the control wild type animal when compared to the homozygous line 1, 4044a founder line animals, but not when compared to the homozygous line 2, 4045a founder line animals in the colon.

## 5.5 Discussion

Since the first gene transfers into mice were successfully executed in 1980, transgenic mice have allowed researchers to observe experimentally what happens to an entire organism during the development and progression of a disease. Transgenic mice have hence become models for studying human diseases and their treatments, and have provided great insights into the pathological role of specific cadherins in disease epidemiology (Calvisi *et al.*, 2004; Perl *et al.*, 1998). As previously mentioned disturbances in cadherin adhesion and expression are thought to contribute to tumour metastasis and invasion in a range of epithelium tumours (Yap, 1998).

Cadherins are important cell adhesion molecules involved in the maintenance of integrity in the gut epithelium (Sanders, 2005). Clues to the functionality of P-cadherin come from previous reported associations with mucosal proliferation, injury, ulceration, repair, and neoplastic change in the GI tract (Hardy *et al.*, 2002a; Jankowski *et al.*, 1998; Sanders *et al.*, 2000). Essentially, co-expression of P-cadherin and E-cadherin is a reversible feature of cells undergoing proliferation and migration and, although P-cadherin upregulation may facilitate mucosal regeneration without much compromise to mucosal integrity, the probable result will be increased permeability (Sanders, 2005).

Animal model experiments have already shown the importance of cadherins in GI tissue integrity and chimaeric mice expressing two lineages of gut cells, one wild type and one a dominant negative with N-cadherin substituted for E-cadherin, developed patchy transmural inflammation in areas of leaky epithelium, characterised by N-cadherin expression (Hermiston and Gordon, 1995b). This suggests that a defect in gut barrier function and increased permeability can lead to a Crohn's disease-like inflammatory bowel disease in the presence of an intact immune system (Sanders, 2005).

In this study forced P-cadherin expression was achieved with a murine model and a FABP promoter to determine the normal and potential pathological roles of P-cadherin expression in the intestine. Firstly, IHC studies were undertaken to analyse P-cadherin protein expression. Despite trying several different antibodies, under a range of various antigen retrieval and detection conditions, it was not possible to satisfactorily optimise these to perform successful P-cadherin IHC in the transgenic mouse experimental population. This study produced data which differed from others in the field where the PCD-1 P-cadherin clone had been reported to be suitable for IHC use on mouse tissue (Nose and Takeichi, 1986; Radice *et al.*, 1997).

This work requires further investigation and no firm conclusions could be drawn from the P-cadherin IHC data as the antibody testing was limited, with only very few samples being examined. However, our findings did show that native P-cadherin was not expressed in the murine oesophageal compartment, which was anticipated due to the human findings. This could potentially highlight the involvement of another cadherin in murine oesophageal tissue.

Examination of the wild type, heterozygous and homozygous transgenic tissues in this study reported all samples to be normal with no sign of ulceration, polyps, or cancer and no significant difference in tissue pathology between each of the animal genotypes. The reason why a phenotype was not present is perhaps due to the promoter system that was utilised. L-FABP is expressed throughout the GI tract in the enterocyte cells and therefore if the P-cadherin is only targeting the enterocytes cells then expression may be limited. While upregulation of P-cadherin may be necessary for a metaplastic phenotype in man, alone it may not be sufficient.

Phosphohistone IHC analysis was performed on the experimental P-cadherin transgenic animals to determine the proliferative phenotype in the experimental tissues. Upon examination of the labelling index scores there was a significant reduction in the homozygous animals when compared to the wild type and heterozygous animals. This indicates a decreased proliferative potential in the homozygous animals and is in direct contrast to the findings of our group and others which suggest P-cadherin can increase mucosal proliferation (Hardy *et al.*, 2002a; Jankowski *et al.*, 1998; Sanders *et al.*, 2000) and that by knocking out P-cadherin in experimental animals, growth of breast tissue is reduced (Radice *et al.*, 1997).

Unpublished work from our group has determined that a fibroblast-like cell line stably transfected with P-cadherin showed statistically significant increase in the number of cells in S-phase when compared to vector-only transfected controls. Silencing of P-cadherin expression in colorectal cell lines using siRNA resulted in arrest in G0/G1 phase and a decrease in cell numbers, therefore implicating P-cadherin in the role of proliferation (Janusz Jankowski, personal communication).

The findings in this study indicate that decreased proliferation in the transgenic experimental animals could be due to several factors. Firstly, when looking at the model *in vivo* it is possible that the cellular interactions are swamping the effects that were observed *in vitro*. Secondly, it is possible that an upregulation of the P-cadherin adhesion molecule may reduce

the migration and proliferation in the tissue due to increased adhesion. Potentially therefore the role of P-cadherin in tumour development could be retention of cells rather than increased proliferation.

Even though there was no marked observable phenotype it was important to demonstrate that the transgene was present and that P-cadherin had been transfected into the experimental animals. To determine this RT-PCR analysis was performed on the homozygous and wild type transgenic animals. Data obtained showed that in three separate homozygous animals P-cadherin expression was variable, being maximally expressed throughout the small and large intestine in one animal, in the small intestine only in the second animal and in the third animal no expression was seen. The L-FABP promoter is expressed throughout the GI tract but it is maximally expressed in small intestine and proximal large bowel and thus these results confirm that the *in vivo* mouse model was a useful research tool. Another point of interest was that RT-PCR data confirmed the P-cadherin IHC data, in that no native expression of P-cadherin was seen in the oesophagus of any of the experimental animals. Native L-FABP expression was present in both the wild type and homozygous animals throughout all tissue samples and this result was quite unexpected. It was accepted that expression should be seen in the small and large intestine and in the liver tissue samples in both the native and transgenic situation. However, as the stomach, oesophageal and caecum tissues do not contain enterocyte cells or native expression of L-FABP and the promoter is tissue specific it was difficult to understand why this was the case.

Once the RT-PCR data had confirmed that the mRNA was present it was important to confirm this by protein analysis. Unfortunately this data proved inconclusive and while attempts to resolve this are ongoing at this time no conclusions can be drawn. It is felt that the use of a promoter with more general expression, such as a stem cell targeted promoter, would be able to target a larger number of cells within the GI tract and would therefore be beneficial to future experimental analysis.

Microscopic analysis was performed to assess proliferation by metaphase arrest (determinant of proliferation/cell cycle population) and crypt bifurcation (surrogate of stem cell division). From a cell cycle point of view, metaphase arrest is of interest as a model for checkpoint control of mitotic entry and exit. Therefore it gives a very accurate idea of everything in the cell cycle and so even with limited counts and sample sizes it is an accurate way of checking proliferation. In the human setting methylation analysis can be used where increased

methylation occurs in the normal situation and then demethylation occurs as cancer progresses. Unpublished data from our group has shown that that increased proliferation is due to P-cadherin hypomethylation in colorectal carcinoma (Janusz Jankowski, personal communication). However, in this study metaphase arrest was used in the transgenic murine model to indicate proliferation.

Data obtained by R.A. Goodlad indicated that the metaphase arrest was less in colon than in the small intestine when examining both wild type and homozygous animals. This data is not unexpected and is due to the fact that the small intestine has a naturally increased proliferation index due to an elevated cell turnover. The data also showed that the metaphase arrest was not affected by genotype and that both the control and experimental animals showed a comparable metaphase arrest figure. This is obviously a positive finding as it means that the forced expression of P-cadherin has not changed the physiology or altered the normal proliferative biology of the animals.

When looking at the data obtained for the crypt fission, (amount of budding on crypts) rather than the metaphase arrest, several interesting points could be made. Firstly, there was a significant increase in the level of crypt bifurcation in the line 1 homozygous colon samples when compared to the controls. While the line 2 homozygous animals also showed an increase compared to the controls, this did not reach statistical significance and may be due to the original breeding crosses which were set up. Incorporation of transgene in the line two experimental animals may have occurred differently and one may have been more successful and thus show increased expression of transgenic P-cadherin, and therefore increased crypt fission.

When looking at the data for the crypt fission percentage in the small intestine a similar pattern is seen to the one observed in the colon, although this does not reach statistical significance. The reason for this may be that more animals were examined in this group or be due to the fact that there is naturally a higher crypt fission rate present in the small intestine and so the difference is less obvious. Increased fission is indicative of increased cell turnover and proliferation as crypt bifurcation is a physiologic mechanism of crypt reproduction.

In conclusion, the data presented in this Chapter demonstrate successful neoexpression of transgenic P-cadherin *in vivo* using a FABP promoter system. Forced expression of P-cadherin was achieved using a specific promoter to target enterocytes throughout the small

and large intestine and was associated with an increased crypt number and fission rate. Further investigation is required to fully evaluate the implications of these findings. It is hoped that with the development of animal model systems and the use of novel promoter systems, such as stem cell specific promoters, the functionality of P-cadherin expression in the GI tract may be elucidated.

## **Chapter 6: Conclusions and Future Perspectives**

The intestinal stem cell remains difficult to isolate, and over the past few decades research has enabled us to identify its location, its life cycle, how its environment regulates its function and, importantly, its role in the development of intestinal neoplasms.

Work presented in this thesis has added to our understanding of expression patterns of potential molecular stem cell markers in altered states of oesophageal biology, mechanisms of regulation of expression of one such molecule, P-cadherin, and possible phenotypic effects of alteration in cadherin expression. It has also been possible to examine the role of bile acid stimulation and suppression in the normal *in vivo* high throughput zebrafish model system, and to evaluate the environmental factors which may have a causative role in the initiation of BM. Most notably the use of a labelling thymidine analogue has allowed the location of the putative stem cell populations in compartments of normal and aberrant oesophageal tissue.

Previous data in our research group has identified that cancer development is associated with altered cadherin adhesion in colorectal cancer. Specifically that P-cadherin, normally absent from healthy colonic mucosa, is aberrantly expressed in early aberrant crypt foci and the subsequent colorectal carcinoma and that genetic mutation or chromosomal duplication of the P-cadherin gene is not involved in this ectopic expression (Hardy *et al.*, 2002b).

In order to fully investigate the phenotypic effects of P-cadherin expression *in vivo* a transgenic murine model which expressed P-cadherin in the small and large intestine, under the control of a FABP promoter was generated in collaboration with Sir Nicolas Wright at the ICRF, Lincoln's Inn Fields, London. It was hoped that this would directly assess the functionality of P-cadherin. Unfortunately while this model was a valuable research tool the choice of promoter was suboptimal. When using the L-FABP promoter, tissue specific targeting successfully forced aberrant P-cadherin expression in the intestine and colon. However, due to the promoter's cell specificity only low levels of expression were observed and unfortunately these were not enough to reach a phenotypic level although a modest increase in stem cell division was determined. In the future it would be useful to use an oesophageal specific promoter ideally one which targets stem cells and is not expressed in the differentiated compartment. One potential marker worthy of investigation is Mustashi-1 (Msi-1).

Msi-1 is a neural RNA binding protein, the mammalian homologue of a *Drosophila* protein, required for asymmetric division of sensory neural precursor cells (Nakamura *et al.*, 1994;

Okabe *et al.*, 2001) and recently demonstrated to be highly expressed in mammalian neural stem cells (Kaneko *et al.*, 2000; Sakakibara *et al.*, 1996). Its functions include upregulation of a transcriptional repressor molecule called Hairy and Enhancer of Split homologue-1 (Hes-1) (Imai *et al.*, 2001). Hes-1 is essential for neural stem cell self-renewal and suppression of neural stem cell differentiation into neuronal lineages (Akazawa *et al.*, 1992; Nakamura *et al.*, 2000; Sasai *et al.*, 1992) and is a downstream target in the Notch signalling pathway of cellular differentiation (Jarriault *et al.*, 1995). Moreover, Msi-1 has recently been demonstrated to positively regulate Hes-1 transcription, suggesting a close interaction between Msi-1 and Hes-1 (Imai *et al.*, 2001).

Msi-1 and Hes-1 proteins are co-expressed in cells just superior to the paneth cells in the small intestine, the postulated stem cell region (Potten *et al.*, 1997). Hes-1 has a more widespread expression than Msi-1 and is also expressed, albeit in reduced levels, in epithelial cells migrating towards the villus tip. It is suggested that co-localisation of Msi-1 and Hes-1 in cells located just above Paneth cells is indicative of the stem cell population in the mouse small intestine, and that Hes-1 expression alone represents proliferating cells committed to differentiation, which have migrated out of the stem cell niche (Kayahara *et al.*, 2003). Msi-1 mRNA and protein expression has also been confirmed in putative stem cells in neonatal and adult intestinal crypts in mice (Potten *et al.*, 2003) and has recently been demonstrated in the human colon in epithelial cells located between positions 1 and 10 in crypts (Nishimura *et al.*, 2003). These studies implicate Msi-1 as a possible GI stem cell marker (Brittan and Wright, 2004).

Interestingly, the expression of communal markers by stem cells of different tissues e.g. Msi-1 expression by both neural and intestinal stem cells, lends support to the belief that adult stem cells may repopulate adult lineages outside of their tissue of origin. Future work may make it possible to identify other GI stem cell markers by investigating expression patterns of known stem cell markers of adult tissues, such as those found in the brain, epidermis and in the cells of the GI tract (Brittan and Wright, 2003). Alternatively there may actually be no definitive marker of GI stem cells because they need to maintain a restricted repertoire of expressed genes in order to remain undifferentiated.

Analysis of the high throughput zebrafish animal model identified a novel system in which to study the pathological effects of bile acid in the normal squamous mucosa. Treatment with DCA produced disease physiology comparable to that observed during the pathogenesis of

human GORD, and an increase of Pan-cadherin staining in the transitional zone epithelium. Anti Pan-cadherin antibodies can cross-react with virtually all members of the cadherin family and due to the previous findings by the research group indicating an increase of P-cadherin in poorly differentiated tissues; it was felt that in this case P-cadherin was the most likely perpetrator. Unfortunately it was not possible to determine this definitively due to the limit of available P-cadherin zebrafish specific antibodies. Work carried out in this thesis highlights the potential of this model as a novel method to investigate the functional significance of environmental factors or pharmacological targets in the hallmarks of disease physiology, such as dysplasia. While this model provides renewed hope and great potential to the scientific researcher it will not be until diagnostic tools are developed, and become as innovative and up to date as the system for which they are being created, that this models true potential will be realised.

Finally attention was focused on stem cell biology in the setting of a clinical trial and tissue was analysed from patients with OA or high grade dysplasia who has received an intravenous infusion of IUdR a halogenated thymidine analogue. Alongside promising results for the ability to highlight LRCs, work in this thesis was able to demonstrate the putative stem cells in areas of resected experimental tissue. This supports work by others in the field, who have already postulated on the location of the oesophageal stem cell compartment (Jankowski and Wright, 1992; Watt and Hogan, 2000) and may be a valuable approach for the resolution of this debate. However, analysis of a larger cohort is needed to validate these findings and longer time intervals are needed between infusion and resection surgery to definitely comment on the location of stem cells in the normal and aberrant oesophageal mucosa. The research group are currently collaborating with colleagues in Glasgow, Gloucester and Oxford to enable the analysis of a large series of OA or high grade dysplasia cases to confirm these preliminary findings.

Several areas that have been investigated in this thesis lend themselves to further exploration, particularly with regard to analysis of phenotypic differences of P-cadherin. As mentioned the transgenic murine model could provide valuable information if investigations were to use an oesophageal stem cell specific promoter to force the expression of P-cadherin or even other molecules of interest may be investigated. An alternative would be to cross P-cadherin transgenic animals with *Min*/<sup>+</sup> mice, and this is currently being investigated by Professor Jankowski's research group.

Most notably, the results for the crypt bifurcation generated as part of this thesis, showed a modest increase in stem cell division in the colon of the generated transgenic animals. It is felt that an indomethacin stress response assay may exaggerate this P-cadherin phenotype (Robert Goodlad, personal communication) as indomethacin causes increased permeability, decreases cellular junctions and causes superficial ulceration. Therefore if P-cadherin is an important stem cell molecule it would be anticipated that, under these conditions, it would show a much exaggerated phenotype by allowing increased proliferation. Currently this work is being undertaken within Professor Jankowski's research group and it is hoped that the functional significance of the P-cadherin gene in cancer progression, such as its role in proliferation, apoptosis and invasion will finally be realised.

There is still a great deal that is not understood when it comes to stem cells in the GI tract. As yet no studies have been able to extract intestinal stem cells and propagate them for study *in vitro* and until this is done many of the functions of these stem cells will remain a matter of conjecture. This is primarily due to the lack of well-defined stem cell markers. In this study IHC proved valuable when examining the location of the stem cell compartment, and perhaps co-staining with molecules highlighted here, such as P-cadherin and the putative stem cell marker, Msi-1 would prove to be worthy of future analysis.

Work carried out in this thesis demonstrated that IUdR labelling can demonstrate putative stem cell identification and that molecular targets can be localised to show an association to particular stem cell zones. As a consequence of these data a dynamic experimental functional assay was conducted where the molecular target was examined in conjunction with a stimulus to see if this is physiologically relevant. This was elucidated by using bile acid as a stimulus and noting an increase in the cadherin level in the zebrafish model proving physiological relevance. Finally, we examined whether the molecule alone, without the physiological stimulus, can drive the same system. In order to examine this P-cadherin was introduced to a transgenic murine model. These data have shown that a phenotype of increased crypt bifurcation is seen and also subtle changes in animal weight are noted, however metaplasia was not present. From this it can be determined that P-cadherin is upregulated and therefore is almost certainly necessary, but not sufficient without the external stimuli, for metaplastic change. Therefore this thesis strengthens the paradigm that a gene plus an environmental interaction is required in order to induce metaplastic conditions such as BO. With this in mind it can be postulated that in stem cell compartments the mechanism almost certainly is that the environment and the gene work together to induce change.

In conclusion this study has extended previous findings by the research group and has generated novel data to support the hypothesis that stem cells play a pivotal role in human disease. The most significant findings of this thesis have resulted from evaluation of clinical trial patients undergoing treatment for OA or high grade dysplasia. From these investigations it would appear that the previously undefined stem cell compartment can now be elucidated and that P-cadherin upregulation is a feature of this location, not only in native oesophagus, but also in Barrett's oesophageal tissue. Further analysis on an increased sample size and varied infusion time points will prove invaluable for the substantiation of this finding.

## **Chapter 7: References**

- Akazawa, C., Sasai, Y., Nakanishi, S., and Kageyama, R. (1992) Molecular Characterization of A Rat Negative Regulator with A Basic Helix-Loop-Helix Structure Predominantly Expressed in the Developing Nervous-System. *Journal of Biological Chemistry* **267**, 21879-21885.
- Alberts, B., Johnston, A., Lewis, J., Raff, M., Roberts, K., and Walter, P. (2002) *Molecular Biology of the Cell*. Garland Science.
- Alferez, D. and Goodlad, R. A. How to get the measure of cell proliferation in the intestine. *Cell Proliferation*. 2006.
- Alison, M. R., Poulson, R., Forbes, S., and Wright, N. A. (2002) An introduction to stem cells. *Journal of Pathology* **197**, 419-423.
- Alison, M. R., Poulson, R., Otto, W. R., Vig, P., Brittan, M., Direkze, N. C., Lovell, M., Fang, T. C., Preston, S. L., and Wright, N. A. (2004) Recipes for adult stem cell plasticity: fusion cuisine or readymade? *Journal of Clinical Pathology* **57**, 113-120.
- Anderson, D. J., Gage, F. H., and Weissman, I. L. (2001) Can stem cells cross lineage boundaries? *Nature Medicine* **7**, 393-395.
- Attwood, S. E., Smyrk, T. C., DeMeester, T. R., Mirvish, S. S., Stein, H. J., and Hinder, R. A. (1992) Duodeno-esophageal reflux and the development of esophageal adenocarcinoma in rats. *Surgery* **111**, 503-510.
- Bailey, T., Biddlestone, L., Shepherd, N., Barr, H., Warner, P., and Jankowski, J. (1998) Altered cadherin and catenin complexes in the Barrett's esophagus-dysplasia-adenocarcinoma sequence: correlation with disease progression and dedifferentiation. *Am J Pathol* **152**, 135-144.
- Balkwill, F. and Mantovani, A. (2001) Inflammation and cancer: back to Virchow? *Lancet* **357**, 539-545.
- Bani-Hani, K., Martin, I. G., Hardie, L. J., Mapstone, N., Briggs, J. A., Forman, D., and Wild, C. P. (2000) Prospective study of cyclin D1 overexpression in Barrett's esophagus: association with increased risk of adenocarcinoma. *J Natl Cancer Inst* **92**, 1316-1321.
- Bardi, G., Johansson, B., Pandis, N., Mandahl, N., Bak-Jensen, E., Lindstrom, C., Tornqvist, A., Frederiksen, H., ndren-Sandberg, A., Mitelman, F. (1993) Cytogenetic analysis of 52 colorectal carcinomas-non-random aberration pattern and correlation with pathologic parameters. *Int J Cancer* **55**, 422-428.
- Bass, N. M. (1985) Function and Regulation of Hepatic and Intestinal Fatty-Acid Binding-Proteins. *Chemistry and Physics of Lipids* **38**, 95-114.
- Beaulieu, J. F. (1992) Differential Expression of the VLA Family of Integrins Along the Crypt-Villus Axis in the Human Small-Intestine. *Journal of Cell Science* **102**, 427-436.
- Booth, C. and Potten, C. S. (2000) Gut instincts: thoughts on intestinal epithelial stem cells. *Journal of Clinical Investigation* **105**, 1493-1499.
- Brem, G. and Wagner, H. G. Transgenic Livestock. Branckaert, R. D. S. World Animal Review Harnessing biotechnology to animal production and health. 1991.

- Bremner, C. G., Lynch, V. P., and Ellis, F. H., Jr. (1970) Barrett's esophagus: congenital or acquired? An experimental study of esophageal mucosal regeneration in the dog. *Surgery* **68**, 209-216.
- Brittan, M. and Wright, N. A. (2004) Stem cell in gastrointestinal structure and neoplastic development. *Gut* **53**, 899-910.
- Brittan, M. and Wright, N. A. (2003) The gastrointestinal stem cell. *Cell Proliferation* **37**, 35-53.
- Bulay, O. and Mirvish, S. S. (1979) Carcinogenesis in rat esophagus by intraperitoneal injection of different doses of methyl-n-aminonitrosamine. *Cancer Res* **39**, 3644-3646.
- Buskens, C. J., Hulscher, J. B., van Gulik, T. M., Ten Kate, F. J., and van Lanschot, J. J. (2006) Histopathologic evaluation of an animal model for Barrett's esophagus and adenocarcinoma of the distal esophagus. *J Surg Res* **135**, 337-344.
- Buttar, N. S. and Wang, K. K. (2004) Mechanisms of disease: Carcinogenesis in Barrett's esophagus. *Nat Clin Pract Gastroenterol Hepatol* **1**, 106-112.
- Cairns, J. (1975) Mutation Selection and Natural-History of Cancer. *Nature* **255**, 197-200.
- Calvisi, D. F., Ladu, S., Conner, E. A., Factor, V. M., and Thorgeirsson, S. S. (2004) Disregulation of E-cadherin in transgenic mouse models of liver cancer. *Lab Invest* **84**, 1137-1147.
- Cameron, A. J., Lombay, C. T., Pera, M., and Carpenter, H. A. (1995) Adenocarcinoma of the esophagogastric junction and barretts-esophagus. *Gastroenterology* **109**, 1541-1546.
- Campbell, F. C., Tait, I. S., Flint, N., and Evans, G. S. (1993) Transplantation of cultured small bowel enterocytes. *Gut* **34**, 1153-1155.
- Chang, W. W. and Leblond, C. P. (1971) Renewal of the epithelium in the descending colon of the mouse. I. Presence of three cell populations: vacuolated-columnar, mucous and argentaffin. *Am J Anat* **131**, 73-99.
- Chen, X., Yang, G., Ding, W. Y., Bondoc, F., Curtis, S. K., and Yang, C. S. (1999) An esophagogastric anastomosis model for esophageal adenocarcinogenesis in rats and enhancement by iron overload. *Carcinogenesis* **20**, 1801-1808.
- Clark, G. W., Smyrk, T. C., Mirvish, S. S., Anselmino, M., Yamashita, Y., Hinder, R. A., DeMeester, T. R., and Birt, D. F. (1994) Effect of gastroduodenal juice and dietary fat on the development of Barrett's esophagus and esophageal neoplasia: an experimental rat model. *Ann Surg Oncol* **1**, 252-261.
- Colnot, S., Niwa-Kawakita, M., Hamard, G., Godard, C., Le, P. S., Houbon, C., Romagnolo, B., Berrebi, D., Giovannini, M., and Perret, C. (2004) Colorectal cancers in a new mouse model of familial adenomatous polyposis: influence of genetic and environmental modifiers. *Lab Invest* **84**, 1619-1630.
- Dahm, R. (2002) Atlas of Embryonic Stages of Development in the Zebrafish. In: *Zebrafish: A Practical Approach*, pp. 234-235. Eds C. Nusslein-Volhard, R. Dahm. Oxford University Press: Oxford.

- Dawkins, R. (2004) *The Ancestor's Tale: A Pilgrimage to the Dawn of Life*. Weidenfeld and Nicholson: UK.
- Devesa, S. S., Blot, W. J., and Fraumeni, J. F., Jr. (1998) Changing patterns in the incidence of esophageal and gastric carcinoma in the United States. *Cancer* **83**, 2049-2053.
- Dorudi, S., Hanby, A. M., Poulson, R., Northover, J., and Hart, I. R. (1995) Level of expression of E-cadherin mRNA in colorectal cancer correlates with clinical outcome. *Br J Cancer* **71**, 614-616.
- Dorudi, S., Sheffield, J. P., Poulson, R., Northover, J. M., and Hart, I. R. (1993) E-cadherin expression in colorectal cancer. An immunocytochemical and in situ hybridization study. *Am J Pathol* **142**, 981-986.
- Evans, G. S., Flint, N., Somers, A. S., Eyden, B., and Potten, C. S. (1992) The development of a method for the preparation of rat intestinal epithelial cell primary cultures. *J Cell Sci* **101 (Pt 1)**, 219-231.
- Evers, C. A. and Starr, L. (2006) *Biology: Concepts and Applications*. Thomson: United States.
- Fass, R. and Sampliner, R. E. (2000) Extension of squamous epithelium into the proximal stomach: a newly recognized mucosal abnormality. *Endoscopy* **32**, 27-32.
- Fearon, E. R. and Vogelstein, B. (1990) A Genetic Model for Colorectal Tumorigenesis. *Cell* **61**, 759-767.
- Fitzgerald, R. C. (2005) Barrett's oesophagus and oesophageal adenocarcinoma: how does acid interfere with cell proliferation and differentiation? *Gut* **54 Suppl 1**, i21-i26.
- Fleming, A., Jankowski, J., and Goldsmith, P. Pre-mammalian *in vivo* analysis of inflammatory bowel disease in zebrafish. Federation of American Societies for Experimental Biology Journal. 2007.
- Fujioka, T., Murakami, K., Kodama, M., Kagawa, J., Okimoto, T., and Sato, R. (2002) Helicobacter pylori and gastric carcinoma - from the view point of animal model. *Keio J Med* **51 Suppl 2**, 69-73.
- Gagliardi, G., Kandemir, O., Liu, D., Guida, M., Benvestito, S., Ruers, T. G., Benjamin, I. S., Northover, J. M., Stamp, G. W., Talbot, I. C. (1995) Changes in E-cadherin immunoreactivity in the adenoma-carcinoma sequence of the large bowel. *Virchows Arch* **426**, 149-154.
- Gahmberg, C. G. and Tolvenen, M. (1996) Why mammalian cell surface proteins are glycoprotein. *TiBS* **21**, 308-311.
- Gallin, W. J. (1998) Evolution of the "classical" cadherin family of cell adhesion molecules in vertebrates. *Mol Biol Evol* **15**, 1099-1107.
- Garcia, S. B., Park, H. S., Novelli, M., and Wright, N. A. (1999) Field cancerization, clonality, and epithelial stem cells: the spread of mutated clones in epithelial sheets. *J Pathol* **187**, 61-81.

- Garewal, H., Bernstein, H., Bernstein, C., Sampliner, R., and Payne, C. (1996) Reduced bile acid-induced apoptosis in "normal" colorectal mucosa: a potential biological marker for cancer risk. *Cancer Res* **56**, 1480-1483.
- Gassmann, M., Rulicke, T., Ledermann, B., and Burki, K. Transgenesis at the millennium. *Experimental Physiology* **85**[6], 587. 2000.
- Geiger, B., Volberg, T., Ginsberg, D., Bitzur, S., Sabanay, I., and Hynes, R. O. (1990) Broad spectrum pan-cadherin antibodies, reactive with the C-terminal 24 amino acid residues of N-cadherin. *J Cell Sci* **97 (Pt 4)**, 607-614.
- Geisinger, K. R., Cassidy, K. T., Nardi, R., and Castell, D. O. (1990) The histologic development of acid-induced esophagitis in the cat. *Mod Pathol* **3**, 619-624.
- Gerdes, J., Lemke, H., Baisch, H., Wacker, H. H., Schwab, U., and Stein, H. (1984) Cell cycle analysis of a cell proliferation-associated human nuclear antigen defined by the monoclonal antibody Ki-67. *J Immunol* **133**, 1710-1715.
- Ghadimi, B. M., Behrens, J., Hoffmann, I., Haensch, W., Birchmeier, W., and Schlag, P. M. (1999) Immunohistological analysis of E-cadherin, alpha-, beta- and gamma-catenin expression in colorectal cancer: implications for cell adhesion and signaling. *Eur J Cancer* **35**, 60-65.
- Goldsmith, P. and Solari, R. The Role of Zebrafish in drug discovery. *Drug Discovery World* 2003. Spring, 74-78. 2003.
- Goldstein, S. R., Yang, G. Y., Chen, X., Curtis, S. K., and Yang, C. S. (1998) Studies of iron deposits, inducible nitric oxide synthase and nitrotyrosine in a rat model for esophageal adenocarcinoma. *Carcinogenesis* **19**, 1445-1449.
- Goodlad, R. A. (1994) Microdissection-based techniques for the determination of cell proliferation in gastrointestinal epithelium: application to animal and human studies. In: *Cell biology: a laboratory handbook*, pp. 205-216. Ed J. E. Celis. San Diego and London: Academic Press.
- Gordon, J. W., Scangos, G. A., Plotkin, D. J., Barbosa, J. A., and Ruddle, F. H. (1980) Genetic transformation of mouse embryos by microinjection of purified DNA. *Proc Natl Acad Sci U SA* **77**, 7380-7384.
- Han, E., Broussard, J., and Baer, K. E. (2003) Feline esophagitis secondary to gastroesophageal reflux disease: clinical signs and radiographic, endoscopic, and histopathological findings. *J Am Anim Hosp Assoc* **39**, 161-167.
- Handschuh, G., Candidus, S., Lubber, B., Reich, U., Schott, C., Oswald, S., Becke, H., Hutzler, P., Birchmeier, W., Hofler, H., and Becker, K. F. (1999) Tumour-associated E-cadherin mutations alter cellular morphology, decrease cellular adhesion and increase cellular motility. *Oncogene* **18**, 4301-4312.
- Hao, X., Frayling, I. M., Willcocks, T. C., Han, W., Tomlinson, I. P., Pignatelli, M. N., Pretlow, T. P., and Talbot, I. C. (2002) Beta-catenin expression and allelic loss at APC in sporadic colorectal carcinogenesis. *Virchows Arch* **440**, 362-366.

- Hao, X., Palazzo, J. P., Ilyas, M., Tomlinson, I., and Talbot, I. C. (1997) Reduced expression of molecules of the cadherin/catenin complex in the transition from colorectal adenoma to carcinoma. *Anticancer Res* **17**, 2241-2247.
- Hardouin, S. N. and Nagy, A. (2000) Mouse models for human disease. *Clin Genet* **57**, 237-244.
- Hardy, R. G., Brown, R. M., Miller, S. J., Tselepis, C., Morton, D. G., Jankowski, J. A., and Sanders, D. S. (2002a) Transient P-cadherin expression in radiation proctitis; a model of mucosal injury and repair. *J Pathol* **197**, 194-200.
- Hardy, R. G., Tselepis, C., Hoyland, J., Wallis, Y., Pretlow, T. P., Talbot, I., Sanders, D. S., Matthews, G., Morton, D., and Jankowski, J. A. (2002b) Aberrant P-cadherin expression is an early event in hyperplastic and dysplastic transformation in the colon. *Gut* **50**, 513-519.
- Helander, H. F. (1981) The cells of the gastric mucosa. *Int Rev Cytol* **70**, 217-289.
- Hermiston, M. L. and Gordon, J. I. (1995a) In vivo analysis of cadherin function in the mouse intestinal epithelium: essential roles in adhesion, maintenance of differentiation, and regulation of programmed cell death. *J Cell Biol* **129**, 489-506.
- Hermiston, M. L. and Gordon, J. I. (1995b) Inflammatory bowel disease and adenomas in mice expressing a dominant negative N-cadherin. *Science* **270**, 1203-1207.
- Hermiston, M. L., Wong, M. H., and Gordon, J. I. (1996) Forced expression of E-cadherin in the mouse intestinal epithelium slows cell migration and provides evidence for nonautonomous regulation of cell fate in a self-renewing system. *Genes & Development* **10**, 985-996.
- Hiscox, S. and Jiang, W. G. (1997) Expression of E-cadherin, alpha, beta and gamma-catenin in human colorectal cancer. *Anticancer Res* **17**, 1349-1354.
- Hofler, H., Becker, K. F., and Keller, G. (2003) [Molecular carcinogenesis of the upper gastrointestinal tract]. *Verh Dtsch Ges Pathol* **87**, 123-129.
- Hopwood, D., Milne, G., and Logan, K. R. (1979) Electron microscopic changes in human oesophageal epithelium in oesophagitis. *J Pathol* **129**, 161-167.
- Hotchin, N. A., Gandarillas, A., and Watt, F. M. (1995) Regulation of Cell-Surface Beta (1) Integrin Levels During Keratinocyte Terminal Differentiation. *Journal of Cell Biology* **128**, 1209-1219.
- Houghton, J., Morozov, A., Smirnova, I., and Wang, T. C. (2006) Stem cells and cancer. *Semin Cancer Biol.*
- Houghton, J., Stoicov, C., Nomura, S., Rogers, A. B., Carlson, J., Li, H. C., Cai, X., Fox, J. G., Goldenring, J. R., and Wang, T. C. (2004) Gastric cancer originating from bone marrow-derived cells. *Science* **306**, 1568-1571.
- Imai, T., Tokunaga, A., Yoshida, T., Hashimoto, M., Mikoshiba, K., Weinmaster, G., Nakafuku, M., and Okano, H. (2001) The neural RNA-binding protein Musashi1 translationally regulates mammalian numb gene expression by interacting with its mRNA. *Molecular and Cellular Biology* **21**, 3888-3900.

- Ishizuya-Oka, A. (2005) Epithelial-connective tissue cross-talk is essential for regeneration of intestinal epithelium. *J Nippon Med Sch* **72**, 13-18.
- Jankowski, J. and Dover, R. (1993) Cell proliferation, differentiation and cell death in epithelial cells of the oesophagus; a critical review of biological markers and their applications to research and diagnosis. *Gullet* **3**, 1-15.
- Jankowski, J., Hopwood, D., Dover, R., and Wormsley, K. G. (1993) Development and Growth of Normal, Metaplastic and Dysplastic Esophageal Mucosa - Biological Markers of Neoplasia. *European Journal of Gastroenterology & Hepatology* **5**, 235-246.
- Jankowski, J. A. and Anderson, M. (2004) Review article: management of oesophageal adenocarcinoma - control of acid, bile and inflammation in intervention strategies for Barrett's oesophagus. *Aliment Pharmacol Ther* **20 Suppl 5**, 71-80.
- Jankowski, J. A., Bedford, F. K., Boulton, R. A., Cruickshank, N., Hall, C., Elder, J., Allan, R., Forbes, A., Kim, Y. S., Wright, N. A., and Sanders, D. S. (1998) Alterations in classical cadherins associated with progression in ulcerative and Crohn's colitis. *Lab Invest* **78**, 1155-1167.
- Jankowski, J. A., Harrison, R. F., Perry, I., Balkwill, F., and Tselepis, C. (2000a) Barrett's metaplasia. *Lancet* **356**, 2079-2085.
- Jankowski, J. A., Perry, I., and Harrison, R. F. (2000b) Gastro-oesophageal cancer: death at the junction. *BMJ* **321**, 463-464.
- Jankowski, J. A., Provenzale, D., and Moayyedi, P. (2002) Esophageal adenocarcinoma arising from Barrett's metaplasia has regional variations in the west. *Gastroenterology* **122**, 588-590.
- Jankowski, J. A. and Wright, N. A. (1992) Epithelial stem cells in gastrointestinal morphogenesis, adaptation and carcinogenesis. *Semin Cell Biol* **3**, 445-456.
- Jankowski, J. A., Wright, N. A., Meltzer, S. J., Triadafilopoulos, G., Geboes, K., Casson, A. G., Kerr, D., and Young, L. S. (1999) Molecular evolution of the metaplasia-dysplasia-adenocarcinoma sequence in the esophagus. *Am J Pathol* **154**, 965-973.
- Jarriault, S., Brou, C., Logeat, F., Schroeter, E. H., Kopan, R., and Israel, A. (1995) Signalling downstream of activated mammalian Notch. *Nature* **377**, 355-358.
- Jiang, Y. H., Henderson, D., Blackstad, M., Chen, A., Miller, R. F., and Verfaillie, C. M. (2003) Neuroectodermal differentiation from mouse multipotent adult progenitor cells. *Proceedings of the National Academy of Sciences of the United States of America* **100**, 11854-11860.
- Jones, P. H. and Watt, F. M. (1993) Separation of Human Epidermal Stem-Cells from Transit Amplifying Cells on the Basis of Differences in Integrin Function and Expression. *Cell* **73**, 713-724.
- Juliano, R. L. and Varner, J. A. (1993) Adhesion molecules in cancer: the role of integrins. *Curr Opin Cell Biol* **5**.

- Kadirkamanathan, S. S., Yazaki, E., Evans, D. F., Hepworth, C. C., Gong, F., and Swain, C. P. (1999) An ambulant porcine model of acid reflux used to evaluate endoscopic gastroplasty. *Gut* **44**, 782-788.
- Kaneko, Y., Sakakibara, S., Imai, T., Suzuki, A., Nakamura, Y., Sawamoto, K., Ogawa, Y., Toyama, Y., Miyata, T., and Okano, H. (2000) Musashi1: An evolutionally conserved marker for CNS progenitor cells including neural stem cells. *Developmental Neuroscience* **22**, 139-153.
- Karam, S. M. (1999) Lineage commitment and maturation of epithelial cells in the gut. *Front Biosci* **4**, D286-D298.
- Karam, S. M. and Leblond, C. P. (1993) Dynamics of epithelial cells in the corpus of the mouse stomach. I. Identification of proliferative cell types and pinpointing of the stem cell. *Anat Rec* **236**, 259-279.
- Karam, S. M. and Leblond, C. P. (1992) Identifying and counting epithelial cell types in the "corpus" of the mouse stomach. *Anat Rec* **232**, 231-246.
- Karatzas, G., Karayiannakis, A. J., Syrigos, K. N., Chatzigianni, E., Papanikolaou, S., Riza, F., and Papanikolaou, D. (1999) E-cadherin expression correlates with tumor differentiation in colorectal cancer. *Hepatogastroenterology* **46**, 232-235.
- Kawaura, Y., Tatsuzawa, Y., Wakabayashi, T., Ikeda, N., Matsuda, M., and Nishihara, S. (2001) Immunohistochemical study of p53, c-erbB-2, and PCNA in barrett's esophagus with dysplasia and adenocarcinoma arising from experimental acid or alkaline reflux model. *J Gastroenterol* **36**, 595-600.
- Kayahara, T., Sawada, M., Takaishi, S., Fukui, H., Seno, H., Fukuzawa, H., Suzuki, K., Hiai, H., Kageyama, R., Okano, H., and Chiba, T. (2003) Candidate markers for stem and early progenitor cells, Musashi-1 and Hes-1, are expressed in crypt base columnar cells of mouse small intestine. *Febs Letters* **535**, 131-135.
- Kimmel, C. B., Ballard, W. W., Kimmel, S. R., Ullmann, B., and Schilling, T. F. (1995) Stages of embryonic development of the zebrafish. *Dev Dyn* **203**, 253-310.
- Kinsella, T. J. (1996) An approach to the radiosensitization of human tumors. *Cancer J Sci Am* **2**, 184-193.
- Kinzler, K. W. and Vogelstein, B. (1996) Lessons from hereditary colorectal cancer. *Cell* **87**, 159-170.
- Kodama, M., Murakami, K., Sato, R., Okimoto, T., Nishizono, A., and Fujioka, T. (2005) Helicobacter pylori-infected animal models are extremely suitable for the investigation of gastric carcinogenesis. *World J Gastroenterol* **11**, 7063-7071.
- Krause, D. S., Theise, N. D., Collector, M. I., Henegariu, O., Hwang, S., Gardner, R., Neutzel, S., and Sharkis, S. J. (2001) Multi-organ, multi-lineage engraftment by a single bone marrow-derived stem cell. *Cell* **105**, 369-377.
- Lanas, A., Royo, Y., Ortego, J., Molina, M., and Sainz, R. (1999) Experimental esophagitis induced by acid and pepsin in rabbits mimicking human reflux esophagitis. *Gastroenterology* **116**, 97-107.

- Lee, N. P., Mruk, D., Lee, W. M., and Cheng, C. Y. (2003) Is the cadherin/catenin complex a functional unit of cell-cell actin-based adherens junctions in the rat testis? *Biol Reprod* **68**, 489-508.
- Li, A., Simmons, P. J., and Kaur, P. (1998) Identification and isolation of candidate human keratinocyte stem cells based on cell surface phenotype. *Proceedings of the National Academy of Sciences of the United States of America* **95**, 3902-3907.
- Lin, J. and Beerm, D. G. (2004) Molecular biology of upper gastrointestinal malignancies. *Semin Oncol* **31**, 476-486.
- Logan, K. R., Hopwood, D., and Milne, G. (1978) Cellular junctions in human oesophageal epithelium. *J Pathol* **126**, 157-163.
- Luo, Y., Ferreira-Cornwell, M. C., Baldwin, H. S., Kostetskii, I., Lenox, J. M., Lieberman, M., and Radice, G. L. (2001) Rescuing the N-cadherin knockout by cardiac-specific expression of N- or E-cadherin. *Development* **128**, 459-469.
- Mann, N. S., Tsai, M. F., and Nair, P. K. (1989) Barrett's esophagus in patients with symptomatic reflux esophagitis. *Am J Gastroenterol* **84**, 1494-1496.
- Marshman, E., Booth, C., and Potten, C. S. (2002) The intestinal epithelial stem cell. *Bioessays* **24**, 91-98.
- McDonald, S. A., Preston, S. L., Lovell, M. J., Wright, N. A., and Jankowski, J. A. (2006) Mechanisms of disease: from stem cells to colorectal cancer. *Nat Clin Pract Gastroenterol Hepatol* **3**, 267-274.
- Mills, S. E. (2006) *Histology for Pathologists*. Lippincott Williams & Wilkins.
- Miwa, K., Sahara, H., Segawa, M., Kinami, S., Sato, T., Miyazaki, I., and Hattori, T. (1996) Reflux of duodenal or gastro-duodenal contents induces esophageal carcinoma in rats. *Int J Cancer* **67**, 269-74.
- Montero, J. A. and Heisenberg, C. P. (2004) Gastrulation dynamics: cells move into focus. *Trends in Cell Biology* **14**, 620-627.
- Moolenbeek, C. and Ruitenberg, E. J. (1981) The "Swiss roll": a simple technique for histological studies of the rodent intestine. *Lab Anim* **15**, 57-59.
- Muller, N., Reinacher-Schick, A., Baldus, S., van Hengel, J., Berx, G., Baar, A., van Roy, F., Schmiegel, W., and Schwarte-Waldhoff, I. (2002) Smad4 induces the tumor suppressor E-cadherin and P-cadherin in colon carcinoma cells. *Oncogene* **21**, 6049-6058.
- Nair, K. S., Naidoo, R., and Chetty, R. (2005) Expression of cell adhesion molecules in oesophageal carcinoma and its prognostic value. *J Clin Pathol* **58**, 343-351.
- Nakamura, M., Okano, H., Blendy, J. A., and Montell, C. (1994) Musashi, a neural RNA-binding protein required for Drosophila adult external sensory organ development. *Neuron* **13**, 67-81.
- Nakamura, Y., Sakakibara, S., Miyata, T., Ogawa, M., Shimazaki, T., Weiss, S., Kageyama, R., and Okano, H. (2000) The bHLH gene *Hes1* as a repressor of the neuronal commitment of CNS stem cells. *Journal of Neuroscience* **20**, 283-293.

- Nishihara, T., Hashimoto, Y., Katayama, M., Mori, S., and Kuroki, T. (1993) Molecular and cellular features of esophageal cancer cells. *J Cancer Res Clin Oncol* **119**, 441-449.
- Nishimura, S., Wakabayashi, N., Toyoda, K., Kashima, K., and Mitsufuji, S. (2003) Expression of Musashi-1 in human normal colon crypt cells: a possible stem cell marker of human colon epithelium. *Dig Dis Sci* **48**, 1523-1529.
- Nose, A., Nagafuchi, A., and Takeichi, M. (1987) Isolation of Placental Cadherin Cdna - Identification of A Novel Gene Family of Cell Cell-Adhesion Molecules. *Embo Journal* **6**, 3655-3661.
- Nose, A. and Takeichi, M. (1986) A novel cadherin adhesion molecule: Its expression patterns associated with implantation and organogenesis of mouse embryos. *Journal of Cell Biology* **103**, 2649-2658.
- Oberg, S., Lord, R. V., Peters, J. H., Chandrasoma, P., Theisen, J., Hagen, J. A., DeMeester, S. R., Bremner, C. G., and DeMeester, T. R. (2000) Is adenocarcinoma following esophagoduodenostomy without carcinogen in the rat reflux-induced? *J Surg Res* **91**, 111-117.
- Okabe, M., Imai, T., Kurusu, M., Hiromi, Y., and Okano, H. (2001) Translational repression determines a neuronal potential in *Drosophila* asymmetric cell division. *Nature* **411**, 94-98.
- Parkin, D. M. (1998) The global burden of cancer. *Seminars in Cancer Biology* **8**, 219-235.
- Pera, M., Cardesa, A., Bombi, J. A., Ernst, H., Pera, C., and Mohr, U. (1989) Influence of esophagojejunostomy on the induction of adenocarcinoma of the distal esophagus in Sprague-Dawley rats by subcutaneous injection of 2,6-dimethylnitrosomorpholine. *Cancer Res* **49**, 6803-6808.
- Pera, M., Trastek, V. F., Carpenter, H. A., Fernandez, P. L., Cardesa, A., Mohr, U., and Pairolero, P. C. (1993) Influence of pancreatic and biliary reflux on the development of esophageal carcinoma. *Ann Thorac Surg* **55**, 1386-1392.
- Perl, A. K., Wilgenbus, P., Dahl, U., Semb, H., and Christofori, G. (1998) A causal role for E-cadherin in the transition from adenoma to carcinoma. *Nature* **392**, 190-193.
- Perry, I., Hardy, R., Tselepis, C., and Jankowski, J. A. (1999) Cadherin adhesion in the intestinal crypt regulates morphogenesis, mitogenesis, motogenesis, and metaplasia formation. *Mol Pathol* **52**, 166-168.
- Polakis, P. (2000) Wnt signaling and cancer. *Genes Dev* **14**, 1837-1851.
- Poorkhalkali, N., Rich, H. G., Jacobson, I., Amaral, J., Migliori, S., Chrostek, C., Biancani, P., Cabero, J. L., and Helander, H. F. (2001) Chronic oesophagitis in the cat. *Scand J Gastroenterol* **36**, 904-909.
- Potten, C. S., Booth, C., and Pritchard, D. M. (1997) The intestinal epithelial stem cell: the mucosal governor. *International Journal of Experimental Pathology* **78**, 219-243.

- Potten, C. S., Booth, C., Tudor, G. L., Booth, D., Brady, G., Hurley, P., Ashton, G., Clarke, R., Sakakibara, S., and Okano, H. (2003) Identification of a putative intestinal stem cell and early lineage marker; Musashi-1. *Differentiation* **71**, 28-41.
- Pow, C. S., Whitehead, J. S., and Moss, M. S. (2000) In: *Pathology of Genetically Engineered Mice*, pp. 23-32. Eds J. M. Ward, J. F. Mahler, R. R. Maronpot, J. P. Sundberg. Iowa State University Press: Iowa.
- Poynton, A. R., Walsh, T. N., O'Sullivan, G., and Hennessy, T. P. (1996) Carcinoma arising in familial Barrett's esophagus. *Am J Gastroenterol* **91**, 1855-1856.
- Preston, S. L., Harrison, L. A., and Jankowski, J. A. Animal Models of Barrett's Oesophagus. *Gut*. 2007.
- Preston, S. L., Wong, W. M., Chan, A. O., Poulson, R., Jeffery, R., Goodlad, R. A., Mandir, N., Elia, G., Novelli, M., Bodmer, W. F., Tomlinson, I. P., and Wright, N. A. (2003) Bottom-up histogenesis of colorectal adenomas: origin in the monocryptal adenoma and initial expansion by crypt fission. *Cancer Res* **63**, 3819-3825.
- Que, F. G. and Gores, G. J. (1996) Cell death by apoptosis: basic concepts and disease relevance for the gastroenterologist. *Gastroenterology* **110**, 1238-1243.
- Radice, G. L., FerreiraCornwell, M. C., Robinson, S. D., Rayburn, H., Chodosh, L. A., Takeichi, M., and Hynes, R. O. (1997) Precocious mammary gland development in P-cadherin-deficient mice. *Journal of Cell Biology* **139**, 1025-1032.
- Radtke, F. and Clevers, H. (2005) Self-renewal and cancer of the gut: two sides of a coin. *Science* **307**, 1904-1909.
- Regaud, C. (1901a) Etudes sur la structure des tubes seminiferes et sur la spermatogenese chez les mammiferes. Part 1. *Archives d'Anatomie microscopiques et de Morphologie experimentale* **4**, 101-156.
- Regaud, C. (1901b) Etudes sur la structure des tubes seminiferes et sur la spermatogenese chez les mammiferes. Part 2. *Archives d'Anatomie microscopiques et de Morphologie experimentale* **4**, 231-280.
- Richards, F. M., McKee, S. A., Rajpar, M. H., Cole, T. R., Evans, D. G., Jankowski, J. A., McKeown, C., Sanders, D. S., and Maher, E. R. (1999) Germline E-cadherin gene (CDH1) mutations predispose to familial gastric cancer and colorectal cancer. *Hum Mol Genet* **8**, 607-610.
- Rockett, J. C., Larkin, K., Darnton, S. J., Morris, A. G., and Matthews, H. R. (1997) Five newly established oesophageal carcinoma cell lines: phenotypic and immunological characterization. *Br J Cancer* **75**, 258-263.
- Roth, K. A., Hertz, J. M., and Gordon, J. I. (1990) Mapping enteroendocrine cell populations in transgenic mice reveals an unexpected degree of complexity in cellular differentiation within the gastrointestinal tract. *J Cell Biol* **110**, 1791-1801.
- Rubinstein, A. (2003) Zebrafish: from disease modelling to drug discovery. *Curr Op Drug Discovery & Development* **6**, 218-223.

- Rubinstein, AL. (2006) Zebrafish assays for drug toxicity screening. *Expert opinion on drug metabolism & toxicology* **2**, 231-240.
- Sakakibara, S., Imai, T., Hamaguchi, K., Okabe, M., Aruga, J., Nakajima, K., Yasutomi, D., Nagata, T., Kurihara, Y., Uesugi, S., Miyata, T., Ogawa, M., Mikoshiba, K., and Okano, H. (1996) Mouse-Musashi-1, a neural RNA-Binding protein highly enriched in the mammalian CNS stem cell. *Developmental Biology* **176**, 230-242.
- Sancho, E., Battle, E., and Clevers, H. (2004) Signaling pathways in intestinal development and cancer. *Annu Rev Cell Dev Biol* **20**, 695-723.
- Sanders, D. S. (2005) Mucosal integrity and barrier function in the pathogenesis of early lesions in Crohn's disease. *J Clin Pathol* **58**, 568-572.
- Sanders, D. S., Bruton, R., Darnton, S. J., Casson, A. G., Hanson, I., Williams, H. K., and Jankowski, J. (1998) Sequential changes in cadherin-catenin expression associated with the progression and heterogeneity of primary oesophageal squamous carcinoma. *Int J Cancer* **79**, 573-579.
- Sanders, D. S., Perry, I., Hardy, R., and Jankowski, J. (2000) Aberrant P-cadherin expression is a feature of clonal expansion in the gastrointestinal tract associated with repair and neoplasia. *J Pathol* **190**, 526-530.
- Sasai, Y., Kageyama, R., Tagawa, Y., Shigemoto, R., and Nakanishi, S. (1992) Two mammalian helix-loop-helix factors structurally related to Drosophila hairy and Enhancer of split. *Genes Dev* **6**, 2620-2634.
- Sato, T., Miwa, K., Sahara, H., Segawa, M., and Hattori, T. (2002) The sequential model of Barrett's esophagus and adenocarcinoma induced by duodeno-esophageal reflux without exogenous carcinogens. *Anticancer Res* **22**, 39-44.
- Schmidt, P. H., Lee, J. R., Joshi, V., Playford, R. J., Poulsom, R., Wright, N. A., and Goldenring, J. R. (1999) Identification of a metaplastic cell lineage associated with human gastric adenocarcinoma. *Lab Invest* **79**, 639-646.
- Scott, P. A. and Jankowski, J. A. (2001) Metaplasia to cancer sequence in Barrett's oesophagus. *Gastrointestinal Cancer* **6**, 2-4.
- Seery, J. P. (2002) Stem cells of the oesophageal epithelium. *Journal of Cell Science* **115**, 1783-1789.
- Seery, J. P. and Watt, F. M. (2000) Asymmetric stem-cell divisions define the architecture of human oesophageal epithelium. *Current Biology* **10**, 1447-1450.
- Seto, Y., Kobori, O., Shimizu, T., and Morioka, Y. (1991) The role of alkaline reflux in esophageal carcinogenesis induced by N-amyl-N-methylnitrosamine in rats. *Int J Cancer* **49**, 758-763.
- Shamblott, M.J., Axelman, J., Wang, S., Bugg, E.M., Littlefield, J.W., Donovan, P.J., Blumenthal, P.D., Huggins, G.R., and Gearhart, J.D. (1998) Derivation of pluripotent stem cells from cultured human primordial germ cells. *Proc. Natl. Acad. Sci. USA* **95**, 13726-13731.

- Shanahan, F. (1996) Cadherins, inflammatory bowel disease and neoplasia. *Gastroenterology* **111**, 261-262.
- Sharma, P. and Sampliner, R. (1997) GERD, DGER, or both in Barrett's esophagus? *Am J Gastroenterol* **92**, 903-904.
- Shih, I. M., Wang, T. L., Traverso, G., Romans, K., Hamilton, S. R., Ben-Sasson, S., Kinzler, K. W., and Vogelstein, B. (2001) Top-down morphogenesis of colorectal tumors. *Proc Natl Acad Sci U S A* **98**, 2640-2645.
- Shimoyama, Y., Yoshida, T., Terada, M., Shimosato, Y., Abe, O., and Hirohashi, S. (1989) Molecular cloning of a human Ca<sup>2+</sup>-dependent cell-cell adhesion molecule homologous to mouse placental cadherin: its low expression in human placental tissues. *J Cell Biol* **109**, 1787-1794.
- Shinohara, T., Avarbock, M. R., and Brinster, R. L. (1999) beta(1)- and alpha(6)-integrin are surface markers on mouse spermatogonial stem cells. *Proceedings of the National Academy of Sciences of the United States of America* **96**, 5504-5509.
- Sloncova, E., Fric, P., Kucerova, D., Lojda, Z., Tuhackova, Z., and Sovova, V. (2001) Changes of E-cadherin and beta-catenin in human and mouse intestinal tumours. *Histochem J* **33**, 13-17.
- Smalley, M. and Ashworth, A. (2003) Stem cells and breast cancer: A field in transit. *Nat Rev Cancer* **3**, 832-844.
- Sodhani, P., Gupta, S., Prakash, S., and Singh, V. (1999) Columnar and metaplastic cells in vault smears: cytologic and colposcopic study. *Cytopathology* **10**, 122-126.
- Spradling, A., Drummond-Barbosa, D., and Kai, T. (2001) Stem cells find their niche. *Nature* **414**, 98-104.
- Su, Y. H., Chen, X. X., Klein, M., Fang, M., Wang, S., Yang, C. S., and Goyall, R. K. (2004) Phenotype of columnar-lined esophagus in rats with esophagogastrroduodenal anastomosis: similarity to human Barrett's esophagus. *Laboratory Investigation* **84**, 753-765.
- Svoboda, K. R., Vijayaraghavan, S., and Tanguay, R. L. (2002) Nicotinic receptors mediate changes in spinal motoneuron development and axonal pathfinding in embryonic zebrafish exposed to nicotine. *J Neurosci* **22**, 10731-10741.
- Sweetser, D. A., Birkenmeier, E. H., Hoppe, P. C., McKeel, D. W., and Gordon, J. I. (1988) Mechanisms underlying generation of gradients in gene expression within the intestine: an analysis using transgenic mice containing fatty acid binding protein-human growth hormone fusion genes. *Genes Dev* **2**, 1318-1332.
- Takeichi, M. (1990) Cadherins: a molecular family important in selective cell-cell adhesion. *Annu Rev Biochem* **59**, 237-252.
- Takeichi, M. (1995) Morphogenetic roles of classic cadherins. *Curr Opin Cell Biol* **7**, 619-627.

- Tani, H., Morris, R. J., and Kaur, P. (2000) Enrichment for murine keratinocyte stem cells based on cell surface phenotype. *Proceedings of the National Academy of Sciences of the United States of America* **97**, 10960-10965.
- Tatematsu, M., Tsukamoto, T., and Mizoshita, T. (2005) Role of *Helicobacter pylori* in gastric carcinogenesis: the origin of gastric cancers and heterotopic proliferative glands in Mongolian gerbils. *Helicobacter* **10**, 97-106.
- The National Center for Biotechnology Information.  
[http://www.ncbi.nlm.nih.gov/About/primer/genetics\\_cell.html](http://www.ncbi.nlm.nih.gov/About/primer/genetics_cell.html) - A Basic Introduction to the Science Underlying NCBI Resources. 2006.
- Thomas, G. J. and Speight, P. M. (2001) Cell adhesion molecules and oral cancer. *Crit Rev Oral Biol Med* **12**, 479-498.
- Thomson, J.A., Itskovitz-Eldor, J., Shapiro, S.S., Waknitz, M.A., Swiergiel, J.J., Marshall, V.S., and Jones, J.M. (1998) Embryonic Stem Cell Lines Derived from Human Blastocysts. *Science* **282**, 1145-1147.
- Tselepis, C., Perry, I., and Boulton, R. e. a. (1999) Endogenous secondary bile acid levels modify epithelial biology in Barrett's oesophagus. *Gut* **45**.
- Tytgat, G. N. J. (1995) Does endoscopic surveillance in esophageal columnar metaplasia (barretts-esophagus) have any real value. *Endoscopy* **27**, 19-26.
- Varki, A. (1993) Biological roles of oligosaccharides: all of the theories are correct. *Glycobiology* **3**, 97-130.
- Vogelstein, B., Fearon, E. R., Hamilton, S. R., Kern, S. E., Preisinger, A. C., Leppert, M., Nakamura, Y., White, R., Smits, A. M., and Bos, J. L. (1988) Genetic alterations during colorectal-tumor development. *N Engl J Med* **319**, 525-532.
- Wang, Q., Li, H., Liu, S., Wang, G., and Wang, Y. (2005) Cloning and tissue expression of chicken heart fatty acid-binding protein and intestine fatty acid-binding protein genes. *Anim Biotechnol* **16**, 191-201.
- Wang, T. C., Goldenring, J. R., Dangler, C., Ito, S., Mueller, A., Jeon, W. K., Koh, T. J., and Fox, J. G. (1998) Mice lacking secretory phospholipase A(2) show altered apoptosis and differentiation with *Helicobacter felis* infection. *Gastroenterology* **114**, 675-689.
- Watt, F. M. (2002) Role of integrins in regulating epidermal adhesion, growth and differentiation. *Embo Journal* **21**, 3919-3926.
- Watt, F. M. and Hogan, B. L. M. (2000) Out of Eden: Stem cells and their niches. *Science* **287**, 1427-1430.
- Westerfield, M. (2000) *The Zebrafish Book: A Guide for the Laboratory Use of Zebrafish (Danio Rerio\*)*. University of Oregon Press: Eugene, Oregon.
- Williams, C. L. (1997) Regulation of cadherin activity by G protein and the actin cytoskeleton (DSG). In: *Cytoskeletal-membrane interactions and signal transduction*, pp. 111-126. Eds C. Cowin, M. W. Klymkowsky. Austin, R.G. Landes Company and Chapman & Hall.

Winters, C., Jr., Spurling, T. J., Chobanian, S. J., Curtis, D. J., Esposito, R. L., Hacker, J. F., III, Johnson, D. A., Cruess, D. F., Cotelingam, J. D., Gurney, M. S. (1987) Barrett's esophagus. A prevalent, occult complication of gastroesophageal reflux disease. *Gastroenterology* **92**, 118-124.

Wright, N. A. (2000) Epithelial stem cell repertoire in the gut: clues to the origin of cell lineages, proliferative units and cancer. *International Journal of Experimental Pathology* **81**, 117-143.

Wright, N. A. and Alison, M. (1984) *The Biology of Epithelial Cell Populations*. Clarendon Press: Oxford.

Yamashita, Y., Homma, K., Kako, N., Clark, G. W., Smyrk, T. C., Hinder, R. A., Adrian, T. E., DeMeester, T. R., and Mirvish, S. S. (1998) Effect of duodenal components of the refluxate on development of esophageal neoplasia in rats. *J Gastrointest Surg* **2**, 350-355.

Yan, T., Seo, Y., Schupp, J. E., Zeng, X. H., Desai, A. B., and Kinsella, T. J. (2006) Methoxyamine potentiates iododeoxyuridine-induced radiosensitization by altering cell cycle kinetics and enhancing senescence. *Molecular Cancer Therapeutics* **5**, 893-902.

Yap, A. S. (1998) The morphogenetic role of cadherin cell adhesion molecules in human cancer: a thematic review. *Cancer Invest* **16**, 252-261.

Zhang, X., Geboes, K., Depoortere, I., Tack, J., Janssens, J., and Sifrim, D. (2005) Effect of repeated cycles of acute esophagitis and healing on esophageal peristalsis, tone, and length. *Am J Physiol Gastrointest Liver Physiol* **288**, G1339-G1346.

**Appendix 1: Study Documentation to Accompany the  
“STEMcell Assessment in Neoplastic Tissues” (SAINT) Clinical  
Trial**

The following drug dosage chart was used in the SAINT Trial for the intravenous infusion of the Iododeoxyuridine, as detailed in section 2.1.2.

## In Vivo Labelling of Barretts' Oesophagus with Iododeoxyuridine

UHL No. 9122

*Principal Investigator:* Prof J Jankowski

*Study Nurse:* Lea-Anne Harrison

### ORDER

Send to Pharmacy IV Lab / Fax 6928

Ward:.....

Date Required: .....

Confirmed? **Yes / No \***

\*Delete as appropriate

Patient Trial No:.....

Patient Name	Ht (cm):.....
D.O.B.	Wt (Kg):.....
Or affix addressograph	SA (m <sup>2</sup> ):..... (cap @ 2m <sup>2</sup> )

**Iododeoxyuridine (200mg/m<sup>2</sup>)**..... in 250ml Sodium Chloride 0.9% Infusion over 30 minutes  
(max dose 400mg)

Signature (RGN/SRN) ..... Date:.....

PRINT NAME .....

**Pharmacy use:**

**Prof Check:**.....

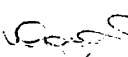
	IODODEOXYURIDINE	
	Initial	Date
Entered in diary by:		
Doc completed in trial file by:		
Dispensed by:		
Checked and released by:		

**One of the signatures in the trial file must be a Pharmacist**

M:\Clinical Trials - Onc,Aseptics\CLINICAL TRIALS Current & Pending\Iododeoxyuridine (IUDR)\iododeoxy order form.doc

Written By: Eoin Barrett

Date: Oct 2005

Checked By: 

Date: .....

The following monitoring chart was used to record all patient observations in the SAINT Trial during the intravenous infusion of the Iododeoxyuridine as detailed in section 2.1.2.

<b>PATIENT OBSERVATIONS</b>								
-----------------------------	--	--	--	--	--	--	--	--

	<b>Pre Infusion Time</b>	<b>Post Infusion Time</b>	<b>½ Hourly</b>	<b>½ Hourly</b>	<b>½ Hourly</b>	<b>½ Hourly</b>	<b>½ Hourly</b>	<b>½ Hourly</b>
<b>BP (Sitting)</b>								
<b>Pulse</b>								
<b>Temp</b>								
<b>SpO<sub>2</sub></b>								

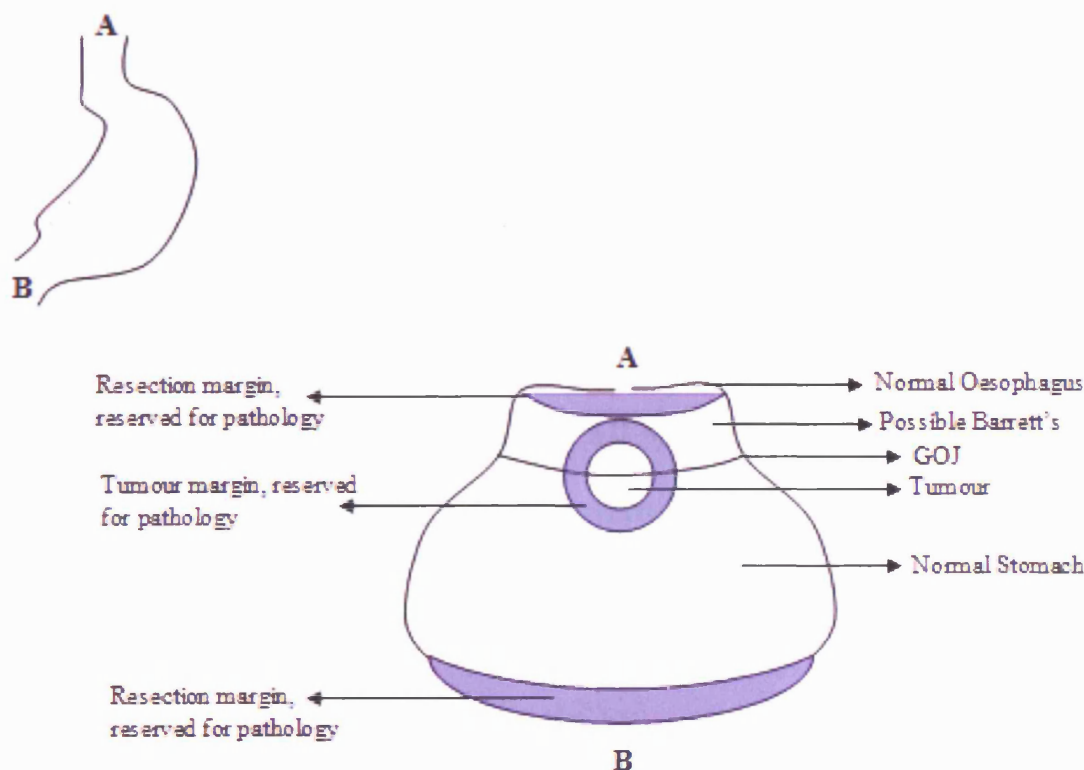
<b>ADVERSE EFFECTS DURING INFUSION (TICK BOX)</b>								
---	--	--	--	--	--	--	--	--

	<b>Pre Infusion Time</b>	<b>Post Infusion Time</b>	<b>½ Hourly</b>	<b>½ Hourly</b>	<b>½ Hourly</b>	<b>½ Hourly</b>	<b>½ Hourly</b>	<b>½ Hourly</b>
<b>Palpitations</b>								
<b>Flushing</b>								
<b>Dizziness/Light Headed</b>								
<b>Pain</b>								
<b>Shortness of Breath</b>								
<b>Other</b>								

<b>DETAILS OF ANY POST INFUSION COMPLICATION</b>								
--	--	--	--	--	--	--	--	--

--

The following diagram represents the way in which patient tissues were processed following enrolment in the SAINT Trial post surgical resection and intravenous infusion of the Iododeoxyuridine, as detailed in section 2.2.1.2.



#### Colour Coding: -

- = Tissue that will go to routine pathology
- = Tissue that will be utilised in our research

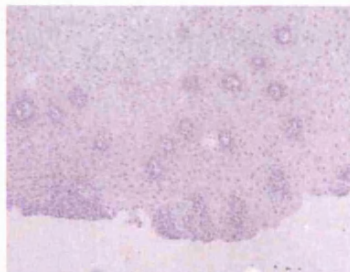
We would like blocks from: -

1. Normal Squamous
2. Barrett's Oesophagus (if present)
3. Tumour
4. Normal Stomach

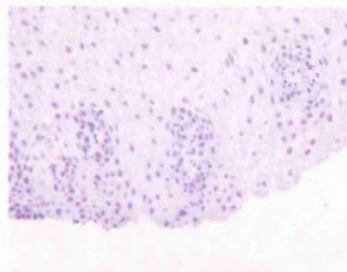
- The specimen will be removed as normal and picked up as fresh tissue from theatre.
- This specimen will be processed by the pathologist for both normal histological samples along with our blocks from the relevant areas.
- We will take blocks for routine processing along with tissue that will be placed onto a filing card, mucosa side down, in long straight lengths.
- This tissue will be fixed in formalin for 24 hours and then transferred to 70% ethanol before being sent to CRUK for processing. **Note:** the tissue can stay in the 70% ethanol for up to one week.

**Appendix 2: IHC Data on All Six Clinical Cases and Each  
Marker Studied**

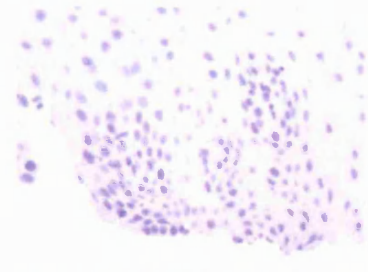
The following contact sheets represent all six clinical cases which were analysed for P-cadherin IHC in gastric, normal squamous, oesophagitis, BM and OA human tissue. A selection of these were utilised to create Figure 3.4, section 3.4.2.



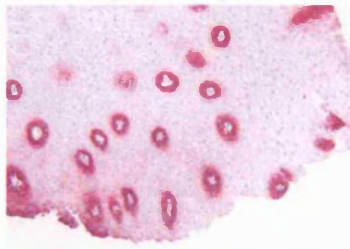
01a 1.100 Negative Norm Squamous Pcad x10.jpg



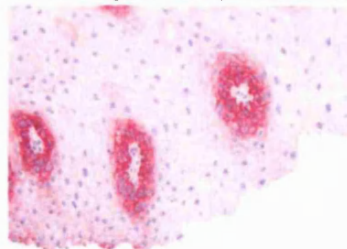
01b 1.100 Negative Norm Squamous Pcad x25.jpg



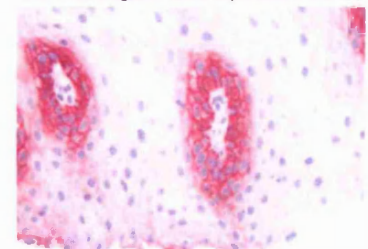
01c 1.100 Negative Norm Squamous Pcad x40.jpg



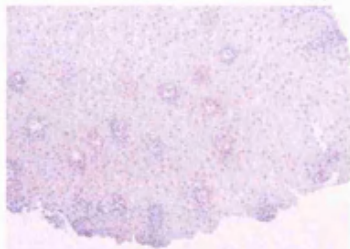
02a 1.100 Norm Squamous Pcad x10.jpg



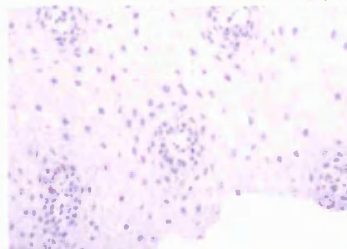
02b 1.100 Norm Squamous Pcad x25.jpg



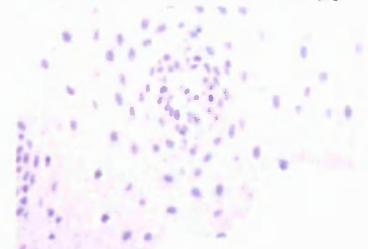
02c 1.100 Norm Squamous Pcad x40.jpg



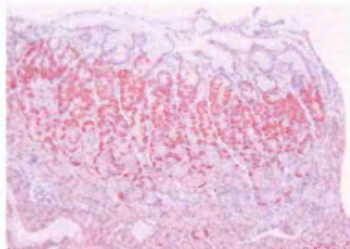
03a 1.100 Isotype Norm Squamous Pcad x10.jpg



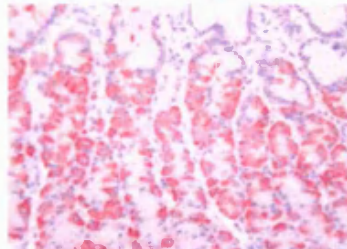
03b 1.100 Isotype Norm Squamous Pcad x25.jpg



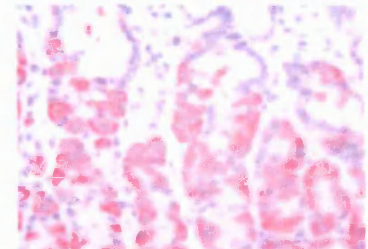
03c 1.100 Isotype Norm Squamous Pcad x40.jpg



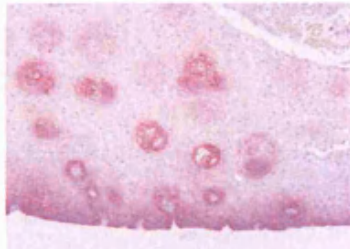
04a 1.100 Case 1 Stomach Pcad x10.jpg



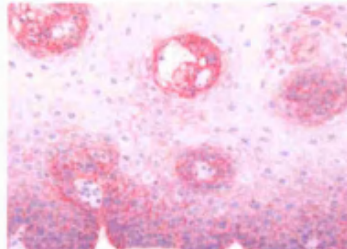
04b 1.100 Case 1 Stomach Pcad x25.jpg



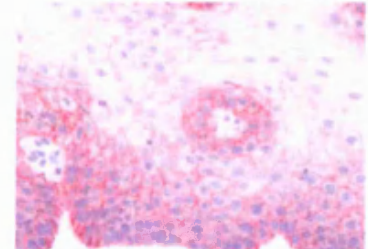
04c 1.100 Case 1 Stomach Pcad x40.jpg



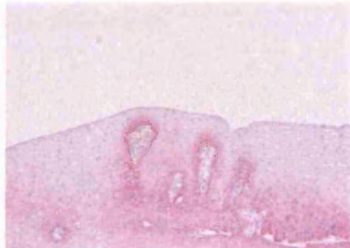
05a 1.100 Case 1 Norm Squamous Pcad x10.jpg



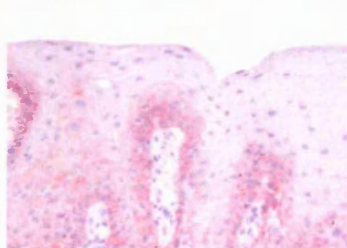
05b 1.100 Case 1 Norm Squamous Pcad x25.jpg



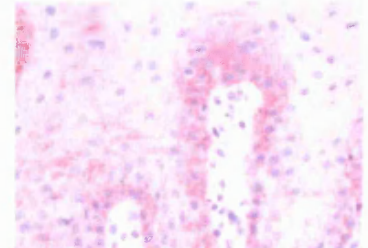
05c 1.100 Case 1 Norm Squamous Pcad x40.jpg



06a 1.100 Case 1 Oesophagitis Pcad x10.jpg



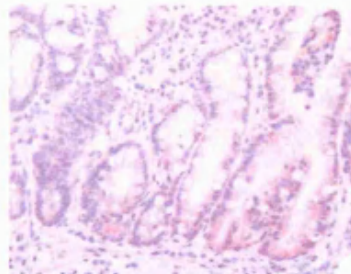
06b 1.100 Case 1 Oesophagitis Pcad x25.jpg



06c 1.100 Case 1 Oesophagitis Pcad x40.jpg



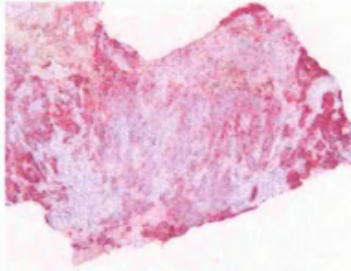
07a 1.100 Case 1 Barretts Pcad x10.jpg



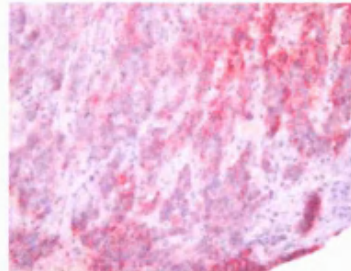
07b 1.100 Case 1 Barretts Pcad x25.jpg



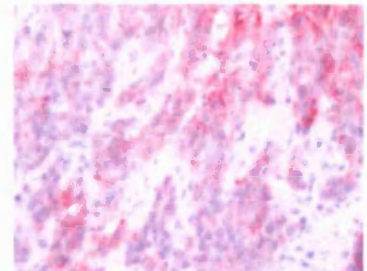
07c 1.100 Case 1 Barretts Pcad x40.jpg



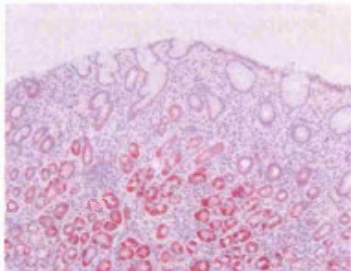
08a 1.100 Case 1 Adeno Pcad x10.jpg



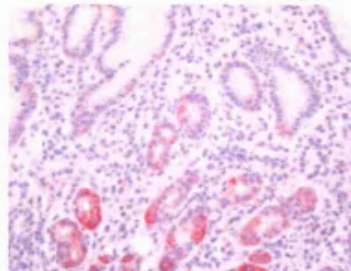
08b 1.100 Case 1 Adeno Pcad x25.jpg



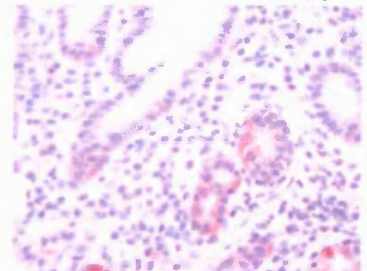
08c 1.100 Case 1 Adeno Pcad x40.jpg



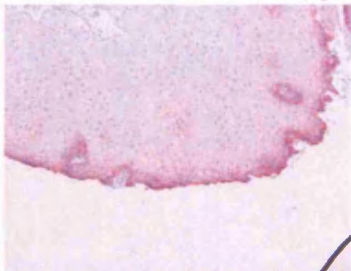
09a 1.100 Case 2 Stomach Pcad x25.jpg



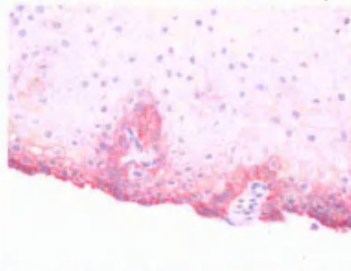
09b 1.100 Case 2 Stomach Pcad x40.jpg



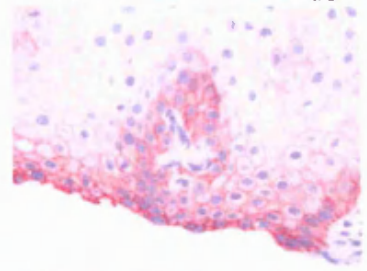
09c 1.100 Case 2 Stomach Pcad x40.jpg



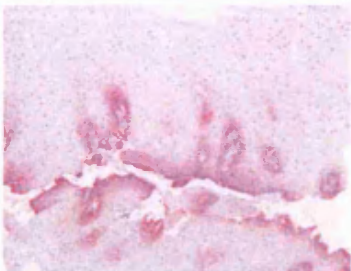
10a 1.100 Case 2 Norm Squamous Pcad x10...



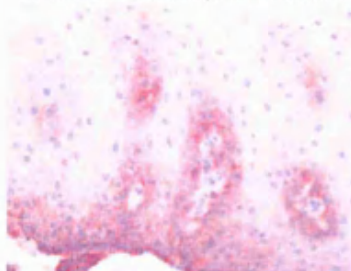
10b 1.100 Case 2 Norm Squamous Pcad x25...



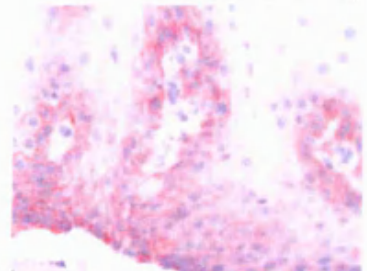
10c 1.100 Case 2 Norm Squamous Pcad x40...



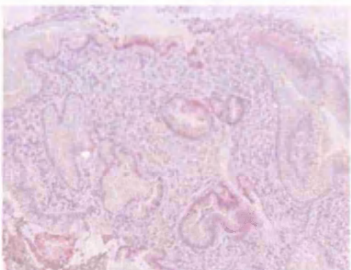
11a 1.100 Case 2 Oesophagitis Pcad x10.jpg



11b 1.100 Case 2 Oesophagitis Pcad x25.jpg



11d 1.100 Case 2 Oesophagitis Pcad x40.jpg



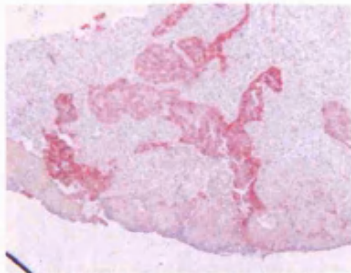
12a 1.100 Case 2 Barretts Pcad x10.jpg



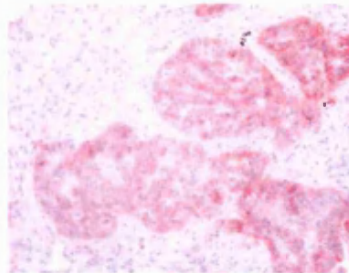
12b 1.100 Case 2 Barretts Pcad x25.jpg



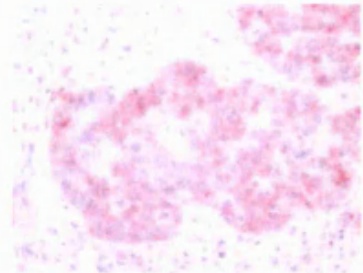
12c 1.100 Case 2 Barretts Pcad x40.jpg



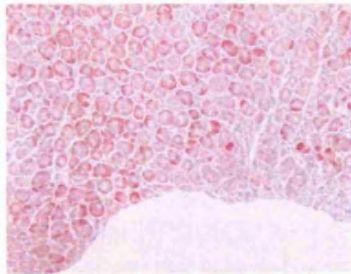
13a 1.100 Case 2 Adeno Pcad x10 .jpg



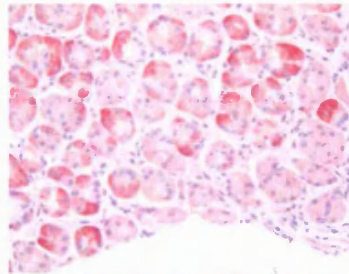
13b 1.100 Case 2 Adeno Pcad x25 .jpg



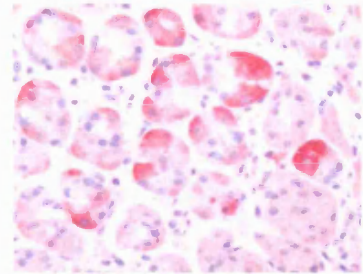
13c 1.100 Case 2 Adeno Pcad x40 .jpg



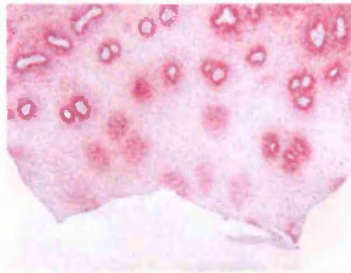
14a 1.100 Case 3 Stomach Pcad x10 .jpg



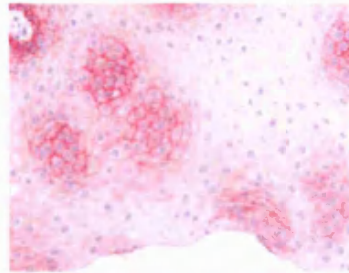
14b 1.100 Case 3 Stomach Pcad x25 .jpg



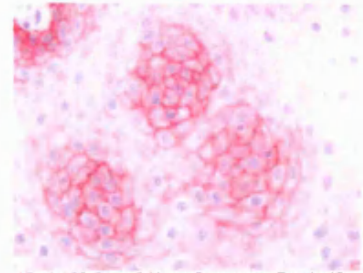
14c 1.100 Case 3 Stomach Pcad x40 .jpg



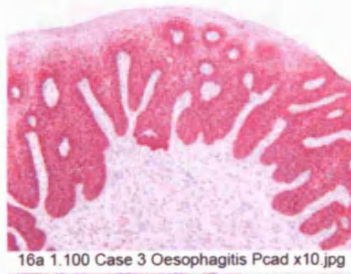
15a 1.100 Case 3 Norm Squamous Pcad x10 .jpg



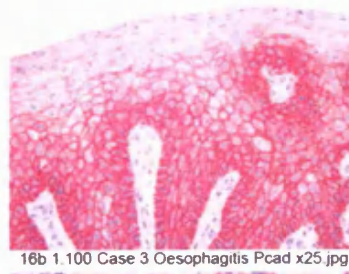
15b 1.100 Case 3 Norm Squamous Pcad x25 .jpg



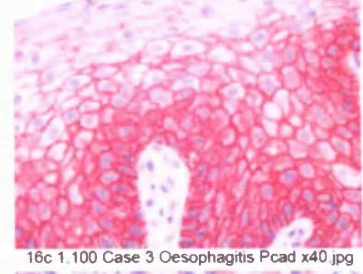
15c 1.100 Case 3 Norm Squamous Pcad x40 .jpg



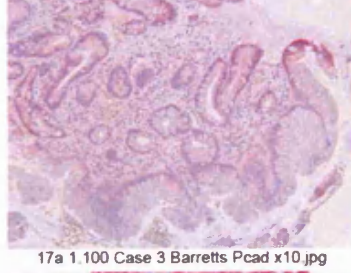
16a 1.100 Case 3 Oesophagitis Pcad x10 .jpg



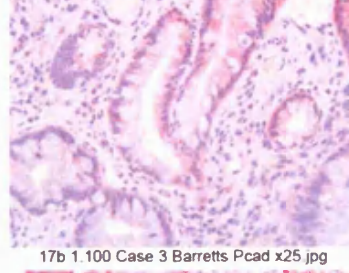
16b 1.100 Case 3 Oesophagitis Pcad x25 .jpg



16c 1.100 Case 3 Oesophagitis Pcad x40 .jpg



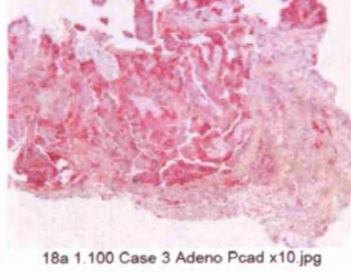
17a 1.100 Case 3 Barretts Pcad x10 .jpg



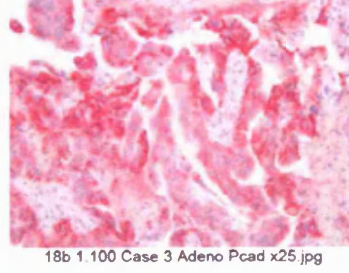
17b 1.100 Case 3 Barretts Pcad x25 .jpg



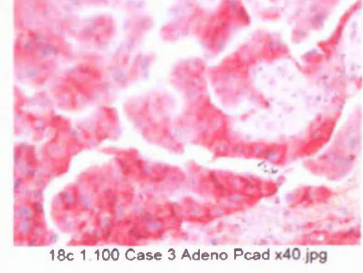
17c 1.100 Case 3 Barretts Pcad x40 .jpg



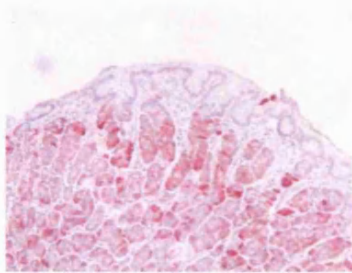
18a 1.100 Case 3 Adeno Pcad x10 .jpg



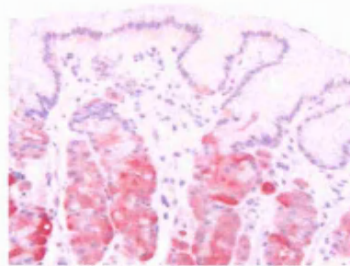
18b 1.100 Case 3 Adeno Pcad x25 .jpg



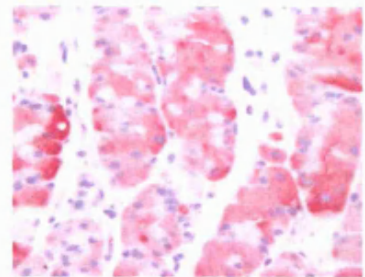
18c 1.100 Case 3 Adeno Pcad x40 .jpg



19a 1.100 Case 4 Stomach Pcad x10.jpg



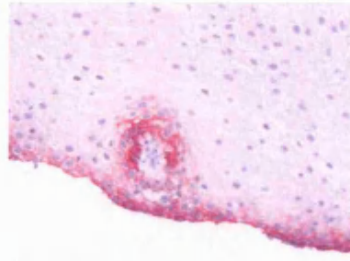
19b 1.100 Case 4 Stomach Pcad x25.jpg



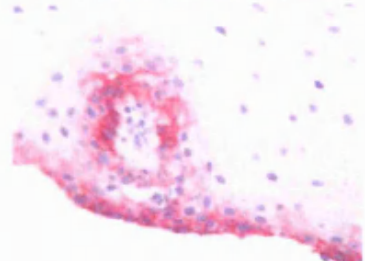
19c 1.100 Case 4 Stomach Pcad x40.jpg



20a 1.100 Case 4 Norm Squamous Pcad x10...



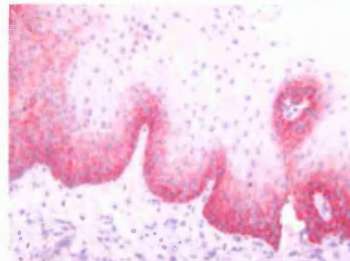
20b 1.100 Case 4 Norm Squamous Pcad x25...



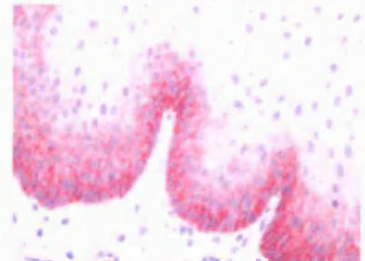
20c 1.100 Case 4 Norm Squamous Pcad x40...



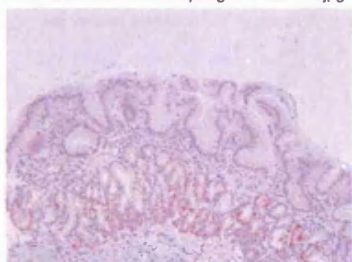
21a 1.100 Case 4 Oesophagitis Pcad x10.jpg



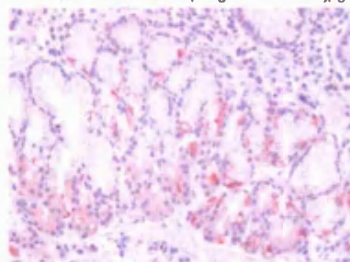
21b 1.100 Case 4 Oesophagitis Pcad x25.jpg



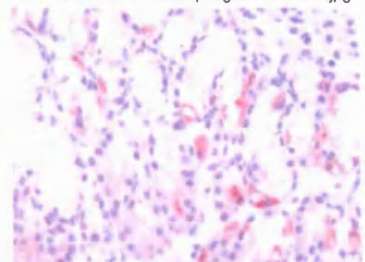
21c 1.100 Case 4 Oesophagitis Pcad x40.jpg



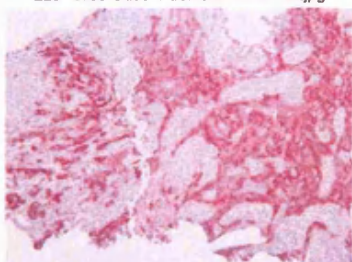
22a 1.100 Case 4 Barretts Pcad x10.jpg



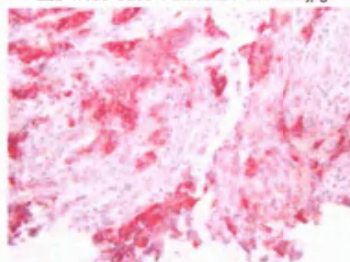
22b 1.100 Case 4 Barretts Pcad x25.jpg



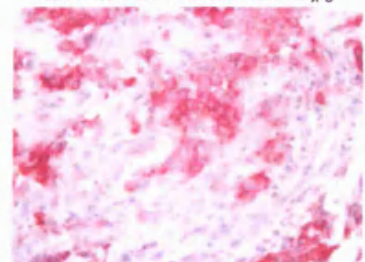
22c 1.100 Case 4 Barretts Pcad x40.jpg



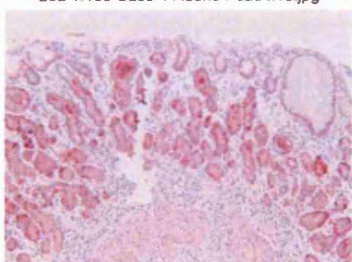
23a 1.100 Case 4 Adeno Pcad x10.jpg



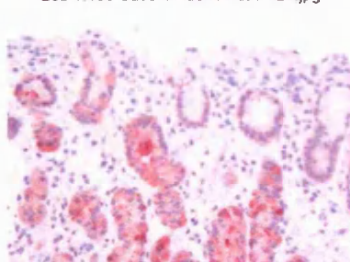
23b 1.100 Case 4 Adeno Pcad x25.jpg



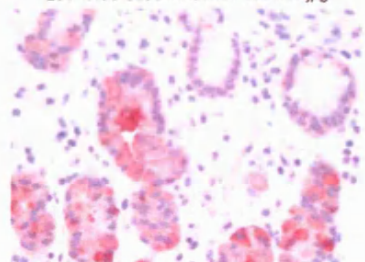
23c 1.100 Case 4 Adeno Pcad x40.jpg



24a 1.100 Case 5 Stomach Pcad x10.jpg



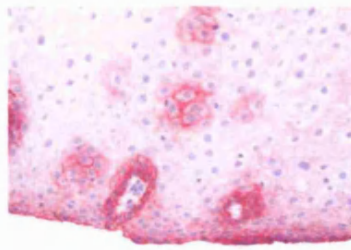
24b 1.100 Case 5 Stomach Pcad x25.jpg



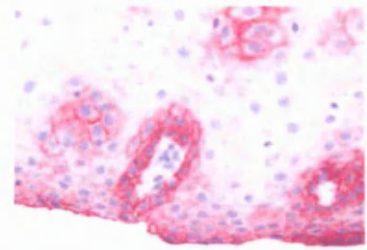
24c 1.100 Case 5 Stomach Pcad x40.jpg



25a 1.100 Case 5 Norm Squamous Pcad x10...



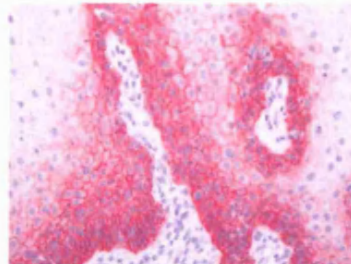
25b 1.100 Case 5 Norm Squamous Pcad x25...



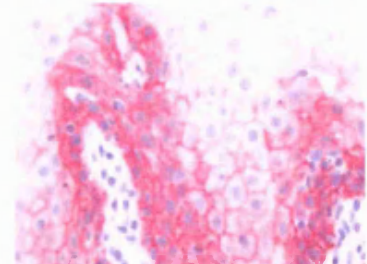
25c 1.100 Case 5 Norm Squamous Pcad x40...



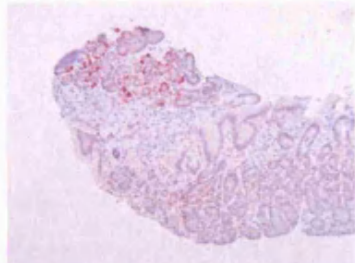
26a 1.100 Case 5 Oesophagitis Pcad x10.jpg



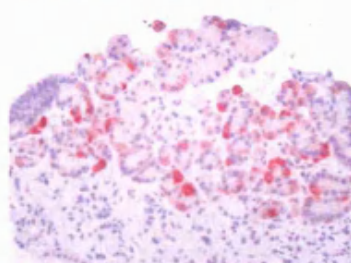
26b 1.100 Case 5 Oesophagitis Pcad x25.jpg



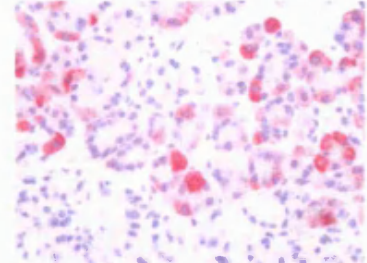
26c 1.100 Case 5 Oesophagitis Pcad x40.jpg



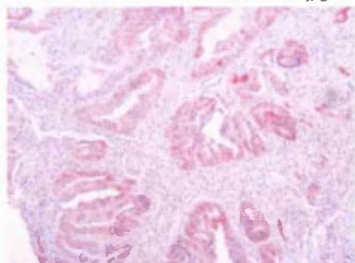
27a 1.100 Case 5 Barretts Pcad x10.jpg



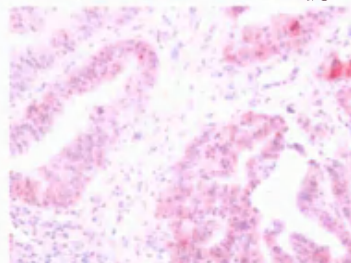
27b 1.100 Case 5 Barretts Pcad x25.jpg



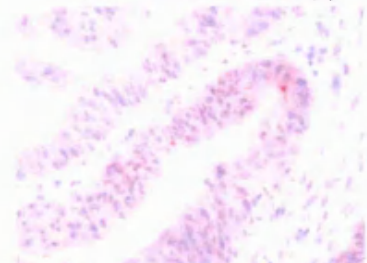
27c 1.100 Case 5 Barretts Pcad x40.jpg



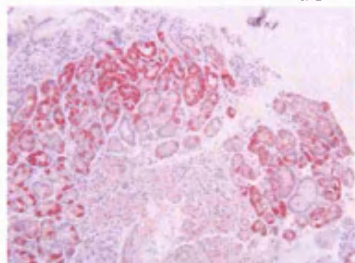
28a 1.100 Case 5 Adeno Pcad x10.jpg



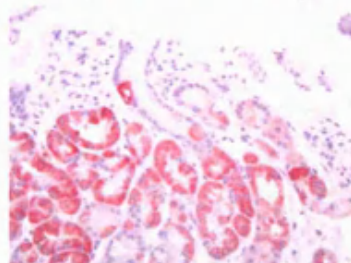
28b 1.100 Case 5 Adeno Pcad x25.jpg



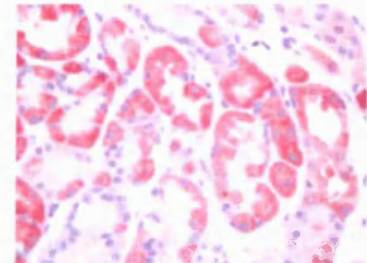
28c 1.100 Case 5 Adeno Pcad x40.jpg



29a 1.100 Case 6 Stomach Pcad x10.jpg



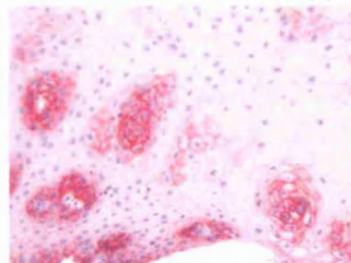
29b 1.100 Case 6 Stomach Pcad x25.jpg



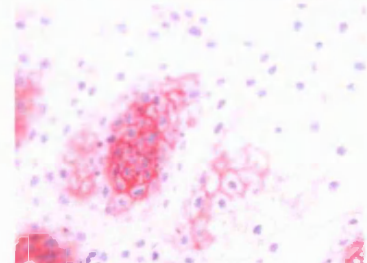
29c 1.100 Case 6 Stomach Pcad x40.jpg



30a 1.100 Case 6 Norm Squamous Pcad x10...



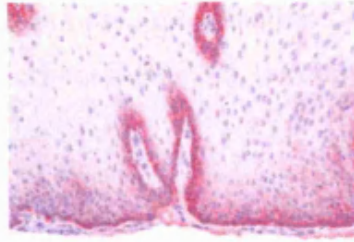
30b 1.100 Case 6 Norm Squamous Pcad x25...



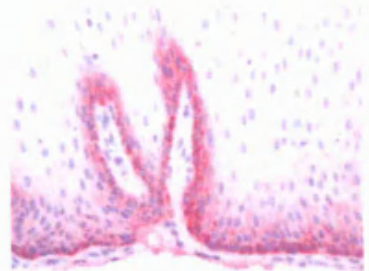
30c 1.100 Case 6 Norm Squamous Pcad x40...



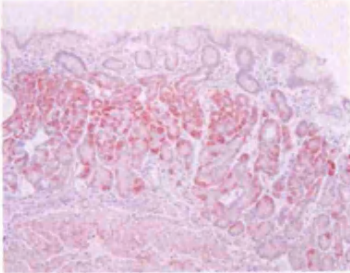
31a 1.100 Case 6 Oesophagitis Pcad x10 .jpg



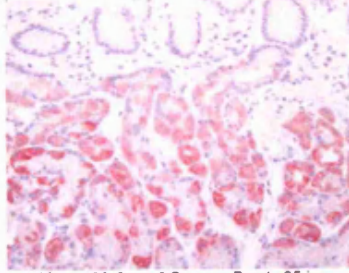
31b 1.100 Case 6 Oesophagitis Pcad x25 .jpg



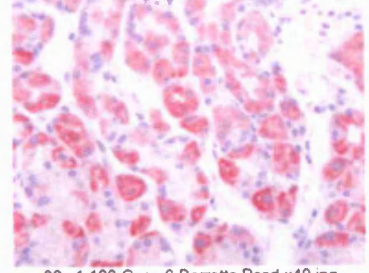
31c 1.100 Case 6 Oesophagitis Pcad x40 .jpg



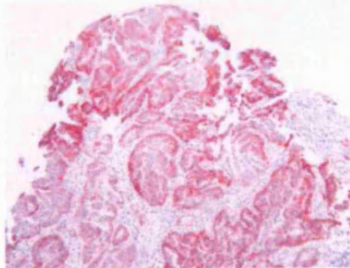
32a 1.100 Case 6 Barretts Pcad x10 .jpg



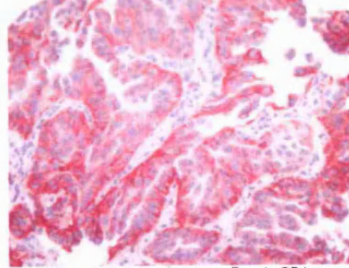
32b 1.100 Case 6 Barretts Pcad x25 .jpg



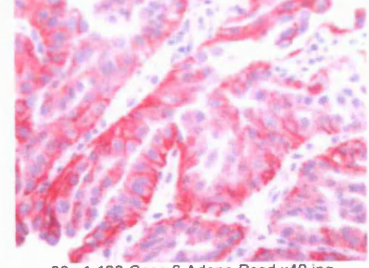
32c 1.100 Case 6 Barretts Pcad x40 .jpg



33a 1.100 Case 6 Adeno Pcad x10 .jpg

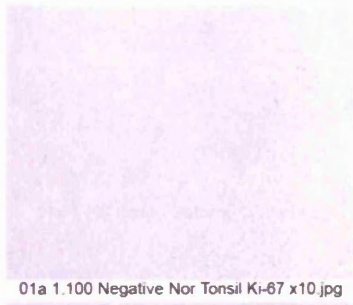


33b 1.100 Case 6 Adeno Pcad x25 .jpg

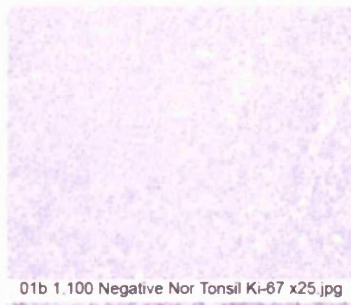


33c 1.100 Case 6 Adeno Pcad x40 .jpg

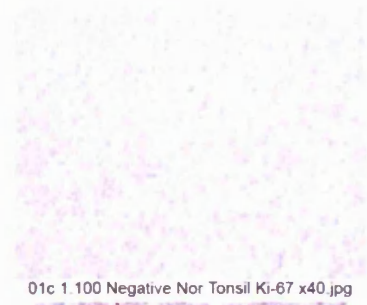
The following contact sheets represent all six clinical cases which were analysed for Ki-67 IHC in gastric, normal squamous, oesophagitis, BM and OA human tissue. A selection of these were utilised to create Figure 3.5, section 3.4.2.



01a 1.100 Negative Nor Tonsil Ki-67 x10.jpg



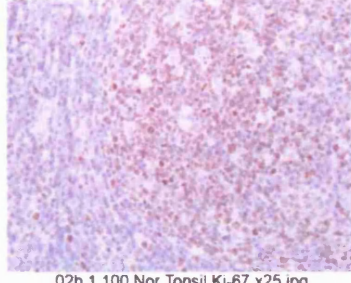
01b 1.100 Negative Nor Tonsil Ki-67 x25.jpg



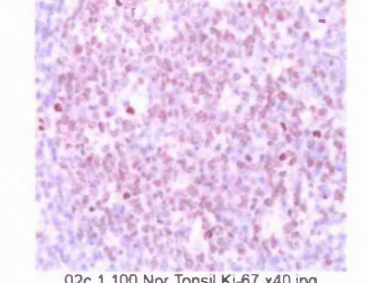
01c 1.100 Negative Nor Tonsil Ki-67 x40.jpg



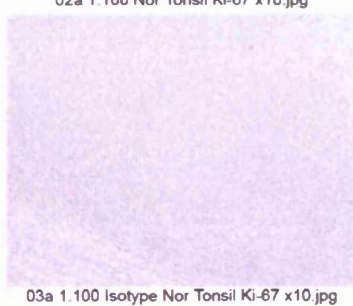
02a 1.100 Nor Tonsil Ki-67 x10.jpg



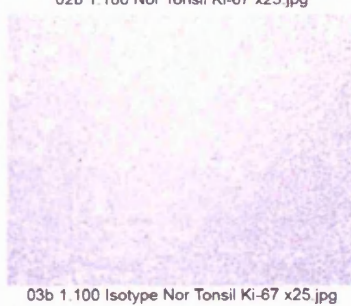
02b 1.100 Nor Tonsil Ki-67 x25.jpg



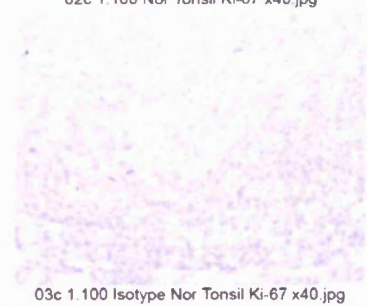
02c 1.100 Nor Tonsil Ki-67 x40.jpg



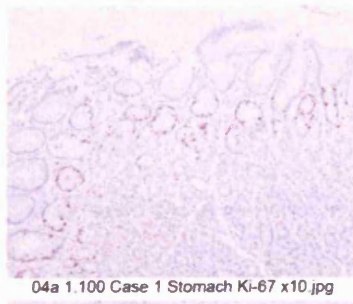
03a 1.100 Isotype Nor Tonsil Ki-67 x10.jpg



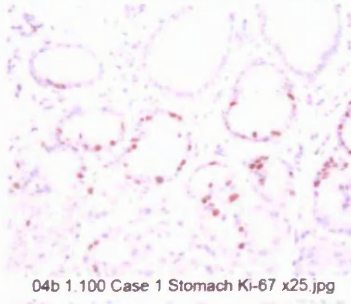
03b 1.100 Isotype Nor Tonsil Ki-67 x25.jpg



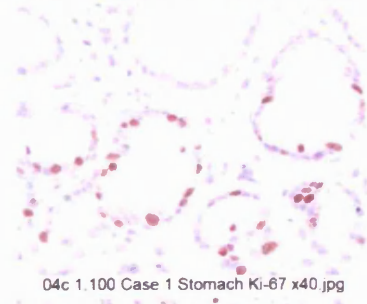
03c 1.100 Isotype Nor Tonsil Ki-67 x40.jpg



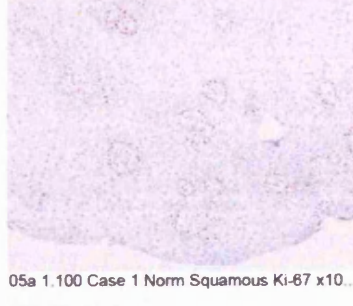
04a 1.100 Case 1 Stomach Ki-67 x10.jpg



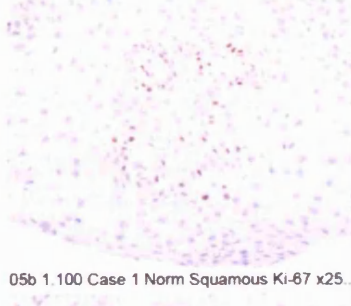
04b 1.100 Case 1 Stomach Ki-67 x25.jpg



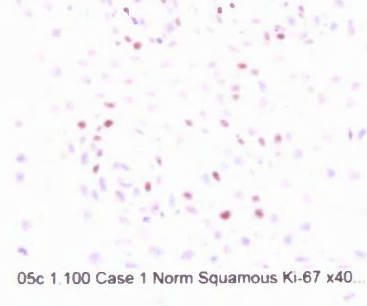
04c 1.100 Case 1 Stomach Ki-67 x40.jpg



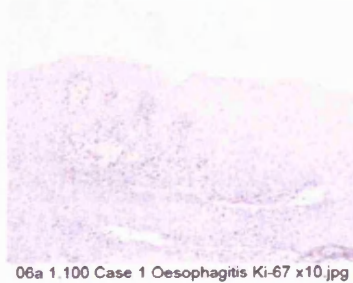
05a 1.100 Case 1 Norm Squamous Ki-67 x10...



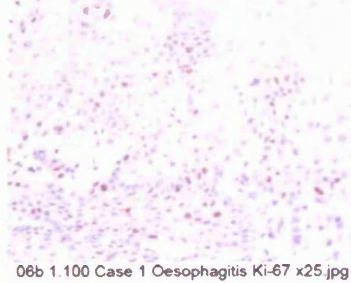
05b 1.100 Case 1 Norm Squamous Ki-67 x25...



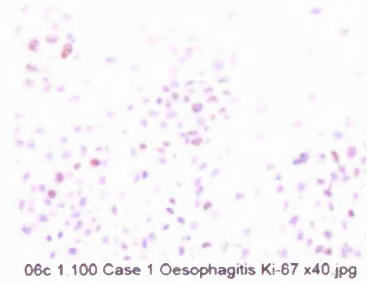
05c 1.100 Case 1 Norm Squamous Ki-67 x40...



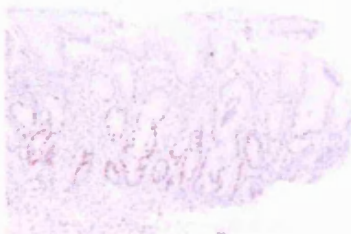
06a 1.100 Case 1 Oesophagitis Ki-67 x10.jpg



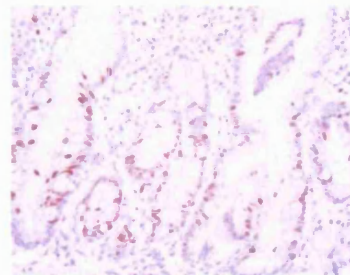
06b 1.100 Case 1 Oesophagitis Ki-67 x25.jpg



06c 1.100 Case 1 Oesophagitis Ki-67 x40.jpg



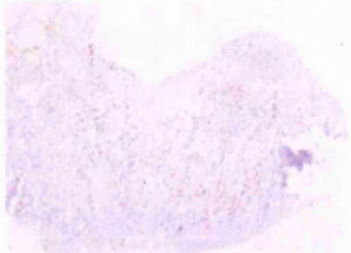
07a 1.100 Case 1 Barretts Ki-67 x10.jpg



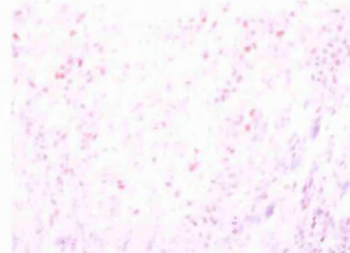
07b 1.100 Case 1 Barretts Ki-67 x25.jpg



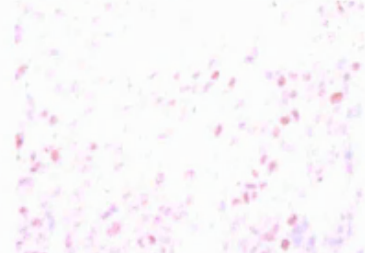
07c 1.100 Case 1 Barretts Ki-67 x40.jpg



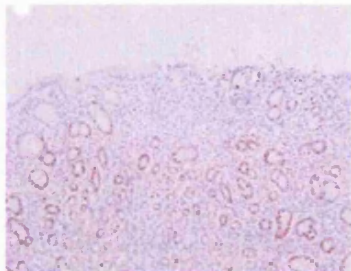
08a 1.100 Case 1 Adeno Ki-67 x10.jpg



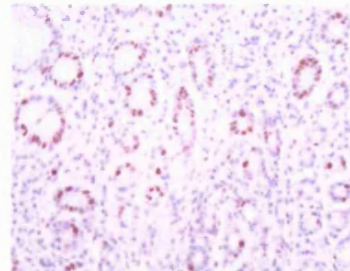
08b 1.100 Case 1 Adeno Ki-67 x25.jpg



08c 1.100 Case 1 Adeno Ki-67 x40.jpg



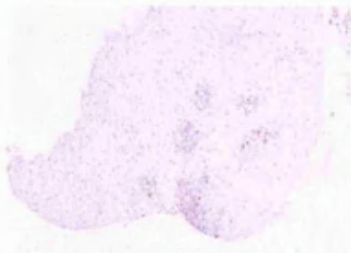
09a 1.100 Case 2 Stomach Ki-67 x10.jpg



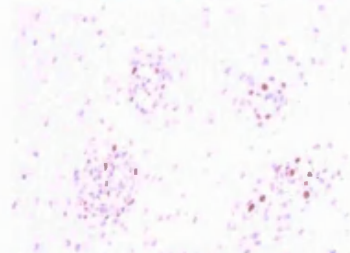
09b 1.100 Case 2 Stomach Ki-67 x25.jpg



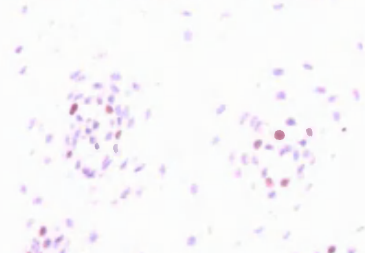
09c 1.100 Case 2 Stomach Ki-67 x40.jpg



10a 1.100 Case 2 Norm Squamous Ki-67 x10...



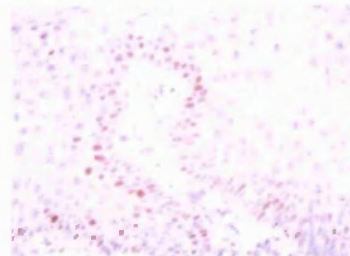
10b 1.100 Case 2 Norm Squamous Ki-67 x25...



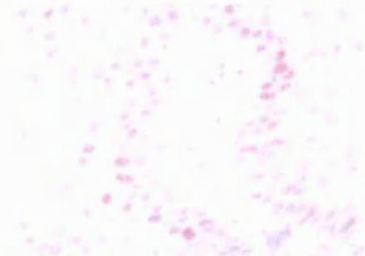
10c 1.100 Case 2 Norm Squamous Ki-67 x40...



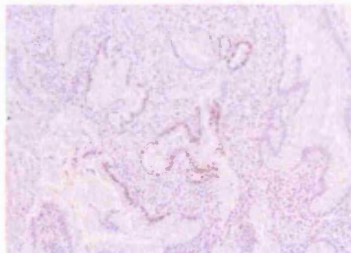
11a 1.100 Case 2 Oesophagitis Ki-67 x10.jpg



11b 1.100 Case 2 Oesophagitis Ki-67 x25.jpg



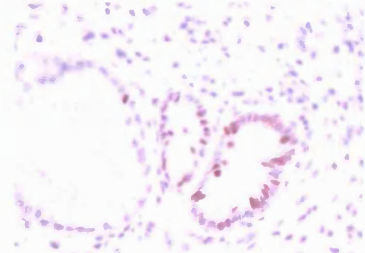
11c 1.100 Case 2 Oesophagitis Ki-67 x40.jpg



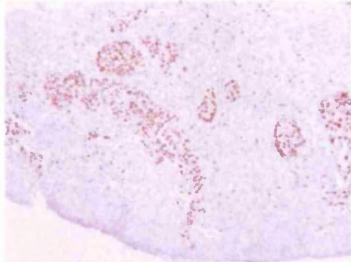
12a 1.100 Case 2 Barretts Ki-67 x10.jpg



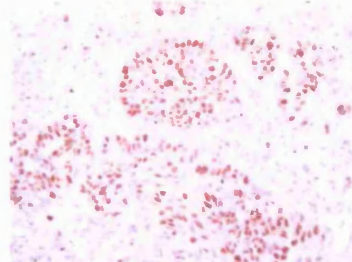
12b 1.100 Case 2 Barretts Ki-67 x25.jpg



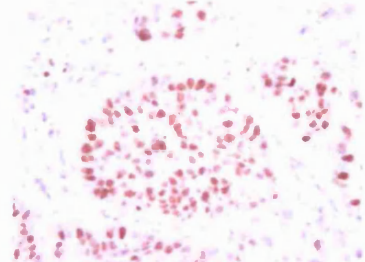
12c 1.100 Case 2 Barretts Ki-67 x40.jpg



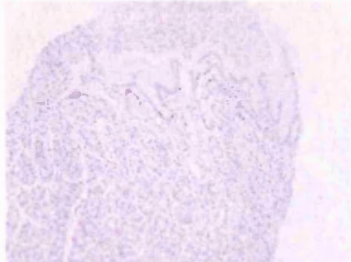
13a 1.100 Case 2 Adeno Ki-67 x10 .jpg



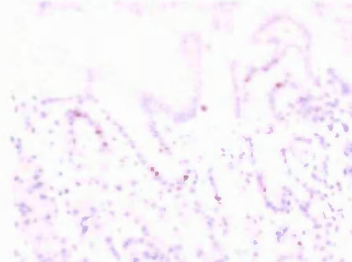
13b 1.100 Case 2 Adeno Ki-67 x25 .jpg



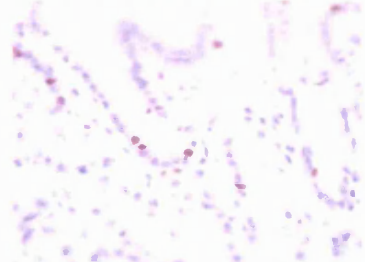
13c 1.100 Case 2 Adeno Ki-67 x40 .jpg



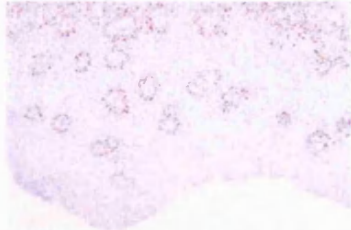
14a 1.100 Case 3 Stomach Ki-67 x10 .jpg



14b 1.100 Case 3 Stomach Ki-67 x25 .jpg



14c 1.100 Case 3 Stomach Ki-67 x40 .jpg



15a 1.100 Case 3 Normal Squamous Ki-67 x...



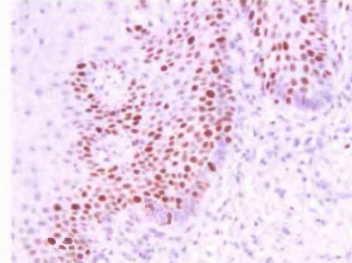
15b 1.100 Case 3 Normal Squamous Ki-67 x...



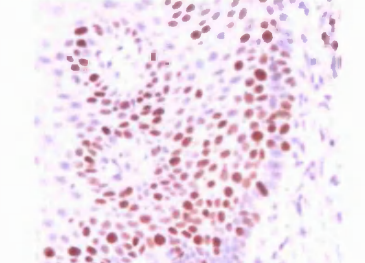
15c 1.100 Case 3 Normal Squamous Ki-67 x...



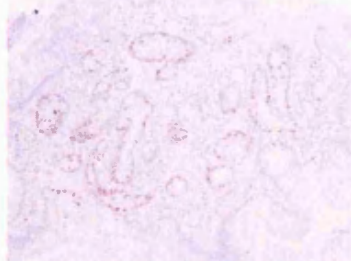
16a 1.100 Case 3 Oesophagitis Ki-67 x10 .jpg



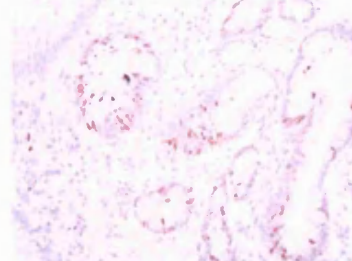
16b 1.100 Case 3 Oesophagitis Ki-67 x25 .jpg



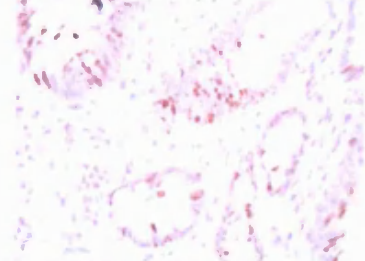
16c 1.100 Case 3 Oesophagitis Ki-67 x40 .jpg



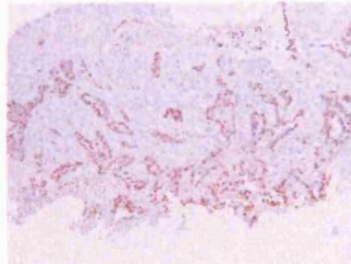
17a 1.100 Case 3 Barretts Ki-67 x10 .jpg



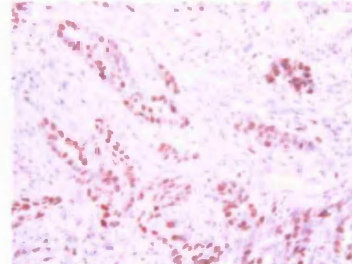
17b 1.100 Case 3 Barretts Ki-67 x25 .jpg



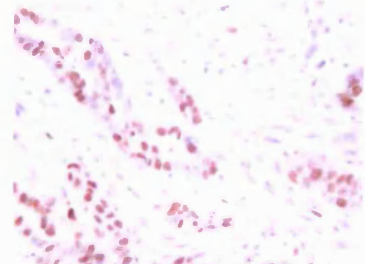
17c 1.100 Case 3 Barretts Ki-67 x40 .jpg



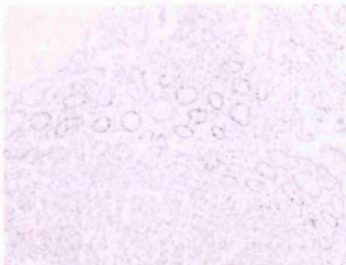
18a 1.100 Case 3 Adeno Ki-67 x10 .jpg



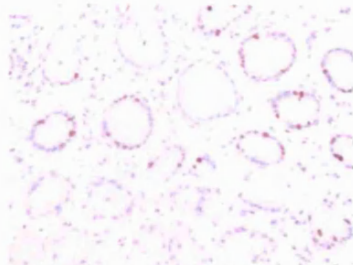
18b 1.100 Case 3 Adeno Ki-67 x25 .jpg



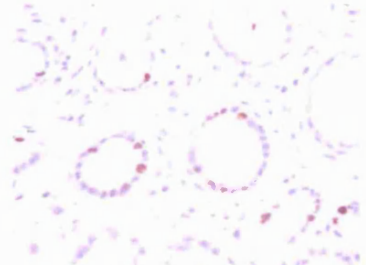
18c 1.100 Case 3 Adeno Ki-67 x40 .jpg



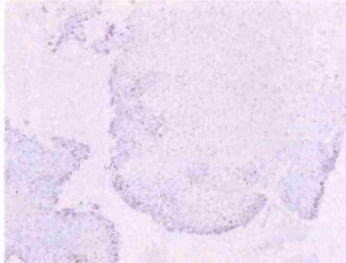
19a 1.100 Case 4 Stomach Ki-67 x10.jpg



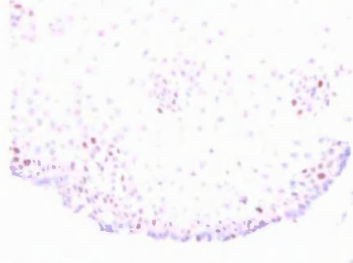
19b 1.100 Case 4 Stomach Ki-67 x25.jpg



19c 1.100 Case 4 Stomach Ki-67 x40.jpg



20a 1.100 Case 4 Norm Squamous Ki-67 x10.jpg



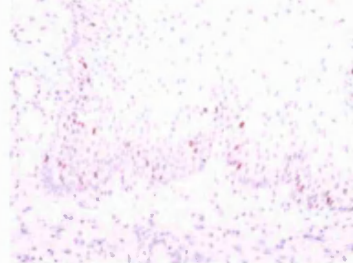
20b 1.100 Case 4 Norm Squamous Ki-67 x25.jpg



20c 1.100 Case 4 Norm Squamous Ki-67 x40.jpg



21a 1.100 Case 4 Oesophagitis Ki-67 x10.jpg



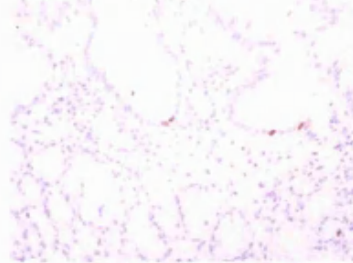
21b 1.100 Case 4 Oesophagitis Ki-67 x25.jpg



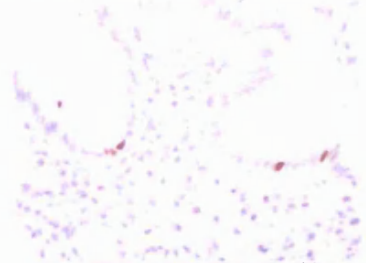
21c 1.100 Case 4 Oesophagitis Ki-67 x40.jpg



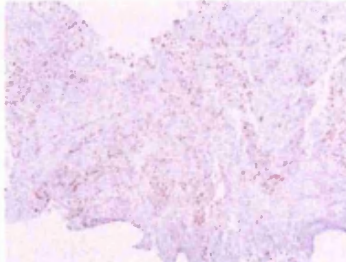
22a 1.100 Case 4 Barretts Ki-67 x10.jpg



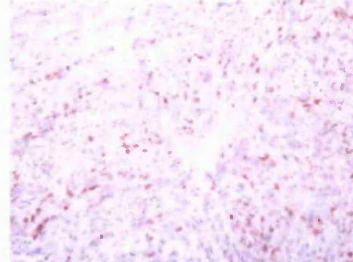
22b 1.100 Case 4 Barretts Ki-67 x25.jpg



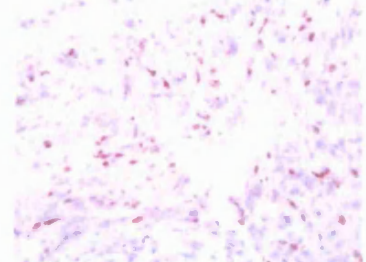
22c 1.100 Case 4 Barretts Ki-67 x40.jpg



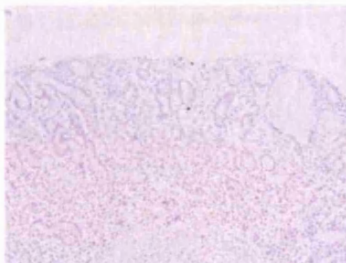
23a 1.100 Case 4 Adeno Ki-67 x10.jpg



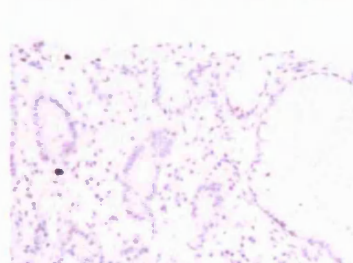
23b 1.100 Case 4 Adeno Ki-67 x25.jpg



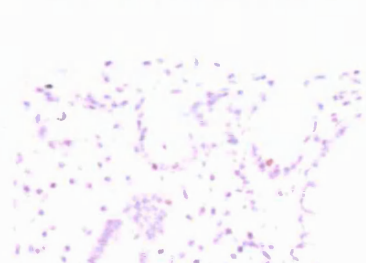
23c 1.100 Case 4 Adeno Ki-67 x40.jpg



24a 1.100 Case 5 Stomach Ki-67 x10.jpg



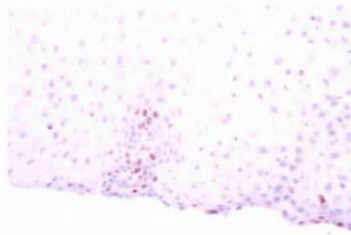
24b 1.100 Case 5 Stomach Ki-67 x25.jpg



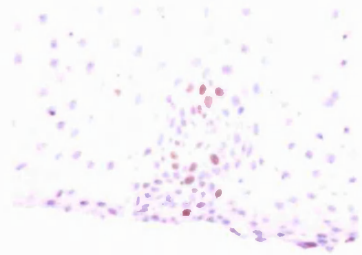
24c 1.100 Case 5 Stomach Ki-67 x40.jpg



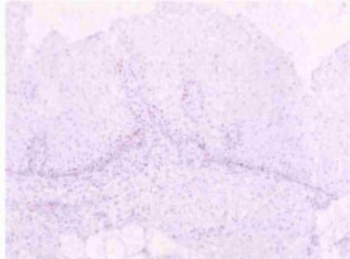
25a 1.100 Case 5 Norm Squamous Ki-67 x10...



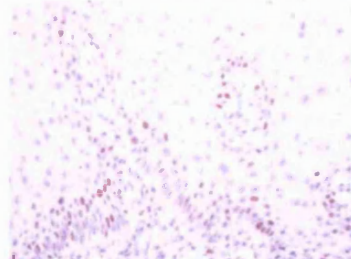
25b 1.100 Case 5 Norm Squamous Ki-67 x25 ...



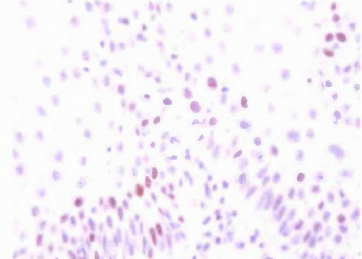
25c 1.100 Case 5 Norm Squamous Ki-67 x40...



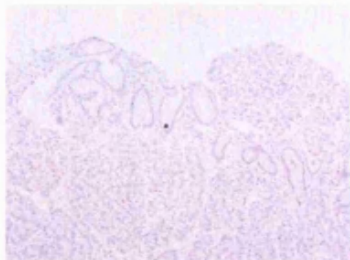
26a 1.100 Case 5 Oesophagitis Ki-67 x10 .jpg



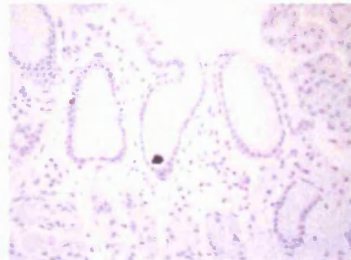
26b 1.100 Case 5 Oesophagitis Ki-67 x25 .jpg



26c 1.100 Case 5 Oesophagitis Ki-67 x40 .jpg



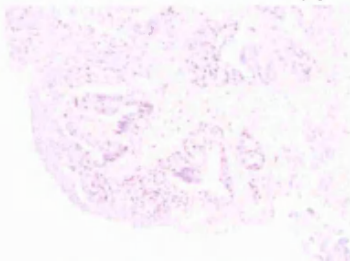
27a 1.100 Case 5 Barretts Ki-67 x10 .jpg



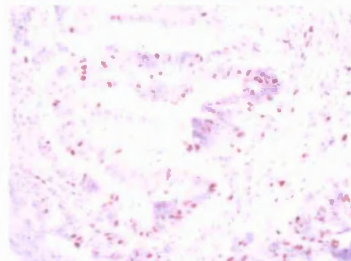
27b 1.100 Case 5 Barretts Ki-67 x25 .jpg



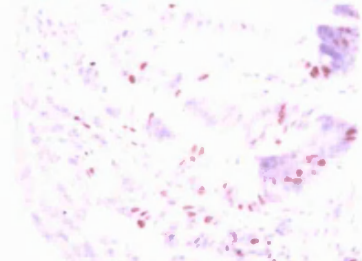
27c 1.100 Case 5 Barretts Ki-67 x40 .jpg



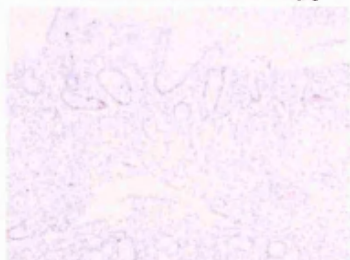
28a 1.100 Case 5 Adeno Ki-67 x10 .jpg



28b 1.100 Case 5 Adeno Ki-67 x25 .jpg



28c 1.100 Case 5 Adeno Ki-67 x40 .jpg



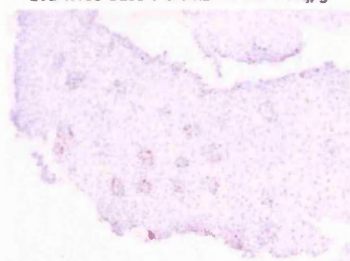
29a 1.100 Case 6 Stomach Ki-67 x10 .jpg



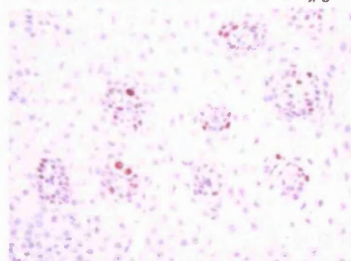
29b 1.100 Case 6 Stomach Ki-67 x25 .jpg



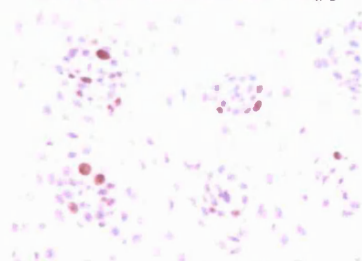
29c 1.100 Case 6 Stomach Ki-67 x40 .jpg



30a 1.100 Case 6 Norm Squamous Ki-67 x10...



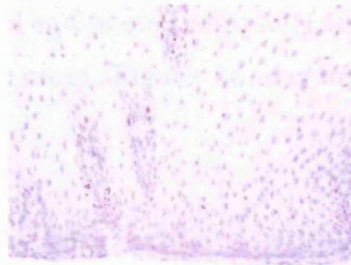
30b 1.100 Case 6 Norm Squamous Ki-67 x25 ...



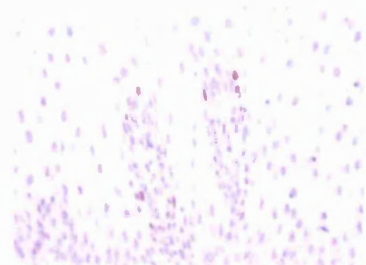
30c 1.100 Case 6 Norm Squamous Ki-67 x40...



31a 1.100 Case 6 Oesophagitis Ki-67 x10.jpg



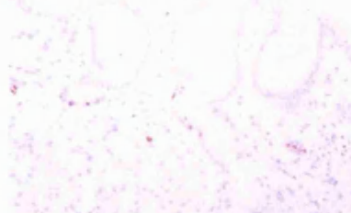
31b 1.100 Case 6 Oesophagitis Ki-67 x25.jpg



31c 1.100 Case 6 Oesophagitis Ki-67 x40.jpg



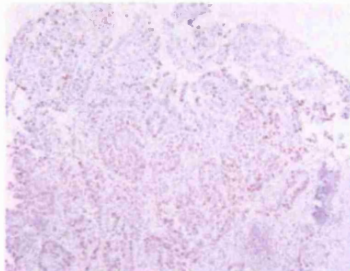
32a 1.100 Case 6 Barretts Ki-67 x10.jpg



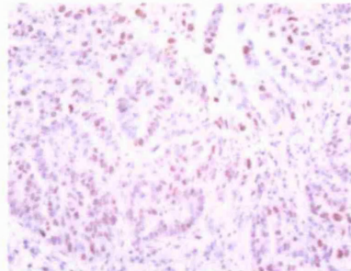
32b 1.100 Case 6 Barretts Ki-67 x25.jpg



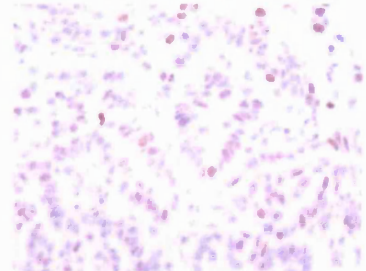
32c 1.100 Case 6 Barretts Ki-67 x40.jpg



33a 1.100 Case 6 Adeno Ki-67 x10.jpg

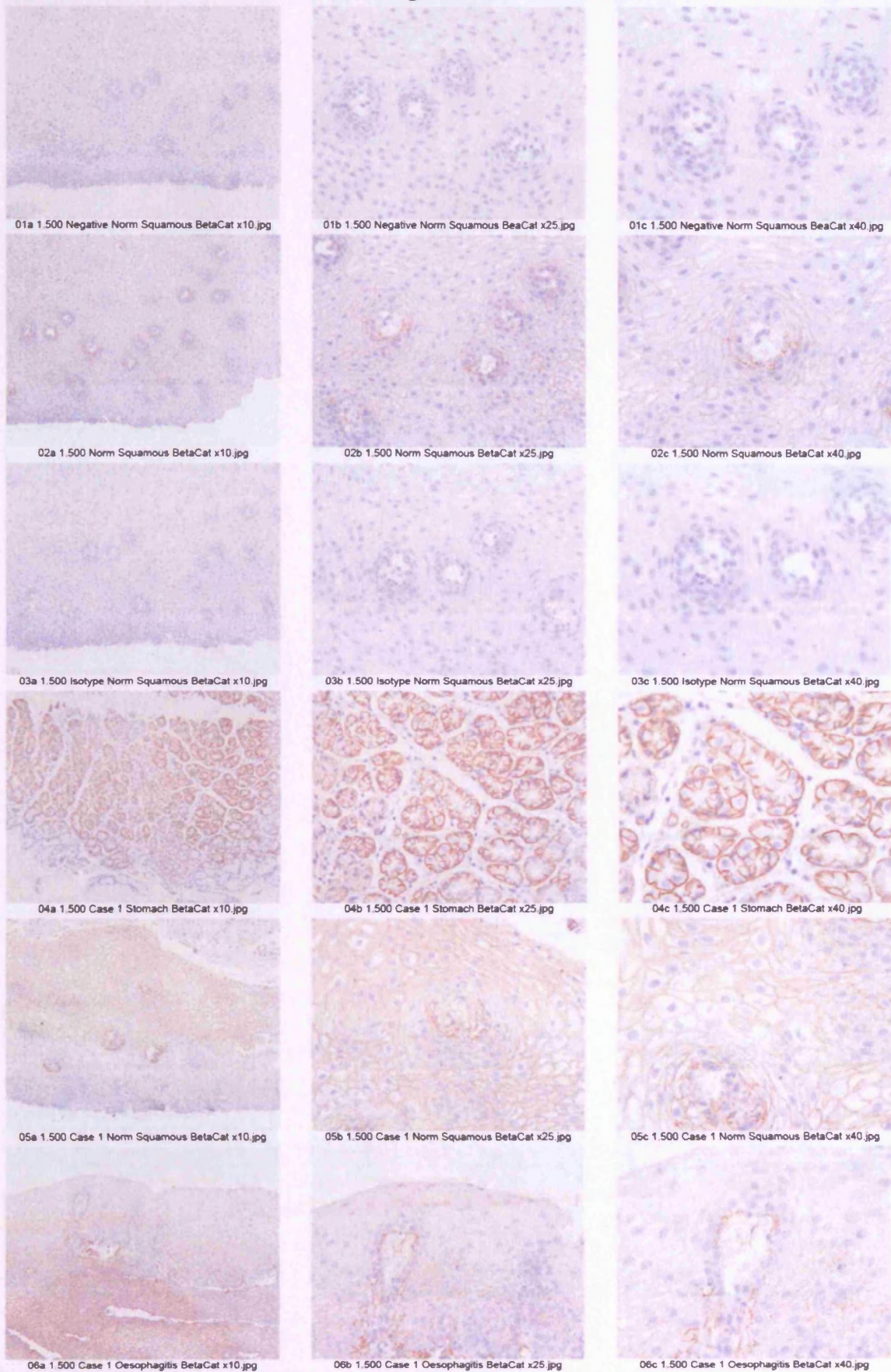


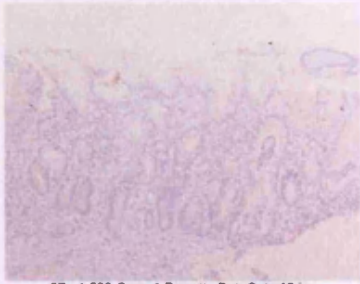
33b 1.100 Case 6 Adeno Ki-67 x25.jpg



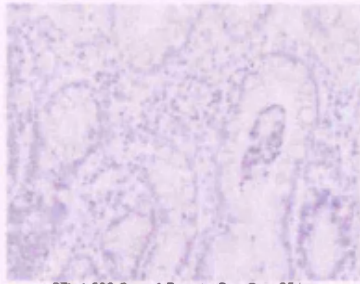
33c 1.100 Case 6 Adeno Ki-67 x40.jpg

The following contact sheets represent all six clinical cases which were analysed for  $\beta$ -catenin IHC in gastric, normal squamous, oesophagitis, BM and OA human tissue. A selection of these were utilised to create Figure 3.6, section 3.4.2.

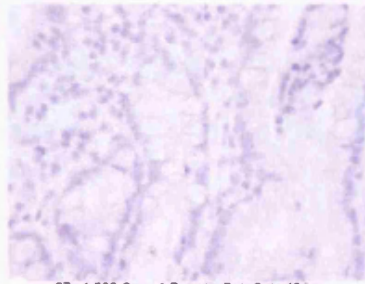




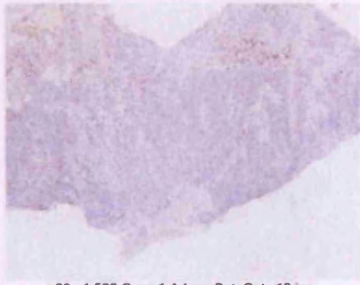
07a 1.500 Case 1 Barretts BetaCat x10.jpg



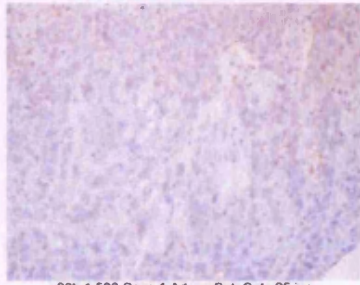
07b 1.500 Case 1 Barretts BetaCat x25.jpg



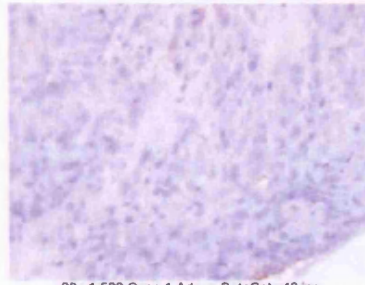
07c 1.500 Case 1 Barretts BetaCat x40.jpg



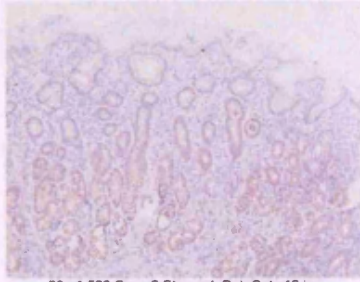
08a 1.500 Case 1 Adeno BetaCat x10.jpg



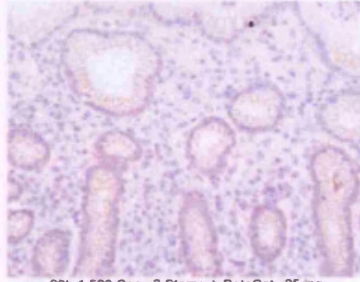
08b 1.500 Case 1 Adeno BetaCat x25.jpg



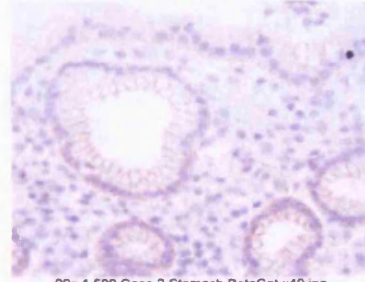
08c 1.500 Case 1 Adeno BetaCat x40.jpg



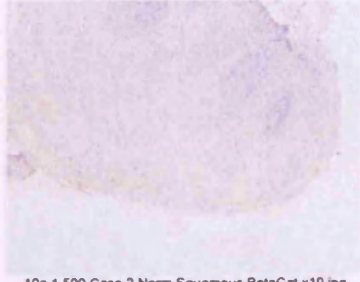
09a 1.500 Case 2 Stomach BetaCat x10.jpg



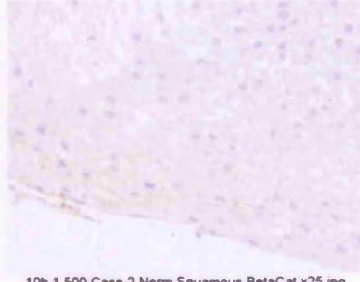
09b 1.500 Case 2 Stomach BetaCat x25.jpg



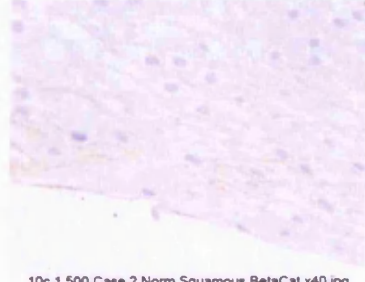
09c 1.500 Case 2 Stomach BetaCat x40.jpg



10a 1.500 Case 2 Norm Squamous BetaCat x10.jpg



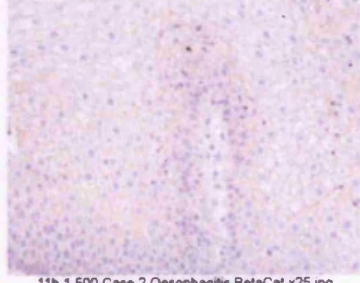
10b 1.500 Case 2 Norm Squamous BetaCat x25.jpg



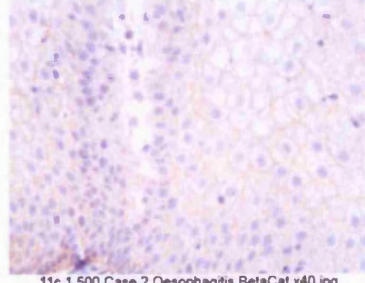
10c 1.500 Case 2 Norm Squamous BetaCat x40.jpg



11a 1.500 Case 2 Oesophagitis BetaCat x10.jpg



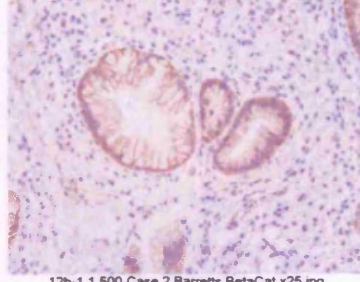
11b 1.500 Case 2 Oesophagitis BetaCat x25.jpg



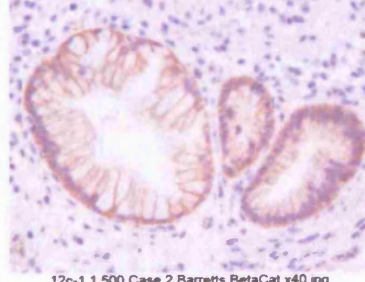
11c 1.500 Case 2 Oesophagitis BetaCat x40.jpg



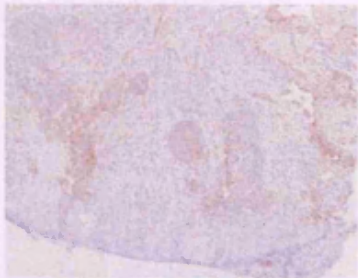
12a 1.500 Case 2 Barretts BetaCat x10.jpg



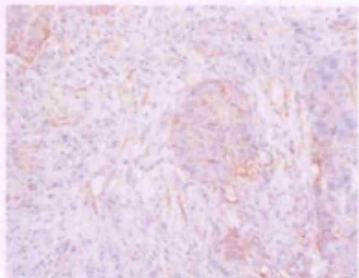
12b-1 1.500 Case 2 Barretts BetaCat x25.jpg



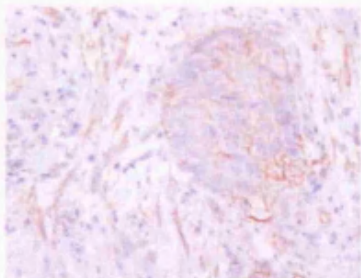
12c-1 1.500 Case 2 Barretts BetaCat x40.jpg



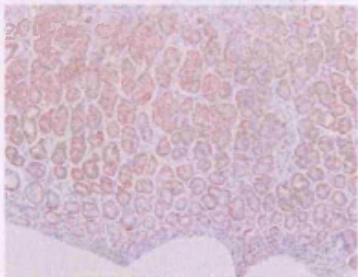
13a 1.500 Case 2 Adeno BetaCat x10.jpg



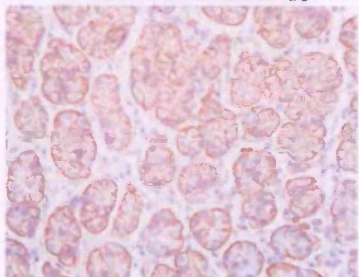
13b 1.500 Case 2 Adeno BetaCat x25.jpg



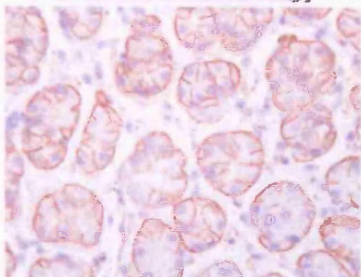
13c 1.500 Case 2 Adeno BetaCat x40.jpg



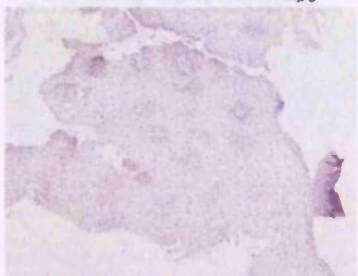
14a 1.500 Case 3 Stomach BetaCat x10.jpg



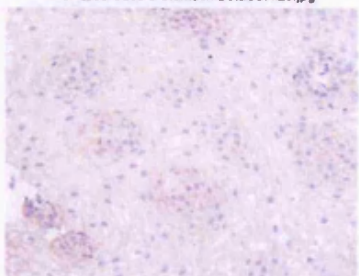
14b 1.500 Case 3 Stomach BetaCat x25.jpg



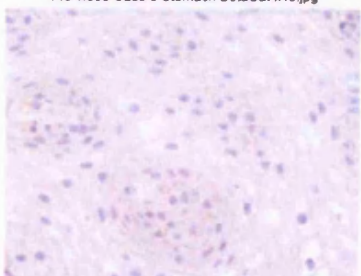
14c 1.500 Case 3 Stomach BetaCat x40.jpg



15a 1.500 Case 3 Norm Squamous BetaCat x10.jpg



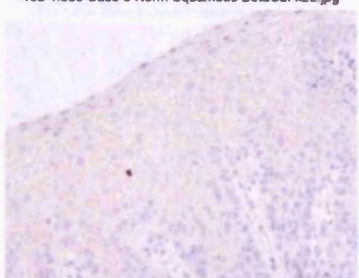
15b 1.500 Case 3 Norm Squamous BetaCat x25.jpg



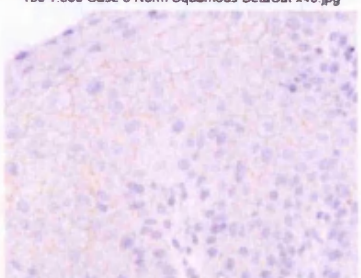
15c 1.500 Case 3 Norm Squamous BetaCat x40.jpg



16a 1.500 Case 3 Oesophagitis BetaCat x10.jpg



16b 1.500 Case 3 Oesophagitis BetaCat x25.jpg



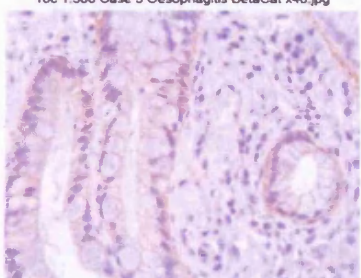
16c 1.500 Case 3 Oesophagitis BetaCat x40.jpg



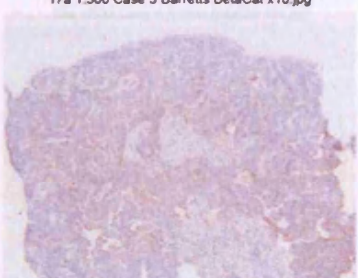
17a 1.500 Case 3 Barretts BetaCat x10.jpg



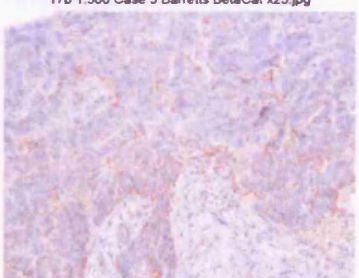
17b 1.500 Case 3 Barretts BetaCat x25.jpg



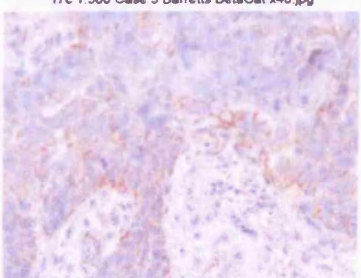
17c 1.500 Case 3 Barretts BetaCat x40.jpg



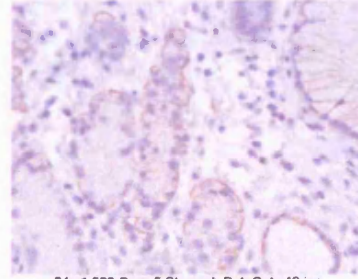
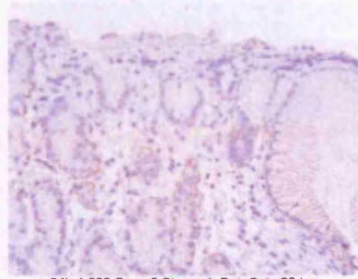
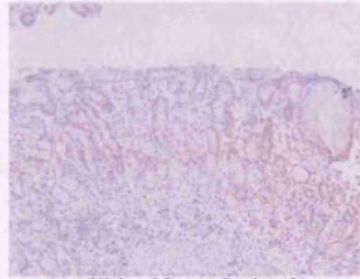
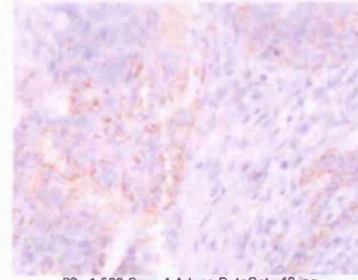
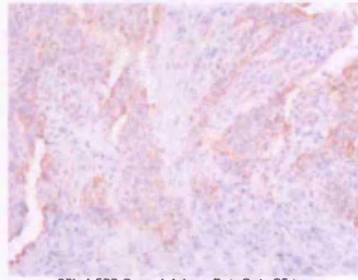
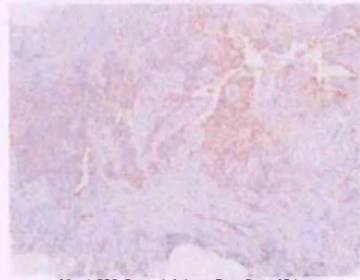
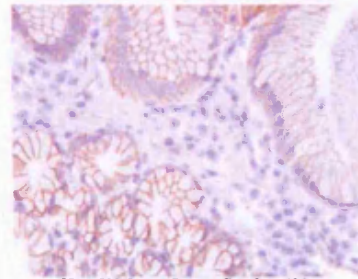
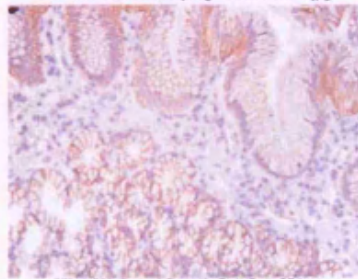
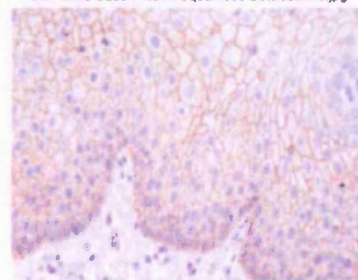
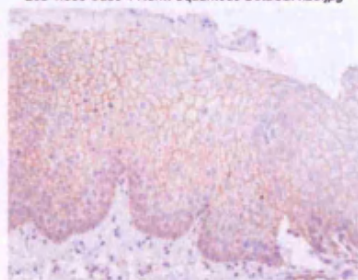
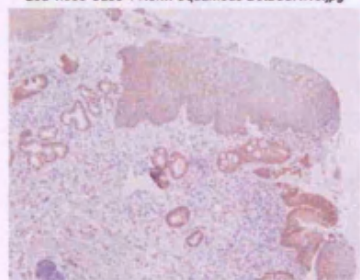
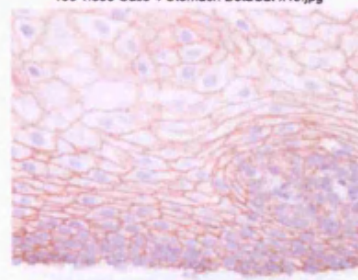
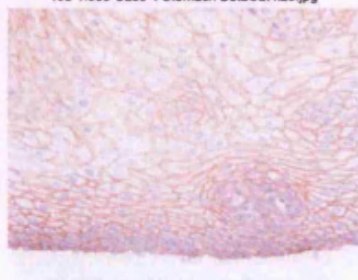
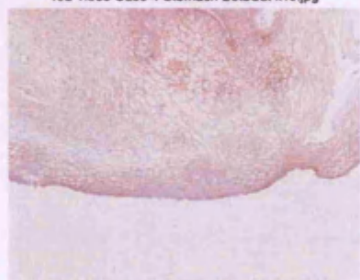
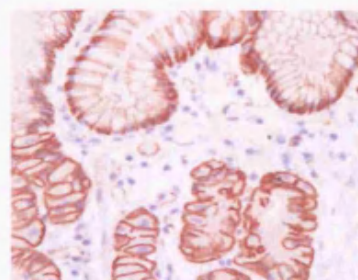
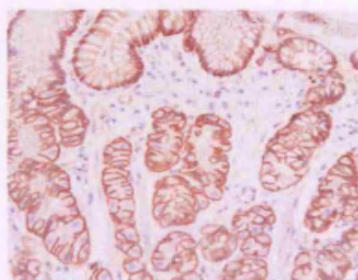
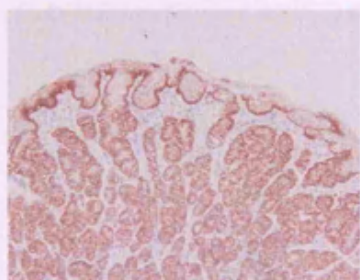
18a 1.500 Case 3 Adeno BetaCat x10.jpg



18b 1.500 Case 3 Adeno BetaCat x25.jpg



18c 1.500 Case 3 Adeno BetaCat x40.jpg

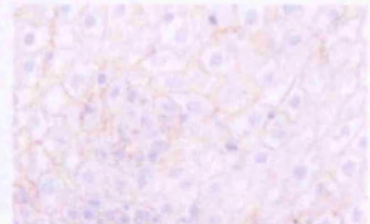




25a 1.500 Case 5 Norm Squamous BetaCat x10 .jpg



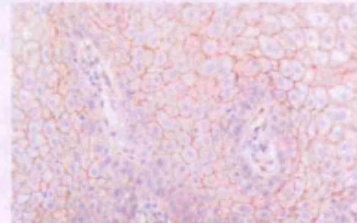
25b 1.500 Case 5 Norm Squamous BetaCat x25 .jpg



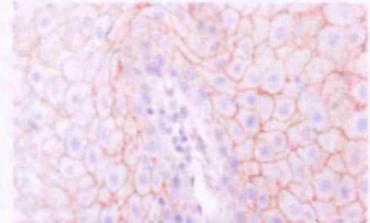
25c 1.500 Case 5 Norm Squamous BetaCat x40 .jpg



26a 1.500 Case 5 Oesophagitis BetaCat x10 .jpg



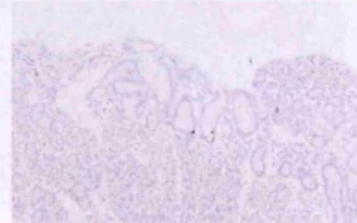
26b 1.500 Case 5 Oesophagitis BetaCat x25 .jpg



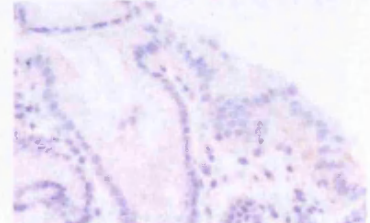
26c 1.500 Case 5 Oesophagitis BetaCat x40 .jpg



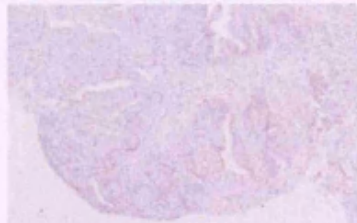
27a 1.500 Case 5 Barretts BetaCat x4 .jpg



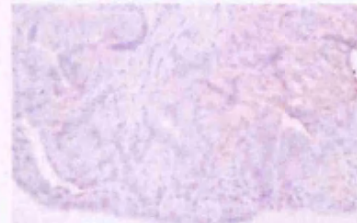
27b 1.500 Case 5 Barretts BetaCat x10 .jpg



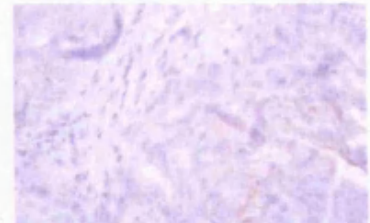
27d 1.500 Case 5 Barretts BetaCat x40 .jpg



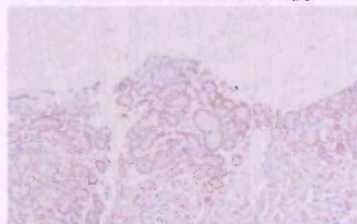
28a 1.500 Case 5 Adeno BetaCat x10 .jpg



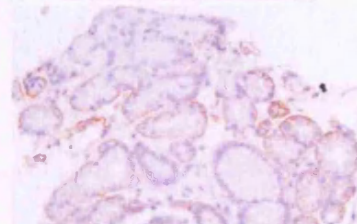
28b 1.500 Case 5 Adeno BetaCat x25 .jpg



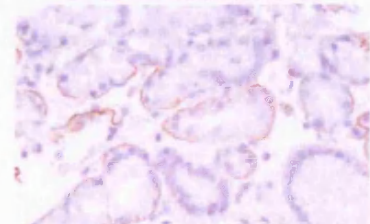
28c 1.500 Case 5 Adeno BetaCat x40 .jpg



29a 1.500 Case 6 Stomach BetaCat x10 .jpg



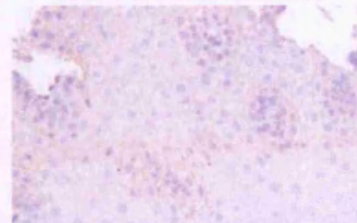
29b 1.500 Case 6 Stomach BetaCat x25 .jpg



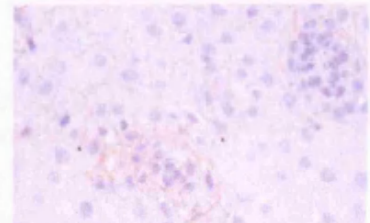
29c 1.500 Case 6 Stomach BetaCat x40 .jpg



30a 1.500 Case 6 Norm Squamous BetaCat x10 .jpg



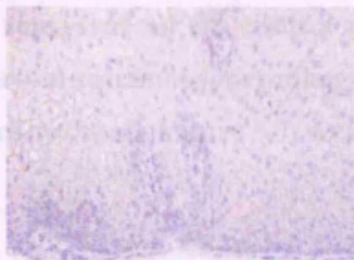
30b 1.500 Case 6 Norm Squamous BetaCat x25 .jpg



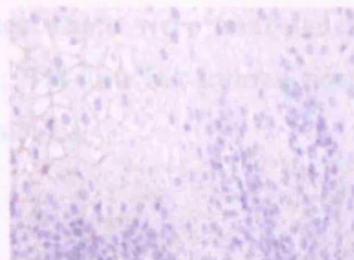
30c 1.500 Case 6 Norm Squamous BetaCat x40 .jpg



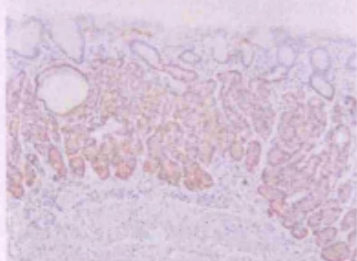
31a 1.500 Case 6 Oesophagitis BetaCat x10.jpg



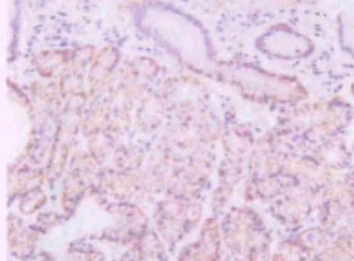
31b 1.500 Case 6 Oesophagitis BetaCat x25.jpg



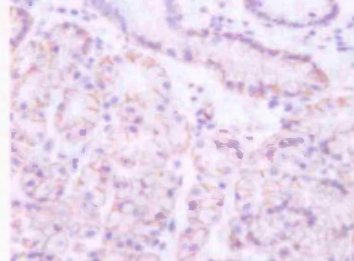
31c 1.500 Case 6 Oesophagitis BetaCat x40.jpg



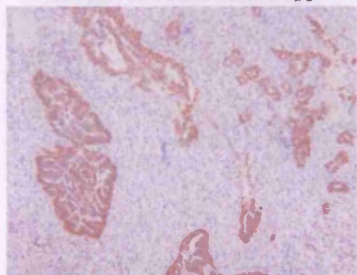
32a 1.500 Case 6 Barretts BetaCat x10.jpg



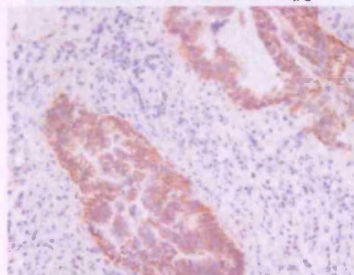
32b 1.500 Case 6 Barretts BetaCat x25.jpg



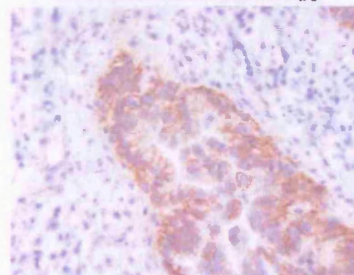
32c 1.500 Case 6 Barretts BetaCat x40.jpg



33a 1.500 Case 6 Adeno BetaCat x10.jpg

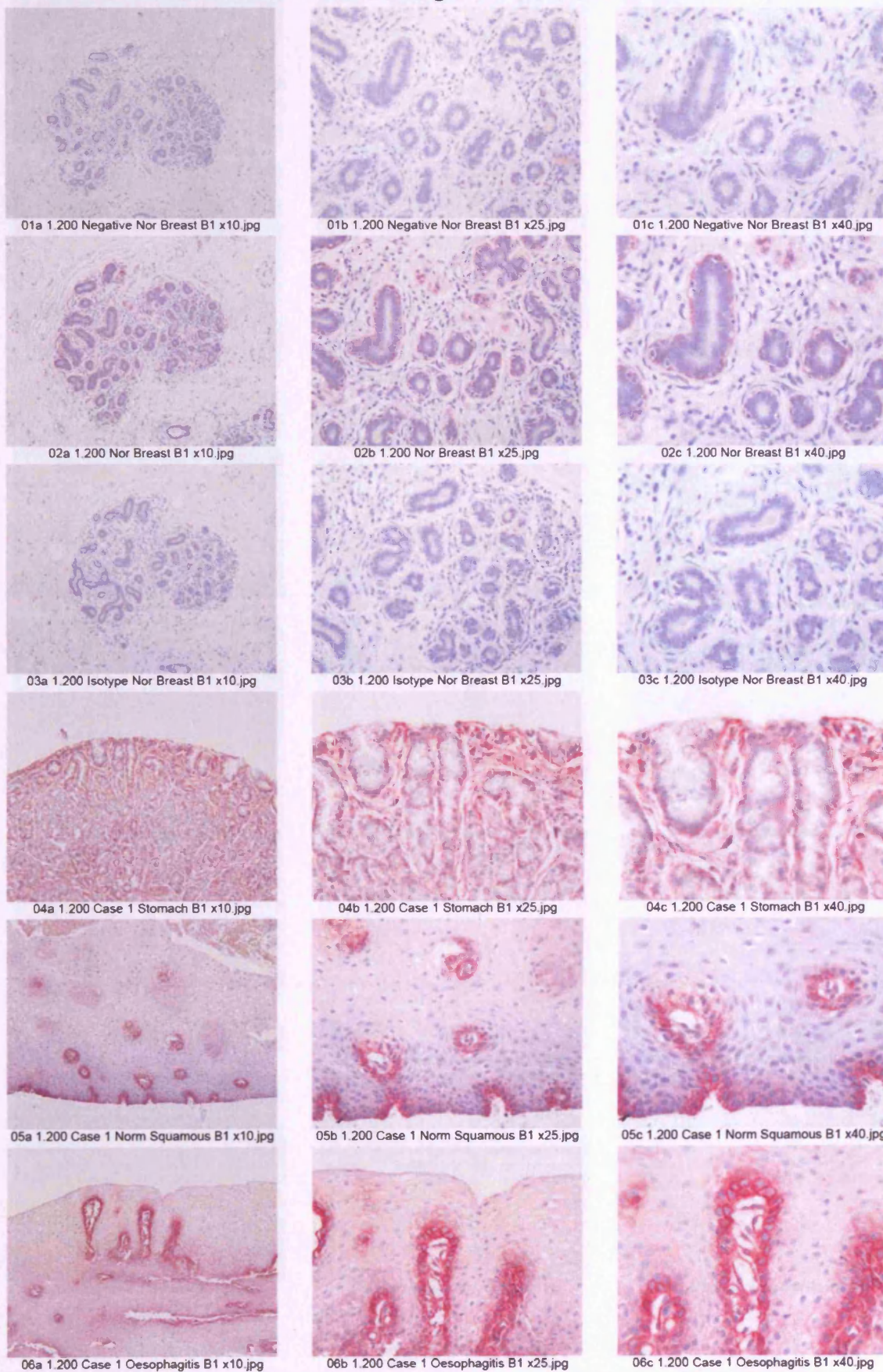


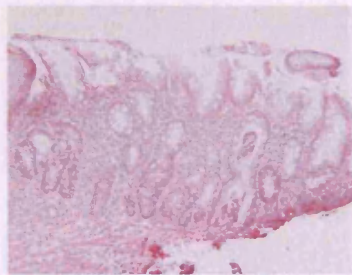
33b 1.500 Case 6 Adeno BetaCat x25.jpg



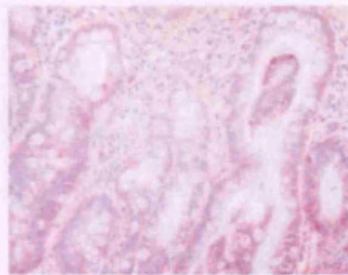
33c 1.500 Case 6 Adeno BetaCat x40.jpg

The following contact sheets represent all six clinical cases which were analysed for  $\beta$ 1-integrin IHC in gastric, normal squamous, oesophagitis, BM and OA human tissue. A selection of these were utilised to create Figure 3.7, section 3.4.2.

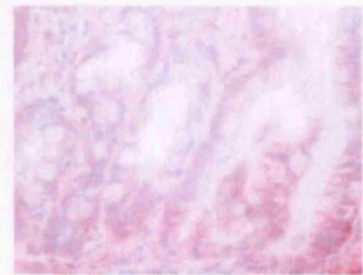




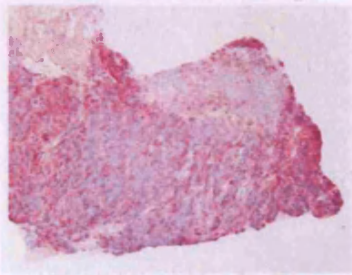
07a 1.200 Case 1 Barretts B1 x10.jpg



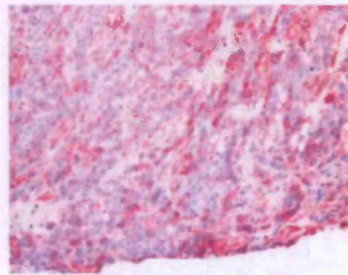
07b 1.200 Case 1 Barretts B1 x25.jpg



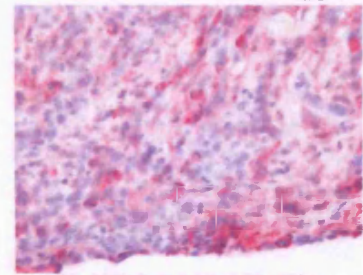
07c 1.200 Case 1 Barretts B1 x40.jpg



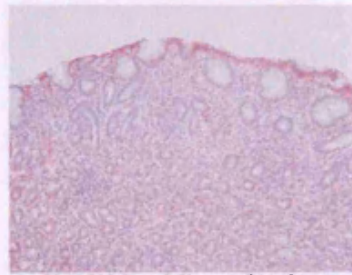
08a 1.200 Case 1 Adeno B1 x10.jpg



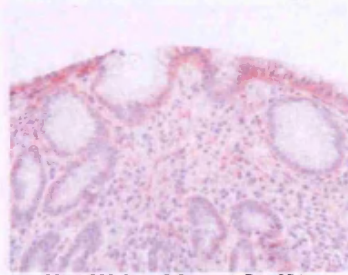
08b 1.200 Case 1 Adeno B1 x25.jpg



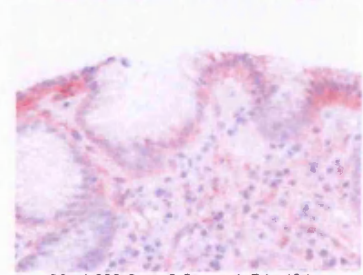
08c 1.200 Case 1 Adeno B1 x40.jpg



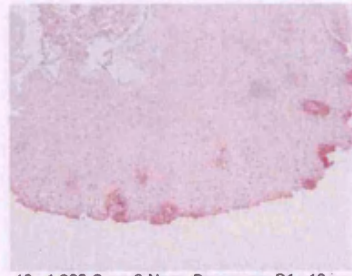
09a 1.200 Case 2 Stomach B1 x10.jpg



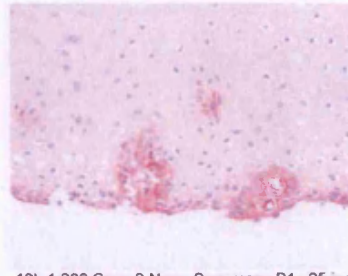
09b 1.200 Case 2 Stomach B1 x25.jpg



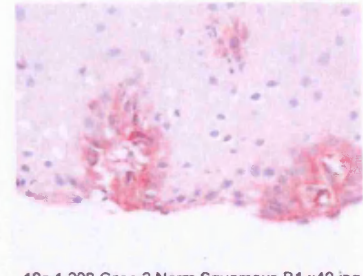
09c 1.200 Case 2 Stomach B1 x40.jpg



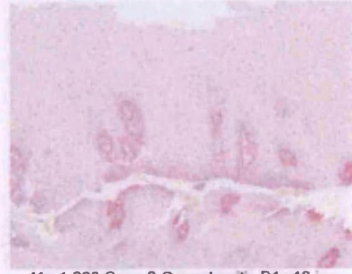
10a 1.200 Case 2 Norm Squamous B1 x10.jpg



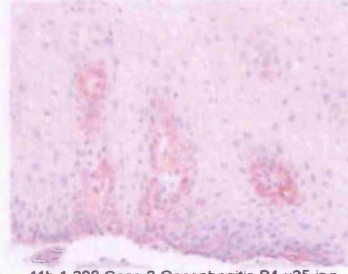
10b 1.200 Case 2 Norm Squamous B1 x25.jpg



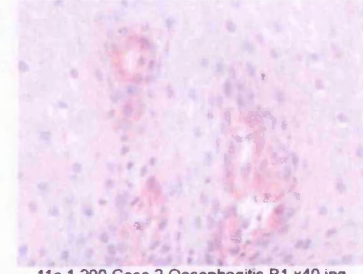
10c 1.200 Case 2 Norm Squamous B1 x40.jpg



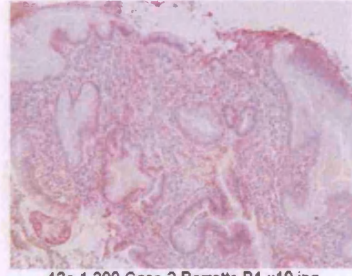
11a 1.200 Case 2 Oesophagitis B1 x10.jpg



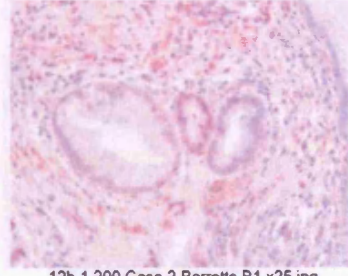
11b 1.200 Case 2 Oesophagitis B1 x25.jpg



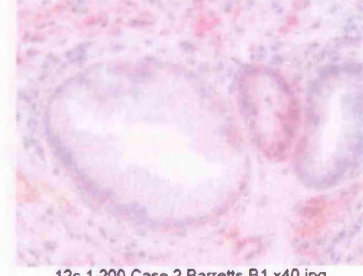
11c 1.200 Case 2 Oesophagitis B1 x40.jpg



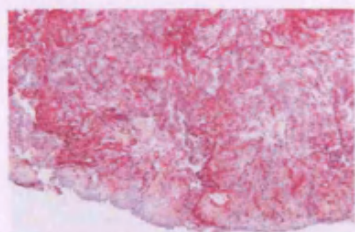
12a 1.200 Case 2 Barretts B1 x10.jpg



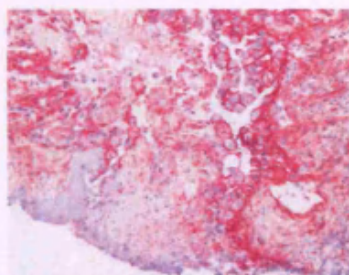
12b 1.200 Case 2 Barretts B1 x25.jpg



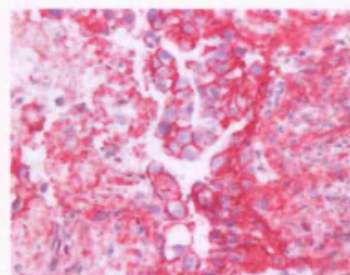
12c 1.200 Case 2 Barretts B1 x40.jpg



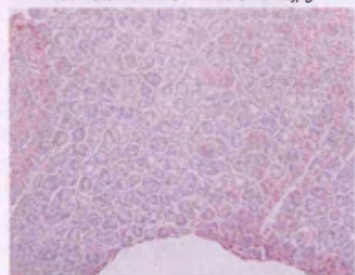
13a 1.200 Case 2 Adeno B1 x10.jpg



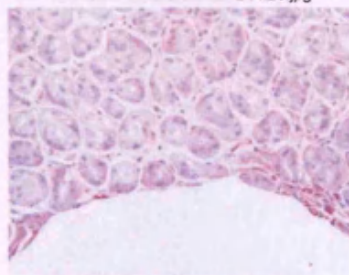
13b 1.200 Case 2 Adeno B1 x25.jpg



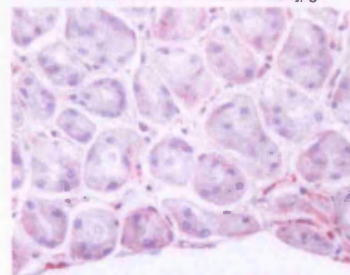
13c 1.200 Case 2 Adeno B1 x40.jpg



14a 1.200 Case 3 Stomach B1 x10.jpg



14b 1.200 Case 3 Stomach B1 x25.jpg



14c 1.200 Case 3 Stomach B1 x40.jpg



15a 1.200 Case 3 Norm Squamous B1 x10.jpg



15b 1.200 Case 3 Norm Squamous B1 x25.jpg



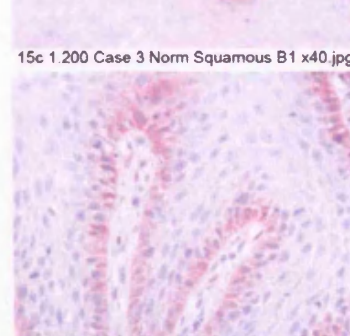
15c 1.200 Case 3 Norm Squamous B1 x40.jpg



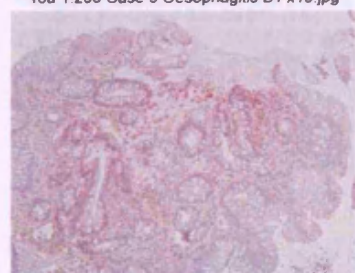
16a 1.200 Case 3 Oesophagitis B1 x10.jpg



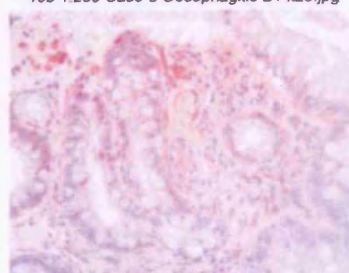
16b 1.200 Case 3 Oesophagitis B1 x25.jpg



16c 1.200 Case 3 Oesophagitis B1 x40.jpg



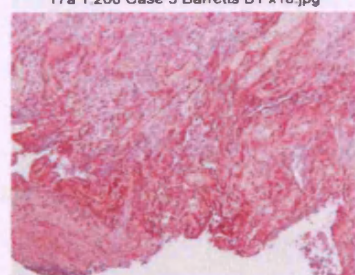
17a 1.200 Case 3 Barretts B1 x10.jpg



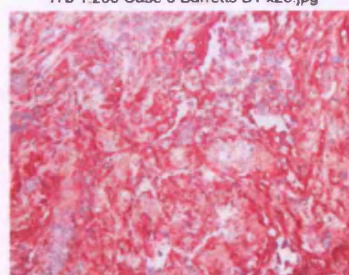
17b 1.200 Case 3 Barretts B1 x25.jpg



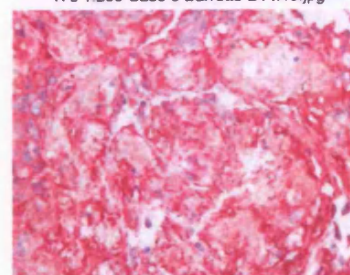
17c 1.200 Case 3 Barretts B1 x40.jpg



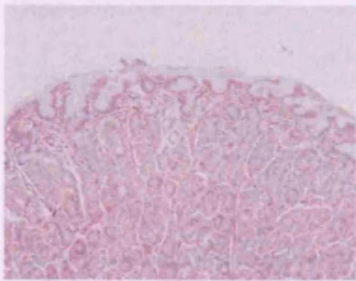
18a 1.200 Case 3 Adeno B1 x10.jpg



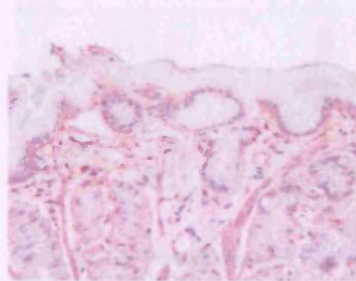
18b 1.200 Case 3 Adeno B1 x25.jpg



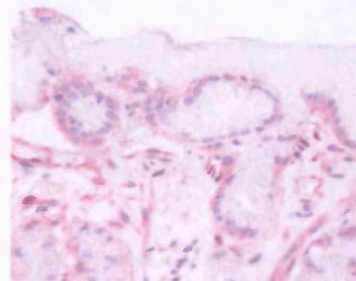
18c 1.200 Case 3 Adeno B1 x40.jpg



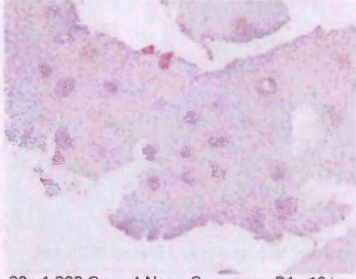
19a 1.200 Case 4 Stomach B1 x10.jpg



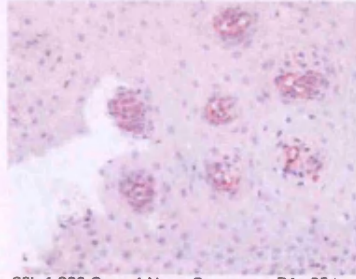
19b 1.200 Case 4 Stomach B1 x25.jpg



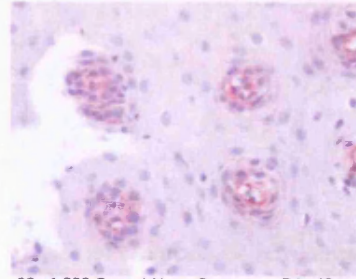
19c 1.200 Case 4 Stomach B1 x40.jpg



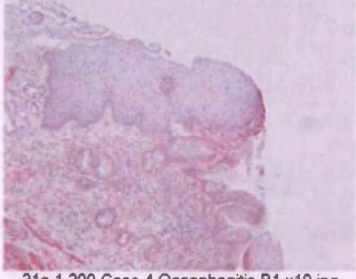
20a 1.200 Case 4 Norm Squamous B1 x10.jpg



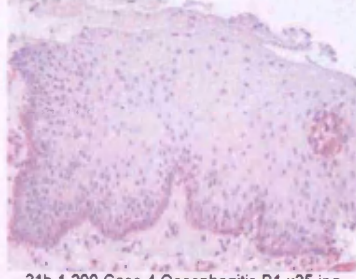
20b 1.200 Case 4 Norm Squamous B1 x25.jpg



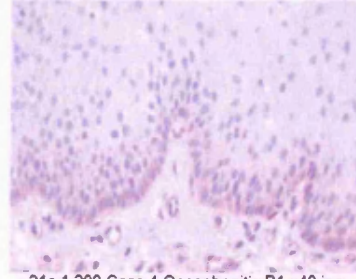
20c 1.200 Case 4 Norm Squamous B1 x40.jpg



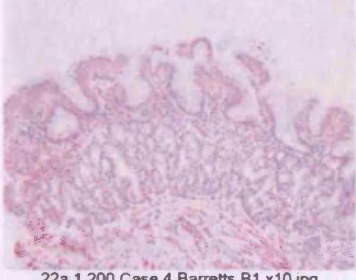
21a 1.200 Case 4 Oesophagitis B1 x10.jpg



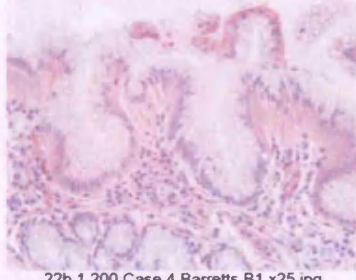
21b 1.200 Case 4 Oesophagitis B1 x25.jpg



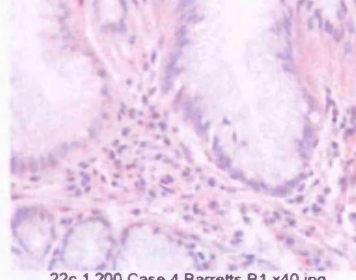
21c 1.200 Case 4 Oesophagitis B1 x40.jpg



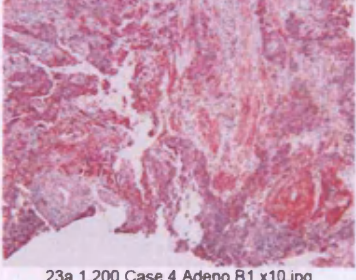
22a 1.200 Case 4 Barretts B1 x10.jpg



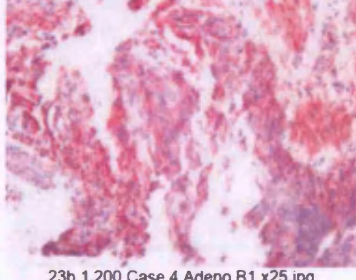
22b 1.200 Case 4 Barretts B1 x25.jpg



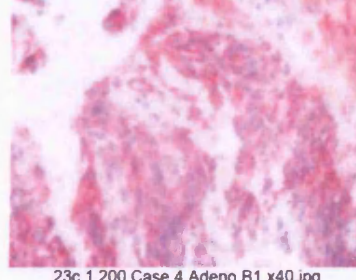
22c 1.200 Case 4 Barretts B1 x40.jpg



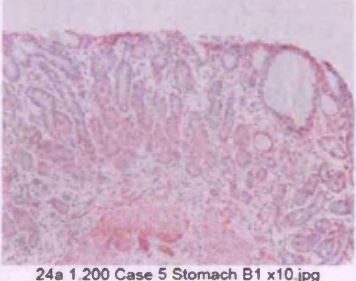
23a 1.200 Case 4 Adeno B1 x10.jpg



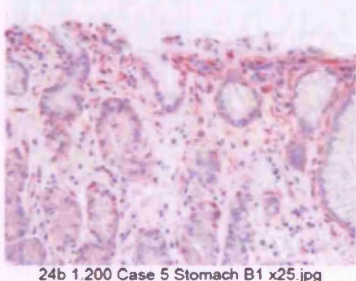
23b 1.200 Case 4 Adeno B1 x25.jpg



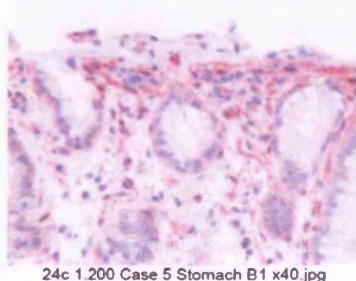
23c 1.200 Case 4 Adeno B1 x40.jpg



24a 1.200 Case 5 Stomach B1 x10.jpg



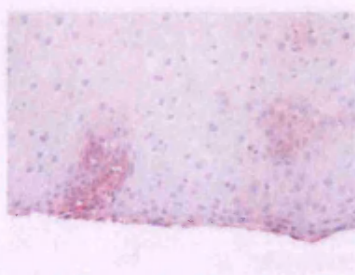
24b 1.200 Case 5 Stomach B1 x25.jpg



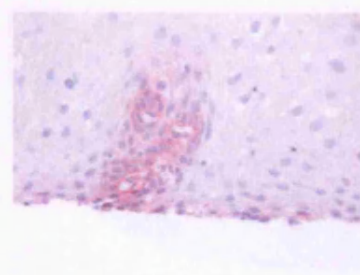
24c 1.200 Case 5 Stomach B1 x40.jpg



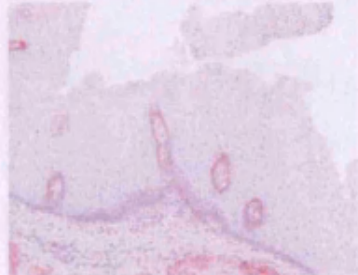
25a 1.200 Case 5 Norm Squamous B1 x10 .jpg



25b 1.200 Case 5 Norm Squamous B1 x25 .jpg



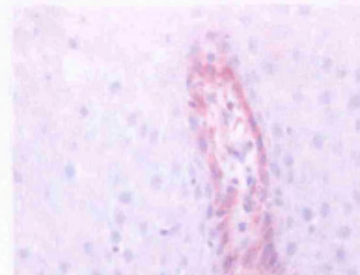
25c 1.200 Case 5 Norm Squamous B1 x40 .jpg



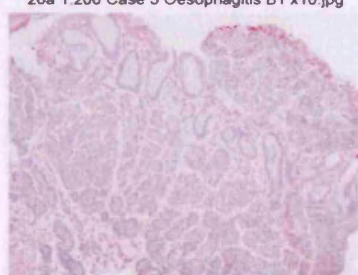
26a 1.200 Case 5 Oesophagitis B1 x10 .jpg



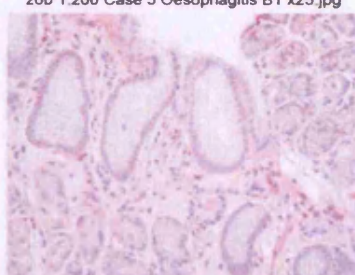
26b 1.200 Case 5 Oesophagitis B1 x25 .jpg



26c 1.200 Case 5 Oesophagitis B1 x40 .jpg



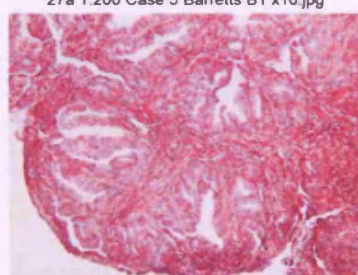
27a 1.200 Case 5 Barretts B1 x10 .jpg



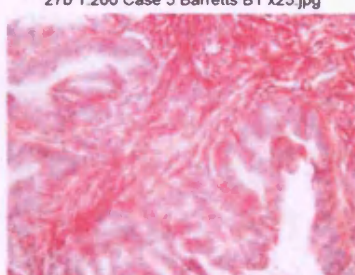
27b 1.200 Case 5 Barretts B1 x25 .jpg



27c 1.200 Case 5 Barretts B1 x40 .jpg



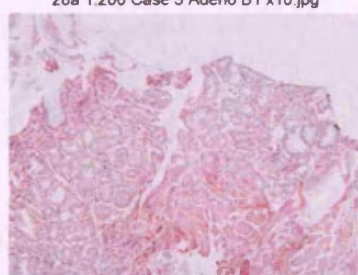
28a 1.200 Case 5 Adeno B1 x10 .jpg



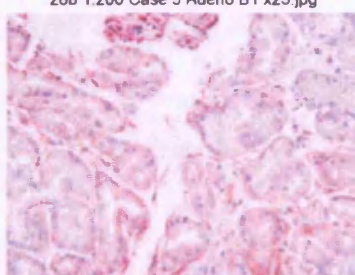
28b 1.200 Case 5 Adeno B1 x25 .jpg



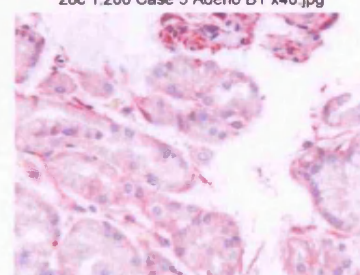
28c 1.200 Case 5 Adeno B1 x40 .jpg



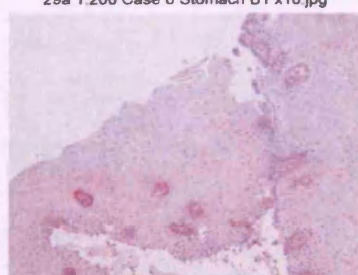
29a 1.200 Case 6 Stomach B1 x10 .jpg



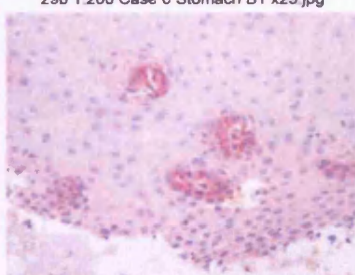
29b 1.200 Case 6 Stomach B1 x25 .jpg



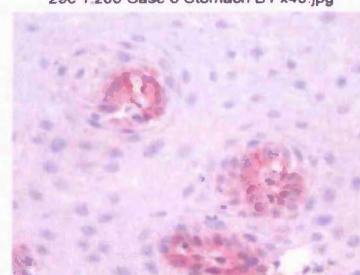
29c 1.200 Case 6 Stomach B1 x40 .jpg



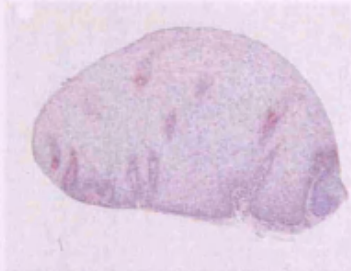
30a 1.200 Case 6 Norm Squamous B1 x10 .jpg



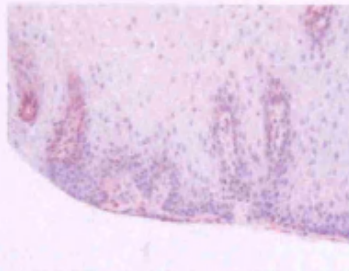
30b 1.200 Case 6 Norm Squamous B1 x25 .jpg



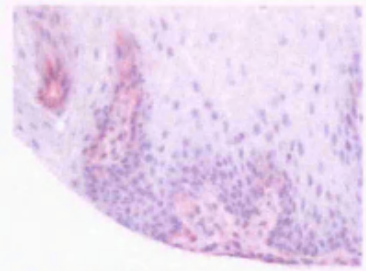
30c 1.200 Case 6 Norm Squamous B1 x40 .jpg



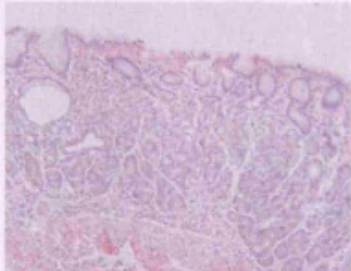
31a 1.200 Case 6 Oesophagitis B1 x10.jpg



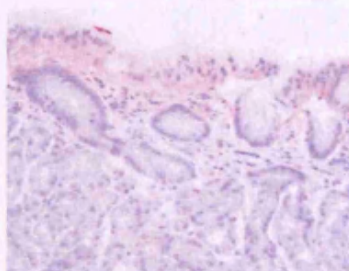
31b 1.200 Case 6 Oesophagitis B1 x25.jpg



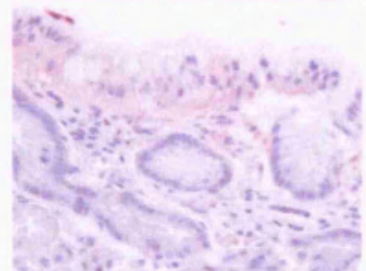
31c 1.200 Case 6 Oesophagitis B1 x40.jpg



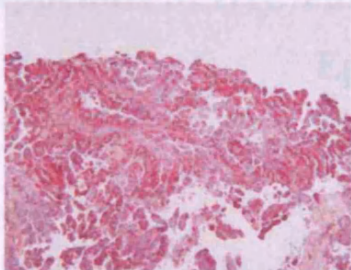
32a 1.200 Case 6 Barretts B1 x10.jpg



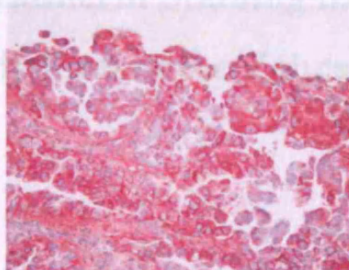
32b 1.200 Case 6 Barretts B1 x25.jpg



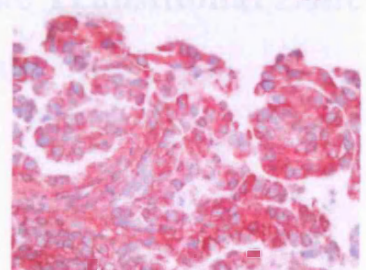
32c 1.200 Case 6 Barretts B1 x40.jpg



33a 1.200 Case 6 Adeno B1 x10.jpg



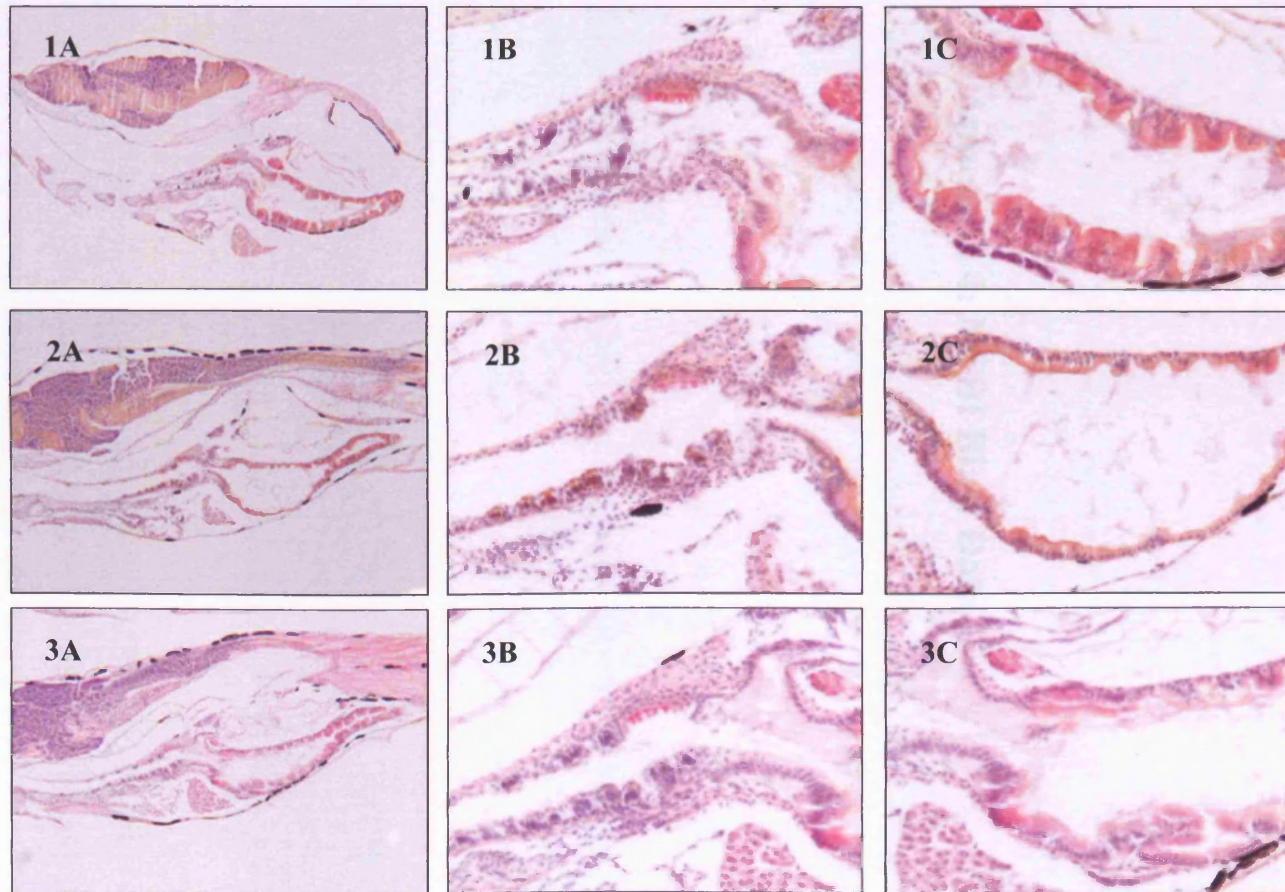
33b 1.200 Case 6 Adeno B1 x25.jpg



33c 1.200 Case 6 Adeno B1 x40.jpg

**Appendix 3: IHC Pan-cadherin Staining in the Transitional Zone  
Epithelium in the Zebrafish**

The following figure details the IHC Pan-cadherin staining in the transitional zone epithelium in the zebrafish, where 1A-C represents the control animal, 2A-C represents the 10 $\mu$ M DCA treated animal and 3A-C represents the 100 $\mu$ M DCA treated animal, each at increased magnification. This information was utilised in section 4.4.2.4 in this works main body of text.



## **Appendix 4: NCBI Blast Data**

The following NCBI blast represents the plot obtained when sequencing into the promoter, bases 398 to 632 of the sequencing plot aligned to bases 464 to 230 of the rat L-FABP sequence. This information was utilised in section 5.4.1 in this works main body of text.

```
>  gi|204085|gb|M13501.1|RATFABPLG G Rat L-FABP gene encoding liver fatty acid binding protein, complete cds
Length=4637

Score = 418 bits (211), Expect = 9e-114
Identities = 227/235 (96%), Gaps = 0/235 (0%)
Strand=Plus/Minus

Query 398 AAATCAGAATGGGCAAGGCAGAAGTTTGTCTAATTCAGCAAACATTAGTGAGTCCAATC 457
          |||
Sbjct 464 AAATCAGAATGGGCAAGGCAGAAGTTTGTCTAATTCAGCAAACATTAGTGAGTCCAATC 405

Query 458 AAGGGCAAAGCTCTCTGTAATGGTGCAATTTTGGTGTCTTATCACCGCTCATGAANTAN 517
          |||
Sbjct 404 AAGGGCAAAGCTCTCTGTAATGGTGCAATTTTGGTGTCTTATCACCGCTCATGAATAA 345

Query 518 NAGTGCATACNTGANATGTATGTTGACAGATGTATATATGTGCAACAGACATGTNAATCA 577
          |||
Sbjct 344 GAGTGCATACATGAAATGTATGTTGACAGATGTATATATGTGCAACAGACATGTGAATCA 285

Query 578 CATCTCTANCAATGCATACATGCATATATACCTATGTGTACNTATGTATGTGTTT 632
          |||
Sbjct 284 CATCTCTAGCAATGCATACATGCATATATACCTATGTGTACATATGTATGTGTTT 230
```

The following NCBI blast represents the plot obtained when sequencing into the first part of the vector, bases 45 to 139 of the sequencing plot aligned to bases 3062 to 3156 in the mouse mRNA for P-cadherin. This information was utilised in section 5.4.1 in this works main body of text.

```
>  gi|50267|emb|X06340.1|MMCADHP    Mouse mRNA for P-cadherin
Length=3187

Score = 147 bits (74), Expect = 1e-32
Identities = 95/95 (100%), Gaps = 0/95 (0%)
Strand=Plus/Plus

Query 45 AAIACTGAGTATATCTAAGTTGICTCGTAnnnnnnnAATTTCCCTGTTATGTGCTGTAGA 104
          |||
Sbjct 3062 AAIACTGAGTATATCTAAGTTGICTCGTATTTTTTATTTTCCCTGTTATGTGCTGTAGA 3121

Query 105 TGGAGAGTGATGACAATCGTGTAAATGTAAGTAGAA 139
          |||
Sbjct 3122 TGGAGAGTGATGACAATCGTGTAAATGTAAGTAGAA 3156
```

The following NCBI blast represents the plot obtained when sequencing into the second part of the vector, bases 174 to 1039 of the sequencing plot aligned to bases 700 to 1565 of the pBluescript cloning vector sequence. This information was utilised in section 5.4.1 in this works main body of text.

```
>  gi|58063|emb|X52328.1|ARBL29KF pBluescript II SK(+) vector DNA, phagemid excised from lambda ZAPII
Length=2961
```

```
Score = 1515 bits (764), Expect = 0.0
Identities = 843/870 (96%), Gaps = 8/870 (0%)
Strand=Plus/Plus
```

```
Query 174 CGAATTCCTGCAGCCCGGGGATCGATCCACTAGTTC TAGAGCGGCCGCCACCGCGGTGG 233
          |||
Sbjct 700 CGAATTCCTGCAGCCCGGGGATC----CACTAGTTC TAGAGCGGCCGCCACCGCGGTGG 755

Query 234 AGCTCCAGCTTTTGTCCCTTTAGTGAGGGTTAATTGCGCGCTTGCGTAATCATGGTCA 293
          |||
Sbjct 756 AGCTCCAGCTTTTGTCCCTTTAGTGAGGGTTAATTGCGCGCTTGCGTAATCATGGTCA 815

Query 294 TAGTGTTTCTGTGTGAAATTGTTATCCGCTCACAAATCCACACAACATACGAGCCGGA 353
          |||
Sbjct 816 TAGTGTTTCTGTGTGAAATTGTTATCCGCTCACAAATCCACACAACATACGAGCCGGA 875

Query 354 AGCATAAAGTGTAAAGCCTGGGGTGCCTAATGAGTGAGCTAACTCACATTAATTGCGTTG 413
          |||
Sbjct 876 AGCATAAAGTGTAAAGCCTGGGGTGCCTAATGAGTGAGCTAACTCACATTAATTGCGTTG 935

Query 414 CGCTCACTGCCCGCTTTCAGTCGGGAAACCTGTCGTGCCAGCTGCATTAATGAATCGGC 473
          |||
Sbjct 936 CGCTCACTGCCCGCTTTCAGTCGGGAAACCTGTCGTGCCAGCTGCATTAATGAATCGGC 995

Query 474 CAACGCGCGGGGAGAGGCGGTTTTCGTATTGGGCGCTCTCCGCTTCTCGCTCACTGAC 533
          |||
Sbjct 996 CAACGCGCGGGGAGAGGCGGTTTTCGTATTGGGCGCTCTCCGCTTCTCGCTCACTGAC 1055

Query 534 TCGCTGCGCTCGGTGTTTCGGCTGCGGCGAGCGGTATCAGCTCACTCAAAGGCGTAATA 593
          |||
Sbjct 1056 TCGCTGCGCTCGGTGTTTCGGCTGCGGCGAGCGGTATCAGCTCACTCAAAGGCGTAATA 1115

Query 594 CGGTTATCCACAGAATCAGGGGATAACCGCAGGAAAGAACATGTGAGCAAAGGCCAGCAA 653
          |||
Sbjct 1116 CGGTTATCCACAGAATCAGGGGATAACCGCAGGAAAGAACATGTGAGCAAAGGCCAGCAA 1175

Query 654 AAGGCCAGGAACCGTAAAAAGGCCGCTTGTGCGGTTTTTCCATAGGCTCCGCCCCCT 713
          |||
Sbjct 1176 AAGGCCAGGAACCGTAAAAAGGCCGCTTGTGCGGTTTTTCCATAGGCTCCGCCCCCT 1235

Query 714 GACGAGCATCACAAAATCGACGCTCAAGTCAGAGGTGGCGAAACCCGACAGGACTATAA 773
          |||
Sbjct 1236 GACGAGCATCACAAAATCGACGCTCAAGTCAGAGGTGGCGAAACCCGACAGGACTATAA 1295

Query 774 AGATAACGAGCGTTTTCCCTGNAAGCTCCCTCGTGCCTCTCCTGTTCCGACCCCTGCCG 833
          |||
Sbjct 1296 AGATAACGAGCGTTTTCCCTGGAAGCTCCCTCGTGCCTCTCCTGTTCCGACCCCTGCCG 1355

Query 834 CTTACCGGATACCTGTCCGCTTTCTCCCTTCGGGAAGCGI-MNGCTTTCTCATAGCTCA 892
          |||
Sbjct 1356 CTTACCGGATACCTGTCCGCTTTCTCCCTTCGGGAAGCGTGGCGCTTTCTCATAGCTCA 1415

Query 893 CGCTGTAGGTATCTCAGTTCGGGT-MNCGTTCGCTCCAAGCTGGGCTGTGNGCACGAA 951
          |||
Sbjct 1416 CGCTGTAGGTATCTCAGTTCGGGTGGTTCGCTCCAAGCTGGGCTGTGNGCACGAA 1475

Query 952 CCCCCGTTTCAGCCCGACCGCTGCGMCTTATCCGGT-ANTATCGTCTTGAGTCC-ACCCN 1009
          |||
Sbjct 1476 CCCCCGTTTCAGCCCGACCGCTGCGMCTTATCCGGTAACTATCGTCTTGAGTCCAAACCCG 1535

Query 1010 GTAAGANNCNACTTATCNCNCNGGAGCA 1039
          |||
Sbjct 1536 GTAAGACACGACTTATCGCCACTGGCAGCA 1565
```

The following NCBI blast represents the plot obtained when sequencing into the FABP promoter region, bases 25 to 1005 of the sequencing plot aligned to bases 5 to 983 of the mouse mRNA for P-cadherin sequence. This information was utilised in section 5.4.1 in this works main body of text.

```
>  gi|50267|emb|X06340.1|MMCADHF    Mouse mRNA for P-cadherin
Length=3187

Score = 1871 bits (944), Expect = 0.0
Identities = 972/981 (99%), Gaps = 2/981 (0%)
Strand=Plus/Plus

Query 25      CGCGCCCCNCCGTCGCGGCAGCCTTCTCACCTCCCTTCAGTTATGGAGCTTCTTAGTGGG 84
                |||
Sbjct 5        CGCGCCCCACCGTCGCGGCA-CCTTCTCACCTCCCTTCAGTTATGGAGCTTCTTAGTGGG 63

Query 85      CCTCACGCGCTTCTGCTCCTCCTGCTCCAGGTTTGTGGCTACGCAGCGTGGTCTCCGAG 144
                |||
Sbjct 64      CCTCACGCGCTTCTGCTCCTCCTGCTCCAGGTTTGTGGCTACGCAGCGTGGTCTCCGAG 123

Query 145     CCTTACCGAGCGGGCTTTCATCGGGGAGGCTGGAGTGACCTTGGAGGTGGAAGGAACTGAC 204
                |||
Sbjct 124     CCTTACCGAGCGGGCTTTCATCGGGGAGGCTGGAGTGACCTTGGAGGTGGAAGGAACTGAC 183

Query 205     CTGGAGCCGAGCCAAGTTCTGGGAAAGTAGCCTTGGCTGGACAGGGCATGCACCATGCA 264
                |||
Sbjct 184     CTGGAGCCGAGCCAAGTTCTGGGAAAGTAGCCTTGGCTGGACAGGGCATGCACCATGCA 243

Query 265     GACAATGGAGACATCATTATGCTGACTAGGGGGACAGTTCAGGGAGGGAAGGATGCGATG 324
                |||
Sbjct 244     GACAATGGAGACATCATTATGCTGACTAGGGGGACAGTTCAGGGAGGGAAGGATGCGATG 303

Query 325     CACTCCCCACCCACCCGCATCTTAAGGAGACGAAAGAGAGAGTGGGTGATGCCACCAATA 384
                |||
Sbjct 304     CACTCCCCACCCACCCGCATCTTAAGGAGACGAAAGAGAGAGTGGGTGATGCCACCAATA 363

Query 385     TTCGTCCTCCGAGAATGGCAAGGGTCCCTTCCCTCAGAGGCTGAATCAGCTCAAATCTAAT 444
                |||
Sbjct 364     TTCGTCCTCCGAGAATGGCAAGGGTCCCTTCCCTCAGAGGCTGAATCAGCTCAAATCTAAT 423

Query 445     AAGGACAGAGGCACCAAGATTTTCTACAGCATCACAGGGCCTGGCGCAGACAGTCCCCCC 504
                |||
Sbjct 424     AAGGACAGAGGCACCAAGATTTTCTACAGCATCACAGGGCCTGGCGCAGACAGTCCCCCC 483

Query 505     GAAGGAGTCTTTCACCATAGAGAAGGAGTGGGCTGGCTGTTGTTGCATATGCCACTGGAC 564
                |||
Sbjct 484     GAAGGAGTCTTTCACCATAGAGAAGGAGTGGGCTGGCTGTTGTTGCATATGCCACTGGAC 543

Query 565     AGGGAGAAGATTGTCAAGTACGAGCTTTATGGCCACGCTGTATCTGAGAATGGTGCCTCT 624
                |||
Sbjct 544     AGGGAGAAGATTGTCAAGTACGAGCTTTATGGCCACGCTGTATCTGAGAATGGTGCCTCT 603

Query 625     GTAGAGGAGCCCATGAACATATCCATCATTGTGACAGACCAGAATGACAACAAGCCCAAG 684
                |||
Sbjct 604     GTAGAGGAGCCCATGAACATATCCATCATTGTGACAGACCAGAATGACAACAAGCCCAAG 663

Query 685     TTCCTCAAGACACCTTCAGAGGGAGTGTCTGGAGGGAGTAAATGCCTGGCACTTCTGTG 744
                |||
Sbjct 664     TTCCTCAAGACACCTTCAGAGGGAGTGTCTGGAGGGAGTAAATGCCTGGCACTTCTGTG 723

Query 745     ATGCAGGTGACAGCCACAGATGAGGACGATGCTGTCAACACTTACAATGGGGTGGTGGCT 804
                |||
Sbjct 724     ATGCAGGTGACAGCCACAGATGAGGACGATGCTGTCAACACTTACAATGGGGTGGTGGCT 783

Query 805     TACTCCATCCATAGCCAAGAGCCGAAGGAGCCACACGACCTCATGTTCAACATCCATAAA 864
                |||
Sbjct 784     TACTCCATCCATAGCCAAGAGCCGAAGGAGCCACACGACCTCATGTTCAACATCCATAAA 843

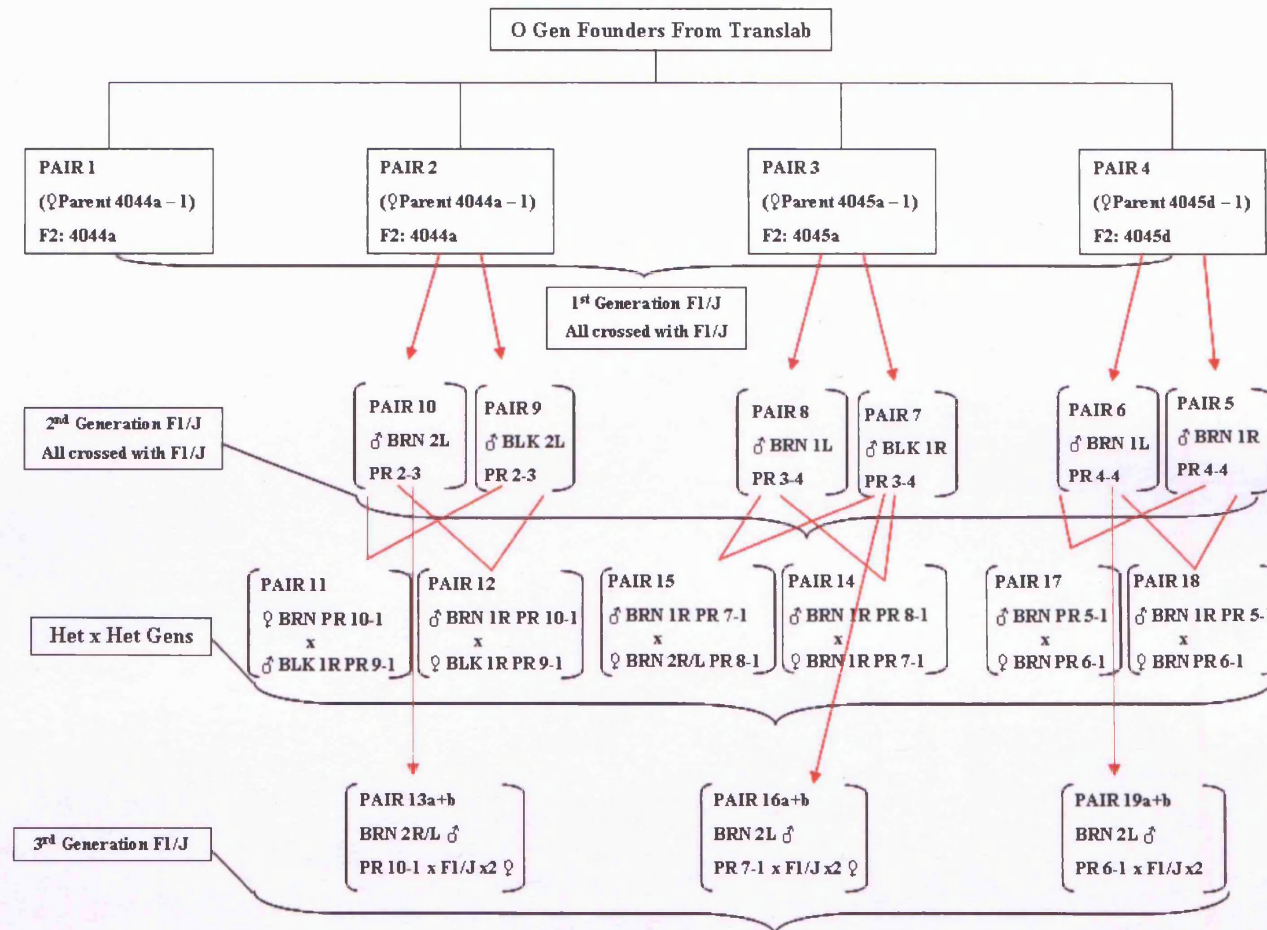
Query 865     AGCACGGGAACCAATTAGCGTCATAICCAAGTGGNCCCTGNACCCGAGAGAAAGTCCCTGAGTA 924
                |||
Sbjct 844     AGCACGGGAACCAATTAGCGTCATAICCAAGTGG-CCTGGACCCGAGAGAAAGTCCCTGAGTA 902

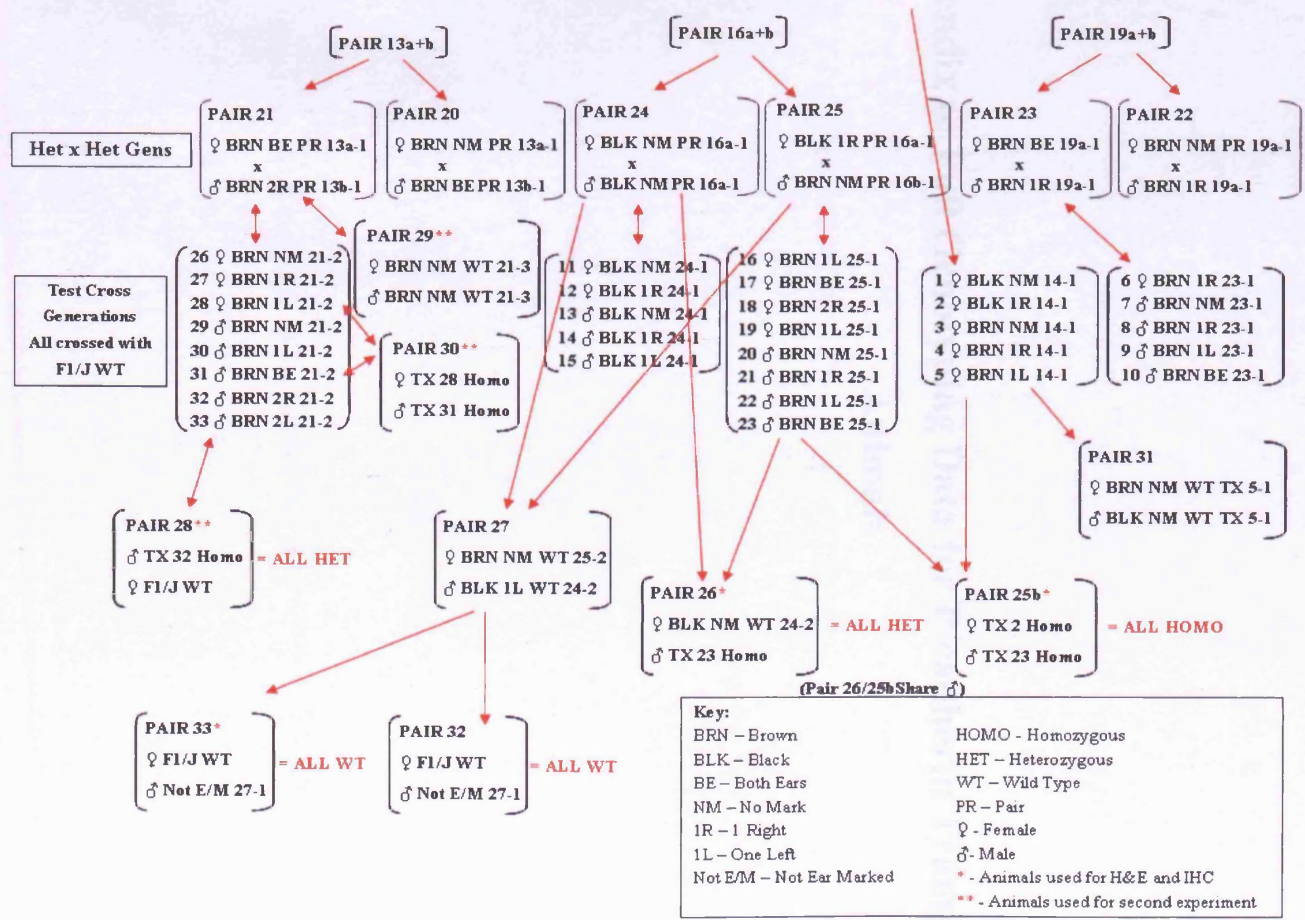
Query 925     CAGACTGACCGTCCAGGCCACAGACNTGGNNGGNGAGGGCTCTACCACGACGGNAGAGGC 984
                |||
Sbjct 903     CAGACTGACCGTCCAGGCCACAGACATGGATGGAGAGGGCTCTACCACGACGGCAGAGGC 962

Query 985     CGTTGTGCAAATCCITGATGC 1005
                |||
Sbjct 963     CGTTGTGCAAATCCITGATGC 983
```

**Appendix 5: Full Version of Mice Breeding Family Tree**

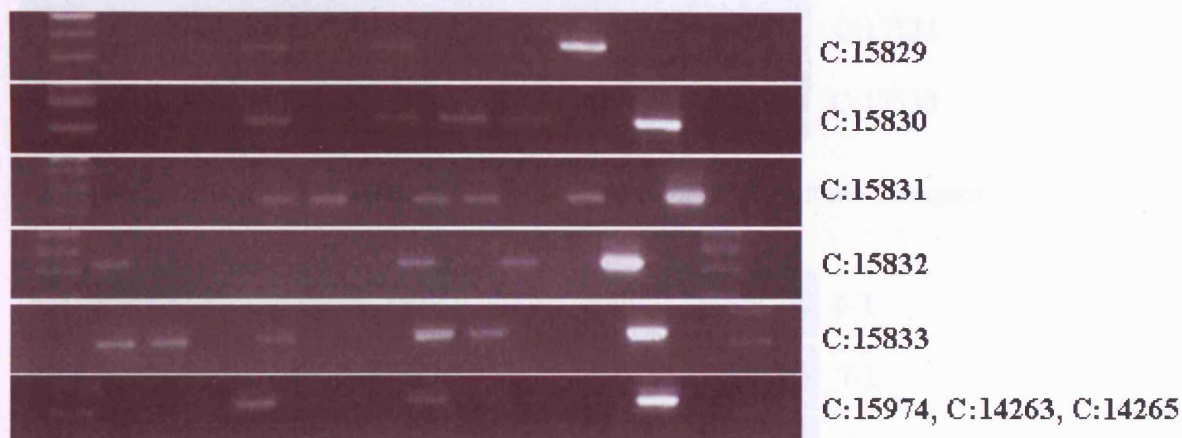
The following family tree diagram represents all animals generated for the P-cadherin transgenic mouse project. Experimental animals were generated from two founder female animals which were either from the 4044a female = line 1 or the 4045a female = line 2. This information was utilised in section 5.4.2 in this works main body of text to create Figure 5.7 and 5.8.



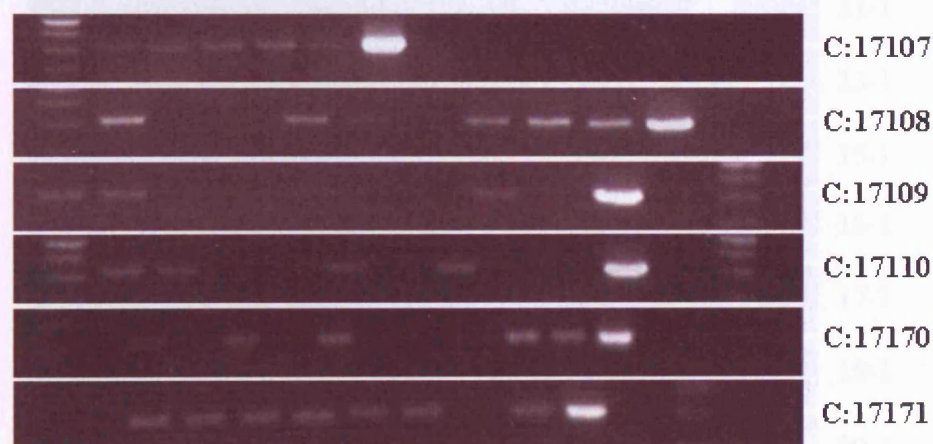


**Appendix 6: Full Genotyping Data for P-cadherin Transgenic  
Animals**

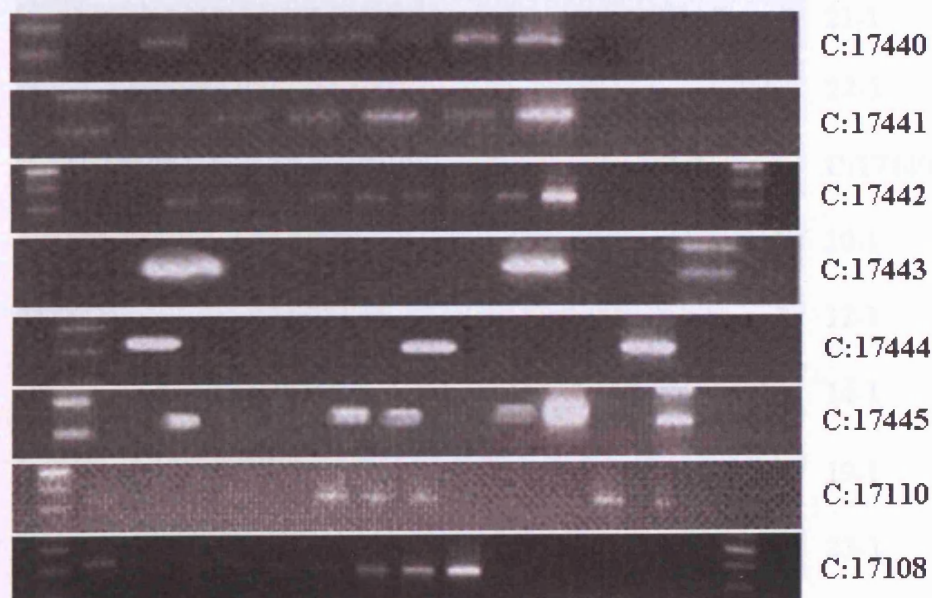
The following gel pictures represent all 505 transgenic P-cadherin animals which were genotyped for the presence of the P-cadherin transgene. This information was utilised in section 5.4.3 in this works main body of text.



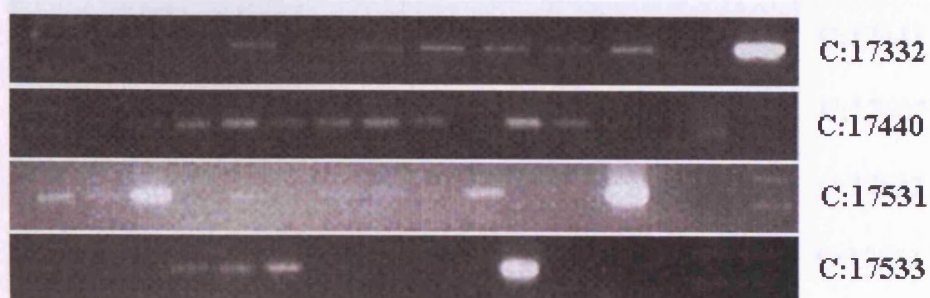
**Round One Genotyping.** 22 animals out of 56 were positive for the P-cadherin Transgene.



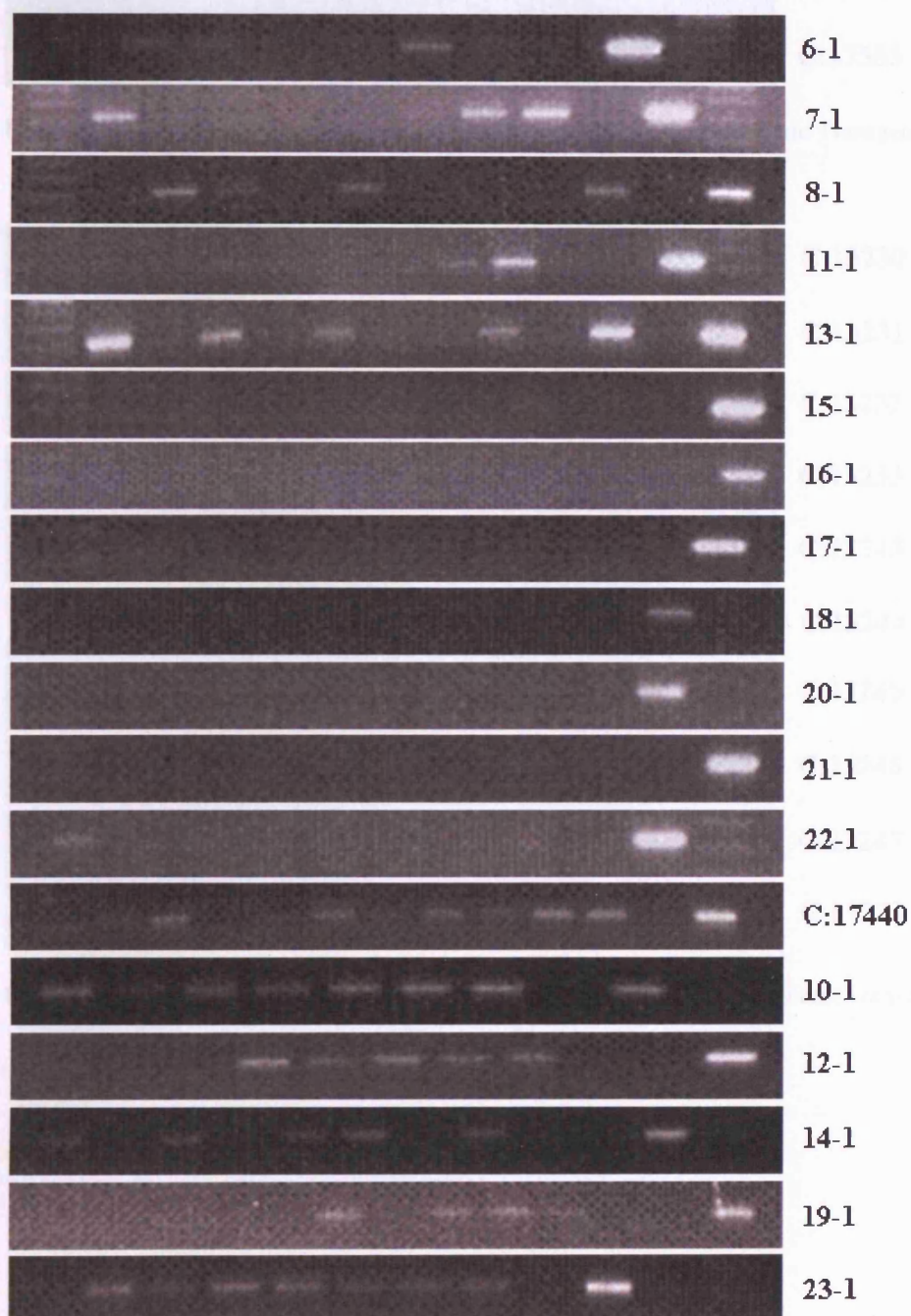
**Round Two Genotyping.** 31 animals out of 53 were positive for the P-cadherin Transgene.



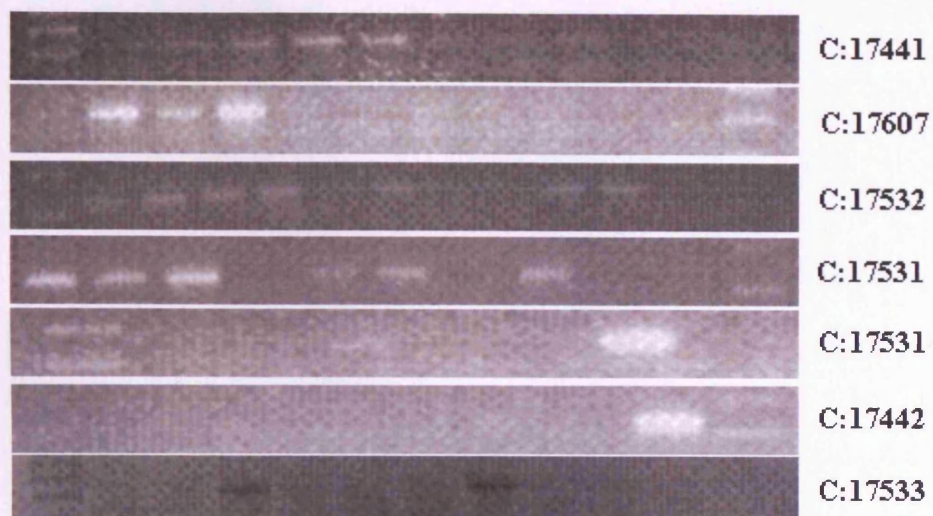
**Round Three Genotyping.** 43 animals out of 65 were positive for the P-cadherin Transgene.



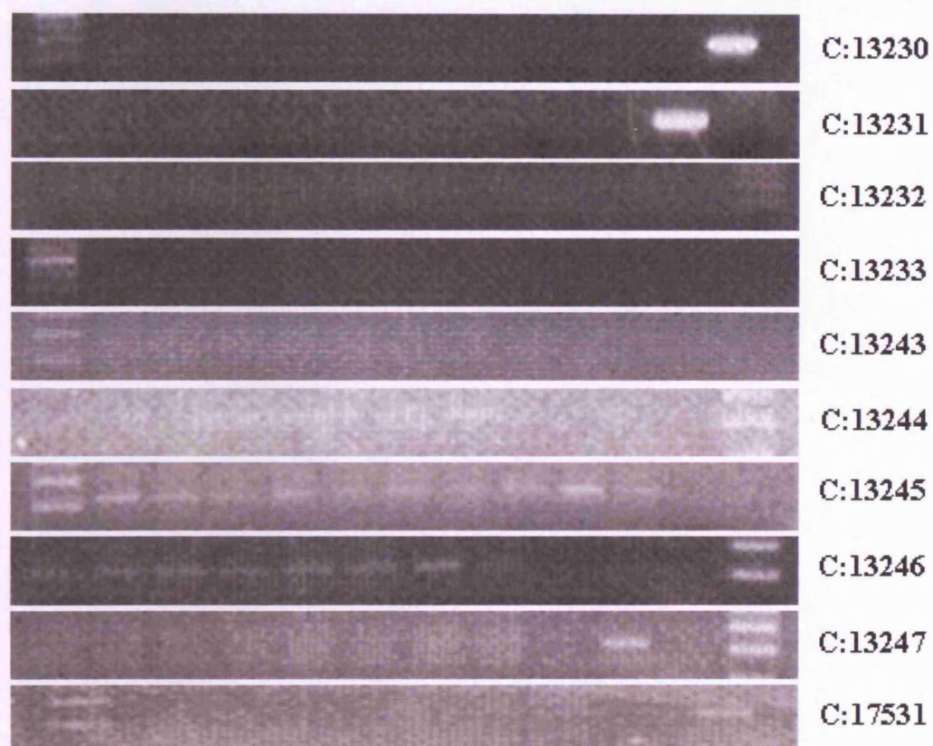
**Round Four Genotyping.** 29 animals out of 41 were positive for the P-cadherin Transgene.



**Round Five Genotyping.** 70 animals out of 153 were positive for the P-cadherin Transgene.



**Round Six Genotyping.** 28 animals out of 54 were positive for the P-cadherin Transgene.



**Round Seven Genotyping.** 27 animals out of 83 were positive for the P-cadherin Transgene.

## **Appendix 7: Statistical Raw Data and Analyses**

The following two tables represent the P-cadherin cytoplasmic staining analysis. The first table details the raw data of the cytoplasmic staining intensity figures obtained for each of the six patients within each topographical location and tissue type, (where  $n > 6$  the data came from the second independent observer, J. Jankowski, who examined a subset of cases). The second table details the statistical analysis using a one-way ANOVA and Tukey's post-hoc test to examine the mean score of the cytoplasmic staining intensity figures between the topographical locations, within different tissue types. \* - The mean difference was either significant at the 0.05 or 0.01 level. This information was utilised in section 3.4.2.6 in this works main body of text to create Tables 3.1 and 3.3.

Cytoplasmic	Basal	Mid	Surface
Stomach - Case 1	2	3	1
Stomach - Case 2	2	2	2
Stomach - Case 3	3	2	2
Stomach - Case 4	3	2	1
Stomach - Case 5	3	2	2
Stomach - Case 6	3	3	1
Additional Count	1	1	-
Average	2.4	2.1	1.5
SE	0.4	0.3	0.3
Normal Squamous - Case 1	2	1	1
Normal Squamous - Case 2	1	1	1
Normal Squamous - Case 3	1	1	1
Normal Squamous - Case 4	1	1	1
Normal Squamous - Case 5	1	1	1
Normal Squamous - Case 6	1	1	1
Average	1.2	1.0	1.0
SE	0.2	0.0	0.0
Oesophagitis - Case 1	2	2	2
Oesophagitis - Case 2	1	1	1
Oesophagitis - Case 3	2	2	1
Oesophagitis - Case 4	2	1	1
Oesophagitis - Case 5	2	1	1
Oesophagitis - Case 6	2	2	1
Additional Count	1	1	-
Average	1.7	1.4	1.2
SE	0.2	0.3	0.2
Barrett's - Case 1	2	1	1
Barrett's - Case 2	2	2	1
Barrett's - Case 3	3	1	1
Barrett's - Case 4	3	2	1
Barrett's - Case 5	2	2	1
Barrett's - Case 6	2	1	1
Average	2.3	1.5	1.0
SE	0.3	0.3	0.0
Adenocarcinoma - Case 1	3	2	3
Adenocarcinoma - Case 2	1	2	2
Adenocarcinoma - Case 3	3	3	3
Adenocarcinoma - Case 4	3	4	4
Adenocarcinoma - Case 5	3	3	3
Adenocarcinoma - Case 6	2	2	3
Additional Count	2	2	2
Additional Count	1	1	1
Additional Count	1	1	1
Average	2.1	2.2	2.4
SE	0.5	0.5	0.5

Dependent Variable	(I) TopoLocation	(J) TopoLocation	Mean Difference (I-J)	Std. Error	Sig.	95% Confidence Interval	
						Lower Bound	Upper Bound
Stomach	Basal	Mid	.286	.368	.723	-.66	1.23
		Surface	.929	.383	.066	-.05	1.91
	Mid	Basal	-.286	.368	.723	-1.23	.66
		Surface	.643	.383	.242	-.34	1.63
	Surface	Basal	-.929	.383	.066	-1.91	.05
		Mid	-.643	.383	.242	-1.63	.34
NormSq	Basal	Mid	.167	.136	.457	-.19	.52
		Surface	.167	.136	.457	-.19	.52
	Mid	Basal	-.167	.136	.457	-.52	.19
		Surface	.000	.136	1.000	-.35	.35
	Surface	Basal	-.167	.136	.457	-.52	.19
		Mid	.000	.136	1.000	-.35	.35
Oesophagitis	Basal	Mid	.286	.259	.524	-.38	.95
		Surface	.548	.269	.134	-.14	1.24
	Mid	Basal	-.286	.259	.524	-.95	.38
		Surface	.262	.269	.603	-.43	.95
	Surface	Basal	-.548	.269	.134	-1.24	.14
		Mid	-.262	.269	.603	-.95	.43
Barretts	Basal	Mid	.833*	.251	.012	.18	1.49
		Surface	1.333*	.251	.000	.68	1.99
	Mid	Basal	-.833*	.251	.012	-1.49	-.18
		Surface	.500	.251	.148	-.15	1.15
	Surface	Basal	-1.333*	.251	.000	-1.99	-.68
		Mid	-.500	.251	.148	-1.15	.15
Adenocarcinoma	Basal	Mid	-.111	.458	.968	-1.26	1.03
		Surface	-.333	.458	.750	-1.48	.81
	Mid	Basal	.111	.458	.968	-1.03	1.26
		Surface	-.222	.458	.879	-1.37	.92
	Surface	Basal	.333	.458	.750	-.81	1.48
		Mid	.222	.458	.879	-.92	1.37

The following two tables represent the P-cadherin membranous staining analysis. The first table details the raw data of the membranous staining intensity figures obtained for each of the six patients within each topographical location and tissue type, (where  $n = >6$  the data came from the second independent observer, J. Jankowski, who examined a subset of cases). The second table details the statistical analysis using a one-way ANOVA and Tukey's post-hoc test to examine the mean score of the membranous staining intensity figures between the topographical locations, within different tissue types. \* - The mean difference was either significant at the 0.05 or 0.01 level. This information was utilised in section 3.4.2.6 in this works main body of text to create Tables 3.2 and 3.3.

Membranous	Basal	Mid	Surface
Somach - Case 1	1	1	1
Somach - Case 2	1	1	1
Somach - Case 3	1	1	1
Somach - Case 4	1	1	1
Somach - Case 5	1	1	1
Somach - Case 6	1	1	1
Additional Count	2	2	-
Average	1.1	1.1	1.0
SE	0.2	0.2	0.0
Normal Squamous - Case 1	3	3	2
Normal Squamous - Case 2	3	2	1
Normal Squamous - Case 3	4	2	1
Normal Squamous - Case 4	4	3	1
Normal Squamous - Case 5	3	2	1
Normal Squamous - Case 6	3	3	1
Additional Count	2	3	-
Additional Count	3	-	-
Average	3.1	2.6	1.2
SE	0.3	0.3	0.2
Oesophagitis - Case 1	1	3	2
Oesophagitis - Case 2	3	3	1
Oesophagitis - Case 3	5	5	3
Oesophagitis - Case 4	4	3	1
Oesophagitis - Case 5	4	3	1
Oesophagitis - Case 6	3	3	1
Additional Count	4	4	-
Additional Count	4	4	-
Average	3.5	3.5	1.5
SE	0.6	0.4	0.4
Barrett's - Case 1	1	1	1
Barrett's - Case 2	1	1	1
Barrett's - Case 3	1	1	1
Barrett's - Case 4	1	1	1
Barrett's - Case 5	1	1	1
Barrett's - Case 6	1	1	1
Additional Count	3	1	-
Additional Count	1	-	-
Additional Count	1	-	-
Average	1.2	1.0	1.0
SE	0.3	0.0	0.0
Adenocarcinoma - Case 1	4	3	4
Adenocarcinoma - Case 2	1	3	1
Adenocarcinoma - Case 3	4	4	4
Adenocarcinoma - Case 4	2	2	2
Adenocarcinoma - Case 5	1	1	1
Adenocarcinoma - Case 6	5	4	5
Additional Count	4	4	4
Additional Count	4	4	4
Additional Count	4	4	4
Average	3.2	3.2	3.2
SE	0.7	0.5	0.7

Dependent Variable	(I) TopoLocation	(J) TopoLocation	Mean Difference (I-J)	Std. Error	Sig.	95% Confidence Interval	
						Lower Bound	Upper Bound
Stomach	Basal	Mid	.000	.170	1.000	-.44	.44
		Surface	.143	.177	.703	-.31	.60
		Mid	.000	.170	1.000	-.44	.44
	Mid	Surface	.143	.177	.703	-.31	.60
		Basal	-.143	.177	.703	-.60	.31
		Mid	-.143	.177	.703	-.60	.31
NormSq	Basal	Mid	.554	.284	.154	-.17	1.28
		Surface	1.958*	.296	.000	1.20	2.71
		Mid	-.554	.284	.154	-1.28	.17
	Mid	Surface	1.405*	.305	.001	.63	2.18
		Basal	-1.958*	.296	.000	-2.71	-1.20
		Mid	-1.405*	.305	.001	-2.18	-.63
Oesophagitis	Basal	Mid	.000	.480	1.000	-1.22	1.22
		Surface	2.000*	.518	.003	.68	3.32
		Mid	.000	.480	1.000	-1.22	1.22
	Mid	Surface	2.000*	.518	.003	.68	3.32
		Basal	-2.000*	.518	.003	-3.32	-.68
		Mid	-2.000*	.518	.003	-3.32	-.68
Barretts	Basal	Mid	.222	.218	.574	-.33	.78
		Surface	.222	.228	.601	-.36	.80
		Mid	-.222	.218	.574	-.78	.33
	Mid	Surface	.000	.241	1.000	-.61	.61
		Basal	-.222	.228	.601	-.80	.36
		Mid	.000	.241	1.000	-.61	.61
Adenocarcinoma	Basal	Mid	.000	.643	1.000	-1.61	1.61
		Surface	.000	.643	1.000	-1.61	1.61
		Mid	.000	.643	1.000	-1.61	1.61
	Mid	Surface	.000	.643	1.000	-1.61	1.61
		Basal	.000	.643	1.000	-1.61	1.61
		Surface	.000	.643	1.000	-1.61	1.61
Surface	Basal	.000	.643	1.000	-1.61	1.61	
	Mid	.000	.643	1.000	-1.61	1.61	

The following two tables represent the Ki-67 nuclear staining analysis. The first table details the raw data of the nuclear staining intensity figures obtained for each of the six patients within each topographical location and tissue type. The second table details the statistical analysis using a one-way ANOVA and Tukey's post-hoc test to examine the mean score of the nuclear staining intensity figures between the topographical locations, within different tissue types. \* - The mean difference was either significant at the 0.05 or 0.01 level. This information was utilised in section 3.4.2.6 in this works main body of text to create Tables 3.4 and 3.5.

Nuclear	Basal	Mid	Surface
Stomach - Case 1	5	5	1
Stomach - Case 2	5	3	1
Stomach - Case 3	3	3	1
Stomach - Case 4	3	1	1
Stomach - Case 5	4	1	1
Stomach - Case 6	3	1	1
Average	3.8	2.3	1.0
SE	0.5	0.8	0.0
Normal Squamous - Case 1	5	5	1
Normal Squamous - Case 2	5	5	1
Normal Squamous - Case 3	4	3	1
Normal Squamous - Case 4	4	3	1
Normal Squamous - Case 5	4	3	1
Normal Squamous - Case 6	5	4	1
Average	4.5	3.8	1.0
SE	0.3	0.5	0.0
Oesophagitis - Case 1	5	5	3
Oesophagitis - Case 2	4	4	3
Oesophagitis - Case 3	3	3	3
Oesophagitis - Case 4	3	3	3
Oesophagitis - Case 5	3	3	4
Oesophagitis - Case 6	2	3	3
Average	3.3	3.5	3.2
SE	0.5	0.4	0.2
Barrett's - Case 1	5	5	1
Barrett's - Case 2	3	4	2
Barrett's - Case 3	4	1	1
Barrett's - Case 4	4	1	1
Barrett's - Case 5	1	1	1
Barrett's - Case 6	3	3	1
Average	3.3	2.5	1.2
SE	0.7	0.9	0.2
Adenocarcinoma - Case 1	2	5	2
Adenocarcinoma - Case 2	2	5	2
Adenocarcinoma - Case 3	2	4	3
Adenocarcinoma - Case 4	4	4	4
Adenocarcinoma - Case 5	3	4	3
Adenocarcinoma - Case 6	4	4	4
Average	2.8	4.3	3.0
SE	0.5	0.3	0.4

Dependent Variable	(I) TopoLocation	(J) TopoLocation	Mean Difference (I-J)	Std. Error	Sig.	95% Confidence Interval	
						Lower Bound	Upper Bound
Stomach	Basal	Mid	1.500	.635	.078	-.15	3.15
		Surface	2.833*	.635	.001	1.18	4.48
		Surface	-1.500	.635	.078	-3.15	.15
	Mid	Surface	1.333	.635	.124	-.32	2.98
		Basal	-2.833*	.635	.001	-4.48	-1.18
		Mid	-1.333	.635	.124	-2.98	.32
NormSq	Basal	Mid	.667	.375	.211	-.31	1.64
		Surface	3.500*	.375	.000	2.53	4.47
		Surface	-1.667	.375	.211	-1.64	.31
	Mid	Surface	2.833*	.375	.000	1.86	3.81
		Basal	-3.500*	.375	.000	-4.47	-2.53
		Basal	-2.833*	.375	.000	-3.81	-1.86
Oesophagitis	Basal	Mid	-.167	.463	.932	-1.37	1.04
		Surface	.167	.463	.932	-1.04	1.37
		Surface	.333	.463	.756	-.87	1.54
	Mid	Basal	.167	.463	.932	-1.04	1.37
		Surface	-.167	.463	.932	-1.37	1.04
		Surface	-.333	.463	.756	-1.54	.87
Barretts	Basal	Mid	.833	.755	.527	-1.13	2.80
		Surface	2.167*	.755	.030	.20	4.13
		Surface	-1.333	.755	.527	-2.80	1.13
	Mid	Surface	1.333	.755	.215	-.63	3.30
		Basal	-2.167*	.755	.030	-4.13	-.20
		Basal	-1.333	.755	.527	-3.30	.63
Adenocarcinoma	Basal	Mid	-1.500*	.475	.017	-2.73	-.27
		Surface	-.167	.475	.935	-1.40	1.07
		Surface	1.500*	.475	.017	.27	2.73
	Mid	Surface	1.333*	.475	.034	.10	2.57
		Basal	.167	.475	.935	-1.07	1.40
		Basal	-1.333*	.475	.034	-2.57	-.10

The following two tables represent the  $\beta$ -catenin membranous staining analysis. The first table details the raw data of the membranous staining intensity figures obtained for each of the six patients within each topographical location and tissue type. The second table details the statistical analysis using a one-way ANOVA and Tukey's post-hoc test to examine the mean score of the membranous staining intensity figures between the topographical locations, within different tissue types. \* - The mean difference was either significant at the 0.05 or 0.01 level. This information was utilised in section 3.4.2.6 in this works main body of text to create Table 3.6.

Membranous	Basal	Mid	Surface
Stomach - Case 1	4	2	1
Stomach - Case 2	4	4	4
Stomach - Case 3	4	4	2
Stomach - Case 4	4	4	4
Stomach - Case 5	3	3	1
Stomach - Case 6	3	3	1
Average	3.7	3.3	2.2
SE	0.3	0.4	0.7
Normal Squamous - Case 1	3	4	4
Normal Squamous - Case 2	2	2	1
Normal Squamous - Case 3	2	2	2
Normal Squamous - Case 4	5	5	5
Normal Squamous - Case 5	3	3	4
Normal Squamous - Case 6	4	3	3
Average	3.2	3.2	3.2
SE	0.6	0.6	0.7
Oesophagitis - Case 1	4	4	4
Oesophagitis - Case 2	4	3	3
Oesophagitis - Case 3	2	2	2
Oesophagitis - Case 4	4	4	4
Oesophagitis - Case 5	4	4	4
Oesophagitis - Case 6	2	2	2
Average	3.3	3.2	3.2
SE	0.5	0.5	0.5
Barrett's - Case 1	1	1	1
Barrett's - Case 2	4	4	4
Barrett's - Case 3	3	3	3
Barrett's - Case 4	4	4	4
Barrett's - Case 5	1	1	1
Barrett's - Case 6	4	3	1
Average	2.8	2.7	2.3
SE	0.7	0.7	0.8
Adenocarcinoma - Case 1	2	2	3
Adenocarcinoma - Case 2	2	4	2
Adenocarcinoma - Case 3	3	4	3
Adenocarcinoma - Case 4	2	4	2
Adenocarcinoma - Case 5	2	2	1
Adenocarcinoma - Case 6	1	1	1
Average	2.0	2.8	2.0
SE	0.3	0.7	0.4

Dependent Variable	(I) TopoLocation	(J) TopoLocation	Mean Difference (I-J)	Std. Error	Sig.	95% Confidence Interval	
						Lower Bound	Upper Bound
Stomach	Basal	Mid	.333	.587	.839	-1.19	1.86
		Surface	1.500	.587	.054	-.02	3.02
		Basal	-.333	.587	.839	-1.86	1.19
	Mid	Surface	1.167	.587	.149	-.36	2.69
		Basal	-1.500	.587	.054	-3.02	.02
		Mid	-1.167	.587	.149	-2.69	.36
NormSq	Basal	Mid	.000	.738	1.000	-1.92	1.92
		Surface	.000	.738	1.000	-1.92	1.92
		Basal	.000	.738	1.000	-1.92	1.92
	Mid	Surface	.000	.738	1.000	-1.92	1.92
		Basal	.000	.738	1.000	-1.92	1.92
		Mid	.000	.738	1.000	-1.92	1.92
Oesophagitis	Basal	Mid	.167	.577	.955	-1.33	1.67
		Surface	.167	.577	.955	-1.33	1.67
		Basal	-.167	.577	.955	-1.67	1.33
	Mid	Surface	.000	.577	1.000	-1.50	1.50
		Basal	-.167	.577	.955	-1.67	1.33
		Mid	.000	.577	1.000	-1.50	1.50
Barretts	Basal	Mid	.167	.837	.978	-2.01	2.34
		Surface	.500	.837	.823	-1.67	2.67
		Basal	-.167	.837	.978	-2.34	2.01
	Mid	Surface	.333	.837	.917	-1.84	2.51
		Basal	-.500	.837	.823	-2.67	1.67
		Mid	-.333	.837	.917	-2.51	1.84
Adenocarcinoma	Basal	Mid	-.833	.574	.341	-2.32	.66
		Surface	.000	.574	1.000	-1.49	1.49
		Mid	.833	.574	.341	-.66	2.32
	Mid	Surface	.833	.574	.341	-.66	2.32
		Basal	.000	.574	1.000	-1.49	1.49
		Mid	-.833	.574	.341	-2.32	.66

The following two tables represent the  $\beta 1$ -integrin cytoplasmic staining analysis. The first table details the raw data of the cytoplasmic staining intensity figures obtained for each of the six patients within each topographical location and tissue type. The second table details the statistical analysis using a one-way ANOVA and Tukey's post-hoc test to examine the mean score of the cytoplasmic staining intensity figures between the topographical locations, within different tissue types. \* - The mean difference was either significant at the 0.05 or 0.01 level. This information was utilised in section 3.4.2.6 in this work's main body of text to create Tables 3.7 and 3.9.

Cytoplasmic	Basal	Mid	Surface
Stomach - Case 1	4	4	4
Stomach - Case 2	2	2	4
Stomach - Case 3	3	3	2
Stomach - Case 4	3	3	3
Stomach - Case 5	2	2	2
Stomach - Case 6	4	4	4
Average	3.0	3.0	3.2
SE	0.4	0.4	0.5
Normal Squamous - Case 1	4	3	2
Normal Squamous - Case 2	3	3	1
Normal Squamous - Case 3	2	2	1
Normal Squamous - Case 4	2	2	1
Normal Squamous - Case 5	4	3	1
Normal Squamous - Case 6	4	3	1
Average	3.2	2.7	1.2
SE	0.5	0.3	0.2
Oesophagitis - Case 1	4	4	4
Oesophagitis - Case 2	3	3	3
Oesophagitis - Case 3	2	4	4
Oesophagitis - Case 4	3	3	3
Oesophagitis - Case 5	3	3	4
Oesophagitis - Case 6	3	3	2
Average	3.0	3.3	3.3
SE	0.3	0.3	0.4
Barrett's - Case 1	4	3	3
Barrett's - Case 2	3	3	3
Barrett's - Case 3	3	3	4
Barrett's - Case 4	3	3	2
Barrett's - Case 5	4	3	2
Barrett's - Case 6	2	3	3
Average	3.2	3.0	2.8
SE	0.4	0.0	0.4
Adenocarcinoma - Case 1	5	4	5
Adenocarcinoma - Case 2	4	4	5
Adenocarcinoma - Case 3	5	4	5
Adenocarcinoma - Case 4	4	4	4
Adenocarcinoma - Case 5	5	5	5
Adenocarcinoma - Case 6	3	3	4
Average	4.3	4.0	4.7
SE	0.4	0.3	0.3

Dependent Variable	(I) TopoLocation	(J) TopoLocation	Mean Difference (I-J)	Std. Error	Sig.	95% Confidence Interval	
						Lower Bound	Upper Bound
Stomach	Basal	Mid	-.167	.509	.943	-1.49	1.16
		Surface	-.333	.509	.793	-1.66	.99
	Mid	Basal	.167	.509	.943	-1.16	1.49
		Surface	-.167	.509	.943	-1.49	1.16
	Surface	Basal	.333	.509	.793	-.99	1.66
		Mid	.167	.509	.943	-1.16	1.49
NormSq	Basal	Mid	.500	.394	.434	-.52	1.52
		Surface	2.000*	.394	.000	.98	3.02
	Mid	Basal	-.500	.394	.434	-1.52	.52
		Surface	1.500*	.394	.005	.48	2.52
	Surface	Basal	-2.000*	.394	.000	-3.02	-.98
		Mid	-1.500*	.394	.005	-2.52	-.48
Oesophagitis	Basal	Mid	-.333	.385	.669	-1.33	.67
		Surface	-.333	.385	.669	-1.33	.67
	Mid	Basal	.333	.385	.669	-.67	1.33
		Surface	.000	.385	1.000	-1.00	1.00
	Surface	Basal	.333	.385	.669	-.67	1.33
		Mid	.000	.385	1.000	-1.00	1.00
Barretts	Basal	Mid	.167	.355	.886	-.76	1.09
		Surface	.333	.355	.625	-.59	1.26
	Mid	Basal	-.167	.355	.886	-1.09	.76
		Surface	.167	.355	.886	-.76	1.09
	Surface	Basal	-.333	.355	.625	-1.26	.59
		Mid	-.167	.355	.886	-1.09	.76
Adenocarcinoma	Basal	Mid	.333	.385	.669	-.67	1.33
		Surface	-.333	.385	.669	-1.33	.67
	Mid	Basal	-.333	.385	.669	-1.33	.67
		Surface	-.667	.385	.226	-1.67	.33
	Surface	Basal	.333	.385	.669	-.67	1.33
		Mid	.667	.385	.226	-.33	1.67

The following two tables represent the  $\beta 1$ -integrin membranous staining analysis. The first table details the raw data of the membranous staining intensity figures obtained for each of the six patients within each topographical location and tissue type. The second table details the statistical analysis using a one-way ANOVA and Tukey's post-hoc test to examine the mean score of the membranous staining intensity figures between the topographical locations, within different tissue types. \* - The mean difference was either significant at the 0.05 or 0.01 level. This information was utilised in section 3.4.2.6 in this works main body of text to create Tables 3.8 and 3.9.

Membranous	Basal	Mid	Surface
Stomach - Case 1	2	2	2
Stomach - Case 2	2	1	3
Stomach - Case 3	3	2	1
Stomach - Case 4	1	1	1
Stomach - Case 5	1	1	1
Stomach - Case 6	2	2	2
Average	1.8	1.5	1.7
SE	0.4	0.3	0.4
Normal Squamous - Case 1	1	1	1
Normal Squamous - Case 2	4	4	1
Normal Squamous - Case 3	1	1	1
Normal Squamous - Case 4	1	1	1
Normal Squamous - Case 5	1	1	1
Normal Squamous - Case 6	1	1	1
Average	1.5	1.5	1.0
SE	0.6	0.6	0.0
Oesophagitis - Case 1	4	4	4
Oesophagitis - Case 2	1	1	1
Oesophagitis - Case 3	1	1	1
Oesophagitis - Case 4	1	1	1
Oesophagitis - Case 5	1	1	1
Oesophagitis - Case 6	1	1	1
Average	1.5	1.5	1.5
SE	0.6	0.6	0.6
Barrett's - Case 1	1	1	1
Barrett's - Case 2	2	4	4
Barrett's - Case 3	1	1	1
Barrett's - Case 4	1	1	1
Barrett's - Case 5	1	1	1
Barrett's - Case 6	1	1	1
Average	1.2	1.5	1.5
SE	0.2	0.6	0.6
Adenocarcinoma - Case 1	1	1	1
Adenocarcinoma - Case 2	5	5	5
Adenocarcinoma - Case 3	4	4	4
Adenocarcinoma - Case 4	1	1	1
Adenocarcinoma - Case 5	3	4	4
Adenocarcinoma - Case 6	4	4	5
Average	3.0	3.2	3.3
SE	0.8	0.9	0.9

Dependent Variable	(I) TopoLocation	(J) TopoLocation	Mean Difference (I-J)	Std. Error	Sig.	95% Confidence Interval	
						Lower Bound	Upper Bound
Stomach	Basal	Mid	.333	.413	.704	-.74	1.41
		Surface	.167	.413	.915	-.91	1.24
	Mid	Basal	-.333	.413	.704	-1.41	.74
		Surface	-.167	.413	.915	-1.24	.91
	Surface	Basal	-.167	.413	.915	-1.24	.91
		Mid	.167	.413	.915	-.91	1.24
NormSq	Basal	Mid	.000	.577	1.000	-1.50	1.50
		Surface	.500	.577	.669	-1.00	2.00
	Mid	Basal	.000	.577	1.000	-1.50	1.50
		Surface	.500	.577	.669	-1.00	2.00
	Surface	Basal	-.500	.577	.669	-2.00	1.00
		Mid	-.500	.577	.669	-2.00	1.00
Oesophagitis	Basal	Mid	.000	.707	1.000	-1.84	1.84
		Surface	.000	.707	1.000	-1.84	1.84
	Mid	Basal	.000	.707	1.000	-1.84	1.84
		Surface	.000	.707	1.000	-1.84	1.84
	Surface	Basal	.000	.707	1.000	-1.84	1.84
		Mid	.000	.707	1.000	-1.84	1.84
Barretts	Basal	Mid	-.333	.593	.842	-1.87	1.21
		Surface	-.333	.593	.842	-1.87	1.21
	Mid	Basal	.333	.593	.842	-1.21	1.87
		Surface	.000	.593	1.000	-1.54	1.54
	Surface	Basal	.333	.593	.842	-1.21	1.87
		Mid	.000	.593	1.000	-1.54	1.54
Adenocarcinoma	Basal	Mid	-.167	1.013	.985	-2.80	2.46
		Surface	-.333	1.013	.942	-2.96	2.30
	Mid	Basal	.167	1.013	.985	-2.46	2.80
		Surface	-.167	1.013	.985	-2.80	2.46
	Surface	Basal	.333	1.013	.942	-2.30	2.96
		Mid	.167	1.013	.985	-2.46	2.80

The following four tables represent the labelling index analysis performed in the SAINT clinical trial tissue. Cell counts were undertaken for gastric, normal squamous, Barrett's and adenocarcinoma tissue, whereby 10 counts of 100 cells were undertaken and the number of cells which had retained the IUDR label, and those which had not, within each 100 cells were detailed. The first table details the raw data of the cell counts which were undertaken in the gastric tissue for both SAINT trial recruits. The second table details the raw data of the cell counts which were undertaken in the normal squamous tissue for both SAINT trial recruits. The third table details the raw data of the cell counts which were undertaken in the Barrett's tissue for both SAINT trial recruits. The fourth table details the raw data of the cell counts which were undertaken in the adenocarcinoma tissue for both SAINT trial recruits. The average number of cells and the standard error information can also be seen in each table. This information was utilised to prepare Table 3.10 in this works main body of text.

	<b>Positive Cells</b>	<b>Negative Cells</b>	<b>Total Count</b>
<b>Gastric ST001</b>	3	97	100
<b>Gastric ST001</b>	4	96	100
<b>Gastric ST001</b>	8	92	100
<b>Gastric ST001</b>	6	94	100
<b>Gastric ST001</b>	3	97	100
<b>Gastric ST002</b>	1	99	100
<b>Gastric ST002</b>	4	96	100
<b>Gastric ST002</b>	3	97	100
<b>Gastric ST002</b>	4	96	100
<b>Gastric ST002</b>	2	98	100
<b>Average</b>	<b>3.8</b>	<b>96.2</b>	<b>100</b>
<b>Standard Error</b>	<b>1.0</b>	<b>1.0</b>	

	<b>Positive Cells</b>	<b>Negative Cells</b>	<b>Total Count</b>
<b>Normal Squamous ST001</b>	2	98	100
<b>Normal Squamous ST001</b>	8	92	100
<b>Normal Squamous ST001</b>	13	87	100
<b>Normal Squamous ST001</b>	3	97	100
<b>Normal Squamous ST001</b>	1	99	100
<b>Normal Squamous ST002</b>	11	89	100
<b>Normal Squamous ST002</b>	5	95	100
<b>Normal Squamous ST002</b>	0	100	100
<b>Normal Squamous ST002</b>	2	98	100
<b>Normal Squamous ST002</b>	14	86	100
<b>Average</b>	<b>5.9</b>	<b>94.1</b>	<b>100</b>
<b>Standard Error</b>	<b>2.6</b>	<b>2.6</b>	

	Positive Cells	Negative Cells	Total Count
Barret's Metaplasia ST002	0	100	100
Barret's Metaplasia ST002	5	95	100
Barret's Metaplasia ST002	7	93	100
Barret's Metaplasia ST002	1	99	100
Barret's Metaplasia ST002	5	95	100
Barret's Metaplasia ST002	4	96	100
Barret's Metaplasia ST002	6	94	100
Barret's Metaplasia ST002	2	98	100
Barret's Metaplasia ST002	3	97	100
Barret's Metaplasia ST002	2	98	100
Average	3.5	96.5	100
Standard Error	1.1	1.1	

	Positive Cells	Negative Cells	Total Count
Adenocarcinoma ST001	21	79	100
Adenocarcinoma ST001	33	67	100
Adenocarcinoma ST001	11	89	100
Adenocarcinoma ST001	23	77	100
Adenocarcinoma ST001	12	88	100
Adenocarcinoma ST002	29	71	100
Adenocarcinoma ST002	19	81	100
Adenocarcinoma ST002	25	75	100
Adenocarcinoma ST002	38	62	100
Adenocarcinoma ST002	26	74	100
Average	23.7	76.3	100
Standard Error	4.3	4.3	

The following three tables represent the labelling index analysis performed in the SAINT clinical trial tissue. Cell counts were undertaken for gastric, normal squamous and Barrett's tissue, whereby the number of cells which had retained the IUDR label within each topographical location were detailed. The first table details the raw data of the cell counts which were undertaken in the gastric tissue for both SAINT trial recruits. The second table details the raw data of the cell counts which were undertaken in the normal squamous tissue for both SAINT trial recruits. The third table details the raw data of the cell counts which were undertaken in the Barrett's tissue for both SAINT trial recruits. The average number of cells and the standard error information can also be seen in each table. This information was utilised to prepare Table 3.11 in this works main body of text.

	Base	Neck	Surface
Gastric ST001	-	2	-
Gastric ST001	-	2	1
Gastric ST001	2	1	-
Gastric ST001	1	2	-
Gastric ST001	2	4	-
Gastric ST002	3	-	-
Gastric ST002	4	2	-
Gastric ST002	-	-	3
Gastric ST002	3	-	-
Gastric ST002	3	3	-
Average	1.8	1.6	0.4
Standard Error	0.5	0.5	0.7

Normal Squamous ST 001	2	-	-
Normal Squamous ST 001	1	5	2
Normal Squamous ST 001	-	8	5
Normal Squamous ST 001	2	1	-
Normal Squamous ST 001	-	1	-
Normal Squamous ST 002	1	1	1
Normal Squamous ST 002	2	6	3
Normal Squamous ST 002	2	3	-
Normal Squamous ST 002	-	-	2
Normal Squamous ST 002	6	4	1
Average	1.6	2.9	1.4
Standard Error	0.9	1.3	0.8

Barret's Metaplasia ST 002	1	-	1
Barret's Metaplasia ST 002	-	2	-
Barret's Metaplasia ST 002	3	3	-
Barret's Metaplasia ST 002	-	2	3
Barret's Metaplasia ST 002	-	1	-
Barret's Metaplasia ST 002	3	1	1
Barret's Metaplasia ST 002	-	2	-
Barret's Metaplasia ST 002	1	1	1
Barret's Metaplasia ST 002	4	-	-
Barret's Metaplasia ST 002	3	1	1
Average	1.5	1.3	0.7
Standard Error	0.6	0.4	0.4

The following three tables represent the IHC double labelling analysis performed in the SAINT clinical trial normal oesophageal tissue. The first table details the raw data of the cell counts which were undertaken for both the number of positive cells which had retained the BrdU or the Ki-67 label, along with those that had not shown any positive staining in the PBL and IBL compartments. The second table details the percentage of cells observed in each area, and the third the standard error figures for the counts and percentage respectively. This information was utilised to prepare Tables 3.12 and 3.13 in this works main body of text.

Counts	PBL IUdR	PBL Ki-67	PBL Negative	PBL Total	IBL IUdR	IBL Ki-67	IBL Negative	IBL Total
Normal Squamous SI001	6	30	50	86	14	29	65	108
Normal Squamous SI001	6	16	32	54	8	18	24	50
Normal Squamous SI001	6	28	12	46	4	8	18	30
Normal Squamous SI001	2	31	31	64	11	24	41	76
Normal Squamous SI001	7	15	39	61	10	30	68	108
Normal Squamous SI002	7	18	42	67	8	39	52	99
Normal Squamous SI002	11	31	39	81	14	28	44	86
Normal Squamous SI002	9	25	20	54	5	8	44	57
Normal Squamous SI002	14	26	48	88	20	40	59	119
Normal Squamous SI002	8	24	43	75	16	34	53	103
Average Count	7.6	24.4	35.6	67.6	11	25.8	46.8	83.6

Percentages	PBL IUdR	PBL Ki-67	PBL Negative	PBL Total	IBL IUdR	IBL Ki-67	IBL Negative	IBL Total
Normal Squamous SI001	7.0	34.9	58.1	100	13.0	26.9	60.2	100
Normal Squamous SI001	11.1	29.6	59.3	100	16.0	36.0	48.0	100
Normal Squamous SI001	13.0	60.9	26.1	100	13.3	26.7	60.0	100
Normal Squamous SI001	3.1	48.4	48.4	100	14.5	31.6	53.9	100
Normal Squamous SI001	11.5	24.6	63.9	100	9.3	27.8	63.0	100
Normal Squamous SI002	10.4	26.9	62.7	100	8.1	39.4	52.5	100
Normal Squamous SI002	13.6	38.3	48.1	100	16.3	32.6	51.2	100
Normal Squamous SI002	16.7	46.3	37.0	100	8.8	14.0	77.2	100
Normal Squamous SI002	15.9	29.5	54.5	100	16.8	33.6	49.6	100
Normal Squamous SI002	10.7	32.0	57.3	100	15.5	33.0	51.5	100
AveragePercentage	11.3	37.1	51.6	100	13.2	30.1	56.7	100

	PBL IUdR	PBL Ki-67	PBL Negative	PBL Total	IBL IUdR	IBL Ki-67	IBL Negative	IBL Total
Standard Error - Counts	1.6	3.0	6.0	7.2	2.5	5.7	8.2	14.7
Standard Error - Percentages	2.0	5.7	6.0	0.0	1.7	3.5	4.4	0.0

The following table represents the DCA stimulation analysis. Statistical analysis was carried out to see if there was a significant difference between the DCA stimulated animals versus the control groups using the Fishers exact test. In total 19 animals were analysed in the DCA group (11 = positive, 8 = negative) and 20 animals in the control group (5 = positive, 15 = negative). A two-tailed probability value of  $P = 0.05$  for the DCA versus control animal group was observed. This information was utilised in section 4.4.3.1 in this works main body of text.

Fishers Exact Test Statistics for DCA Zebrafish Stimulation Experiment

Observed	Gp 1	Gp 2	
Class 1:	11	5	16
Class 2:	8	15	23
	19	20	39

*p*-values:

Calculate this tail: 0.0384280

Reset other tail: 0.9926454

both tails: 0.0535509

Status: Status okay

The following two tables represent the phosphohistone analysis. The first table details the raw data of the labelling indexes obtained for each of the four animals in each area of the intestinal mucosa. The second table details the statistical analysis using a one-way ANOVA and Tukey's post-hoc test to examine the mean score of the labelling index figures from 4 animals in each sample group for each area of the intestinal mucosa. \* - The mean difference is significant at the 0.05 level. This information was utilised in section 5.4.4.5 in this works main body of text to create Table 5.4 and Figure 5.15.

	SB1	SB2	SB3	LB1	Caecum
<b>Wild Type</b>	2.10	1.90	2.50	0.60	2.80
<b>Wild Type</b>	2.10	3.10	2.70	1.80	1.40
<b>Wild Type</b>	1.30	1.60	1.20	2.10	2.40
<b>Wild Type</b>	1.10	2.10	1.70	1.10	1.90
<b>Average</b>	<b>1.65</b>	<b>2.18</b>	<b>2.03</b>	<b>1.40</b>	<b>2.13</b>
<b>Standard Error</b>	<b>0.26</b>	<b>0.33</b>	<b>0.04</b>	<b>0.34</b>	<b>0.30</b>
<b>Homozygous</b>	1.50	0.20	0.70	0.30	0.30
<b>Homozygous</b>	0.60	0.30	0.40	0.20	0.30
<b>Homozygous</b>	0.30	0.50	0.50	0.20	0.20
<b>Homozygous</b>	0.30	0.30	0.40	0.10	0.10
<b>Average</b>	<b>0.68</b>	<b>0.33</b>	<b>0.50</b>	<b>0.20</b>	<b>0.23</b>
<b>Standard Error</b>	<b>0.28</b>	<b>0.06</b>	<b>0.07</b>	<b>0.04</b>	<b>0.05</b>
<b>Heterzygous</b>	2.00	2.30	1.90	1.00	1.00
<b>Heterzygous</b>	1.50	1.30	0.70	1.40	0.10
<b>Heterzygous</b>	1.70	2.10	1.40	0.60	1.30
<b>Average</b>	<b>1.75</b>	<b>2.03</b>	<b>1.55</b>	<b>1.03</b>	<b>0.85</b>
<b>Standard Error</b>	<b>0.10</b>	<b>0.25</b>	<b>0.33</b>	<b>0.17</b>	<b>0.26</b>

Dependent Variable	(I) Genotype	(J) Genotype	Mean Difference (I-J)	Std. Error	Sig.	95% Confidence Interval	
						Lower Bound	Upper Bound
SB1	Wild type	Homo	.97500*	.32724	.037	.0614	1.8886
		Het	-.10000	.32724	.950	-1.0136	.8136
	Homo	Wild type	-.97500*	.32724	.037	-1.8886	-.0614
		Het	-1.07500*	.32724	.023	-1.9886	-.1614
SB2	Wild type	Homo	.10000	.32724	.950	-.8136	1.0136
		Homo	1.07500*	.32724	.023	.1614	1.9886
	Homo	Wild type	1.85000*	.33850	.001	.9049	2.7951
		Het	.15000	.33850	.899	-.7951	1.0951
SB3	Wild type	Homo	-1.85000*	.33850	.001	-2.7951	-.9049
		Het	-1.70000*	.33850	.002	-2.6451	-.7549
	Homo	Wild type	-1.50000	.33850	.899	-1.0951	.7951
		Homo	1.70000*	.33850	.002	.7549	2.6451
LB1	Wild type	Homo	1.52500*	.39564	.010	.4204	2.6296
		Het	.47500	.39564	.482	-.6296	1.5796
	Homo	Wild type	-1.52500*	.39564	.010	-2.6296	-.4204
		Het	-1.05000	.39564	.062	-2.1546	.0546
Caecum	Wild type	Homo	1.20000*	.30979	.009	.3351	2.0649
		Het	-.37500	.30979	.477	-.4899	1.2399
	Homo	Wild type	-1.20000*	.30979	.009	-2.0649	-.3351
		Het	-.82500	.30979	.061	-1.6899	.0399
Caecum	Wild type	Homo	1.90000*	.32872	.001	.9822	2.8178
		Het	1.27500*	.32872	.009	.3672	2.1928
	Homo	Wild type	-1.90000*	.32872	.001	-2.8178	-.9822
		Het	-.62500	.32872	.194	-1.5428	.2928
Homo	Wild type	-1.27500*	.32872	.009	-2.1928	-.3572	
	Het	.62500	.32872	.194	-.2928	1.5428	

## **Appendix 8: Publications Arising from this Work**

---

The following abstract was for poster presentation at the BSCB annual conference, September 2003.

### **Transgenic mouse model for P-cadherin expression**

J.Obszynska, L.Harrison, R.Harrison, N.Wright\*, and J.Jankowski.

Digestive Diseases Centre, University Department of Cancer Studies and Molecular Medicine, University of Leicester, Leicester, UK.

\*Histopathology Unit, Cancer Research UK, London, UK.

#### Hypothesis:

“P-cadherin over expression is believed to have no additional phenotypic change in the gastrointestinal (GI) tract”.

#### Objectives:

We aimed to force the expression of P-cadherin within a site of the GI tract where it is not normally expressed. We will look at P-cadherin expression throughout the GI tract. Also we will look at the association of P-cadherin expression and disease status. In addition we aim to force the expression in murine intestine using fatty acid binding protein.

#### Methods:

A total of 58 animals were genotyped for the presence of P-cadherin.

#### Results:

36 animals (62%) were identified as homozygous for human P-cadherin gene.

#### Conclusions:

It would appear that P-cadherin is expressed in normal stratified tissue and also in transgenic animals.

---

The following abstract was for oral presentation at the BSG annual conference, March 2006 and was also published in *Gut* 2006; 55 (suppl II) A9-A9, 032.

### Transgenic mouse model for P-cadherin expression

LA.Harrison<sup>1</sup>, E. Nye<sup>3</sup>, G. Stamp<sup>3</sup>, NA. Wright<sup>2</sup>, R. Goodlad<sup>2</sup>, and JA. Jankowski<sup>1</sup>

<sup>1</sup>Digestive Diseases Centre, University Department of Cancer Studies and Molecular Medicine, Leicester Medical School at University Hospitals Trust, Leicester, UK,

<sup>2</sup>Histopathology Unit, Cancer Research UK, London, UK, <sup>3</sup>Experimental Pathology Laboratory, Cancer Research UK, London, UK.

Epithelial (E), neuronal (N) and placental (P) cadherin isoforms belong to a highly conserved superfamily of calcium dependent cellular adhesion molecules. They are involved in the development and homeostasis of normal tissue function. P-cadherin upregulation in particular has been associated with the early stages of cancer in the gastrointestinal (GI) tract. P-cadherin has also been shown to have a proliferative effect on the GI tract.

Transgenic mouse models have provided great insights into the pathological role of specific cadherins in the intestine. Our hypothesis was to test if cadherins could have a proliferative effect in the GI tract. To study the mechanism of action of P-cadherin, an *in vivo* model was designed consisting of transgenic animals and a fatty acid binding promoter was used to force the expression of P-cadherin within a site of the GI tract where it is not normally expressed.

Test-crosses were set up between F1 and transgene positive animals to generate a homozygous mouse model stable for P-cadherin expression. A total of 6 animals (2 animals from each genotype of wild type, heterozygous and homozygous) were examined blindly. The pathology report determined that all organs samples were normal, with no sign of Crohn's disease and no significant difference between the wild type, heterozygous or homozygous animals.

In conclusion it would appear that while P-cadherin upregulation may be necessary for a metaplastic or dysplastic phenotype in man, it may alone not be sufficient. Subtle changes of P-cadherin on mucosal biology will be discussed.

---

**The following abstract was selected for oral presentation at the Leicestershire Research Prize Day, June 2006 and was awarded first prize.**

### **Transgenic mouse model for P-cadherin expression**

LA.Harrison<sup>1</sup>, E. Nye<sup>3</sup>, G. Stamp<sup>3</sup>, NA. Wright<sup>2</sup>, R. Goodlad<sup>2</sup>, and JA. Jankowski<sup>1</sup>

<sup>1</sup> - Digestive Diseases Centre, University Department of Cancer Studies and Molecular Medicine, Leicester Medical School at University Hospitals Trust, Leicester, UK

<sup>2</sup> - Histopathology Unit, Cancer Research UK, London, UK

<sup>3</sup> - Experimental Pathology Laboratory, Cancer Research UK, London, UK

Epithelial (E), neuronal (N) and placental (P) cadherin isoforms belong to a highly conserved superfamily of calcium dependent cellular adhesion molecules. They are involved in the development and homeostasis of normal tissue function. P-cadherin upregulation in particular has been associated with the early stages of cancer in the gastrointestinal (GI) tract. P-cadherin has also been shown to have a proliferative effect on the GI tract.

Transgenic mouse models have provided great insights into the pathological role of specific cadherins in the intestine. Our hypothesis was to test if cadherins could have a proliferative effect in the GI tract. To study the mechanism of action of P-cadherin, an *in vivo* model was designed consisting of transgenic animals and a fatty acid binding promoter was used to force the expression of P-cadherin within a site of the GI tract where it is not normally expressed.

Test-crosses were set up between F1 and transgene positive animals to generate a homozygous mouse model stable for P-cadherin expression. A total of 6 animals (2 animals from each genotype of wild type, heterozygous and homozygous) were examined blindly. The pathology report determined that all organs samples were normal, with no sign of Crohn's disease and no significant difference between the wild type, heterozygous or homozygous animals.

RT-PCR work has revealed that homozygous animals showed forced transgene P-cadherin expression present within the small intestine. Analysis of variance for fission data has shown subtle changes in crypt bifurcation.

In conclusion it would appear that P-cadherin seems to be expressed within the stem cell compartment, not only within native oesophagus, but also within Barrett's oesophagus. Secondly, that by using the L-FABP cadherin promoter we have been able to show that the mouse is a viable model system. Thirdly, upregulation may be necessary for a metaplastic phenotype in man, but it may alone not be sufficient. Finally a modest increase in stem cell division is shown which may show an exaggerated P-cadherin phenotype if an indomethacin stress response assay was used. Subtle changes of P-cadherin on mucosal biology will be discussed.

---

The following abstract was for oral presentation at the BSG annual conference, March 2007.

## **THE SAINT TRIAL (STEM CELL ANALYSIS AND IDENTIFICATION BY IUDR LABELLING OF NEOPLASTIC TISSUE); IDENTIFICATION OF BARRETT'S STEM CELLS**

L. Harrison(1), A. M. Nicholson\*(2), R. Harrison(1), S. McDonald(3), G. Wilson(4), N. Wright(3), P. A. Atherfold(2), J. A. Jankowski(2)

(1)Digestive Disease Centre, Leicester Royal Infirmary, Leicester.

(2)Clinical Pharmacology, University of Oxford, Oxford.

(3)Histopathology, Cancer Research UK, London, United Kingdom.

(4)Digestive Disease Centre, Karmanos Institute, Michigan, United States.

**INTRODUCTION:** A gastrointestinal epithelial cell will be shed from the epithelial surface into the lumen and replaced from below by the progeny of a stem cell. Since stem cells are the only long-residing cells within the gastrointestinal epithelium, it is logical that they are to be the target for mutations that may lead to the aberrant epithelial biology seen in Barrett's Metaplasia, a pre-malignant condition that can lead to oesophageal adenocarcinoma. To date, the identification of the putative stem cell within the epithelium of a Barrett's metaplastic lesion remains elusive.

**AIMS & METHODS:** We utilised iododeoxyuridine (IUdR) a nucleoside and a thymidine analogue which is incorporated into the DNA of replicating cells, as a marker to identify the putative Barrett's stem cell. Since transit amplifying cells are lost from the lumen and replaced from below in about 3-7 days, we expect the label retaining cells (LRCs) to contain the putative Barrett's stem cell. Two patients diagnosed with oesophageal adenocarcinoma having previously undergone chemotherapy were scheduled to undergo oesophagectomy. These two patients were recruited to the SAINT clinical trial. Seven days prior to their surgery each patient was infused with IUdR. After resection, tissue samples of normal oesophagus, Barrett's, normal stomach and tumour were extracted and fixed in neutral buffered formalin for approximately 8 hours. Routine immunohistochemistry was performed on 6 micron sections of all tissue types.

**RESULTS:** Infusion three days or less in vitro in transformed cells and explants revealed appropriate abundant staining of the proliferative compartments. However, labelling at 7 days in both patients *ex vivo* showed positive discrete staining of LRCs within various gastrointestinal tissue types including Barrett's Metaplasia. These LRCs were seen in the parabasal layer and basal layer of the squamous epithelium, this is in line with the current dogma of the location of the oesophageal stem cell. LRCs were seen at several locations in metaplastic tissue both at the base of the gland and in the neck region.

**CONCLUSION:** This is the first report of LRCs within the human oesophagus. Our findings correlate with the hypothesised location of stem cells in the squamous epithelium. More importantly LRCs were also located in the basal and neck region of the Barrett's gland, implying that these are the locations of Barrett's stem cells. Future studies underway include looking at 14 days post-IUdR infusion pre-surgery as well as molecular characterisation of the stem cells and their niche.